國立成功大學

太空與電漿科學研究所

碩士論文

National Cheng Kung University
Institute of Space and Plasma Science
Master Thesis

磁控電子束轟擊金屬離子推進器中電子軌跡之探討

Study of Electron Trajectories in Metal Ion Thruster using Magnetron E-beam Bombardment (MIT-MEB)

研究生: 林宛儀
Author: Wan-Yi Lin
指導教授: 張博宇 博士
Advisor: Po-Yu Chang, Ph.D
中華民國109年11月

doi:10.6844/NCKU202003198

國立成功大學

碩士論文

磁控電子束轟擊金屬離子推進器中電子軌跡之探討
Study of Electron Trajectories in Metal Ion Thruster using Magnetron E-beam Bombardment (MIT-MEB)

研究生：林宛儀

本論文業經審查及口試合格特此證明

論文考試委員：

張博宇　李汉元　郭詠仝

指導教授：張博宇

系(所)主管：電漿所所長河森榮一郎

中　華　民　國　109　年　11　月　25　日

摘要

我們的團隊藉由電子蒸鍍的概念開發了一種利用磁控電子束轟擊金屬靶材的離子推進器—Metal Ion Thruster using Magnetron E-beam Bombardment (MIT-MEB)，此論文是透過實驗與模擬電子軌跡來研究此推進器中電子的行爲。此推進器分爲三個部分：金屬離子產生器、離子加速器和中和器。利用加速電壓V_{acc}提供的電場加速電子槍(E-gun)中熱燈絲產生的自由電子轟擊鋅製成的金屬靶材，使靶材被加熱蒸發。在靶材後方有放置磁鐵，因此電子會沿著磁力線轟擊靶材中心。一部分的金屬蒸氣被熱燈絲發射出的電子碰撞而游離，這些離子再經由電場加速排出產生推力，並帶走中和器提供的電子來保持推進的電中性。因此，電子的運行軌跡在此推進器中扮演很重要的角色。我們分別使用V_{acc}等於500、750和1000 V的加速電壓進行了一系列的實驗。從實驗結果我們發現，在使用較低的V_{acc}時，抵達靶材的電子會少於使用較高的V_{acc}。我們認爲電子會被電場力加速往靶材移動，但磁鏡力會將它反彈回電子槍的燈絲，造成電子無法抵達靶材。因此，當V_{acc}較低時，較多的電子會被磁鏡力反彈。所以，我們利用模擬來探討電子軌跡。然而，在模擬中一旦V_{acc}大於1 V，電子就不會被磁鏡力反彈。透過簡單的模型中，只要$V_{\mathrm{acc}} \geqq 0.13$ V就足以加速電子克服磁鏡效應，這符合模擬的結果。所以，我們排除了MIT-MEB中的磁鏡效應對電子軌跡的影響。然而，若我們將燈絲放置於偏心的位置，使得電場力中平行於磁鏡力方向的分量變小，便有機會利用磁鏡效應將電子侷限於燈絲與靶材之間。未來我們需要使用其他可模擬熱電子發射的模擬方式來探討MIT-MEB中電子的行爲並更改推進器的設計。

關鍵字: 磁控電子束轟擊金屬靶材的離子推進器 (MIT-MEB)；電場力；磁鏡力；力的競爭；電子軌跡

doi:10.6844/NCKU202003198

Abstract

The Metal Ion Thruster using Magnetron E-beam Bombardment (MIT-MEB), which uses the principle of electron-beam (E-beam) evaporation, was developed in our group. In this thesis, we studied electron behaviors in both experiments and simulations. There are three parts in the MIT-MEB: a metal evaporator, an ion accelerator, and a neutralizer. Electrons emitted by the heated filament of the E-gun are accelerated toward the target made of Zinc by the electric field provided by an accelerating voltage V_{acc}. A magnet is placed behind the target so that electrons follow the magnetic field lines and reach the center of the target. The target is heated and evaporated when electrons bombard on it. When the metal vapor is impacted by electrons emitted from the thermal filament, part of the vapor is ionized. Ions are then accelerated by the applied electric field providing thrusts. Electrons from the neutralizer would leave the thruster with ions and keep the thruster in neutral. Therefore, electron trajectories play an important role in MIT-MEB. We did a series of experiments with V_{acc} equal to 500, 750, and 1000 V. We found that fewer electrons reach the target in lower V_{acc} than that in higher V_{acc} in experiments. We suspected that the electric force would accelerate electrons toward the target while the magnetic-mirror force would reflect electrons back to the filament of the E-gun preventing them to reach the target. More electrons might be returned in lower V_{acc} than that in higher V_{acc}. Therefore, we studied electron trajectories in simulations. However, in simulations, no electrons were reflected by the magnetic mirror force once there was an electric force from V_{acc} greater than 1 V. It coincided with a simple analytic model where $V_{\mathrm{acc}} \geqq 0.13$ V was sufficient to accelerate electrons overcoming the magnetic-mirror effect. So, we have rolled out the magnetic-mirror effect in the MIT-MEB. Nevertheless, we can move the filament of the E-gun sideway. In this case , the component of the electric field parallel to the magnetic-mirror force much smaller than the magnetic-mirror force will potentially reduce. Thus, electrons may be reflected by the magnetic-mirror force. Therefore, using other simulations which could simulate the thermionic electron emission, and changing the design of the MIT-MEB need to be conducted as future work.

Keyword: MIT-MEB； thermionic electron emission, electric force； magnetic-mirror effect； force competition； electron trajectories

doi:10.6844/NCKU202003198

致謝

很高興能來到太空與電漿科學研究所，在這遇到了許多很棒的老師、學長、同學、學妹與學弟們，讓我在研究所的期間可以愉快的研究、學習與成長。特別感謝張博宇教授，耐心地指導我研究上的各種疑難雜症，且不斷地給我鼓勵和信心，在生活與未來規劃上的問題也會傾聽和給予建議，並營造了PGS這個歡樂大家庭，我一定會懷念和實驗室的夥伴們一起講幹話、互相吐槽的日子。非常謝謝學長國益，在他身上學到很多知識與實驗技巧，很榮幸可以承接MIT-MEB有關的研究。也感謝成大航太系提供了COMSOL這套軟體讓我可以模擬，完成論文。最後謝謝我的家人和朋友們，就算不清楚我在做什麼，依舊無條件的支持、包容我。

doi:10.6844/NCKU202003198

Contents

doi:10.6844/NCKU202003198

doi:10.6844/NCKU202003198

doi:10.6844/NCKU202003198

List of Tables

doi:10.6844/NCKU202003198

List of Figures

doi:10.6844/NCKU202003198

doi:10.6844/NCKU202003198

doi:10.6844/NCKU202003198

1 Introduction

The thrust of the propulsion is produced by the momentum change from ejecting propellants. There are different requirements for different space missions. For example, the rocket launching needs a large thrust. The attitude control, however, may need small thrusts for precision controls. On the other hand, the attitude control and deep-space mission need to carry a lot of propellants. Further, the thrust needs to be low in power consumption and can provide a large final velocity, especially for deep-space missions. The specific impulse (I_{sp}), a measure of how efficient the propellant is used, and thrusts can help us to determine the better type of thrusters for different space missions.

The thrust of an ion thruster is from the exhaust of ions accelerated by an electric force. It can be adjusted by changing the electric field strength. Although the ion thruster only produces the thrust in the range of millinewton (mN), its I_{sp} is in thousands of seconds, i.e., very efficient. Therefore, the spacecraft using an ion thruster can reach a very high speed. If the ion thruster uses a high-density propellant which is easy to be stored and cheap, we can reduce the size as well as the cost. That means the new development of an ion thruster opens up more possibilities for space missions.

1.1 Principle of thrusters

In order to understand the characteristics of the thruster, we must know several parameters, such as thrusts and specific impluses.

1.1.1 Thrusts

The thrust is provided by the reaction force from the accelerated and exhausted propellant. Assuming that the propellant is ejected with a constant exhaust speed v_{ex}, we can calculate the thrust F as

$$F = -\frac{d}{dt}(mv_{\mathrm{ex}}) = -\dot{m}v_{\mathrm{ex}} \equiv \dot{m}_{\mathrm{prop}}v_{\mathrm{ex}} \tag{1}$$

where m is the total mass of the vehicle and m_{prop} is the ejected propellant mass. Notice that v_{ex} is a positive number. The mass reduction rate of the vehicle $\dot{m}$, which is less than 0, equals

doi:10.6844/NCKU202003198

to the negative of the ejected propellant mass rate $\dot{m}_{\text{prop}}$.

1.1.2 Specific impulse (I_{sp})

Specific impulse, I_{sp}, is a parameter that measures the thrust efficiency. It indicates how long a kilogram of propellant can provide 9.8 N of thrusts. The larger, the better. Specific impulse is only related to exhaust speed of the propellant v_{ex}, defined in Eq. 2.

$$I_{\text{sp}} \equiv \frac{F}{\dot{m}_{\text{prop}} g} = \frac{v_{\text{ex}}}{g} \text{ (sec)} \tag{2}$$

where g is the gravitational acceleration. The larger I_{sp} means higher efficiency when the propellant is exhausted with higher speed. From the conservation of linear momentum, we can obtain that a spacecraft has a higher final speed using a thruster with a higher I_{sp}.

$$p(t) = p(t + dt) \tag{3}$$

$$\Rightarrow mv = (m - dm_{\text{prop}})(v + dv) + dm_{\text{prop}}(v - v_{\text{ex}}) \tag{4}$$

$$\Rightarrow dv = -v_{ex}\frac{dm}{m} \text{ where } dm_{\text{prop}}dv \text{ is neglected and } dm_{\text{prop}} = -dm \tag{5}$$

$$\Rightarrow v_{\text{f}} = v_{\text{i}} + v_{\text{ex}} \ln\left(\frac{m_{\text{i}}}{m_{\text{f}}}\right) = v_{\text{i}} + I_{\text{sp}} g \ln\left(\frac{m_{\text{i}}}{m_{\text{f}}}\right) \tag{6}$$

where p is the total linear momentum of the whole system, m is the total mass, m_{prop} is the ejected propellant mass, m_{i} and m_{f} are the initial and final mass, respectively, and v_{i} and v_{f} are the initial and final velocity, respectively. According to Eq. 6, we need either larger $m_{\text{i}}/m_{\text{f}}$ or larger I_{sp} to obtain higher final speed of the spacecraft. However, a thruster with a higher I_{sp} does not necessarily have a larger thrust. The larger thrust can be provided by a larger mass flow of ejected propellants such as chemical rockets. Fig. 1[1, 2] is the comparison between different types of thrusters. Although ion thrusters provide larger I_{sp}, i.e., higher final speed, their thruster density defined as thrusts per unit area is generally too small for a vehicle to overcome the gravitational force on earth. Therefore, an ion thruster is not suitable to be used under the gravitational influence from the earth, but it is one of the best options for deep-space missions after thespacecraft enters the outer space.

doi:10.6844/NCKU202003198

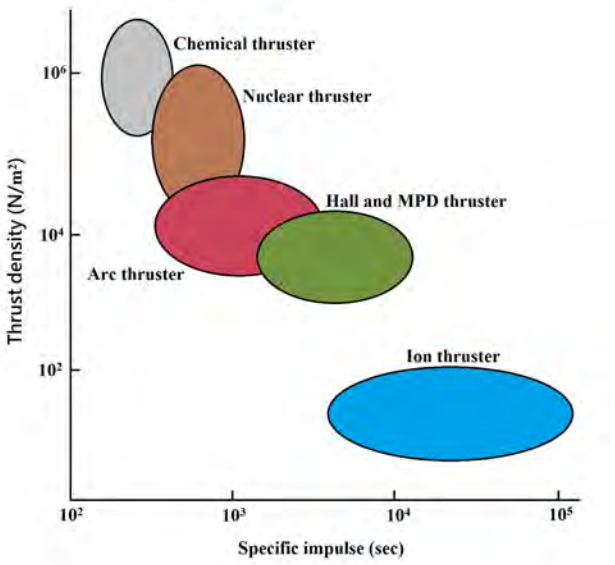

Figure 1: Thrust density vs specific impulse for different types of thrusters.

1.2 Different types of electric thrusters

Categories of electric thrusters are depended on how propellants are accelerated. They are electrothermal, electrostatic, and electromagnetic thrusters. One example for each category is introduced below. They are the resistojet, the gridded-ion thruster, and the pulsed-plasma thruster. The Hall thruster is also introduced below.

1.2.1 Electrothermal thruster – Resistojet

The propellant of the electrothermal thruster is heated electrically. Shown in Fig. 2[3], the gas can be heated via efficient ohmic heating by flowing electrical current through resistors. When the propellant expands after leaving a nozzle, its thermal energy is converted to directional kinetic energy. Finally, the gas leaves the thruster with a high speed to provide thrusts. It is used for orbit insertion, attitude control, and deorbit.

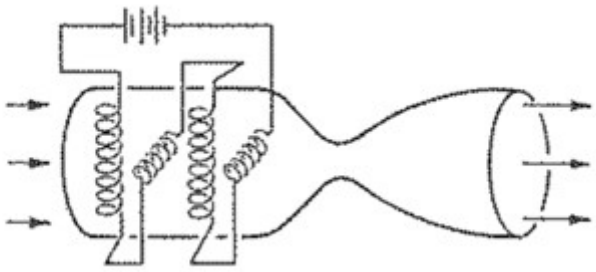

Figure 2: Resistojet.

doi:10.6844/NCKU202003198

1.2.2 Electrostatic – Gridded-ion thruster

The electrostatic thruster uses the electric field to accelerate and exhaust ionized propellant with high speed. The gridded-ion thruster shown in Fig. 3[4] is a classical electrostatic thruster. It usually uses inert gas with a large atomic mass as the propellant, like Xenon gas. The gas in the device is ionized by the electron impact ionization where electrons are provided by an electron gun (E-gun). The accelerating grids consist of the positive grid and negative grid to provide the electric field. When the charges diffuse to the accelerating grids, the ions are accelerated while electrons are decelerated. Finally, ions are exhausted with electrons emitted from the neutralizing electron gun so that the thruster is kept neutral. The gridded ion thruster usually provides a moderate specific impulse (2000–4000 s) with a thrust of 20–200 mN by exhausting high-speed ions. Therefore, it is usually used for deep-space missions.

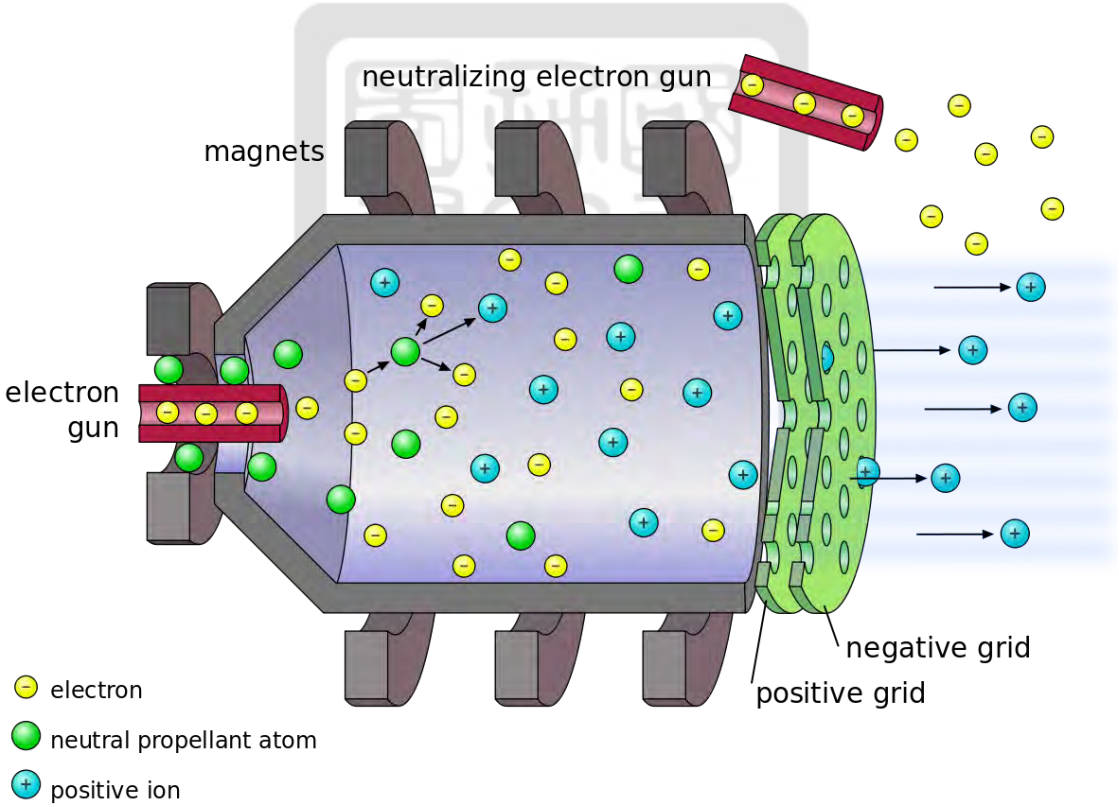

Figure 3: Schematic of gridded ion thrusters.

doi:10.6844/NCKU202003198

1.2.3 Electromagnetic – Pulsed-plasma thruster (PPT)

The electromagnetic thruster uses electromagnetic forces and pressure from the high temperature gas to accelerate the propellant, which is an electrically conducting fluid. Pulsed-plasma thruster (PPT) shown in Fig. 4[5] is one example of the electromagnetic thruster. An arc discharge is initiated between the cathode and the anode. The solid propellant heated, vaporized, and ionized by the arc current. The plasma is then accelerated by the Lorentz force. On the other hand, the gas diffuses with the high thermal energy at the same time. Therefore, the thrusts are provided by both the high-speed plasma and the high-temperature vapors. The pulsed-plasma thruster has a low ionization rate and I_{sp}. However, it has a higher thrust compared to ion thrusters because it has a larger mass flow rate. The size of the pulsed-plasma thruster can be small. Therefore, it is usually used for the CubeSat.

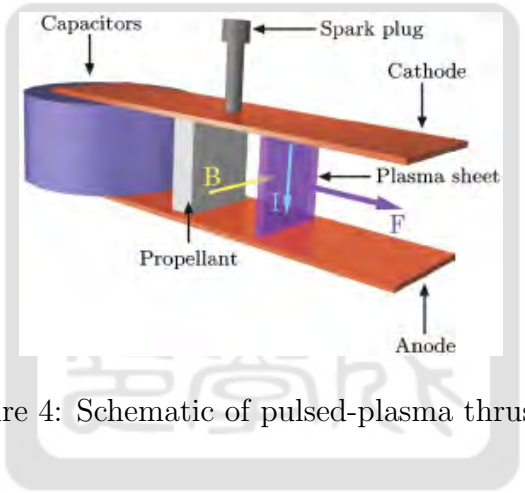

Figure 4: Schematic of pulsed-plasma thruster.

1.2.4 Metal-vapor Hall Thruster

Fig. 5[6] is the schematic of a Hall thruster. The gaseous propellant is injected into the circular chamber from the anode and ionized by the electrons generated from the hollow cathode. The axial electric field and the magnetic fields generated by the radial magnetic coils located at the center cylinder induce the $\overrightarrow{E} \times \overrightarrow{B}$ drift of electrons. Therefore, the electrons are confined and move around the cylinder forming the electron Hall current. It increases the confinement time of electrons in the chamber and improves ionization efficiency. Since ions are too heavy to be magnetized by the magnetic field, they are accelerated by the electric field in the quasi-neutral plasma, leave the thruster with high speed and provide the thrust. The same hollow cathode is also a neutralizing electron gun to keep the thruster neutral. Hall thrusters usually provide a moderate specific impulse (1000–5000 s) with a thrust of 40–600 mN. Therefore, it is

doi:10.6844/NCKU202003198

usually used for deep-space missions.

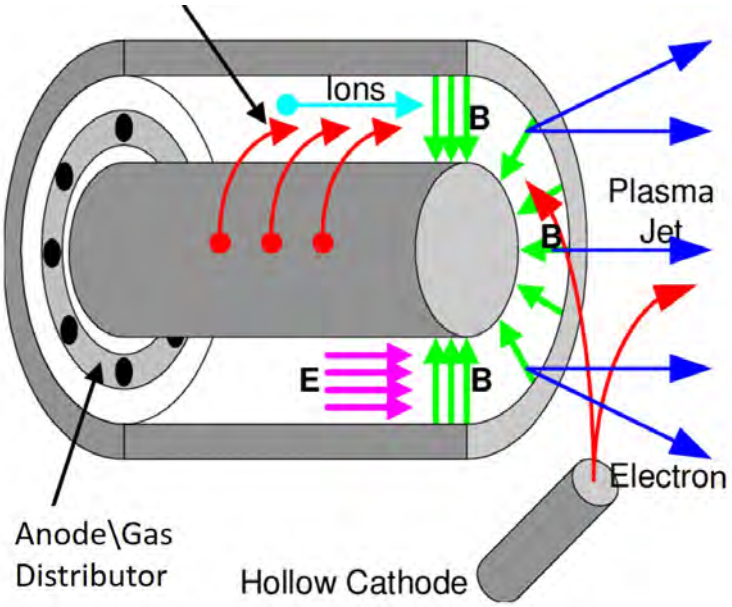

Figure 5: Schematic of Hall thruster.

The conventional hall thruster usually uses Xe gas as the propellant. Xe is expensive and with low density. The solid propellants such as Bi, Mg, and Zn were used to replace Xe [7]. They are in high density, plentiful, non-toxic, and cheap. To use the solid metals as propellant, the metal-vapor Hall thruster is separated into two parets. One part is a metal evaporator. The other part includes the acceleration channel, an anode, and a hollow cathode. It is like a conventional Hall thruster with a metal vapor.

For the example shown in Fig. 6[7], the left part is a separated, temperature-controlled reservoir and the right part includes the acceleration channel, the anode and the hollow cathode. There is a heated line connecting the anode and the reservoir. The condensed zinc in a reservoir is heated and produces the vapor. The feed rate is thus determined by the temperature of the slug. The other elements should be hot enough to prevent condensation of the vapor. The vapor diffuses into anode will be ionized by the electrons provided from the hollow cathode flowing Zn gas. The electrons provided from the hollow cathode also neutralize the thruster[7].

doi:10.6844/NCKU202003198

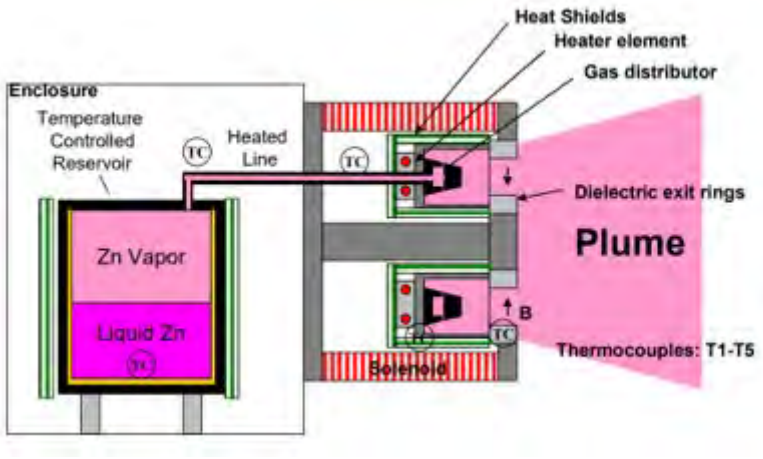

Figure 6: Zinc demonstration system of Metal Vapor Hall Thruster.

We also use Zn as a propellant in the MIT-MEB, where we use E-beam to evaporate and ionize the metal. Moreover, the source of the electrons is from the thermionic electron emission of a tungsten filament to reduce the volume of the thruster.

1.3 Metal Ion Thruster using Magnetron Ebeam Bombardment (MIT-MEB)

The Metal Ion Thruster using Magnetron E-beam Bombardment (MIT-MEB) is a new ion thruster developed by the formal student Kuo-Yi Cheng[8]. Different from the conventional ion thrusters, the MIT-MEB uses the metal instead of the inert gas as the propellant. The solid propellant has many advantages, such as high density, easy to be stored, cheap, and safe. In this section, I will introduce the basic principles of the MIT-MEB, and explain how we designed the thruster. Finally, how we are going to improve the performance of the MIT-MEB and the physics we would like to study based on the principle will be given.

1.3.1 Background principles of the MIT-MEB

We want to use the metal target instead of the inert gas as the propellant because the solid is high density, easy to be stored, cheap, and safe. First, we need to find a way to make the target change its phase from soild to vapor in an ultra-high vacuum. Therefore, we can avoid bringing the gas cylinder to outer space. The second step is to convert the vapor to plasma. We use the ideal of the physical vapor deposition (PVD) to achieve the two steps.

doi:10.6844/NCKU202003198

Shown in Fig. 7[8] is the processes of generating thrust in the MIT-MEB. First, the thermionic electrons provided by the heating filament are accelerated by the external electric field. When the thermionic electrons bombard the target, they heat the target so that it is vaporized. Then, the vapor is ionized by the electron impact ionization. Afterward, ions are accelerated by the electric field and exhausted. They attract electrons provided by the neutralizer so that the thruster is kept neutral. Therefore, the thermionic electron emission, the electron-beam evaporation, and the electron-impact ionization are the basic principles we should understand.

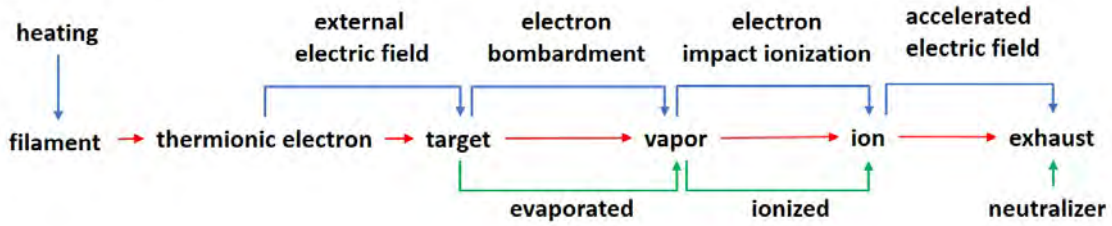

Figure 7: The processes of the MIT-MEB.

1.3.1.1 Physical vapor deposition (PVD) Physical vapor deposition is commonly used for the processes of semiconductor manufacture. The physical mechanism of the PVD is the phase change of matter. It is a vacuum deposition method that can be used to produce thin films and coatings. The most common PVD processes are evaporation and sputtering.

In evaporation, the target is evaporated by being heated directly, such as joule heating, laser heating, and electron-beam (E-beam) heating. The materials most commonly used to hold the evaporated material are tungsten and molybdenum because they have high electrical resistance, high melting point and are difficult to form alloys with other metals. The evaporated material is attached to the tungsten wire or carried in tungsten boats. The evaporated material is evaporated by the heating tungsten as the result of the high temperature. Then, the vapor forms a film on the substrate whose temperature is low.

In sputtering, the target is bombarded by high-energy ions in the plasma. The ions and plasma are provided by the inert gas ionized by a DC or AC high-voltage discharge. Ions as the working particles are accelerated toward the target by the external electric field. Then, the atoms of the target detach from the surface when working particles bombard on it and transfer their kinetic energy to the target. Finally, leaving atoms form a film on the substrate whose

doi:10.6844/NCKU202003198

temperature is low. Since ions and electrons in the plasma are charged, they can be controlled by magnetic fields. Therefore, ions can be guided to specific areas of the target by magnetic fields to increase the efficiency of sputtering.

Evaporation and sputtering work differently. Nevertheless, no matter which method is used, the purpose of PVD is to change the material from a solid state into a gaseous state.

1.3.1.2 The thermionic electron emission When the temperature of a metal rises, the kinetic energy of electrons in the metal increases. The number of electrons whose kinetic energy exceeds the work function, also gradually increases. If the temperature of the metal is over a certain degree, a large number of electrons escape from the metal. This phenomenon is called the thermionic electron emission. In 1901, Richardson gave the mathematical form of the thermal emission [9]:

$$J = \lambda_{\mathrm{R}} A_{\mathrm{G}} T^2 e^{-\frac{w}{k_{\mathrm{B}} T}} \tag{7}$$

where J is the emitted current density, T is the temperature of the metal, w is the work function of the metal, k_{B} is the Boltzmann constant, λ_{R} is a correction factor for different material and A_{G} is a universal constant. The constant A_{G} equals to $4\pi m k_{\mathrm{B}}^2 e/h^3$. The value is 1.2×10^6 ($\mathrm{Am^{-2}K^{-2}}$). The constant λ_{R}, on the other hand, is typically in the order of 0.5. We use tungsten filaments due to its high melting point.

The thermionic emission from a tungsten wire as a function of temperature is shown in Fig. 8[10]. If the temperature of the metal is above 1000 K, a large number of electrons can escape from the metal. However, the escaping hot electrons accumulate near the metal surface as shown in Fig. 9[11]. They prevent more hot electrons from being emitted. Therefore, we have to apply an external electric field to pull out the electrons so that electrons are emitted continuously.

doi:10.6844/NCKU202003198

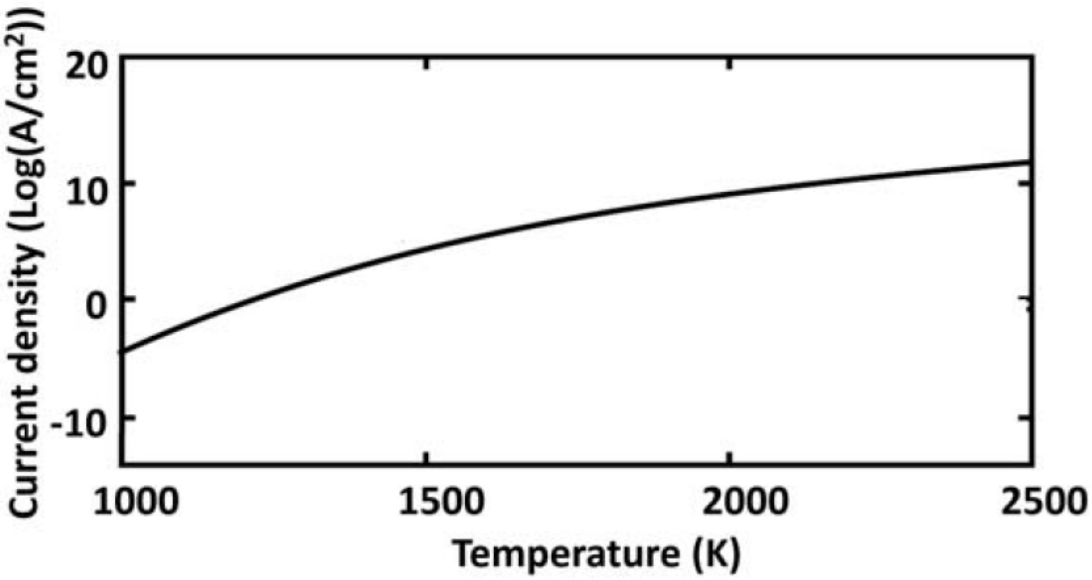

Figure 8: Saturation current densities of the thermionic emission from tungsten as a function of temperature.

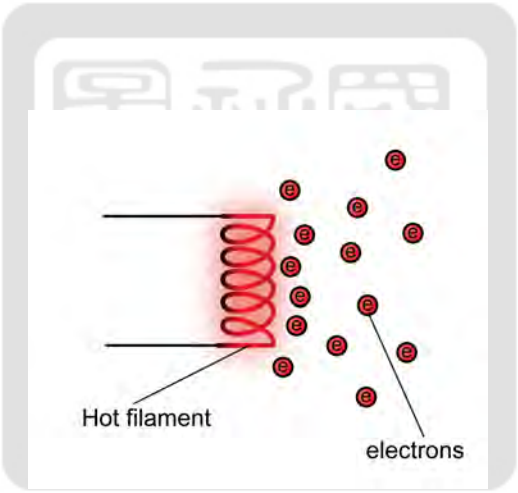

Figure 9: Hot filament emits free electrons.

1.3.1.3 The electron beam evaporation Electron-beam (E-beam) evaporation uses accelerated electrons to bombard the coating material. Therefore, the kinetic energy of the electron is connected to the thermal energy of the coating material. Therefore, the material is heated and vaporized. The design of a conventional E-beam evaporator is shown in Fig. 10[12]. There is a heating filament at the bottom as an electron source using the thermal-emission effect. The free electrons are accelerated by an external electric field to get kinetic energy. Then, we can deflect the E-beam using a magnetic field to control the bombardment location. Thus, the coating material is heated and evaporated when electrons bombard on it and transfer their kinetic energy to the thermal energy of the material. Eventually, the coating material forms a

doi:10.6844/NCKU202003198

film on the substrate. Materials can be heated to temperatures up to 3000˜6000 °C locally because the E-beam heating provides extremely high energy density. Therefore, refractory metals or compounds can still be evaporated. Both incoming electrons and secondary electrons on the target surface generated by high-energy electrons bombardments may ionize residual gas molecules. It is a good way for us to evaporate the solid propellant and provide the ions.

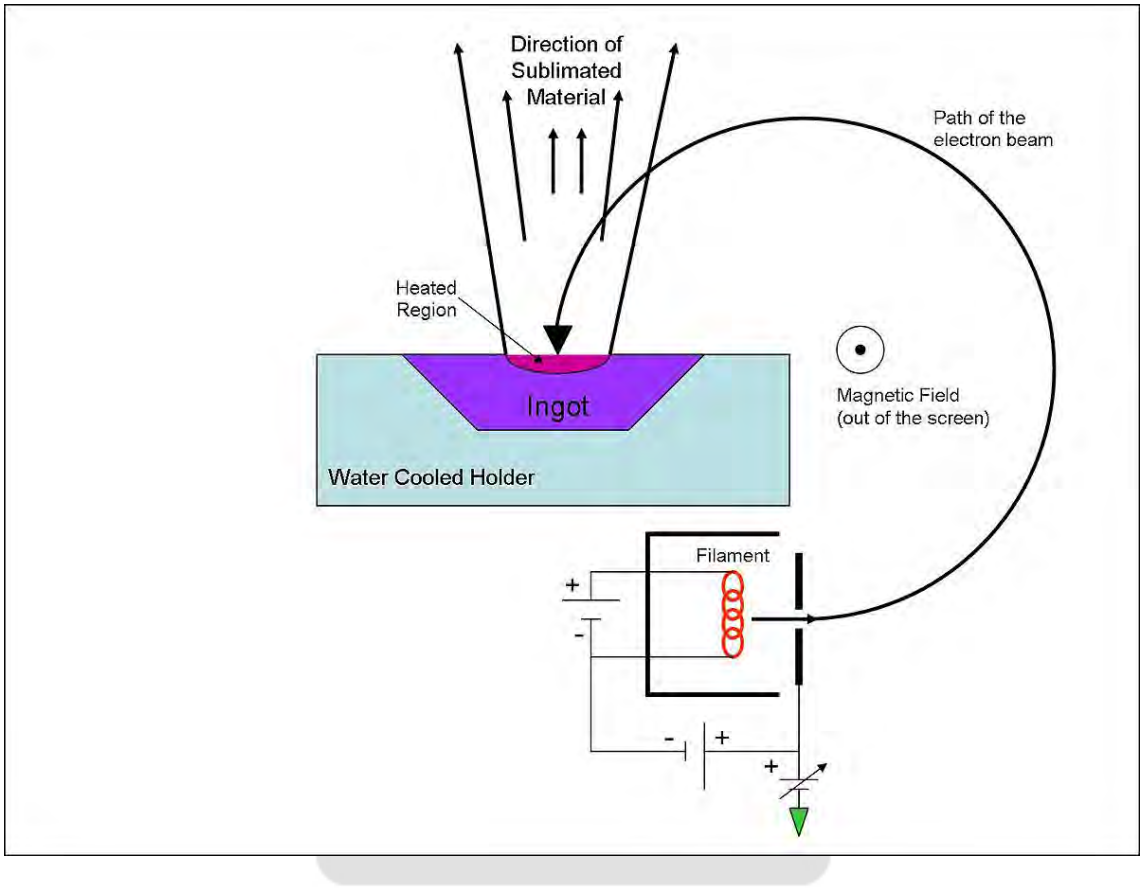

Figure 10: Electron beam evaporation deposition.

1.3.1.4 Temperature of the tungsten filament The tungsten temperature and the thermal velocity are important parameters for the simulation I will perform in Chap. 3. It is because the thermal velocity is assumed to be the initial velocity of the thermionic electrons in MIT-MEB. The estimated tungsten temperature is used to estimate the thermal velocity

$$v_{\text{thermal}} = \sqrt{\frac{2k_{\text{B}}T}{m_{\text{e}}}} \tag{8}$$

where v_{thermal} is the thermal velocity, $k_{\text{B}} = 1.38 \times 10^{-23}$ J/K is Boltzmann constant, $m_{\text{e}} = 9.11 \times 10^{-31}$ kg is the mass of the electron, and T (K) is the tungsten temperature. From Fig. 8 and Eq. 7, the thermionic emission current is a function of temperature. However, we do not

doi:10.6844/NCKU202003198

know emitted electrons would leave the filament freely or return back to the filament. In other words, we can't obtain the temperature of the tungsten filament by measuring the emitted current. All alternative way to estimate the tungsten temperature is required. Then, we can compare the difference between the measured electric current and the predicted electric current from the estimated filament temperature.

The tungsten is heated by the eletric power P. We can estimate the tungsten temperture T by the balance between the heating power and the radiation power. The radiation power can be estimated using the Stefan-Boltzmann law[13] as

$$\phi = \frac{P\,(\mathrm{W})}{A\,(\mathrm{m}^3)} = \epsilon\sigma T^4 \tag{9}$$

where ϕ is the black-body radiant emittance, which is the total energy radiated per unit surface area of a black body across all wavelengths per unit time, A is the surface area of the filament, σ is the Stefan–Boltzmann constant, and ϵ is the emissivity of the object. The Stefan–Boltzmann constant σ is $\frac{2\pi^5 k^4}{15c^2h^3} = 5.67 \times 10^{-8}$ $(\mathrm{J\,s^{-1}m^{-2}K^{-4}})$. The parameter ϵ of an absolute black body is 1 while ϵ of a grey body is less than 1. We use $\epsilon = 0.5$ to estimate the tungsten temperature. On the other hand, the heating power from the power supply is writen as

$$P = IV \tag{10}$$

where I is the current flowing through the filament, and V is the voltage of across filament. By substituting Eq. 10 into Fig. 9, we can estimate the temperature of the the tungsten filament. Then, the temperature can be used to estimate the thermal velocity of emitted electron using Eq. 8 for the simulation. It can also be used to calculate the saturation current densities of the thermionic emission from tungsten and be compared with the electric current we measure in experiments.

1.3.1.5 Vapor pressure of the common metals at different temperature To pick the material as the propellant, the easier it is vaporized, the better it is as the propellant. It is because the metal materials which are easier to be vaporized require less heating power. Note that materials with lower melting points do not mean they are evaporated easier. For example, the melting point of Tin is only 231.9 °C while Zinc needs 419.5 °C to be melted. However,

doi:10.6844/NCKU202003198

to achieve the same vapor pressure such as 10^{-3} Torr, 1315 °C is needed for Tin achieved while only 565 °C is needed for Zin as shown Table 1[14]. Moreover, Zinc is cheap, easy to be obtained, and low toxic. Therefore, we choose Zinc to be the propellant.

Table 1: Temperature (T) in kelvin for different vapor pressure (PE) in torr for different metallic materials

PE (torr) / T (K) / Material	10^{-3}	10^{-2}	10^{-1}	10^{0}	10^{1}	10^{2}
Al ($M = 27.0$ amu)	1162	1269	1396	1552	1760	2022
Fe ($M = 55.8$ amu)	1583	1720	1875	2056	2312	2633
Cu ($M = 63.5$ amu)	1414	1546	1705	1901	2152	2480
Zn ($M = 65.4$ amu)	565	616	678	760	866	1009
Ag ($M = 107.9$ amu)	1209	1320	1457	1626	1848	2138
Sn ($M = 118.7$ amu)	1315	1462	1646	1882	1976	2241
Au ($M = 197.0$ amu)	1589	1738	1919	2140	2427	2794
Pb ($M = 207.2$ amu)	898	991	1105	1248	1440	1690

1.3.1.6 Electron impact ionizations Electron impact ionizations use high energy electrons to impact atoms or molecules to achieve ionization. There are two kinds of sources providing electrons to ionize the vapor. A common method is first using a hot filament as an electron source to provide electrons. Then, electrons are accelerated by an external electric field and confined by the magnetic field between the target and the filament. The other ones are the secondary electron with lower energy, including backscattered and true secondary electrons. They are also confined by the electric potential and the magnetic field in a small region forming an electron cloud on top of the target surface. When atoms or molecules are collided by those electrons, the electron of the atoms or molecules is possible to be removed. The ionization reaction formula can be written as

$$\mathrm{M} + \mathrm{e}^- \rightarrow \mathrm{M}^+ + 2\mathrm{e}^- \tag{11}$$

where M is the atom, e^- is the electron. The kinetic energy of the electron must be greater than the first ionization energy of the target elements.

The relationship between the first ionization energy and the atomic number is shown in Fig. 11[15]. The material we choose as the propellant is Zinc (Zn) whose atomic number is 30. The first ionization energy of Zn is 9.4 eV. Therefore, we should provide the electrons with the energy over 9.4 eV to impact the Zinc vapor to achieve ionization.

doi:10.6844/NCKU202003198

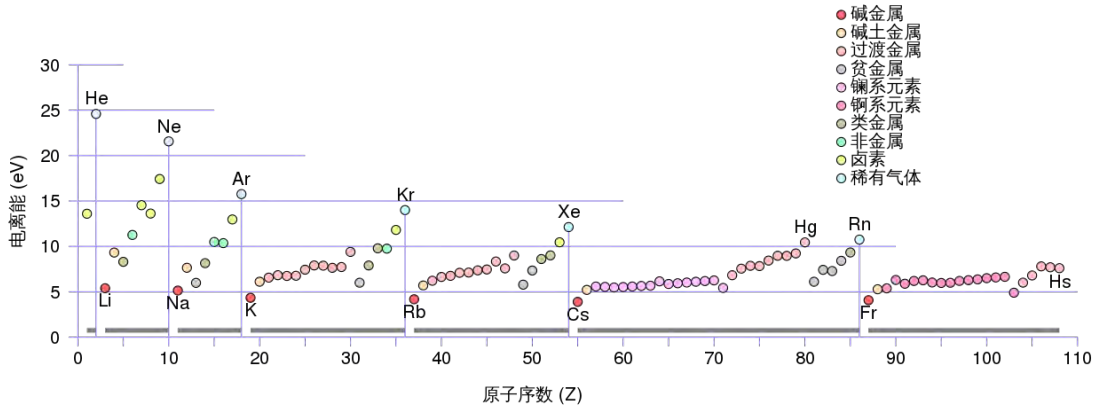

Figure 11: Relationship between first ionization energy and atomic number.

1.3.2 The design of the MIT-MEB

Shown in Fig.12[8], there are two parts of the MIT-MEB: a metal evaporator combining with an ion accelerator and a neutralizer. Similar to an E-beam evaporation, free electrons around the heated filament are accelerated by the high electric field and bombard the target. The target is heated when electrons transfer their kinetic energy to the thermal energy of the target when they bombard on it. As a result, the metal vapor is generated when the target is hot enough. A high-density electron cloud is confined by a magnetic field between the metallic target and the heated filament (E-gun) provided by a focusing magnet. When the metal vapor passes the electrons cloud, a part of the vapor will be ionized by being collided by the high-energy electrons. Those ions are then accelerated by the applied electric field. When ions leave the thruster, they attract electrons provided by the neutralizer so that the thruster is kept neutral.

doi:10.6844/NCKU202003198

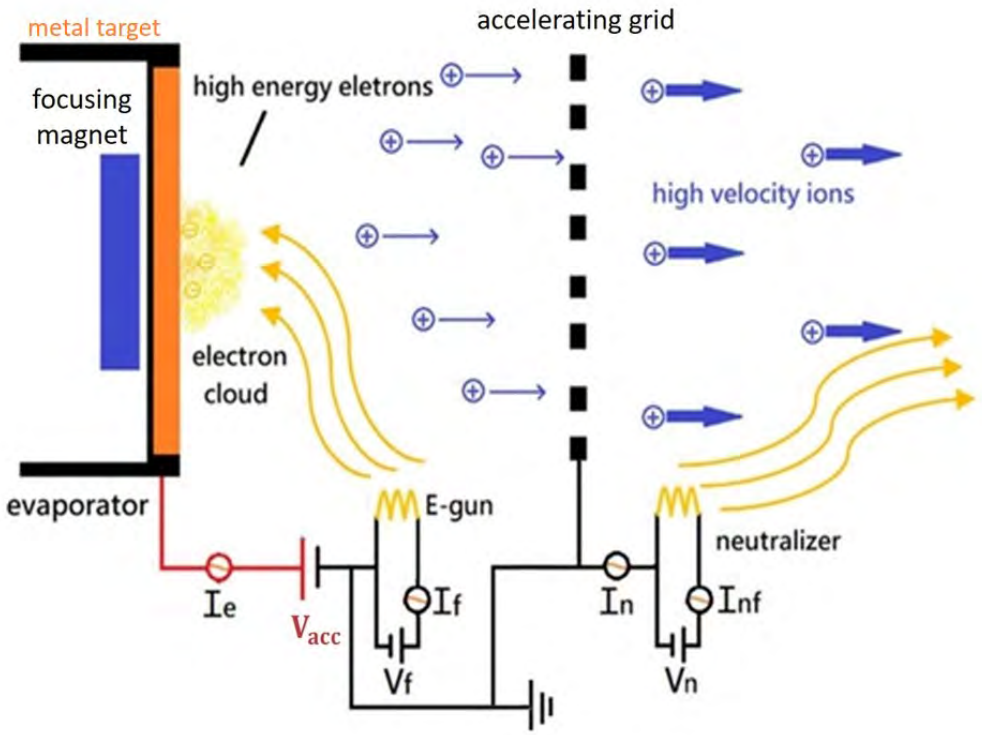

Figure 12: Regular MIT-MEB.

1.3.2.1 The structure of MIT-MEB Shown in Fig. 13 is the modified MIT-MEB we test. The only difference between Fig. 12 and Fig. 13 is an extra voltage V_{ag} keeping the potential of the accelerating grid lower than the E-gun and the neutralizer. The high electric field is provided by V_{acc}, and I_e is the electric current that heats the target. The thermal energy of the free electrons around the filament of the E-gun and the neutralizer is provided by the current I_f and I_{nf}, respectively. V_f and V_{nf} are the voltages of the E-gun and the neutralizer, respectively. The parameter V_{ag} between the accelerating grid and the E-gun and the neutralizer is used to prevent the electrons from the E-gun and the neutralizer passing through the accelerating grid. Therefore, the potential of the accelerating grid is lower than that of the E-gun and the neutralizer providing the small electric fields toward accelerating grid at both sides of the accelerating grid. When ions leave the thruster, they attract electrons with the same charge number to keep the thruster neutral. It can be seen from the equivalent circuit of the MIT-MEB shown in Fig. 14[16]. The current I_{ne} is provided by leaving electrons which equals to the ion current I_{ion}. And the current I_{nf} for the filament of the neutralizer and I_{ne} merge at point d. Then, I_R including by I_{ne} and I_{nf} goes through the resistance R_n of the neutralizer. When I_R arrives at point b, I_R will break into I_b and I_n. I_b is the same as the

doi:10.6844/NCKU202003198

current I_{nf} back to the cathode of the neutralizer. Therefore, I_n is equal to I_{ne} and also equal to the ion current I_{ion}. It is the reason why we measure the ion current with the current monitor between the neutralizer and the accelerating grid to get the ion current I_{ion}.

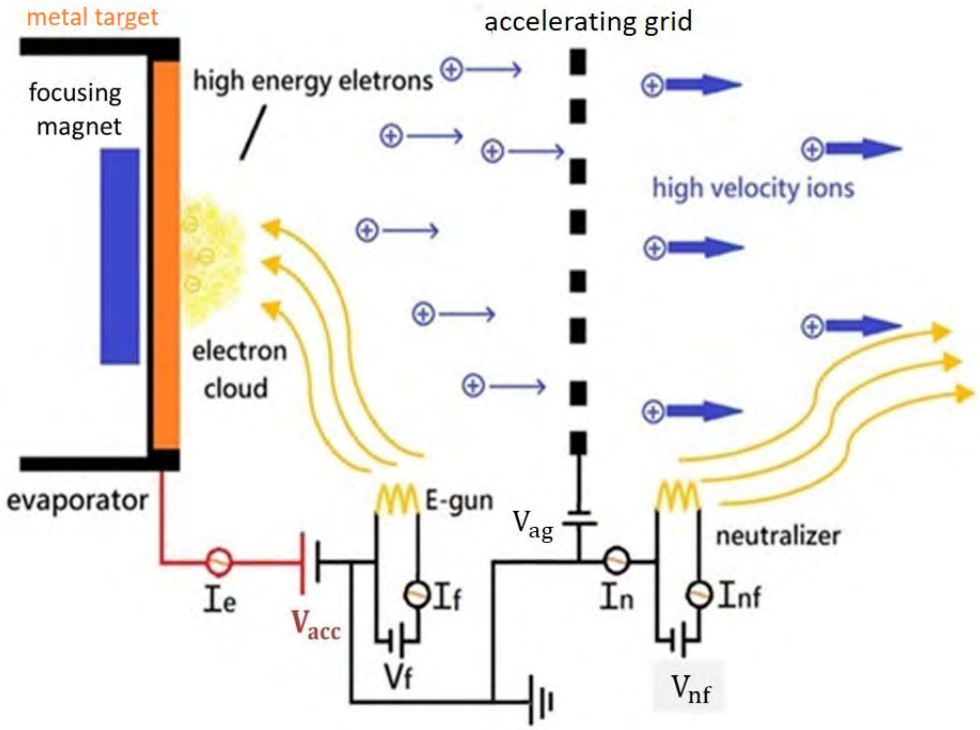

Figure 13: The structure of MIT-MEB.

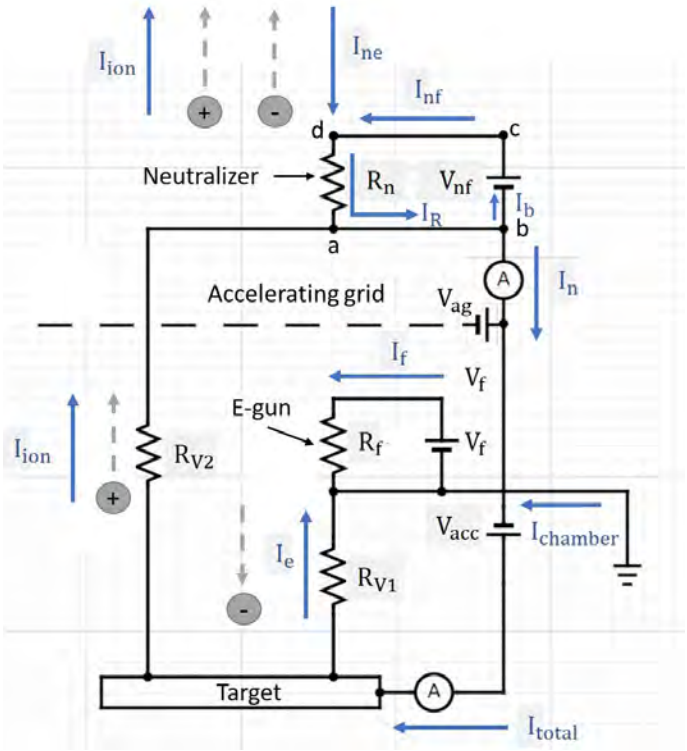

Figure 14: The equivalent circuit of MIT-MEB.

doi:10.6844/NCKU202003198

1.3.2.2 The prototype of the MIT-MEB Shown in Fig. 15 is the design of the MIT-MEB according to the structure given in Fig. 13. We use three focusing magnets whose radius and height are both 10 mm. They are stacked on top of each other. They are placed underneath the metal target such that the gap between the top surface of the magnet and the bottom of the target is 2 mm. The radius of the metal target is 15 mm and the thickness is 0.5 mm. The E-gun is placed 3.5 mm above the metal target. The accelerating grid is 7 mm above the E-gun. Finally, the neutralizer is 7 mm above the accelerating grid . The length of the filaments of the E-gun and neutralizer are both 10 mm. We use this format to build the prototype as shown in Fig. 16[8].

Shown in Fig. 16 (a) and (b), the outer cases of the MIT-MEB are either quartz or ceramics. The melting point and the density of ceramics are 2054 ° C and 3.97 g/cm^3, respectively. This material is strong, durable and heat-resistant so that it is good for experiments. On the other hand, the melting point and the density of the quartz are 1650 ° C and 2.65 g/cm^3, respectively. Although it is crystal brittle, it is easier for observation because it is transparent. We use the prototype with the ceramics outer case to conduct experiments and prototypes with the quartz outer case for exhibition.

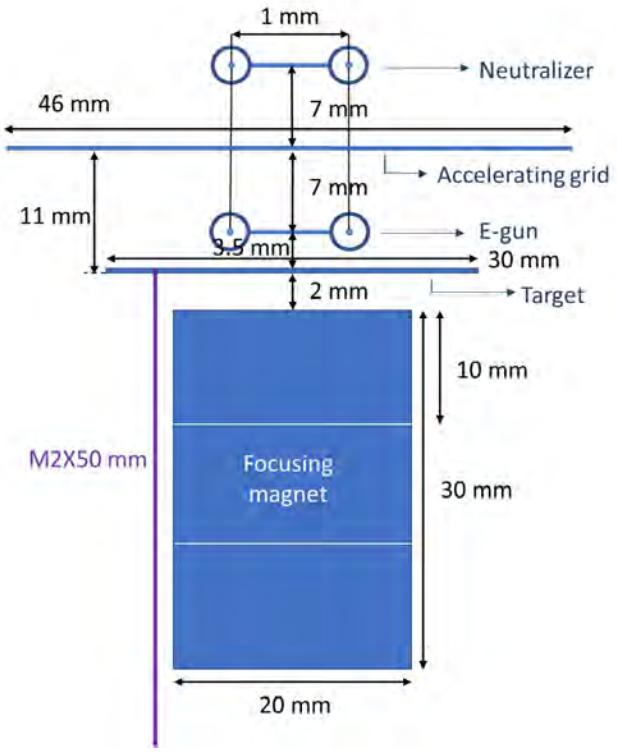

Figure 15: Design of the prototype.

doi:10.6844/NCKU202003198

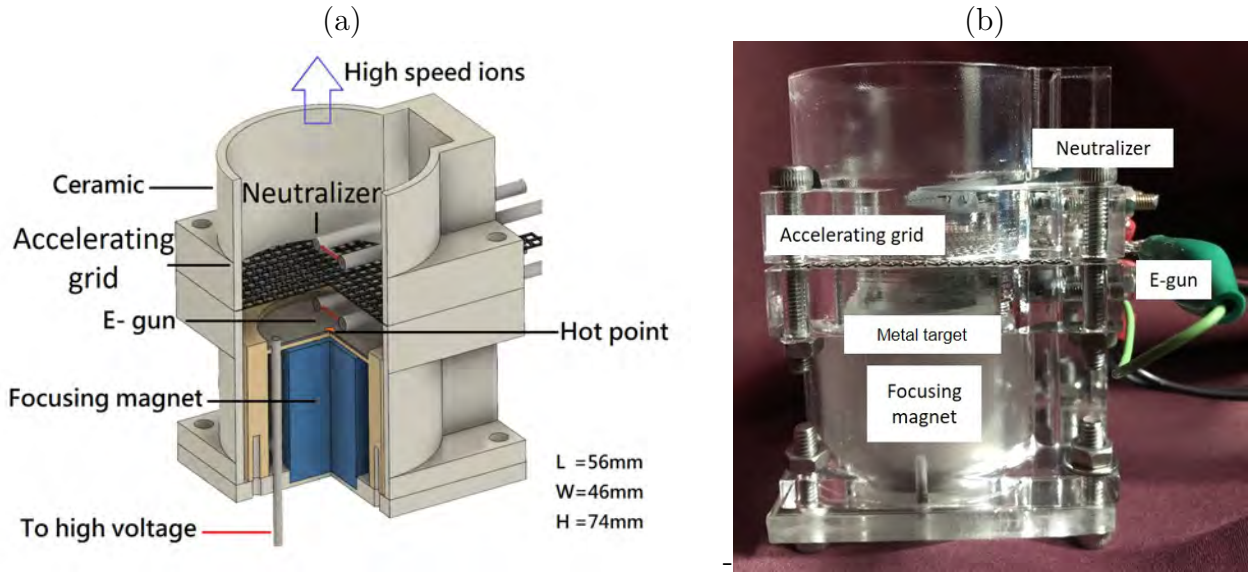

Figure 16: (a) The (CAD) drawing of prototype, and (b) the photograph of the MIT-MEB.

1.3.2.3 Previous results In Kuo-Yi's thesis[8], he did experiments with the accelerated voltage V_{acc} equal to 1 and 5 kV. Different electric currents were used to keep the power of the E-beam equal to 15 W. His experimental results are shown in Table 2. The total power was including the powers of E-beam, E-gun, and the neutralizer. We can see that the evaporation rate of using 5 kV was higher than that of using 1 kV. However, the ionization rate of using 5 kV is less than that of using 1 kV. It means that larger V_{acc} had better evaporation capability but lower the ability of ionizing gas. It is important to understand how different V_{acc} influence the performance of the MIT-MEB. Therefore, I did experiments and simulations with different V_{acc}.

Table 2: Comparison of thruster parameters of 1 kV and 5 kV of MIT-MEB under same E-beam power.

Condition	Total power (W)	Evaporation rate (g/s)	Ionization rate (%)
5 kV/3 mA	24.8 ± 1.1	$(2.2 \pm 0.4) \times 10^{-4}$	0.03 ± 0.01
1 kV/15 mA	26.2 ± 0.7	$(1.8 \pm 0.3) \times 10^{-5}$	1.10 ± 0.30

1.3.2.4 Cross section of electron impact ionization for zinc The cross section of electron impact ionization strongly depends on the electron energy. Larger cross-section means the atom is ionized by the electron impact easier. Therefore, the cross-section for electron impact ionization needs to be considered. As shown in Fig. 17c[17], the cross section of electron impact ionization for Zinc peaks at 60 eV. The voltages, 1 kV and 5 kV, Kou-Yi used in his experiments were too high. Therefore, we should decrease the acceleration voltage to

doi:10.6844/NCKU202003198

increase the cross-section of electron impact ionization for Zinc so that the ionization fraction can be increased. However, the electrons are not only used to ionize the vapor but also to generate vapor so that the acceleration voltage should not be too small. Therefore, I want to study the performance of MIT-MEB with lower voltage.

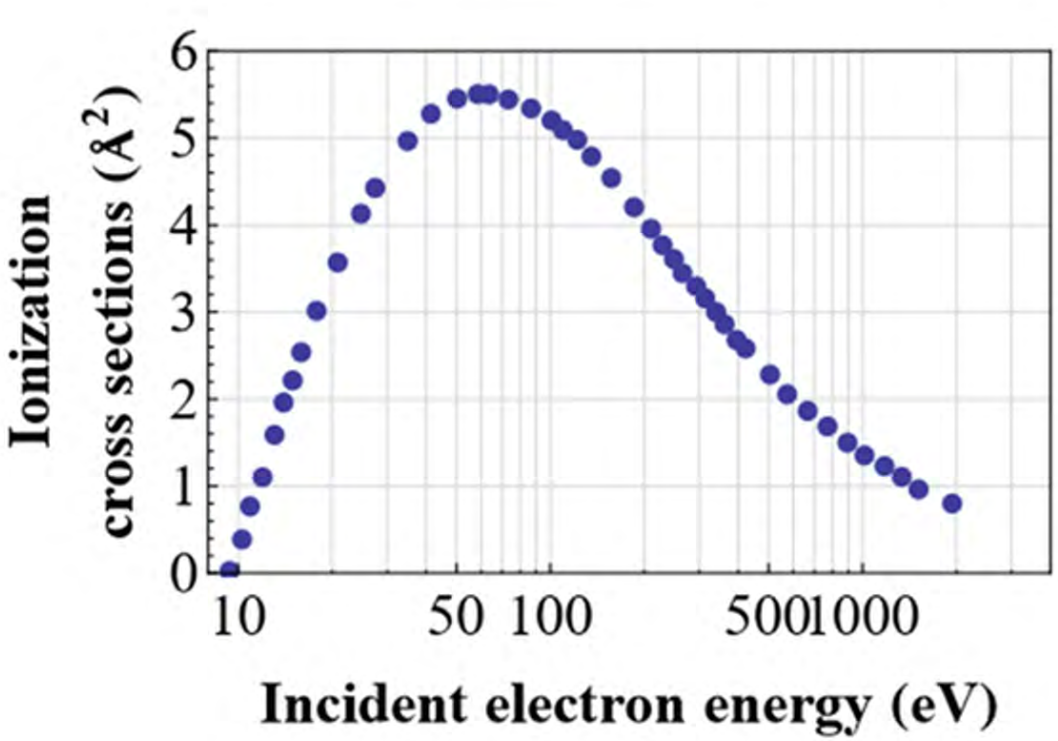

Figure 17: . The cross section of electron impact ionization for Zin.

1.4 Force competitions

Charged particles interact with electromagnetic fields. The Lorentz force $\overrightarrow{F}$ is the force felt by a charged particle in an electromagnetic field:

$$\overrightarrow{F} = q\left(\overrightarrow{E} + \overrightarrow{v} \times \overrightarrow{B}\right) \tag{12}$$

where $\overrightarrow{F}$ is the Lorentz force, q is the charge of the charged particle, $\overrightarrow{E}$ is the electric field, $\overrightarrow{V}$ is the velocity of the charged particle, and $\overrightarrow{B}$ is the magnetic field. It can be used to describe the interactions between charged particles and electromagnetic fields. Therefore, we are able to control the energy and directions of electrons by electromagnetic forces. As shown in Fig. 18 (a) and (b), the electrons are accelerated by the electric field. On the other hand, they gyro around magnetic field lines. Since the magnetic field is not uniform, electrons can be reflected

doi:10.6844/NCKU202003198

by the magnetic-mirror effect. Therefore, the trajectories of electrons are determined by the competition between the two forces as shown in Fig. 18 (c).

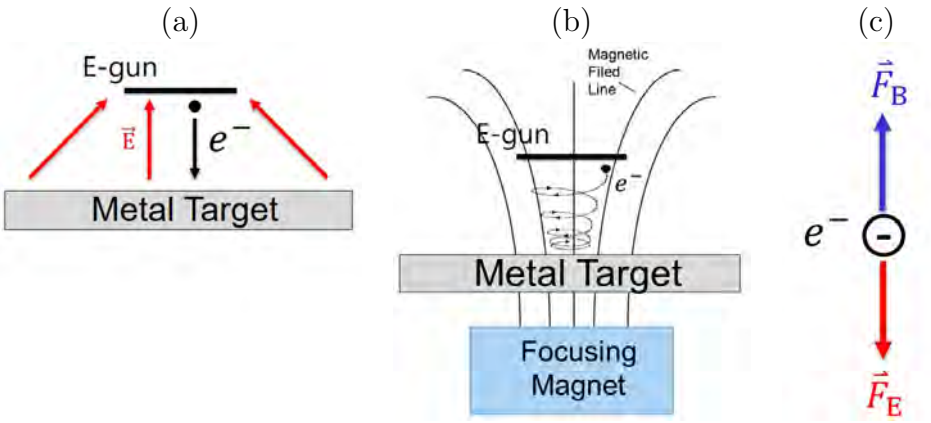

Figure 18: Influence of (a) electric field, (b) magnetic field, and(c) force competition in the MIT-MEB

1.4.1 The electric force

The positive charge in the electric field is accelerated in the same direction of the electric field, but the negative charge in the electric field is accelerated in the anti direction. Therefore, the electric force of the charged particle is the term $q\overrightarrow{E}$ in Eq. 12. Then, a charged particle can obtain the kinetic energy from the acceleration of the electric field. We can express the electric force:

$$\overrightarrow{F}_{\mathrm{E}} = q\overrightarrow{E} = q\left(-\nabla V\right) \tag{13}$$

where V is the electric potential. An electron accelerated by an electric potential of 1 volt obtained the kinetic energy 1 eV equal to 1.6×10^{-19} J as shown in Fig.19. So, we can change the electric potential $V = V_{\mathrm{acc}}$ in the MIT-MEB to provide different strength of the electric field and thus give the charged particle different kinetic energy.

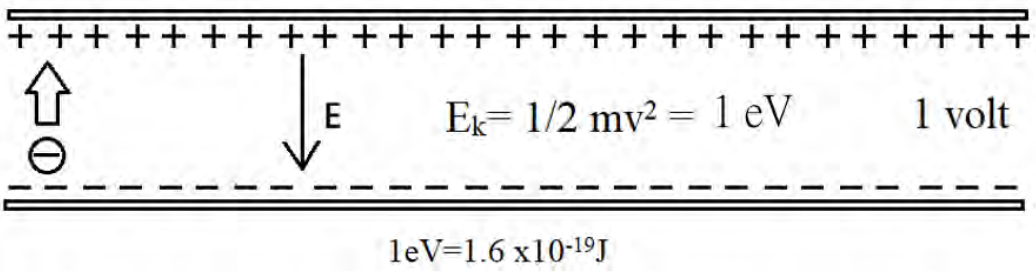

Figure 19: The electrons are accelerated by electric fields.

doi:10.6844/NCKU202003198

1.4.2 The magnetic mirror effect

The magnetic force can be categorized into two cases:

1. An uniform magnetic field.

2. A non-uniform magnetic field.

How charged particles behave in these two cases are giving in the following.

1.4.2.1 Uniform magnetic fields The term in Eq. 12, $q\overrightarrow{v} \times \overrightarrow{B}$, represents the magnetic force acting on the charged particle. The direction of the force is perpendicular to the direction of the magnetic field and the velocity of the charged particle. The charged particles change their directions as shown in Fig. 20[18]. Therefore, we can use the magnetic field to control the directions of electrons.

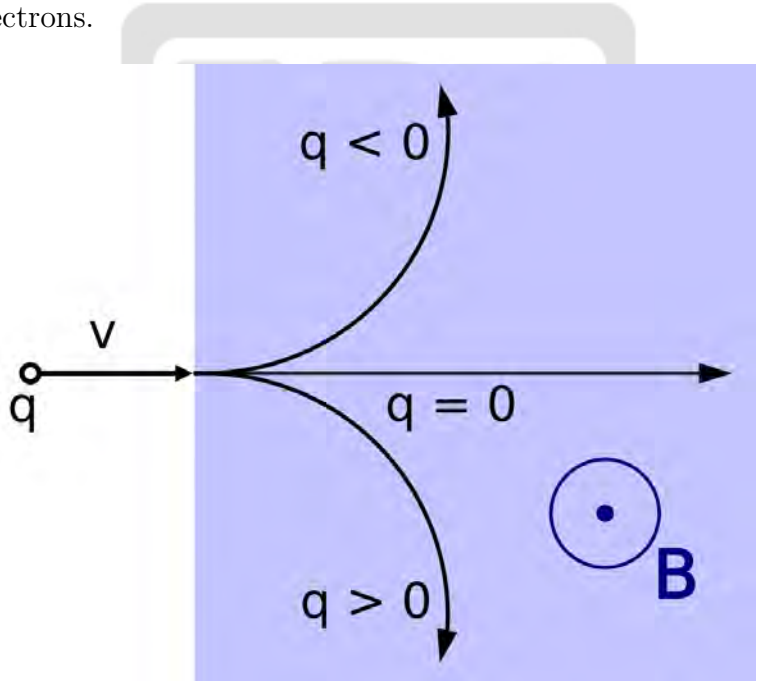

Figure 20: The charge is deflected by the influence of the magnetic field.

Since the magnetic force is the centripetal force for the charged particle in a circular motion, we can have the gyroradius defined as the radius of the circular motion of the charged particle in the presence of a uniform magnetic field. It is given by:

$$r_{\mathrm{L}} = \frac{mv_{\perp}}{|q|B} \tag{14}$$

doi:10.6844/NCKU202003198

where r_{L} is the Larmor radius, m is the mass of the particle, $v_{\perp}$ is the component of the velocity perpendicular to the direction of the magnetic field, q is the electric charge of the particle and B is the strength of the magnetic field.

We can use the Larmor radius to estimate the period of the electron circular motion given in Eq. 15. Then, we can use the Larmor radius to check if the simulation with the magnetic field is correct and use the period to estimate the time step used in the simulation.

$$T = \frac{2\pi r_{\perp}}{v_{\perp}} \tag{15}$$

1.4.2.2 Non-uniform magnetic fields In a non-uniform magnetic field, charged particles are also reflected by the magnetic-mirror effect when charged particles move from the region with a weaker magnetic field into the region with a stronger magnetic field. The reflection force is represented as

$$\overrightarrow{F}_{\mathrm{B}} = -\mu \nabla_{\parallel} |\overrightarrow{B}| \tag{16}$$

where $\overrightarrow{F}_{\mathrm{B}}$ is the magnetic-mirror force, $\nabla_{\parallel}\overrightarrow{B}$ is the gradient of the magnetic field along the magnetic field. The parameter μ is the magnetic moment of the gyrating particles defined as

$$\mu \equiv \frac{\frac{1}{2}mv_{\perp}^2}{|B|} \tag{17}$$

The magnetic moment μ is a constant for a charged particle in any magnetic field without forcesalong with the magnetic force other twins magnetic force. As the charged particle moves into the region with stronger B, its $v_{\perp}$ becomes higher. On the contrary, $v_{\parallel}$, which is the component of the velocity parallel to the direction of the magnetic field, becomes lower according to the energy conservation:

$$\frac{d}{dt}\left(\frac{1}{2}mv^2\right) = \frac{d}{dt}\left(\frac{1}{2}mv_{\parallel}^2 + \frac{1}{2}mv_{\perp}^2\right) = 0 \tag{18}$$

where m is the mass of the charged particle, and v is the total velocity. When the whole kinetic energy transfers into the term of $v_{\perp}$, the charged particle will be reflected as a result of $v_{\parallel} = 0$ as shown in Fig. 21[19]. The position where the charged particle is reflected is called the mirror

doi:10.6844/NCKU202003198

point.

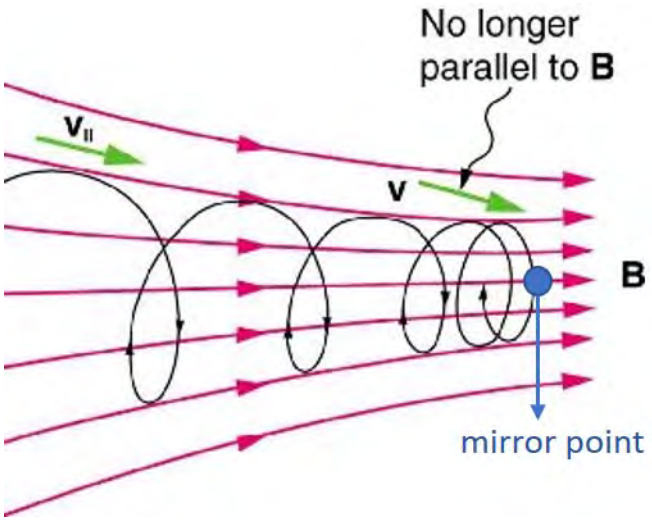

Figure 21: The magnetic mirror effect.

Although charged particles are slow down due to the magnetic-mirror effect, not all charged particles are reflected. Assume that we have a charged particle with the initial velocity $\overrightarrow{v_0}$ which is composed by $\overrightarrow{v_{\perp 0}}$ and $\overrightarrow{v_{\parallel 0}}$. Velocities $\overrightarrow{v_{\perp 0}}$ and $\overrightarrow{v_{\parallel 0}}$ are components perpendicular and parallel to the direction of the magnetic field, respectively. When the ratio $v_{\perp 0}/v_{\parallel 0}$ is too small, $v_{\parallel}$ is too large to be decelerated to zero by the magnetic-mirror force. In other words, the initial velocity v_0 can not be transferred completely into the component of $v_{\perp}$ in the strong-field region. So, the charged particle will go through the strong magnetic field region.

In the case there is no external force parallel to the magnetic field, the magnetic moment μ is an invariant and $v_{\perp}$ in the different field region can be assumed by:

$$\frac{1}{2}\frac{mv_{\perp 0}^2}{B} = \frac{1}{2}\frac{mv_{\perp}^{\prime 2}}{B^{\prime}} \tag{19}$$

where B_0 is the magnetic field of the initial location at which the charged particle is, $B^{\prime}$ is the magnetic field at any location other than the initial location, and $v_{\perp}^{\prime}$ is the velocity perpendicular to the magnetic field $B^{\prime}$ at the same location. Assuming that the location with the magnetic field $B^{\prime}$ is the charged particle stopped, the velocity $v_{\parallel}^{\prime}$ parallel to $B^{\prime}$ becomes zero. Then, conservation of energy requires

$$v_0^2 = v_{0\perp}^2 + v_{0\parallel}^2 = v_{\perp}^{\prime 2}\,. \tag{20}$$

doi:10.6844/NCKU202003198

Therefore,

$$\frac{B_0}{B'} = \frac{v_{\perp 0}^2}{v_{\perp}'^2} = \frac{v_{\perp 0}^2}{v_0^2} \equiv \sin^2\theta \tag{21}$$

where θ is the pitch angle of $\overrightarrow{v_0}$ relative to $\overrightarrow{B_0}$. Assuming that $B_{\rm m}$ is the magnetic field at the location where we want the charged particle to be stopped, which is the mirro point, we can get the angle $\theta_{\rm m}$ by

$$\sin^2\theta_{\rm m} = \frac{B_0}{B_{\rm m}}\,. \tag{22}$$

If θ is smaller than $\theta_{\rm m}$, it means B' is larger than $B_{\rm m}$. In the other words, $B_{\rm m}$ is too small to stop the charged particle with the initial velocity $\overrightarrow{v_0}$ with the pitch angle θ. Therefore, we can get a boundary of a region in velocity space in a cone. This region is called the loss cone as shown in Fig. 22[20].

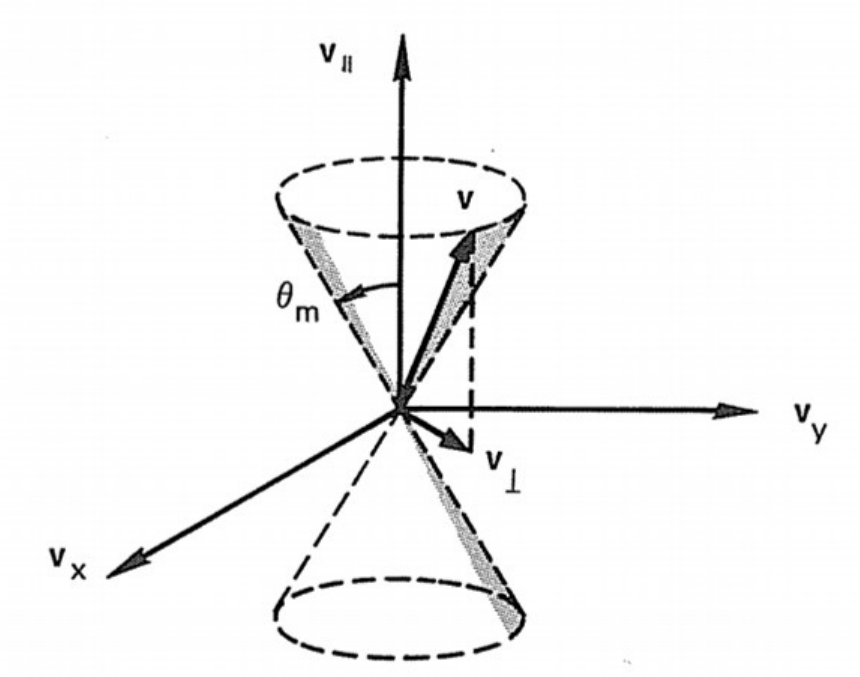

Figure 22: The loss cone.

For particles not in the loss cone, they are reflected. On the other hand, particles in the loss cone would penetrate through the mirro point. In the MIT-MEB, the magnetic field is not uniform. Electrons in the loss cone can arrive the target and evaporate it. On the contrary, electrons not in the loss cone, they are trapped forming an electron cloud. The loss cone of the system is important to be studied in simulations.

doi:10.6844/NCKU202003198

1.4.3 The competition between the electric field and the magnetic-mirror force

We can imagine that if $v_{\parallel}$ of the charged particle is larger enough, it can go through the region with the strongest magnetic field. The larger the electric field gives the electron more kinetic energy in the term of $v_{\parallel}$, the position of the mirror point is closer to the target in MIT-MEB. As shown in Fig. 23 (a), h_1 and h_2 are the distance between $Mirror\ Point_{1,2}$ and the target, respectively. When the electric field E_1 is smaller than E_2, h_1 is larger than h_2. Therefore, the location of the electron cloud is determined by the competition between the electric force and the magnetic-mirror force. If we use a larger electric field, the electron cloud is confined closer to the target as shown in Fig. 23 (b). However, if we use a smaller electric field, the electron cloud is confined farther away from the target as shown in Fig. 23 (c). When the electron cloud is closer to the target, electrons are easier to arrive and evaporate the target. However, the ionization rate is lower as a result of fewer electrons stay in the electron cloud for ionizing the vapor. On the contrary, if the electric field is lower, the electron cloud is farther away from the target. As a result, fewer electrons reach the target leading to a smaller evaporation rate. Nevertheless, the electron cloud may have higher electron density leading to a higher ionization rate. There will be an optimal electric field for providing a sufficient evaporation rate and a higher ionization rate.

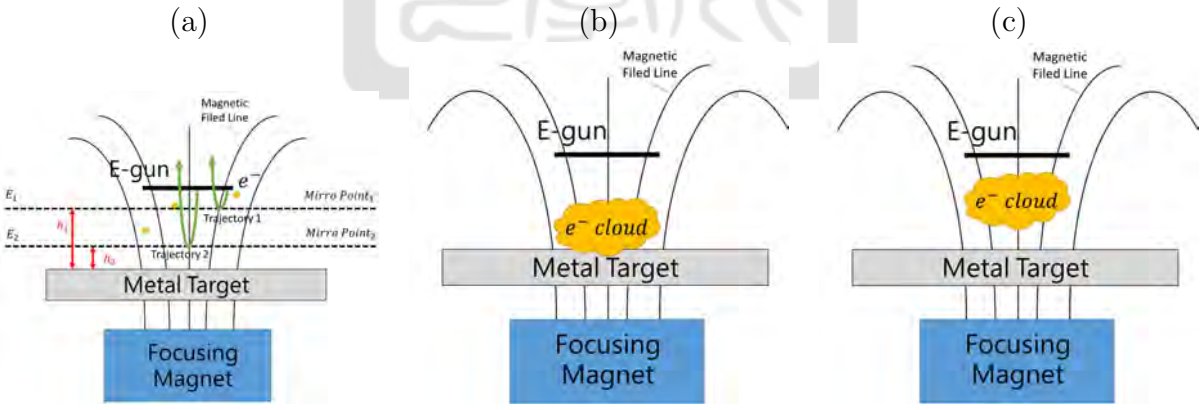

Figure 23: (a) The positions of the mirror point with different eletric fields (b) The position of the electron cloud in the large electric field (c) The position of the electron cloud in the small electric field

1.5 Goal

The MIT-MEB is a new ion thruster developed by the formal student Kuo-Yi Chen. In his thesis, the ionization rates in the MIT-MEB were too small for practical uses. It is important to

doi:10.6844/NCKU202003198

study the electron behaviors and potentially increase the efficiency of the MIT-MEB. We would like to focus on the force competitions between the electric force and the magnetic-mirror force. Both experiments and simulations were conducted. In Chap. 2, I will show the experimental results using different V_{acc}. In Chap. 3, I will show the simulation results for studying the force competitions. Then, the discussion will be shown in Chap. 4. Finally, the summary will be given in Chap. 5.

doi:10.6844/NCKU202003198

2 Experiments

In this chapter, I will introduce experiments of testing the MIT-MEB including the vacuum system, experimental setup, standard operation procedure (SOP) of experiments, and experimental results.

2.1 Parameters in the MIT-MEB

The thrust and the specific impulse are the important parameters of the thruster to be measured. It is not easy to measure them directly. However, the evaporation rate and the ionization rate are the parameters easier for us to measure. Therefore, we use the evaporation rate and ionization rate to calculate the thrust and the specific impulse of the MIT-MEB.

2.1.1 Evaporation rates

The thrust is provided by an exhausted propellant. First, we need to know how many solid propellants become vapor. It is difficult to measure the instant vapor flow during the experiment. So, we measure the mass differences of the target before and after each experiment to calculate the averaged evaporation rate $\dot{m}_{\mathrm{Metal}}$ defined as

$$\dot{m}_{\mathrm{Metal}} = \frac{m_{\mathrm{i}} - m_{\mathrm{f}}}{\triangle t} \tag{23}$$

where m_{i} is the mass of the target before the experiment, m_{f} is the mass of the target after the experiment, and $\triangle t$ is the time difference before and after the experiment.

We used the electronic scale, Sartorius TE124S, shown in Fig. 24 to measure the mass of the target. The precision of the scale is 0.0001 g. Therefore, only the mass difference over 0.001 g was treated as a significant difference when we calculated the averaged evaporation rate.

doi:10.6844/NCKU202003198

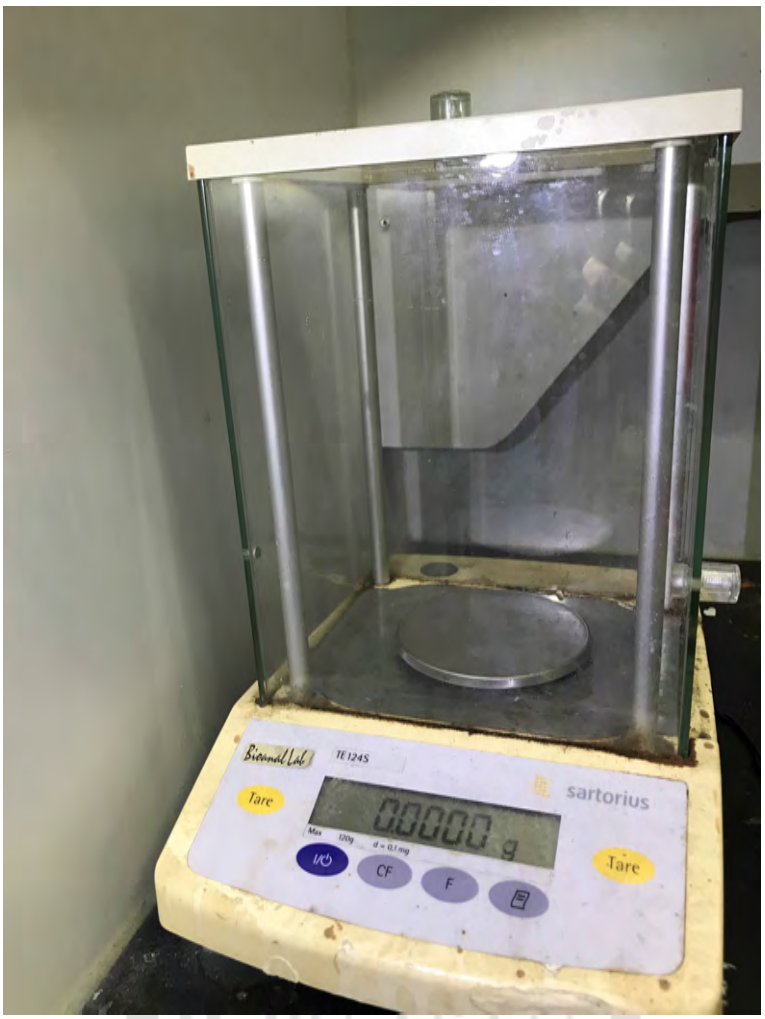

Figure 24: The electronic scale Sartorius TE124S.

2.1.2 Ionization rates

The vapor is ionized via electron impact ionization by electrons located between the target and the E-gun in the MIT-MEB. However, not all vapors are ionized. We measured the ion current to know how many ions were exhausted per second. Then, we could calculate the ratio between the number of ions to the number of neutral gas called ionization rate β as

$$\beta = \frac{I_{\mathrm{n}}}{q} \times \left(\frac{\dot{m}_{\mathrm{Metal}}}{m_{\mathrm{atom}}} \right)^{-1} \tag{24}$$

where I_{n} is the ion current measured according to the equivalent circuit of the MIT-MEB in Fig. 14, $q = 1.6 \times 10^{-19}$ coulomb is the elementary charge, and m_{atom} is the mass of a metal particle.

doi:10.6844/NCKU202003198

2.1.3 Thrusts and I_{sp}

From Eq. 1, thrusts are from the ejected propellant mass per second with a constant exhaust speed. In the MIT-MEB, the thrusts are provided by both vapor and ions. So, we can express the total thrust F_{total} as

$$F_{total} = F_{vapor} + F_{ion} = \dot{m}_{vapor} v_{vapor} + \dot{m}_{ion} v_{ion} = \dot{m}_{Metal} (1 - \beta) \sqrt{\frac{2k_B T_{vapor}}{m_{atom}}} + \dot{m}_{Metal} \beta \sqrt{\frac{2qV_{acc}}{m_{atom}}} \tag{25}$$

where thrusts from vapor and from ions are F_{vapor} and F_{ion}, respectively. The exhaust speed of the vapor, v_{vapor}, is the thermal velocity $\sqrt{\frac{2k_B T_{vapor}}{m_{ion}}}$ where T_{vapor} is the temperature of the vapor. It is smaller than the exhaust speed of the ions $\sqrt{\frac{2qV_{acc}}{m_{ion}}}$. Therefore, more ions, higher thrusts.

Then, we can express Eq. 2 with Eq. 25 as

$$I_{sp} = \frac{F_{total}}{\dot{m}_{Metal} g} = \frac{1}{g} \left[(1 - \beta) \sqrt{\frac{2k_B T_{vapor}}{m_{ion}}} + \beta \sqrt{\frac{2qV_{acc}}{m_{ion}}} \right]. \tag{26}$$

The electrical energy qV_{acc} is easier to control than the thermal energy $k_B T_{vapor}$. Most importantly, qV_{acc} is generally much higher than $k_B T_{vapor}$. Therefore, we want to get higher β in the MIT-MEB to make this thruster have higher thrusts and I_{sp}. However, we only focused on evaporation rates in this thesis.

2.2 Vacuum system

The experiment was done in a vacuum chamber. It was because the tungsten wire used in the Neutralizer and the E-gun would be oxidized and damaged in the atmosphere. On the other hand, the mean free path must be larger than the size of the experimental environment in order to avoid the loss of energy due to the collision of accelerated electrons with ions and background gas molecules. Moreover, we can verify whether it can operate in the space environment in the future.

doi:10.6844/NCKU202003198

2.2.1 Design of the vacuum system

The design of the vacuum system I used is shown in Fig. 25. I used the quartz tube as the vacuum chamber whose diameter, height, and wall thickness were 200 mm, 250 mm, and 5 mm, respectively. There were two stainless-steel plates as the top cover plate and the bottom cover plate.

1. The top cover plate: It had five KF 25 flanges for connecting the ball valve, the low vacuum gauge, the ion gauge, and two electronic feedthroughs.

2. The bottom cover plate: It had one KF 50 flange and four KF 16 flanges.

   (a) KF 50 flange: It was for connecting the high vacuum pump. I used a diffusion pump to be the high vacuum pump instead of the turbomolecular pump Kuo-Yi used. Back of the diffusion pump was connected to a KF25 Radius 90° Elbow.

   (b) KF 16 flanges: One of them was connected to the electronic feedthrough for V_{acc}. The others were not used.

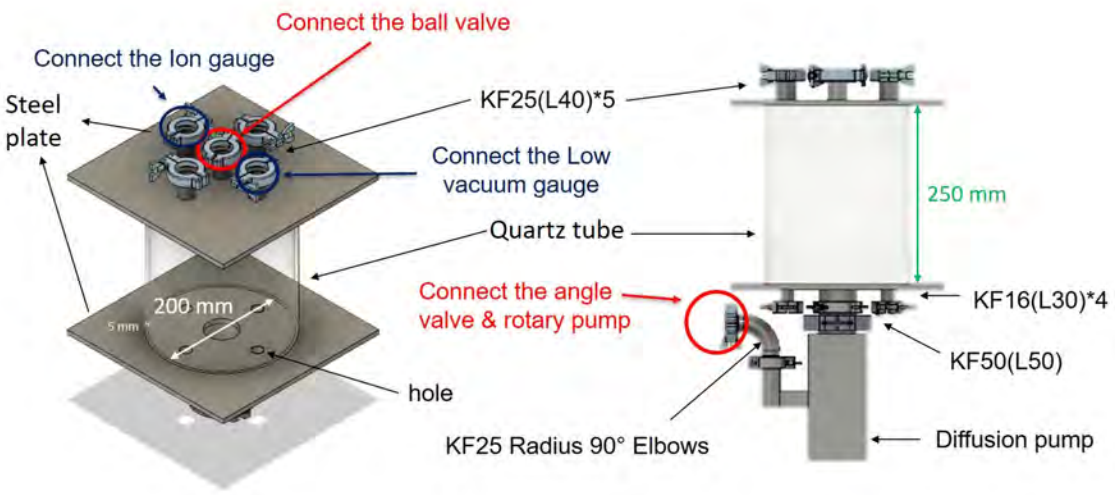

Figure 25: Design and setting of the vacuum system

Another side of the KF25 Radius 90° Elbow was connected to the angle valve and the rotary pump originally. According to the airflow path of the vacuum system shown in Fig. 26(a), I added a gate valve between the chamber and the diffusion pump and a ball valve between the diffusion pump and the rotary pump. Therefore, it reduced the time for experiments since we don't need to vent the chamber after the diffusion pump was cooled down. The SOP of

doi:10.6844/NCKU202003198

the vacuum system is in Appendix A. The actual experiment setup of the MIT-MEB in the vacuum system is shown in Fig. 26(b).

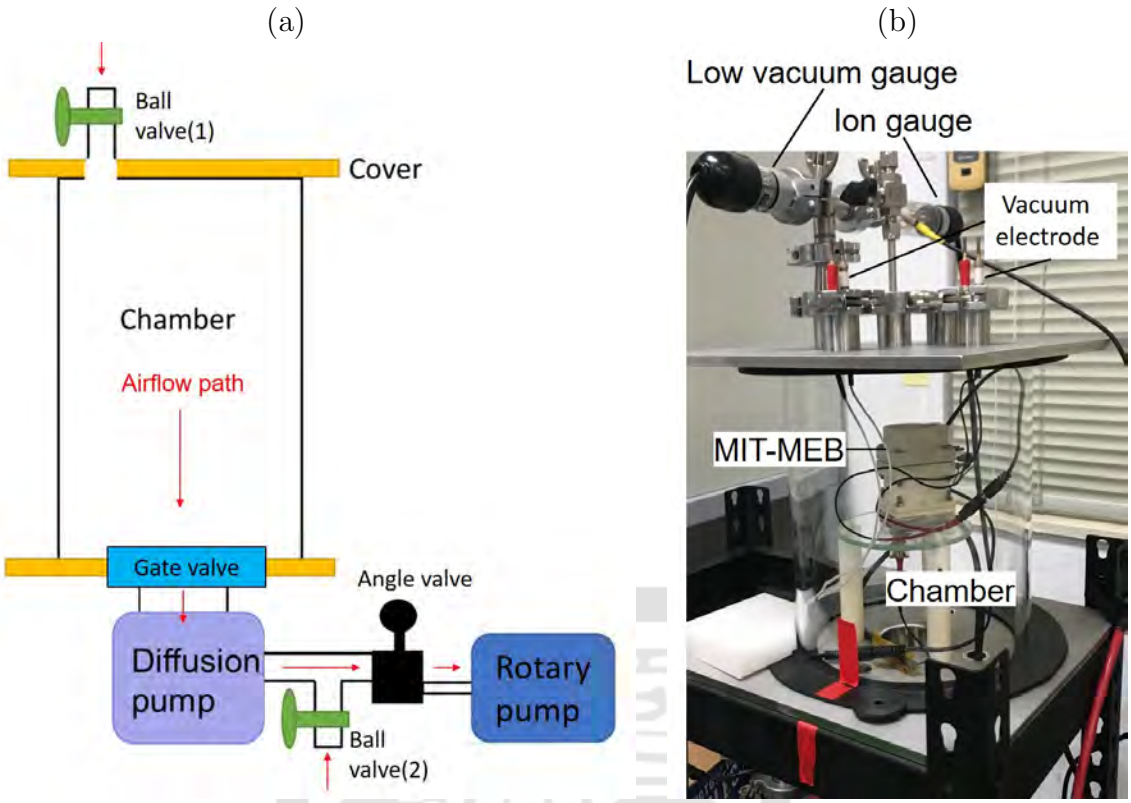

Figure 26: (a)Airflow path of the vacuum system (b) Realistic vacuum system

In Kuo-Yi Cheng's thesis, the background pressure he started to do experiments was about 1.3×10^{-3} Pa (1×10^{-5} torr).[8] However, the diffusion pumps in my vacuum system only provided about 7.3×10^{-3} Pa (5.5×10^{-5} torr) as the background pressure. The mean free path is $5.9 \times 10^{-1} \sim 5.9 \times 10^{0}$ m for pressure equal to $10^{-2} \sim 10^{-3}$ Pa. The size of the chamber is smaller than the mean free path. Therefore, I did experiments in this vacuum system even the background pressure was a little higher than that in Kuo-Yi's experiments.

2.3 Experimental setting

According to Fig. 13, I needed some power supplies to provide voltages and currents to the MIT-MEB. I also had the multimeter and the vacuum gauge to measure the ion current and the background pressure. The instruments I used were shown in Fig. 27.

doi:10.6844/NCKU202003198

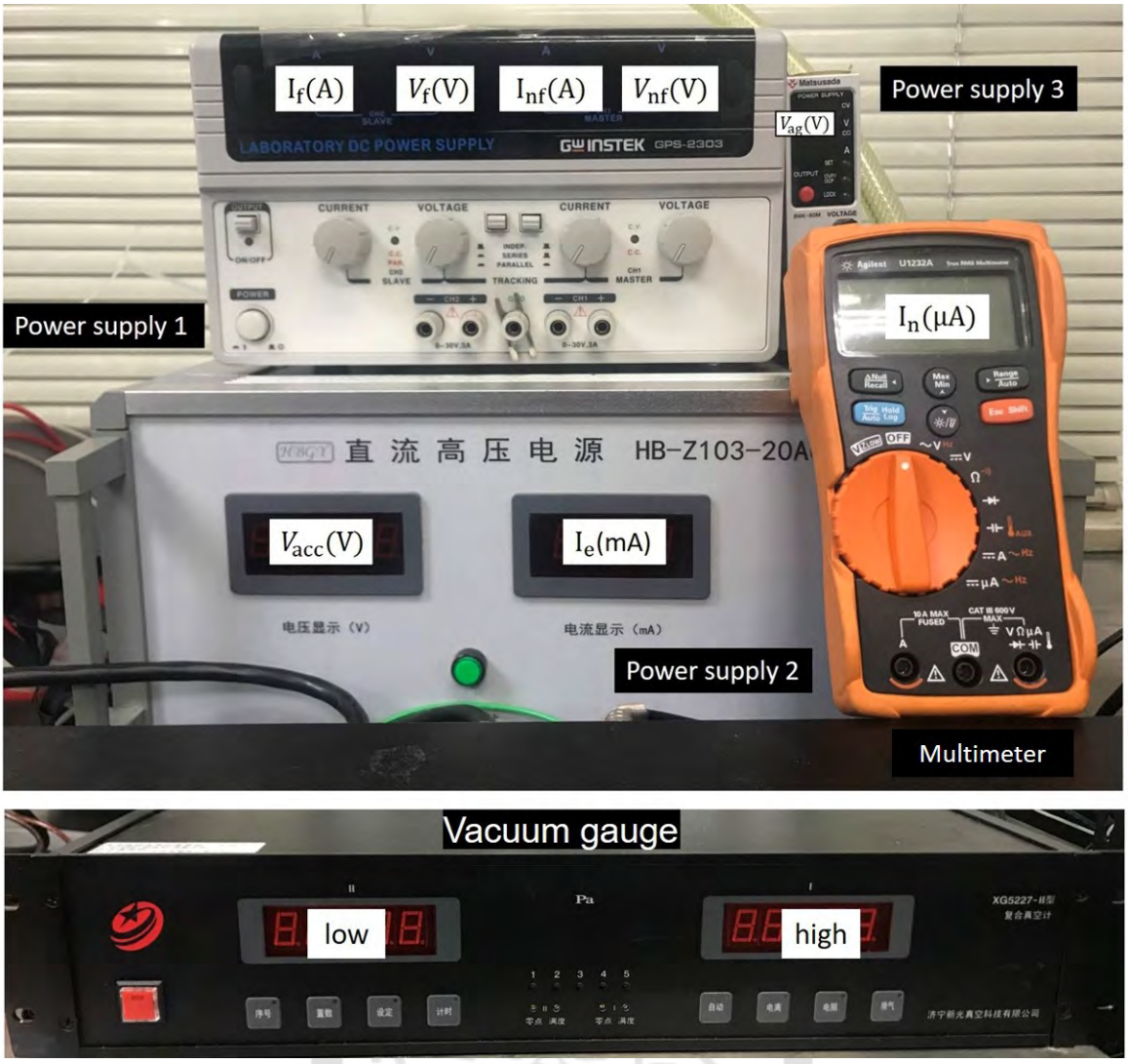

Figure 27: Power supply system of MIT-MEB.

1. Power supply 1:

   It provided the currents and the voltage for controlling the filament temperature. The filament temperature influenced the amount of electron emission.

   (a) I_f and V_f: They were the current and the voltage of the E-gun, respectively. Adjusting I_f could control the emitted electron current I_e from the filament.

   (b) I_{nf} and V_{nf}: They were the current and the voltage of the neutralizer, respectively.

2. Power supply 2:

   (a) V_{acc}: The voltage between the E-gun and the target for providing the high electric field. Electrons from the E-gun were accelerated by this electric field to bombard the target. The ions were also accelerated by this electric field to exhaust the thruster.

doi:10.6844/NCKU202003198

(b) I_e: The electric current that heated the target. It was determined by the ability to release free electrons from the E-gun filament. It is controlled by adjusting I_f.

3. Power supply 3: It provided the voltage V_{ag} between the accelerating grid and the E-gun and the neutralizer. The potential of the accelerating grid was lower than that of the E-gun and the neutralizer to provide the small electric fields at both sides of the accelerating grid. It prevented electrons from passing through the accelerating grid.

4. Multimeter: It was to measure I_n which equaled the ion current I_{ion} as a result of the equivalent circuit of the MIT-MEB shown in Fig. 14.

5. Vacuum gauge:

   (a) Low: It showed the pressure measured by the Pirani vacuum gauge whose range was $10^5 \sim 10^{-1}$ Pa, which was a low vacuum condition.

   (b) High: It showed the pressure measured by the ion gauge whose range was $1 \sim 10^{-5}$ Pa, which was a high vacuum condition. It was turned on only if the pressure in the chamber was less than 6.7 Pa or the diffusion pump had been turned on for over one hour.

I label all terminals of the MIT-MEB and the instruments as shown in Fig. 28. It can help to connect the instruments and the MIT-MEB with Table 3.

doi:10.6844/NCKU202003198

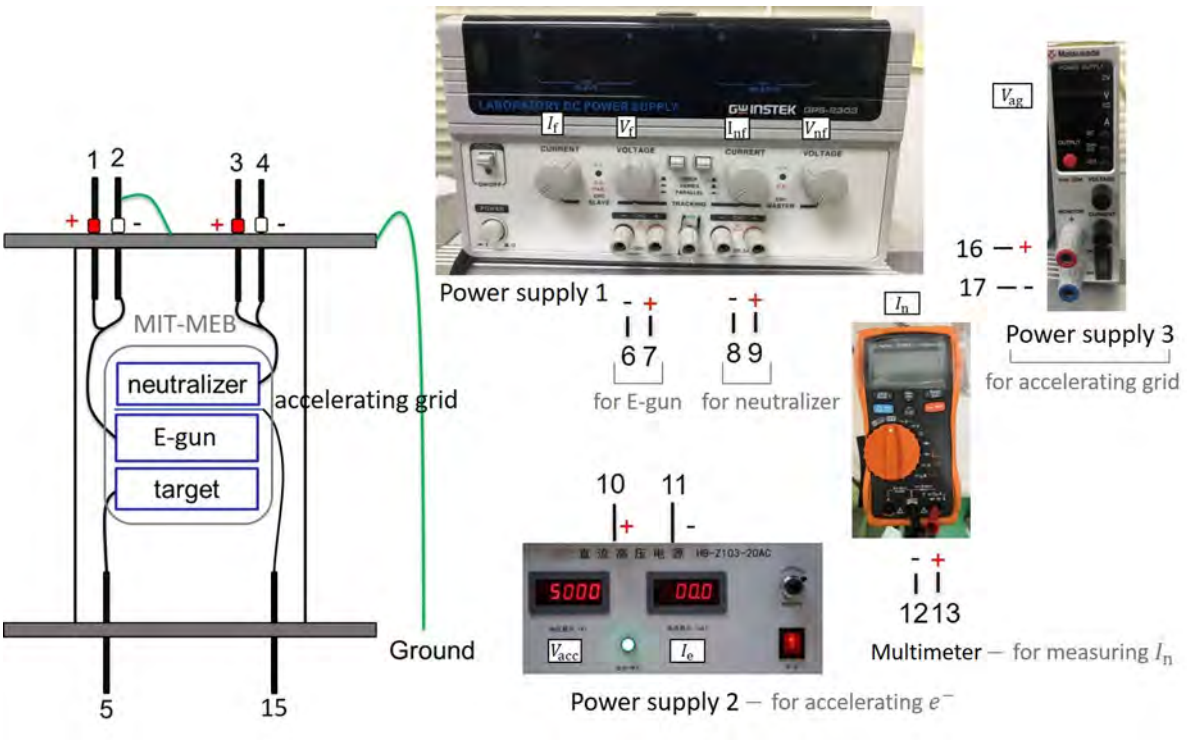

Figure 28: Numbers of the MIT-MEB and the instruments

Table 3: Numbers of the item and connect item

Item	Number	Connect Numbers
E-gun +	1	7
E-gun -	2	6, 11, 12, 16, Ground
neutralizer +	3	9
neutralizer -	4	8, 13
target	5	10
accelerating grid	15	17

2.4 SOP of experiments

1. Put the MIT-MEB without the focusing magnet into the vacuum chamber, and connect terminals of the thruster to the corresponding feedthrough shown in Table 3.

2. Pump the pressure of the vacuum chamber down to 4.5×10^{-5} torr (6.0×10^{-3} Pa).

3. Bake the MIT-MEB.

   (a) Connect E-gun and neutralize to the power supply 1 (power 1).

   Note: Refer to Fig. 28, connect 1 and 7, 2 and 6, 3 and 9, 4 and 8 by wires with alligator clips.

   (b) Set V_f, V_{nf}, I_f and I_{nf} to zero.

doi:10.6844/NCKU202003198

(c) Turn on Power supply 1 and press the "output" button.

(d) Turn V_{f} and V_{nf} to more than 4 V.

(e) Turn I_{f} and I_{nf} to 2 A to make filament glow and bake the thruster.

Note: In order to drive I_{f} and I_{nf} to the set current, V_{f} and V_{nf} need to be high enough so that the power supply is at constant-current (C.C.) mode.

(f) The pressure may increase when the MIT-MEB is being baked.

(g) Check if the pressure decreases back to the original pressure or if the MIT-MEB has been baked for two hours.

4. Turn off power supply for driving the E-gun and the neutralizer.

5. Vent the chamber.

6. Take MIT-MEB out of the chamber and measure the mass of the target immediately.

7. Put the focusing magnet in the MIT-MEB.

8. Put the MIT-MEB with the focusing magnet into the vacuum chamber. Connect all terminals of MIT-MEB to the corresponding feedthroughs.

9. Pump the pressure of the vacuum chamber down to 4.5×10^{-5} torr (6.0×10^{-3} Pa).

10. Repeat step 3 and step 4 to bake the MIT-MEB again to dry the MIT-MEB.

11. Connect all terminals of the MIT-MEB to all instruments according to Fig. 28 and Table 3.

12. Zeroing

(a) Set V_{f}, V_{nf}, I_{f} and I_{nf} to zero.

(b) Turn on Power supply 2 and adjust V_{acc} to the voltage required for the experiment.

(c) Turn on Power supply 1 and press the "output" button.

(d) Turn V_{nf} to more than 3 V.

(e) Turn I_{nf} to $2.33 \sim 2.55$ A.

(f) Turn on Power supply 3 and press the "output" button.

doi:10.6844/NCKU202003198

(g) Adjust V_{ag} until I_n becomes zero.

(h) Turn off Power supply 2 without adjusting the output voltage.

(i) Turn V_{nf} to zero.

13. Turn on Power supply 2.

14. Turn on Power supply 1 and adjust V_f to more than 3 V for driving the E-gun.

15. Adjust I_f and observe I_e until I_e reaches the set current.
    Note: I_f should not be over 3 A to prevent the filament from being broken.

16. Turn V_{nf} to 3 V.

17. Use the camera to record all data and experimental time or write down experimental time manually.

18. Turn all Power supply off.

19. Vent the chamber.

20. Take the MIT-MEB out of the chamber and measure the mass of the target immediately.

21. Calculate the averaged evaporation rate and the ionization rate using Eq. 23 and Eq. 24.

2.5 Experimental results

I did experiments with the accelerated voltage V_{acc} equal to 500, 750, and 1000 V. Different electric current I_e were used to keep the power of E-beam equal to 7.5 W. To provide different I_e, different filament current I_f was used. Therefore, I show the experimental results include I_f, power of the E-gun, I_e, power of E-beam, actual V_{acc}, and evaporation rate with different V_{acc}.

2.5.1 Actual V_{acc}

Power supply 2 might not provide stable V_{acc}. Actual V_{acc} shown in Table 4 are the averaged voltages I used in experiments. In Fig. 29, the x-axis is the set V_{acc}, and the y-axis is the ratio between actual V_{acc} and the set V_{acc}. The ratio of each V_{acc} was around 1. It means V_{acc} was well controlled.

doi:10.6844/NCKU202003198

Table 4: Actual V_{acc}

V_{acc} (V)	ActualV_{acc} (V)	ActualV_{acc}/set V_{acc}
500	505 ± 1	1.0 ± 0.0
750	753 ± 2	1.0 ± 0.0
1000	1003 ± 1	1.0 ± 0.0

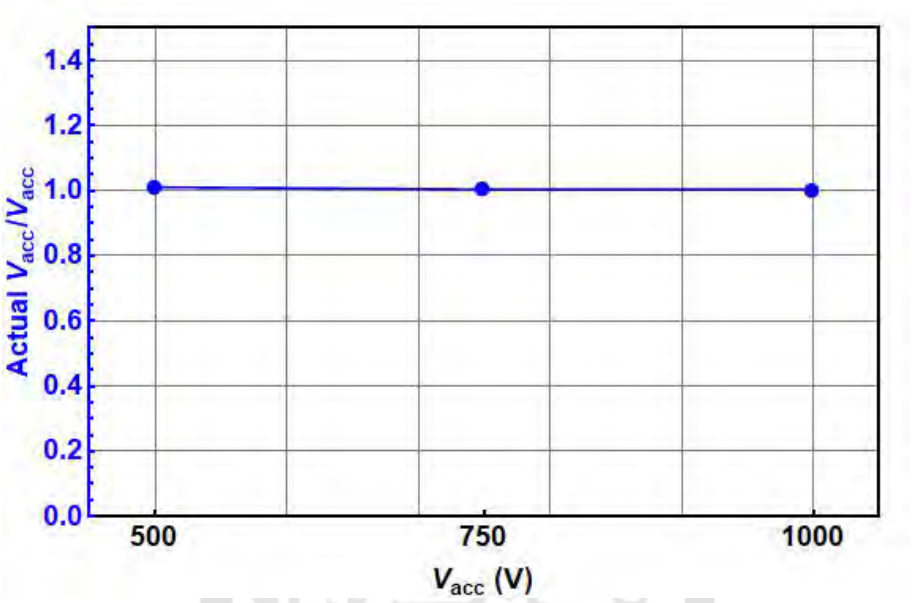

Figure 29: The ratio between actual V_{acc} and goal V_{acc}.

2.5.2 Electron currents I_e and Powers of E-beam

I would like to study how evaporation rates depend on V_{acc}. In order to keep the powers of E-beams in all experiments the same, the electron currents I_e were different with different V_{acc}. The power was kept at 7.5 W. The electron currents I_e are shown in Table 5. The corresponding powers are shown in Table 6 and Fig. 30. Therefore, I can exclude the influence of the power of the E-beam on the evaporation rate.

Table 5: I_e with different V_{acc}.

V_{acc} (V)	I_e (mA)
500	15.0 ± 0.5
750	10.0 ± 0.5
1000	7.5 ± 0.3

Table 6: Power of E-beam with different V_{acc}.

V_{acc} (V)	Power of E-beam (W)
500	7.6 ± 0.2
750	7.5 ± 0.4
1000	7.5 ± 0.3

doi:10.6844/NCKU202003198

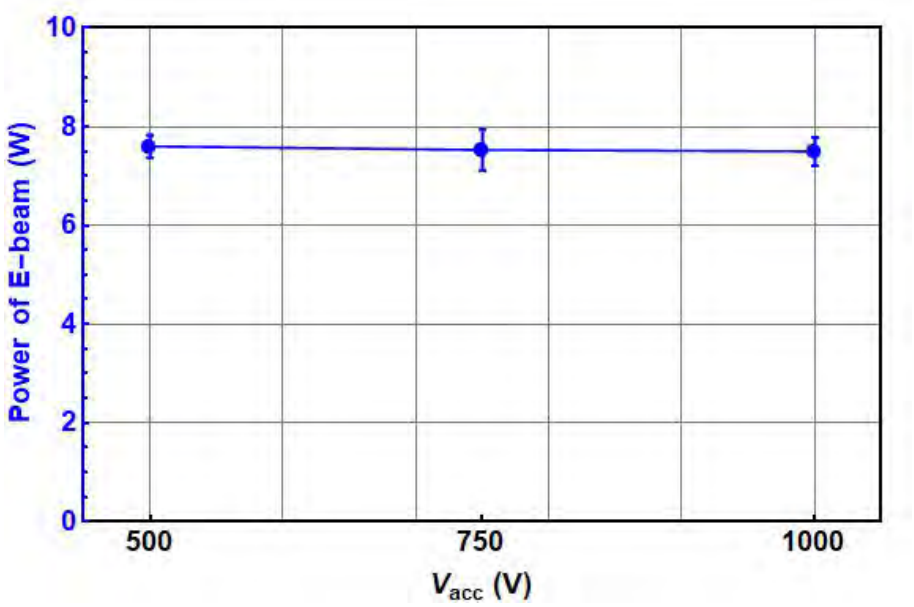

Figure 30: Power of E-beam with different V_{acc}.

2.5.3 Characteristic of the E-gun

Electrons of the electron current I_e were provided by the tungsten filament as the E-gun heated by the current I_f. Table 7 and Fig. 31 are the current I_f and the voltage V_f of the tungsten filament with different V_{acc}. The powers of the tungsten filament with different V_{acc} were calculated by the current I_f and the voltage V_f. I calculated the temperatures of the tungsten filament according to the heating powers of different V_{acc} using Eq. 9 and show them in Table 8 and Fig. 32. These temperatures influenced the thermionic electron emission. I got the emission current density J using Eq. 7 with the calculated temperatures of the tungsten filament shown in Fig. 33. When I_e and J were compared to each other and as shown in Fig. 34 and 35, I found that I_e was much smaller than the current emitted from the tungsten filament with V_{acc} equal to 500 V. It means emitted electrons may not reach the target contributing to the current I_e if the accelerating voltage V_{acc} deceased.

Table 7: I_f and V_f with different V_{acc}.

V_{acc} (V)	I_f (A)	V_f (V)
500	2.19 ± 0.05	3.6 ± 0.1
750	2.06 ± 0.02	2.8 ± 0.1
1000	1.95 ± 0.01	2.8 ± 0.1

doi:10.6844/NCKU202003198

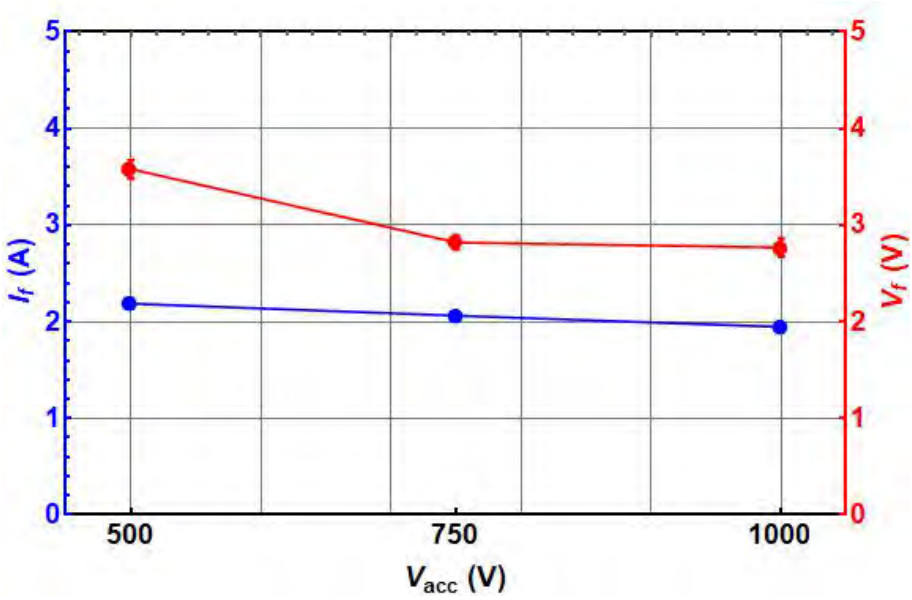

Figure 31: I_f and V_f with different V_{acc} with different V_{acc}.

Table 8: Power of E-gun nd the tungsten temperature with different V_{acc}.

V_{acc} (V)	Power of E-gun (W)	Temperature (K)
500	7.8 ± 0.3	3060 ± 30
750	5.8 ± 0.2	2840 ± 20
1000	5.4 ± 0.2	2790 ± 20

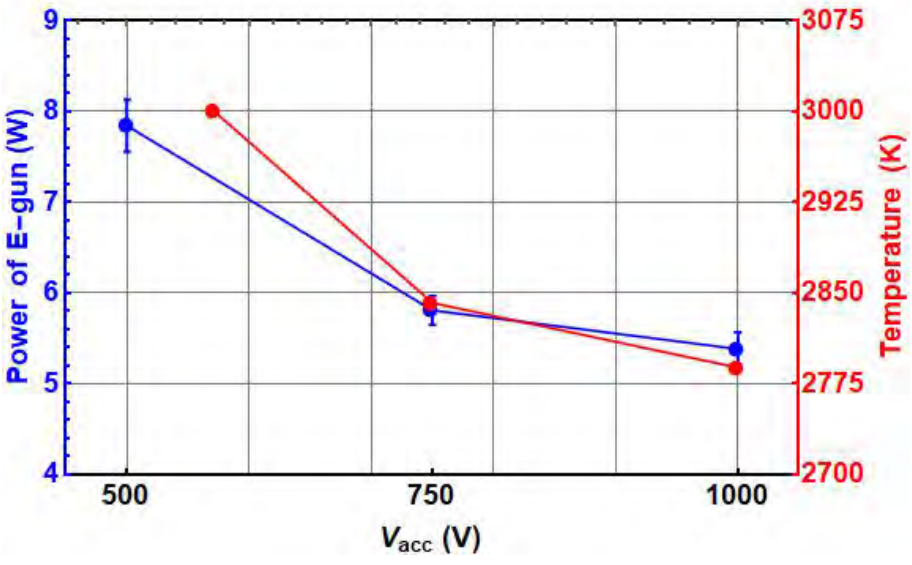

Figure 32: Power of E-gun and the tungsten temperature with different V_{acc}.

doi:10.6844/NCKU202003198

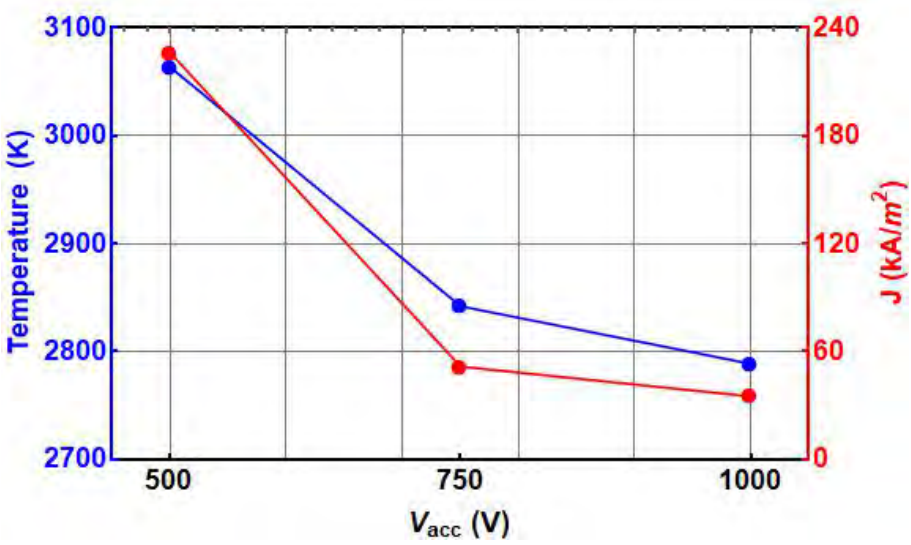

Figure 33: I_{f} and the tungsten temperature with different V_{acc}.

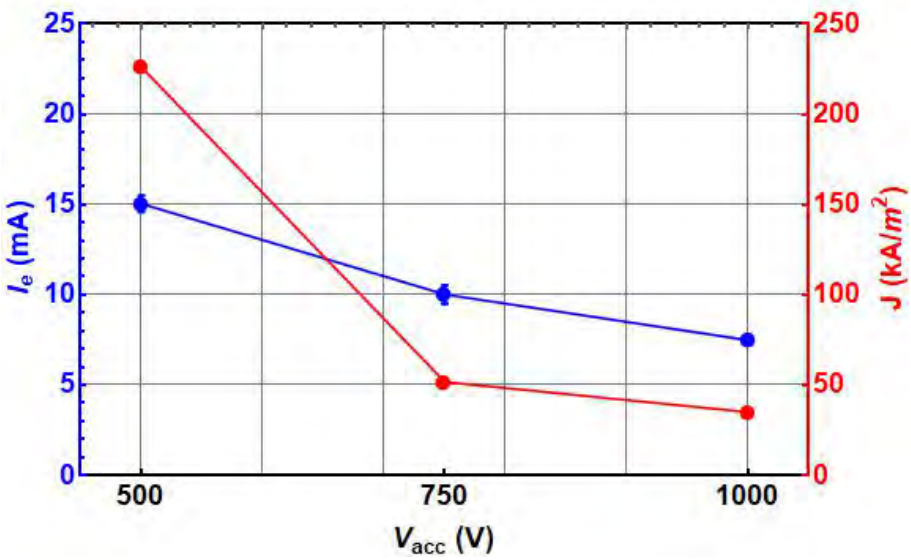

Figure 34: I_{e} and J with different V_{acc}.

doi:10.6844/NCKU202003198

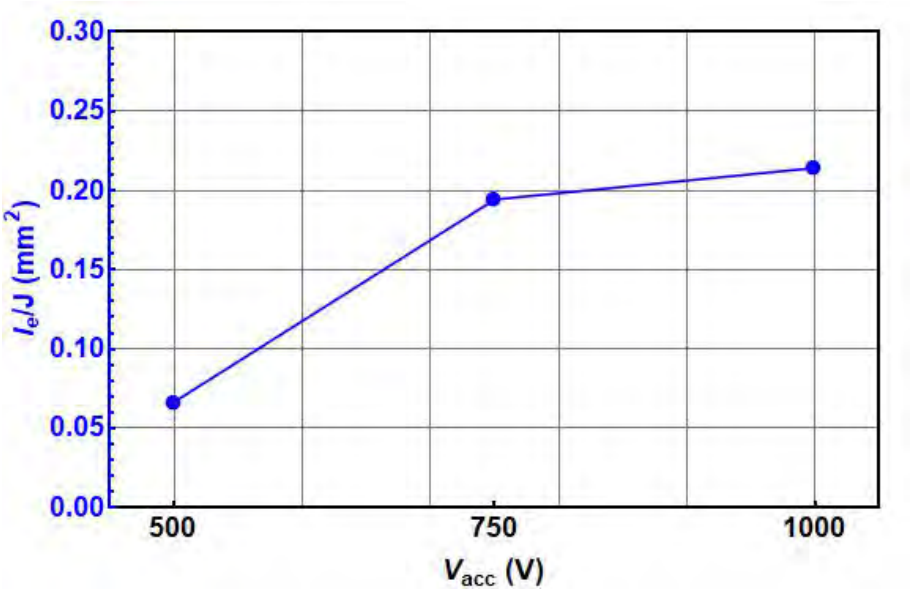

Figure 35: The ratio between I_e and J with different V_{acc}.

2.5.4 Evaporation rates

Table 9 shows evaporation rates with different V_{acc} calculated using Eq. 23. Evaporation rates in experiments with 750 V was an order higher than evaporation rates in experiments with the other two cases. However, the variation of evaporation rates in experiments with 750 V was very large. That means the position of the electron cloud in experiments with 750 V was not stable.

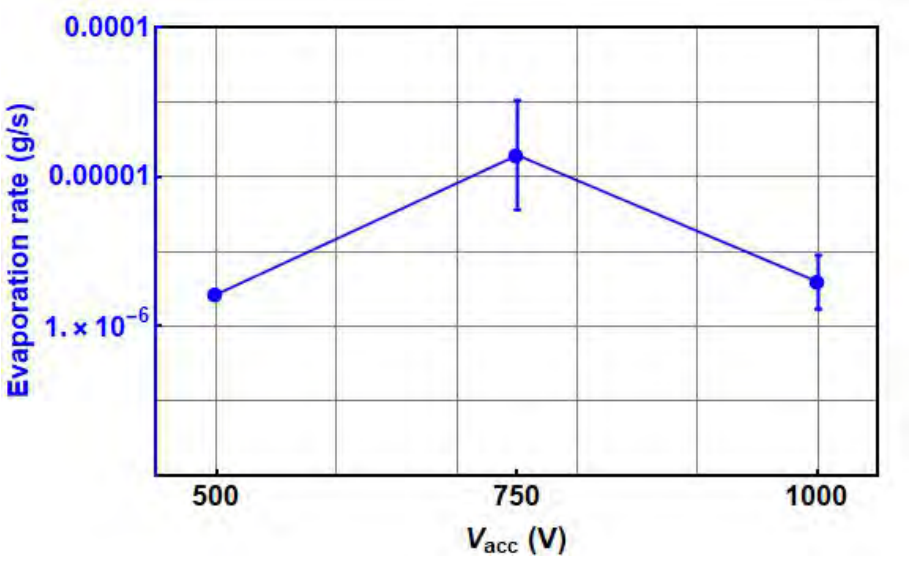

Figure 36: Evaporation rate with different V_{acc}.

doi:10.6844/NCKU202003198

Table 9: Evaporation rate with different V_{acc}.

V_{acc} (V)	$\dot{m}_{\mathrm{Metal}}$ (g/s)
500	$(1.6 \pm 0.1) \times 10^{-6}$
750	$(1.4 \pm 1.9) \times 10^{-5}$
1000	$(2.0 \pm 1.0) \times 10^{-6}$

2.6 Summary

In experimental results, the variation of evaporation rates with 750 V showed that the position of the electron cloud in experiments with 750 V was not stable. Then, I_{e} was much smaller than the current emitted from the tungsten filament if the accelerating voltage V_{acc} deceased. I suspected that emitted electrons did not reach the target contributing to the current I_{e}. The hypothesis is that force competitions between the force from the electric field and that from the magnetic field as described in section 1.4 play an important role in the MIT-MEB. Therefore, I did the simulation of the electron trajectories and show them in Chap 3 to verify the hypothesis.

doi:10.6844/NCKU202003198

3 Simulations

After I did experiments with different $V_{\rm acc}$, I found that the electric currents $I_{\rm e}$ were much smaller than the expected current emitted from the filament as the E-gun due to the thermal emission. In other words, emitted electrons may not reach the target contributing to the current $I_{\rm e}$. So, as described in section 1.4, I thought force competitions between the force from the electric field and that from the magnetic field would influence the electron trajectories. Therefore, I did the simulations on electron trajectories using COMSOL[21] to check if this hypothesis is correct or not.

We have done the following simulation to check our hypothesis:

1. $\overrightarrow{E} \times \overrightarrow{B}$ drift: it was used to verify that COMSOL could simulate electron trajectories with the electric field and the magnetic field.
2. Simplified Model: it was used to simplify the electric field and the magnetic field to axial symmetric.
3. The electric field and the magnetic field : they were simulated first without electrons.
4. Electron trajectories with the electric field only: to check if electrons were accelerated by the electric field.
5. Electron trajectories with the magnetic field only: to check if electrons had the gyro motion in the magnetic field and were reflected by the magnetic mirror force.
6. Electron trajectories with the electric field and the magnetic field.
   (a) Electron trajectories with the electric field and the magnetic field with different initial pitch angles: to check if some electrons accelerated by the electric field were in the loss cone while some electrons were still outside the loss cone.
   (b) Electron trajectories with the electric field and the magnetic field with different $V_{\rm acc}$: to find the best $V_{\rm acc}$ which can support the hypothesis of the force competitions.

doi:10.6844/NCKU202003198

3.1 $\overrightarrow{E} \times \overrightarrow{B}$ drift

I need to check whether the electron trajectories with the electric field and the magnetic field simulated using COMSOL is correct or not. Therefore, we simulated the $\overrightarrow{E} \times \overrightarrow{B}$ drift and compared it with the analytical solution. When the charged particle moves in the uniform electric field and an uniform magnetic field which are not parallel to each other, the particle drifts across the magnetic field lines. The electron gyro around a guiding center while the guiding center drifts in the direction perpendicular to the electric field and the magnetic field. This drift is called $\overrightarrow{E} \times \overrightarrow{B}$ drift. The $\overrightarrow{E} \times \overrightarrow{B}$ drift is a simple case to check if we can simulate the charged particle trajectory using COMSOL.

First, I set the model as shown in Fig. 37. Second, I set the uniform electric field $\overrightarrow{E} = 1$ V/m in $\hat{x}$ and the uniform magnetic field $\overrightarrow{B} = 1$ T in $\hat{z}$. Third, I put a charged particle whose mass was 1 kg and charge was -1 coul at the origin. Fourth, the total simulation time I set was 4 seconds. The number of steps was 4001. The charged-particle trajectory is shown in Fig. 38. The guiding center of the gyromotion drifts in $-\hat{y}$. The drift velocity of the guiding center $V_{\rm gc}$ in theory[20] is

$$\overrightarrow{V}_{\rm gc,th} = \frac{\overrightarrow{E} \times \overrightarrow{B}}{B^2} = -1\,({\rm m/s})\hat{y} \tag{27}$$

where B is the amplitude of $\overrightarrow{B}$.

I picked the drift distance L of the guiding center during the time different $\triangle t$ shown in Fig. 39 to calculate the drift velocity of the guiding center in simulation:

$$V_{\rm gc,sim} = \frac{L}{\triangle t} = \frac{-2.00 - (-0.42)\,({\rm m})}{1.57\,({\rm s})} = \frac{-1.576\,({\rm m})}{1.57\,({\rm s})} = -1.003\,({\rm m/s})\,. \tag{28}$$

The difference between the analytical solution and the simulation result is less than 1 %. We can simulate the electron trajectories using COMSOL.

doi:10.6844/NCKU202003198

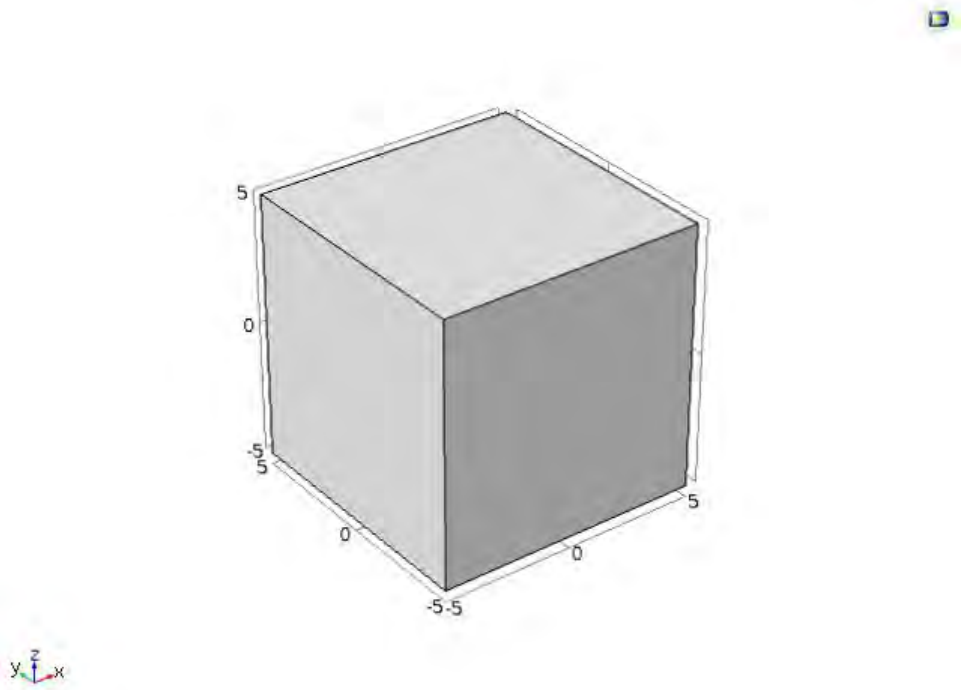

Figure 37: The cube model.

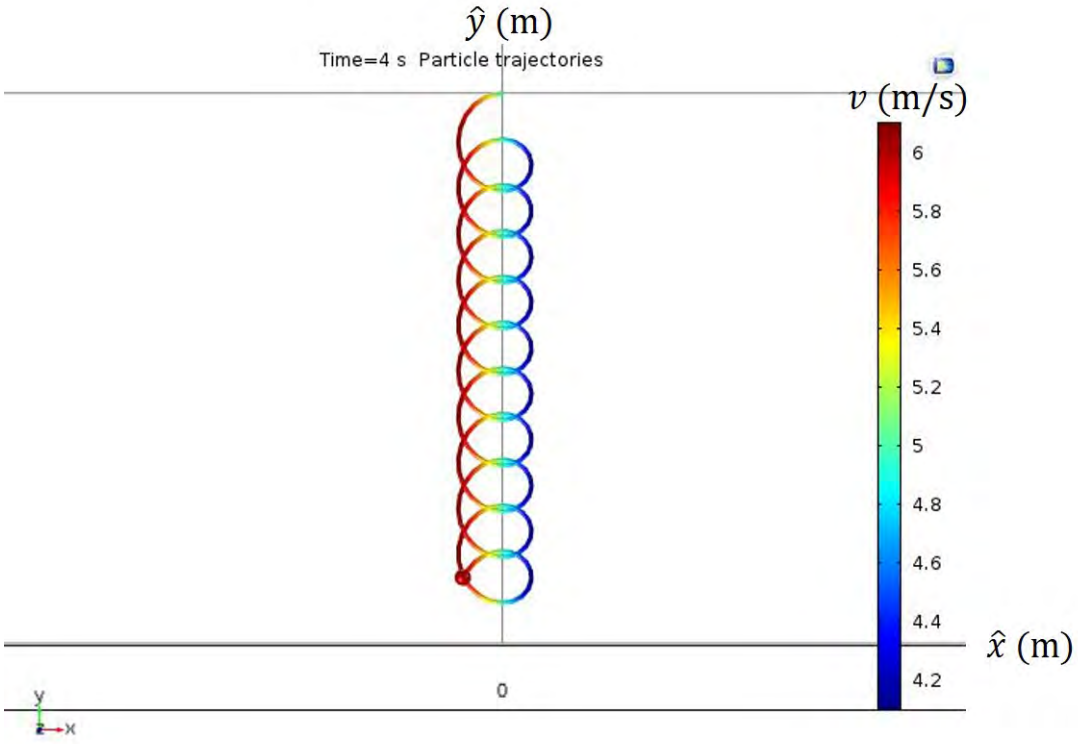

Figure 38: The $\overrightarrow{E} \times \overrightarrow{B}$ drift of the charged particle.

doi:10.6844/NCKU202003198

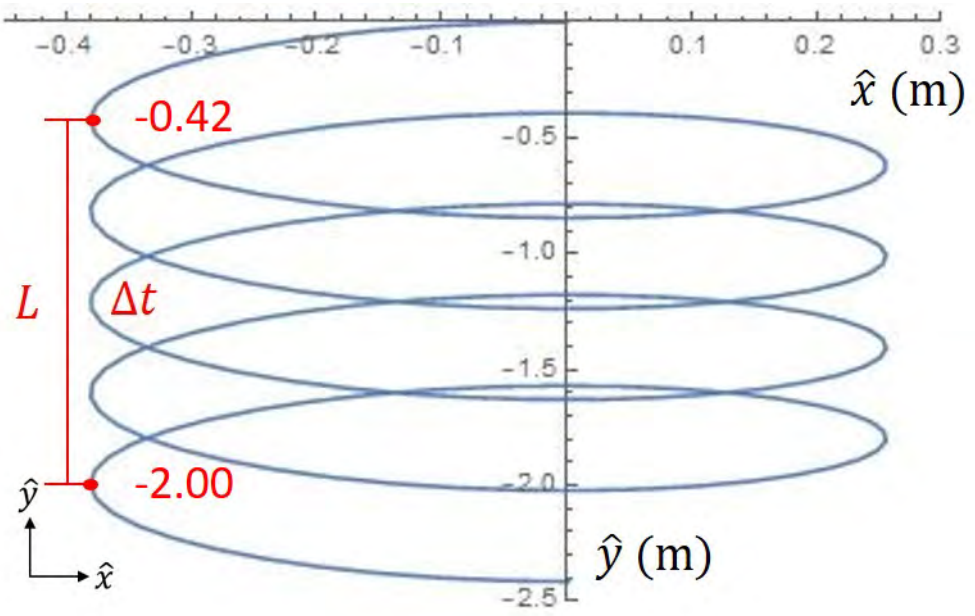

Figure 39: The drift distance of the guiding center.

3.2 Simplified Model

Shown in Fig. 40 is the simplified model of MIT-MEB in simulation. The filament of the E-gun is replaced by a disc filament whose radius is the same as the length of the filament. In this case, the electric field and the magnetic field are simplified to axial symmetric. However, electron trajectories are simulated in 3D.

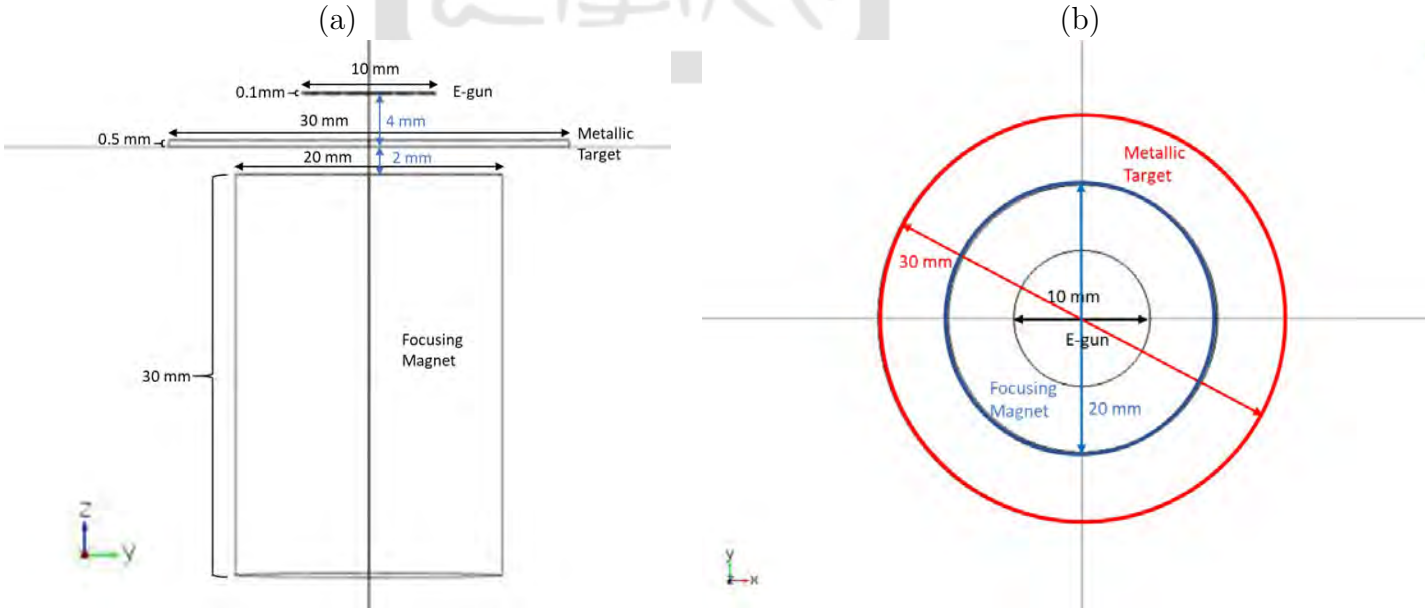

Figure 40: The Simplified Model of MIT-MEB (a) in y-z plan, and (b) in x-y plan.

doi:10.6844/NCKU202003198

3.3 The electric field and the magnetic field

Shown in Fig. 41–43 is the electric potential and the electric field lines in y-z plane with V_{acc} equal to 500 V, 750 V and 1000 V, respectively. Shown in Fig. 44–46 is the electric field and the electric field lines in y-z plane with V_{acc} equal to 500 V, 750 V and 1000 V, respectively. I set the filament at ground and the target at V_{acc}. The electric fields around the center of the filament are uniform. Therefore, I can use this region to check if the electron trajectory with only the electric field is correct or not.

Shown in Fig. 47 is the magnetic flux density and the magnetic field lines in y-z plane. I use 1050,000 [A/m] for the magnetization of the magnet according to Kuo-Yi's thesis[8]. The magnetic field line at the center of the filament is a straight line. Therefore, I can use this field line to check if the electron trajectory with the magnetic field in this simulation is correct or not.

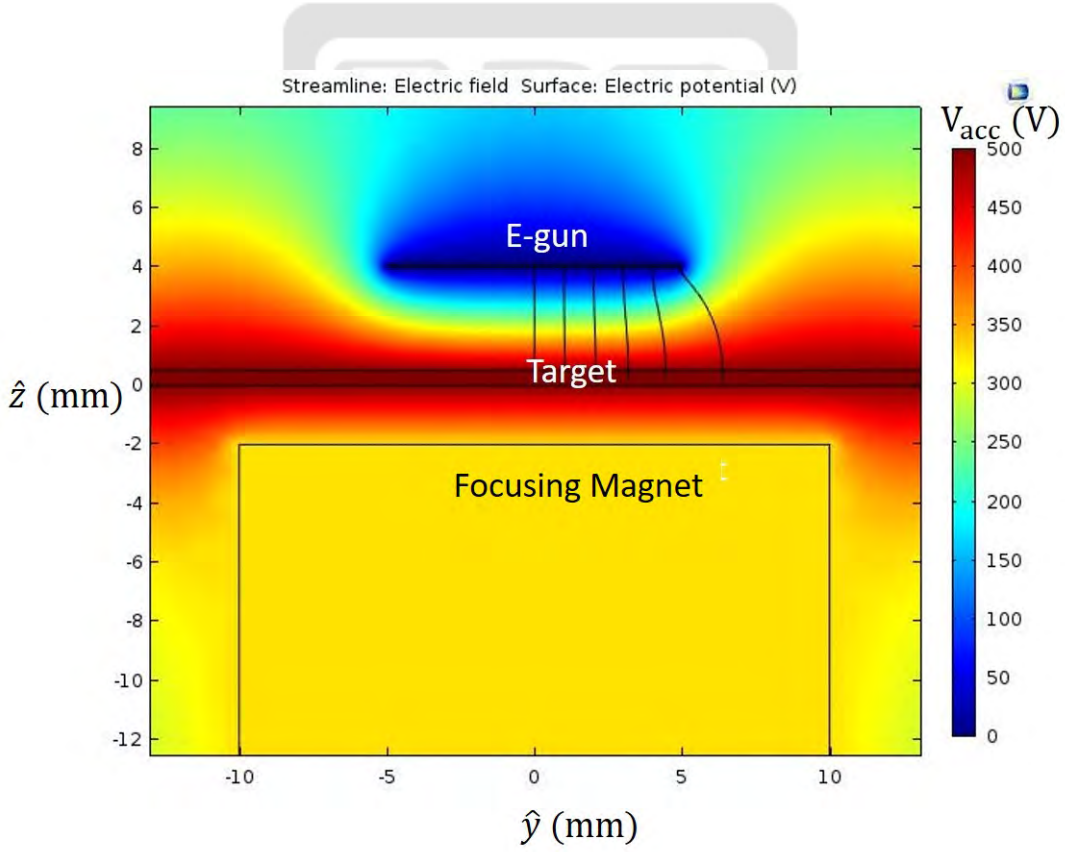

Figure 41: The electric potential and the electric field lines with V_{acc} which is equal 500 V.

doi:10.6844/NCKU202003198

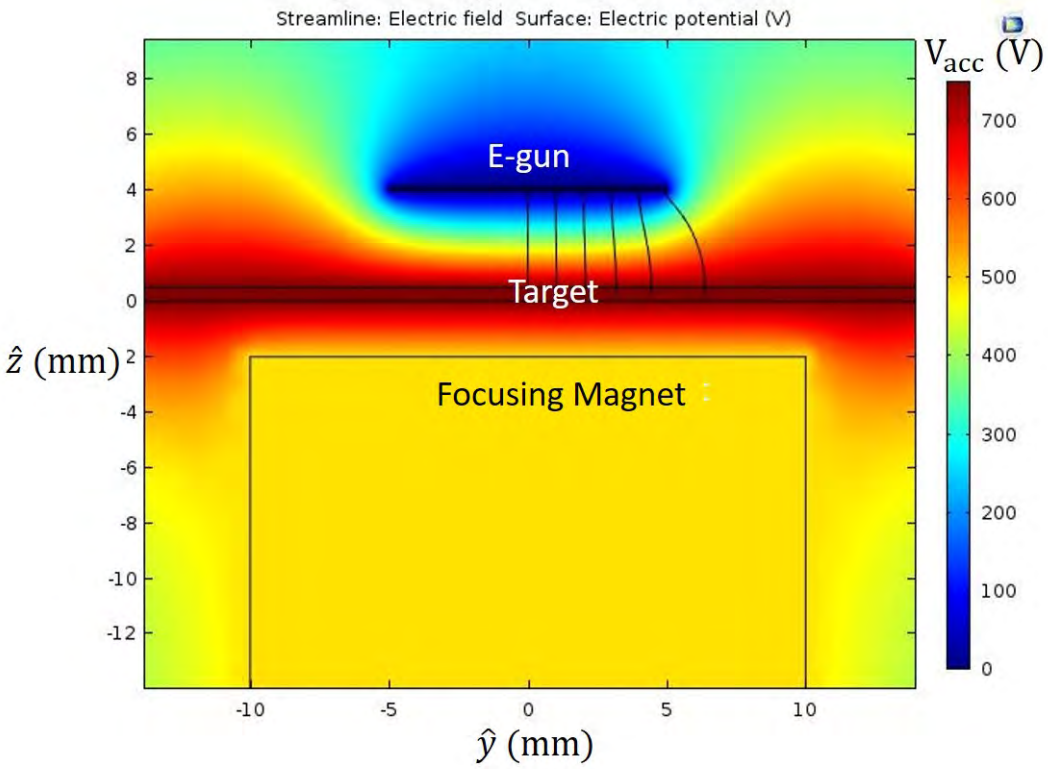

Figure 42: The electric potential and the electric field lines with V_{acc} which is equal 750 V.

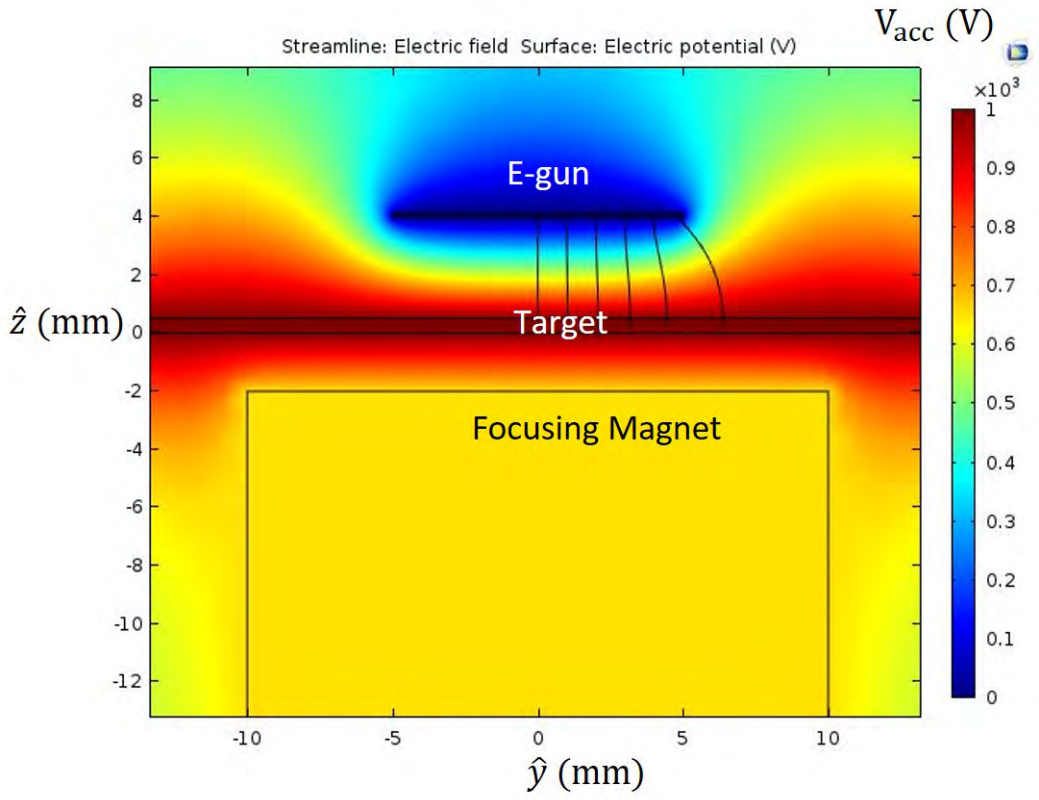

Figure 43: The electric potential and the electric field lines with V_{acc} which is equal 1000 V.

doi:10.6844/NCKU202003198

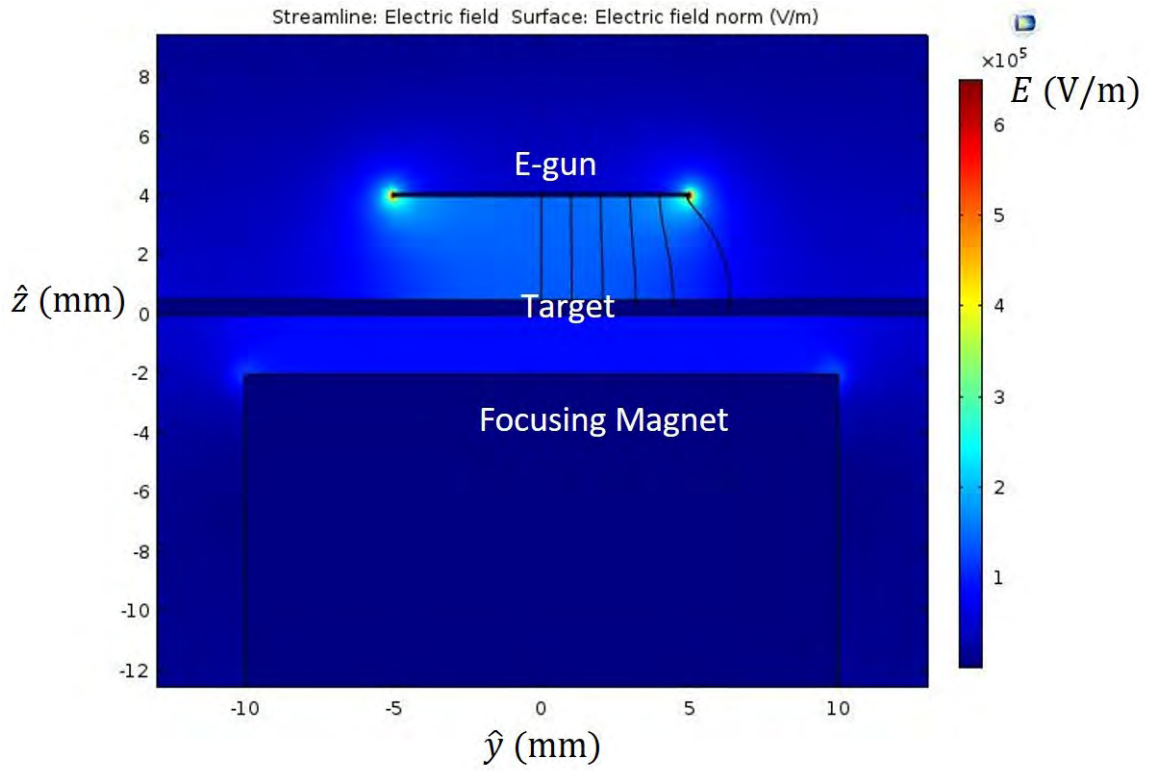

Figure 44: The electric field and the electric field lines with V_{acc} which is equal 500 V.

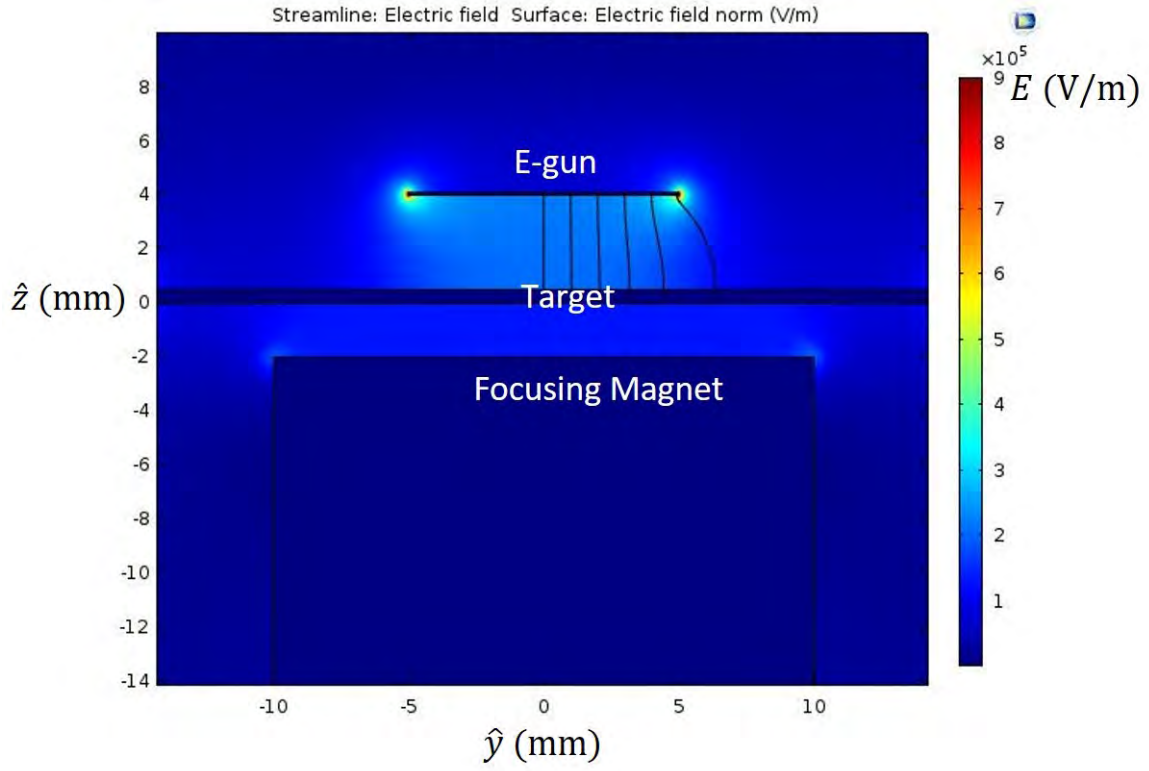

Figure 45: The electric field and the electric field lines with V_{acc} which is equal 750 V.

doi:10.6844/NCKU202003198

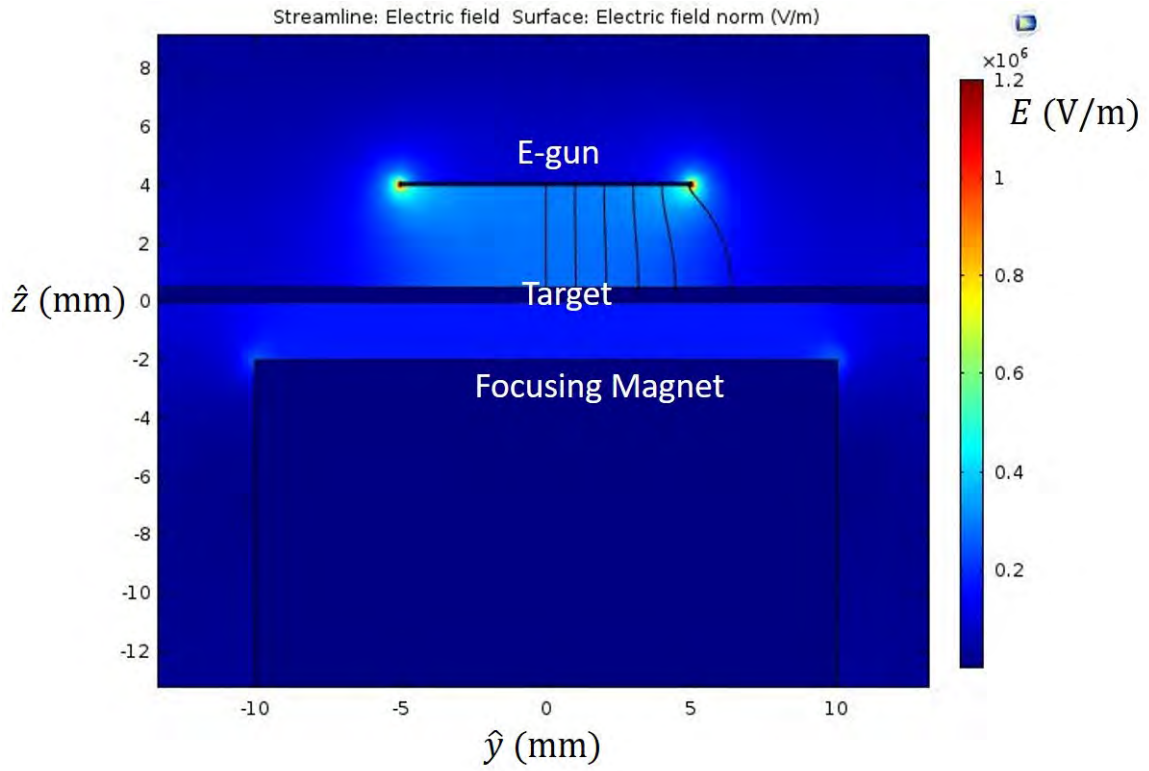

Figure 46: The electric field and the electric field lines with V_{acc} which is equal 1000 V.

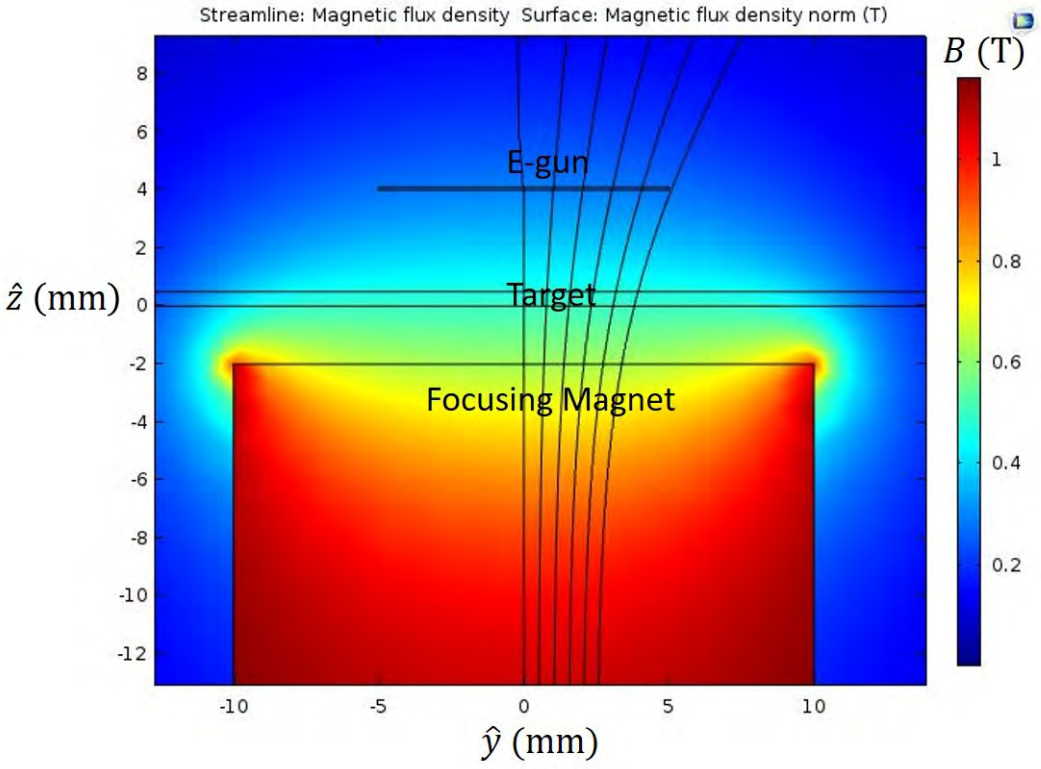

Figure 47: The magnetic flux density and the magnetic field.

doi:10.6844/NCKU202003198

3.4 Electron trajectories with the electric field

Shown in Fig. 48–50 are the electron trajectories in y-z plane with the electric field of V_{acc} equal to 500 V, 750 V and 1000 V, respectively.

Points in figures are locations of electrons at the end of each simulation. All electrons were from the same initial positions with an initial velocity equal to zero. The initial positions in x-z plane were $0\hat{x} + 3.8\hat{z}$. The initial positions in $\hat{y}$ were from 0 to 5 after each interval of 1 mm. The total simulated time was 5×10^{-10} seconds with 1001 steps. Electrons without a magnetic field moved along electric field lines. However, the electron from the edge of the filament was accelerated too fast such that the trajectory was not totally aligned with electric field lines. The electron acceleration from the electric field is smaller when V_{acc} is lower. As a result, the electrons accelerated by 500 V are futher away from the focusing magnet than the electrons accelerated by 1000 V at the end of the simulations.

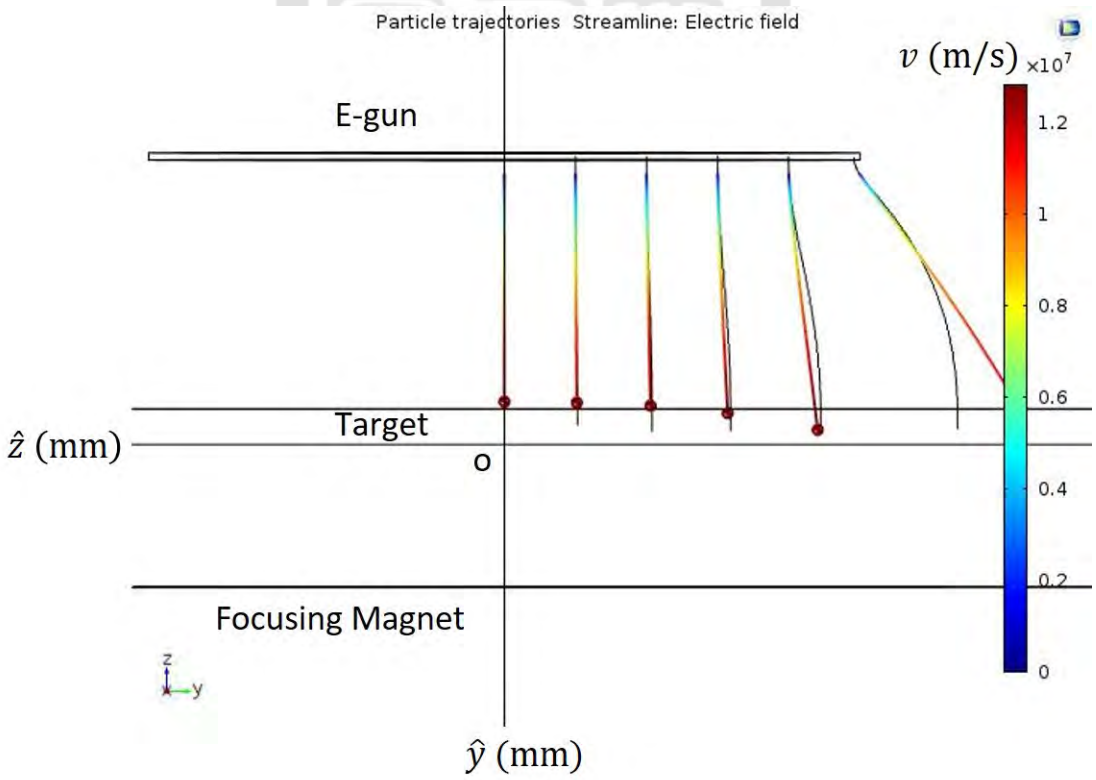

Figure 48: The electron trajectories with the electric field in V_{acc} which is equal 500 V.

doi:10.6844/NCKU202003198

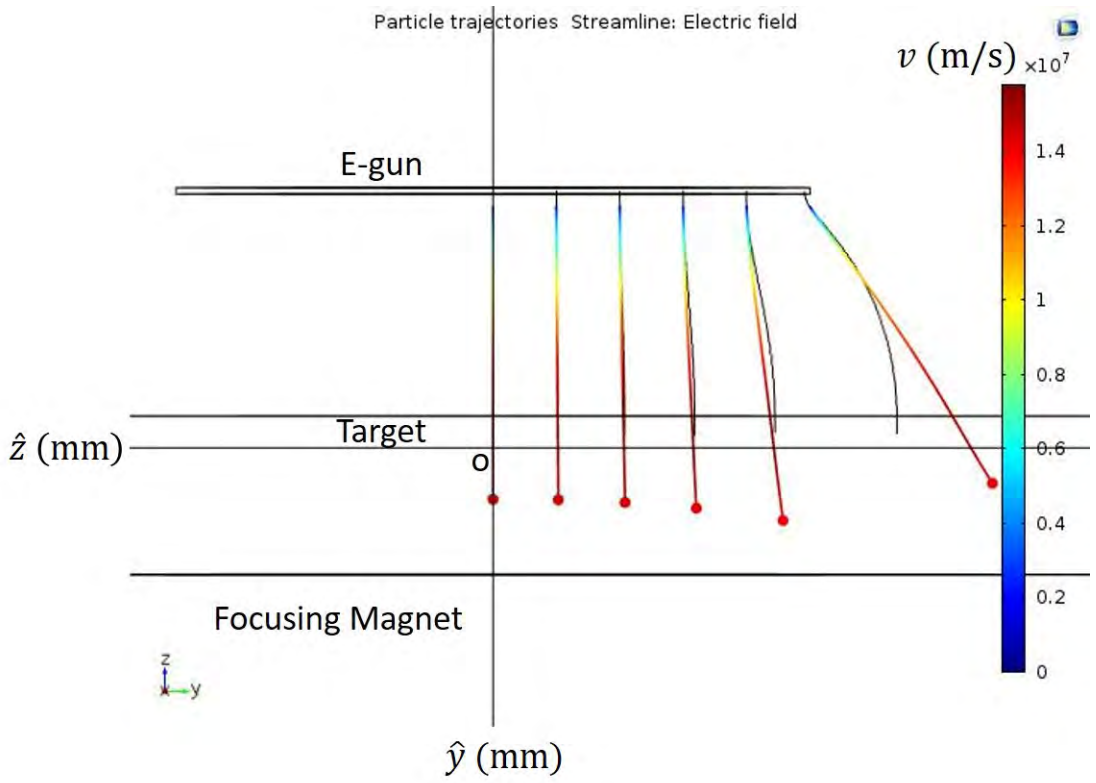

Figure 49: The electron trajectories with the electric field in V_{acc} which is equal 750 V.

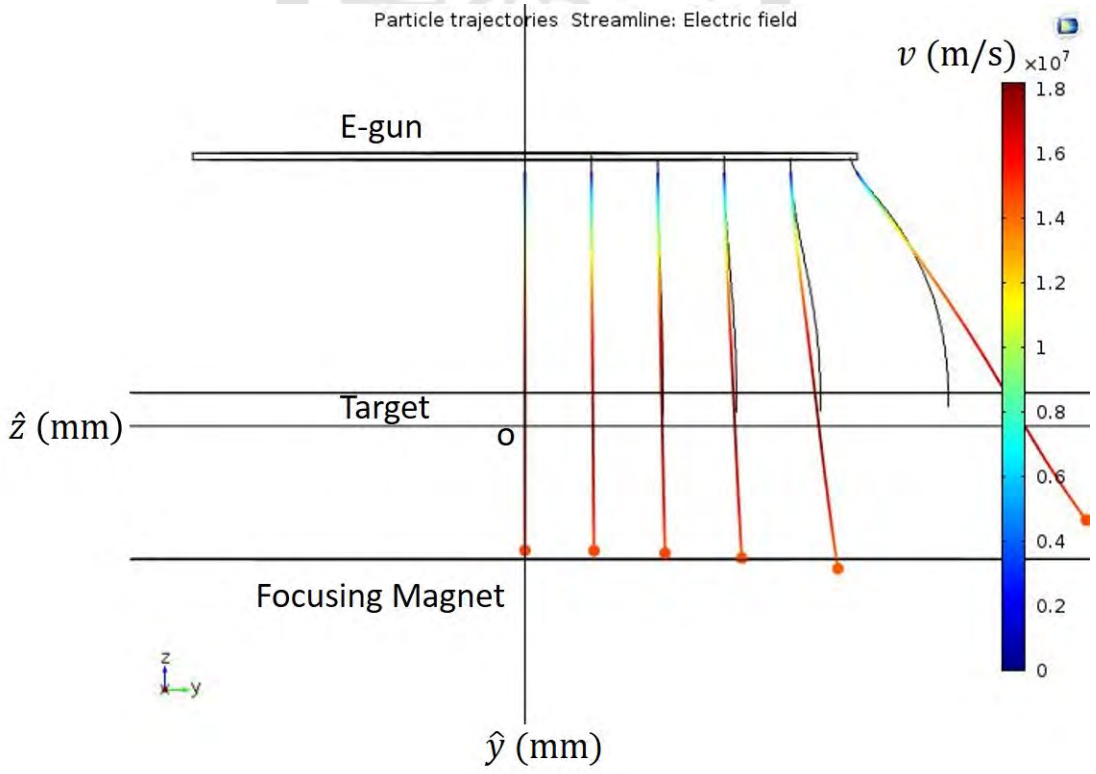

Figure 50: The electron trajectories with the electric field in V_{acc} which is equal 1000 V.

I chose the electron at the center of the filament to check if the simulated electron trajectory with the electric field was correct or not. Table 10 shows the displacements of electrons at

doi:10.6844/NCKU202003198

the center from the analytic calculations and from simulations in different $V_{\rm acc}$. D is the displacement from the simulation, and S is the displacement from the analytic calculation. S is calculated using Eq. 29 and 30.

$$F = m_{\rm e}a = qE \approx q\frac{V_{\rm acc}}{d}, \tag{29}$$

$$S = \frac{1}{2}at^2 = \frac{1}{2}\frac{qV_{\rm vacc}}{m_{\rm e}d}t^2 \tag{30}$$

where F is the electric force, $m_{\rm e}$ is the mass of the electron equal to 9.1×10^{-31} kg, a is the acceleration of the electron by the electric field E, and d is the distance between the filament and the target equal to 3.5 mm.

Differences between D and S are 2 %. It means that the electron trajectory with the electric field in simulation is promising.

Table 10: The displacement of simulation and the calculation in different $V_{\rm acc}$.

$V_{\rm acc}$ (V)	time (s)	D (mm)	S (mm)	S/D
500	5.00×10^{-10}	3.20	3.14	0.98
750	4.10×10^{-10}	3.22	3.17	0.98
1000	3.55×10^{-10}	3.22	3.17	0.98

3.5 Electron trajectories with the magnetic field

I set the value of initial velocity as the thermal velocity calculated by Eq. 8 and 9. The value of initial velocity is about 3×10^{-5} m/s. The magnetic field in MIT-MEB was not uniform. Electrons might be trapped by the magnetic-mirror effect. The angle of the loss cone in MIT-MEB supposed to be

$$\sin^2\theta = \frac{B_0}{B'} = \frac{0.3(\mathrm{T})}{0.45(\mathrm{T})} = \frac{2}{3} \Rightarrow \theta = 54.7^{\rm o} \tag{31}$$

where B_0 is the magnetic field at the center of the disc filament and B' is the magnetic field above the center of the target. Then, I built Table 11 which shows initial angles and their corresponding initial velocities whose value is around 3.00×10^5 m/s. $v_{\rm y}$ is the initial velocity in $\hat{y}$ and v_z is the initial velocity in $\hat{z}$. I can follow this table to set the initial velocities in simulations.

doi:10.6844/NCKU202003198

Table 11: The initial angle and the initial velocity.

The initial angle	v_y (m/s)	v_z (m/s)
54.8°	2.45×10^5	-1.73×10^5
56.4°	2.50×10^5	-1.66×10^5
60.0°	2.60×10^5	-1.50×10^5
70.0°	2.82×10^5	-1.03×10^5
80.0°	2.95×10^5	-0.52×10^5
90.0°	3.00×10^5	0.00×10^5

To show that electrons not in loss cone will be reflected by the magnetic-mirror froce, I did simulations of electron trajectories where the pitch angles of the initial velocity relative to the magnetic field line larger the angle of the loss cone. The total simulated time was 4×10^{-8} seconds with 40001 steps. Shown in Fig. 51 and Fig. 52 are the electron trajectories with the magnetic field in y-z plane with the initial angles equal to 54.8° and 56.4°, respectively. The points in the figures are the locations where the electrons at the end of the simulation. In both cases, we can see electrons are reflected back up due to the magnetic mirror effect. To show that electrons do gyro motion around magnetic field lines, I chose the electron from the center of the filament in both cases. Shown in Fig. 53 and Fig. 54 are electron trajectories with the magnetic field in x-y plane with initial angles equal to 54.8° and 56.4°, respectively. The trajectories are looked like a lot of circles. It means converged. Then, I can also check that electrons have gyro motions in simulations in the x-y plane when they have the initial velocity perpendicular to the magnetic field at the center of the filament.

doi:10.6844/NCKU202003198

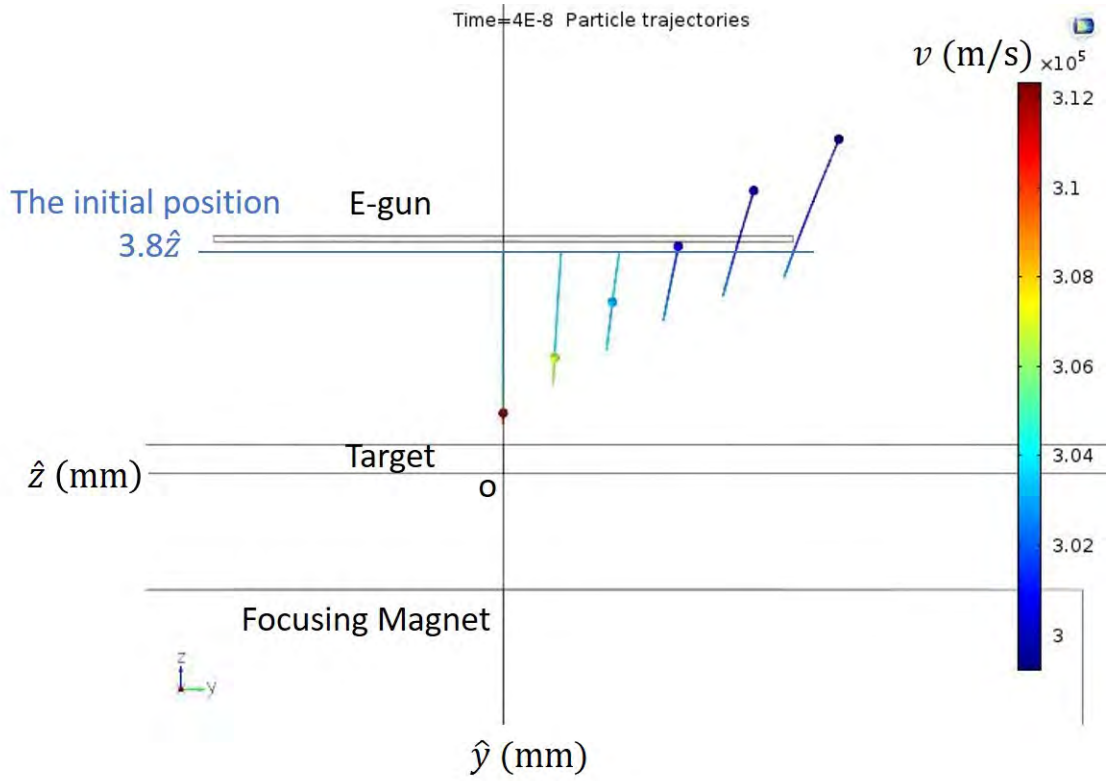

Figure 51: The electron trajectory with the magnetic field and the initial angle equal to 54.8° in the y-z plane.

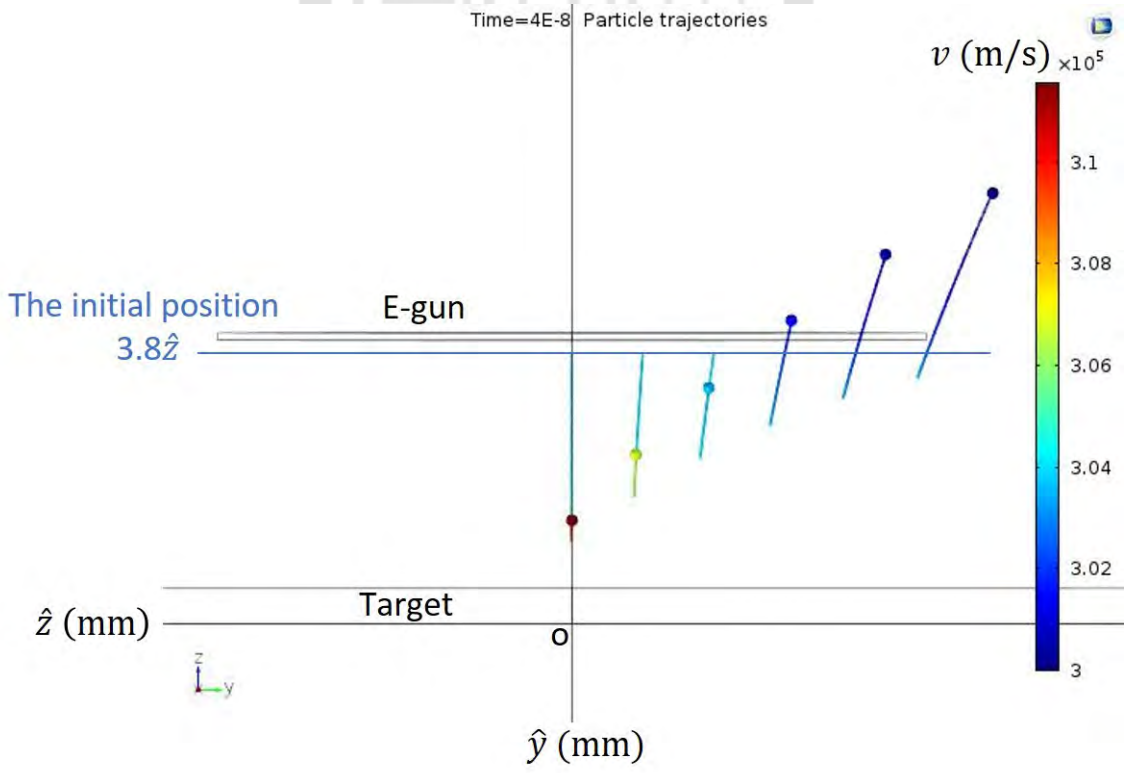

Figure 52: The electron trajectory with the magnetic field and the initial angle equal to 56.4° in the y-z plane.

doi:10.6844/NCKU202003198

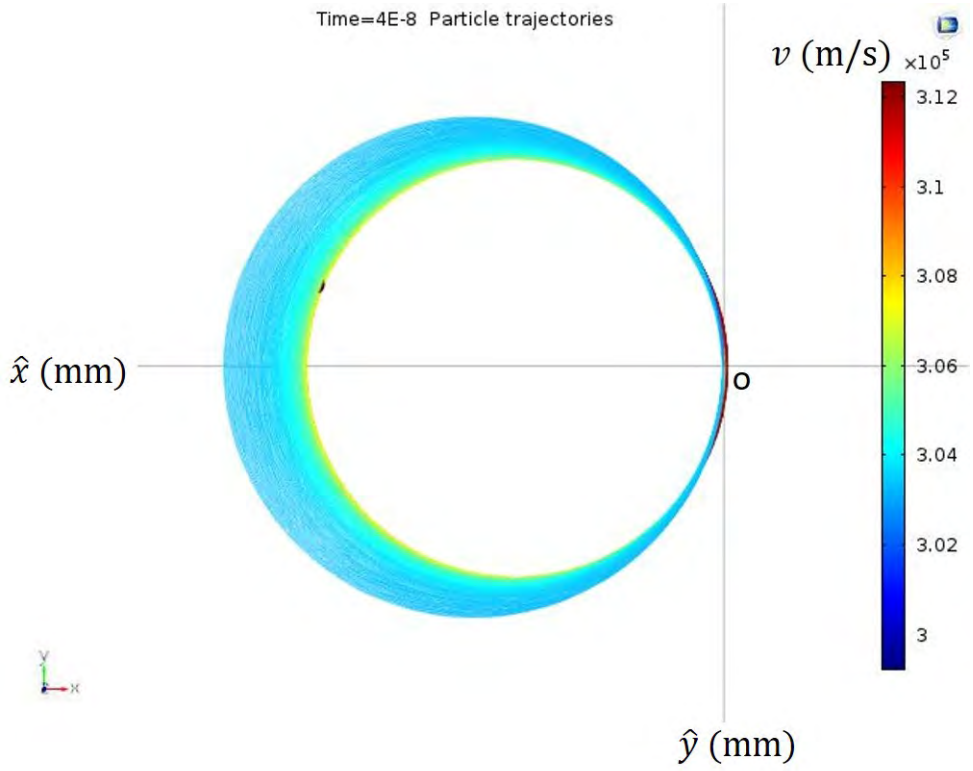

Figure 53: The electron trajectory with the magnetic field and the initial angle equal to 54.8° in the x-y plane.

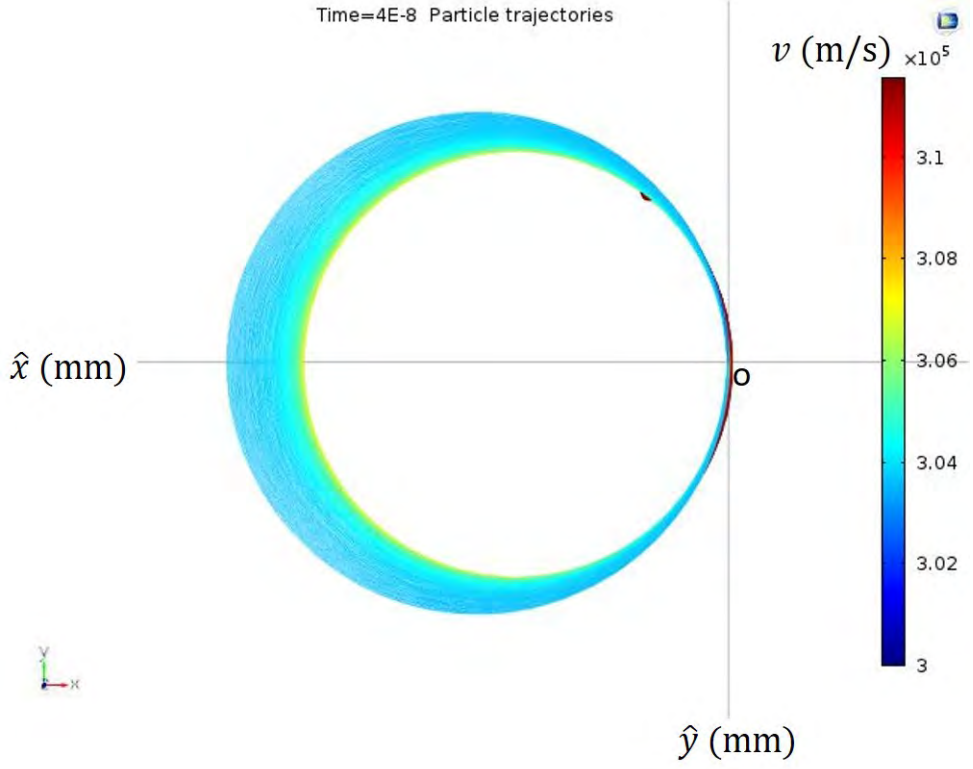

Figure 54: The electron trajectory with the magnetic field and the initial angle equal to 56.4° in the x-y plane.

To show that electrons do gyro motions around magnetic field lines, I chose the electron

doi:10.6844/NCKU202003198

from the center of the filament in the case with the initial angle equal to 56.4°. Top view of the simulated trajectry is shown in Fig. 55. We found the radius of the circle, which was the gyrodadius of the first circle. The gyroradius of the fitting was 4.73×10^{-3} mm. The gyroradius of the calculation was 4.74×10^{-3} using the Eq.

$$r = \frac{m_e v_\perp}{|q| B_0} \tag{32}$$

where $v_\perp$ is 2.5×10^5 m/s. The difference between the simulated radius and the calculated radius was less than 0.5 %. The gyroradius from the fitting and the calculation were similar. Therefore, the simulated electron trajectory with the magnetic field was correct.

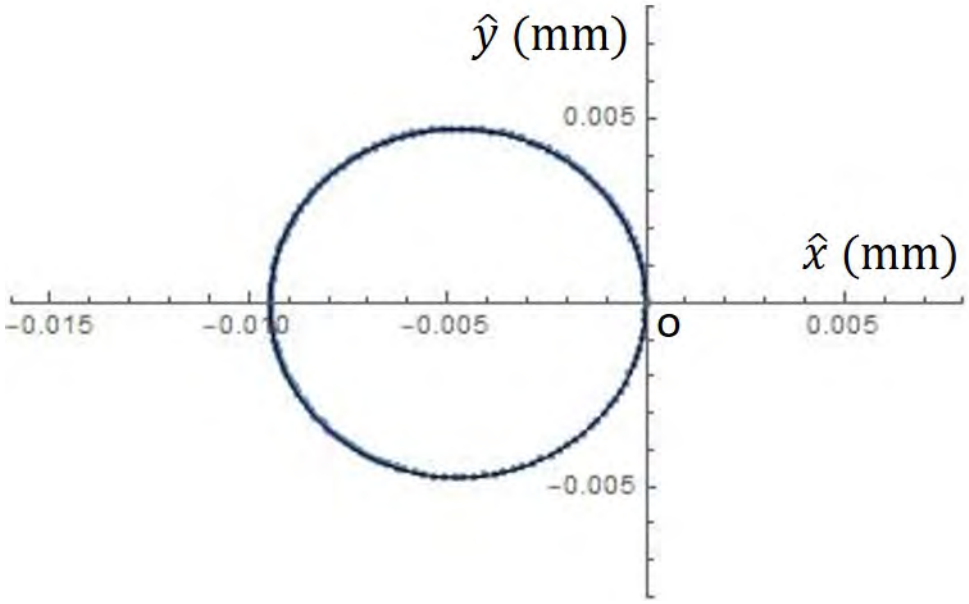

Figure 55: The fitting of the gyroradius.

To show that the electrons are not reflected in the loss cone. I did the simulation with the magnetic field and initial velocities of all electrons equal to -3×10^5 m/s $\hat{z}$ as shown in Fig. 56. Electrons were magnetized so that they follow magnetic field lines and pass through the target.

doi:10.6844/NCKU202003198

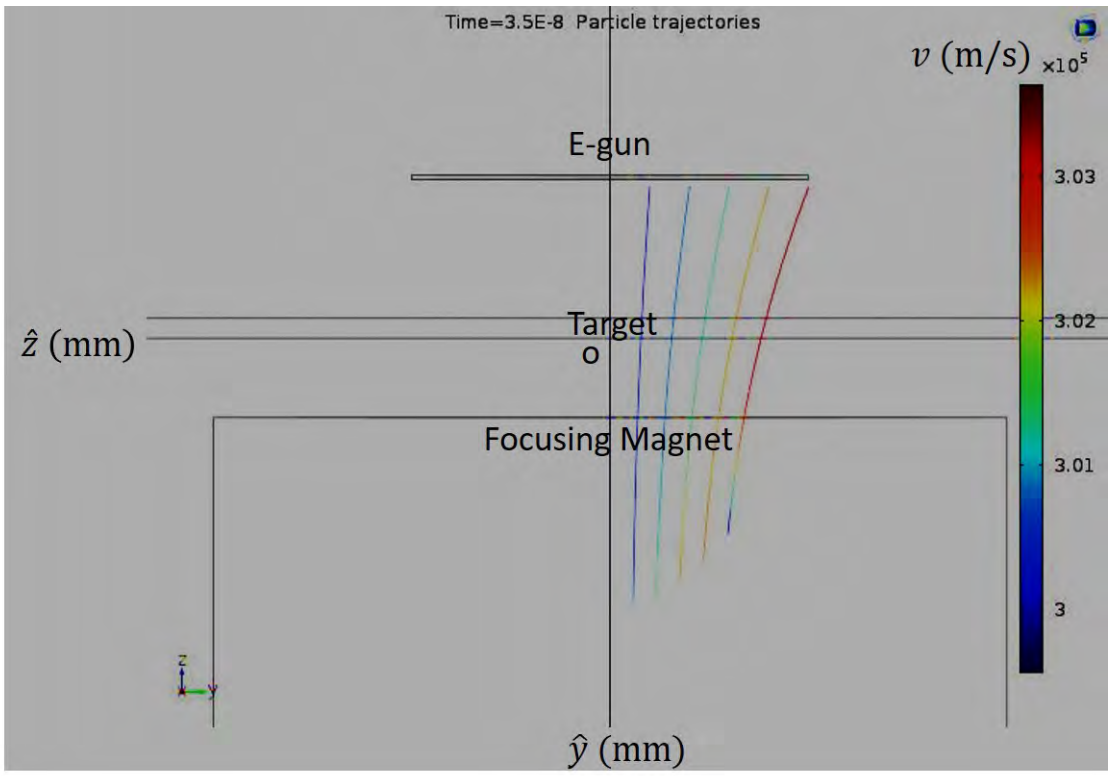

Figure 56: The electron trajectory with the magnetic field and the initial velocity at z-axis.

In summary, for electrons in loss cone as shown in Fig. 56, they penetrate through the mirror point and reach the target. They follow magnetic field lines and collide the center of the target. Contrary, electrons in loss cone as shown in 51 and 52, they were reflected by the magnetic mirror effect.

3.6 Electron trajectories in electric fields and magnetic fields

I did experiments with V_{acc} equal to 500 V, 750 V and 1000 V. In the case where V_{acc} equal to 500 V, the electric force was the smallest. Therefore, I chose this case to simulate the electron trajectory in the electric field and the magnetic field with electrons with different initial pitch angles relative to the magnetic field lines. Shown in Fig. 57–61 are the electron trajectories in the y-z plane with the initial angle equal to 54.8°, 60.0°, 70.0°, 80.0° and 90.0°, respectively. The corresponding initial velocities are shown in Table 11. The total simulated time was 6×10^{-10} with 601 steps. I found that electrons in all cases were magnetized so that they followed magnetic field lines. However, they were not returned and reached the target in all case. It means the electric force in V_{acc} equal to 500 V was large enough such that all electrons were accelerated downward and were in the loss cone. For example, in the case where

doi:10.6844/NCKU202003198

the initial pitch angle was 54.8°, electrons were reflected as shown in Fig. 51. However, with electric fields, electrons were not reflected.

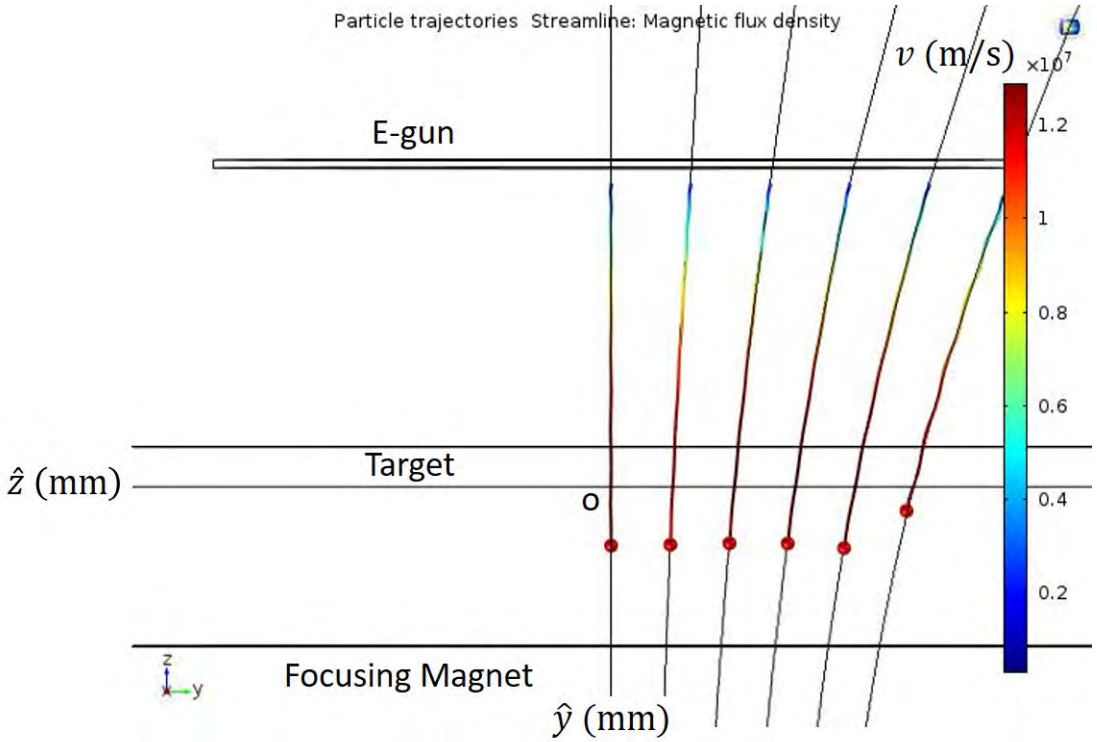

Figure 57: The electron trajectories with the initial angle equal to 54.8° in the y-z plane.

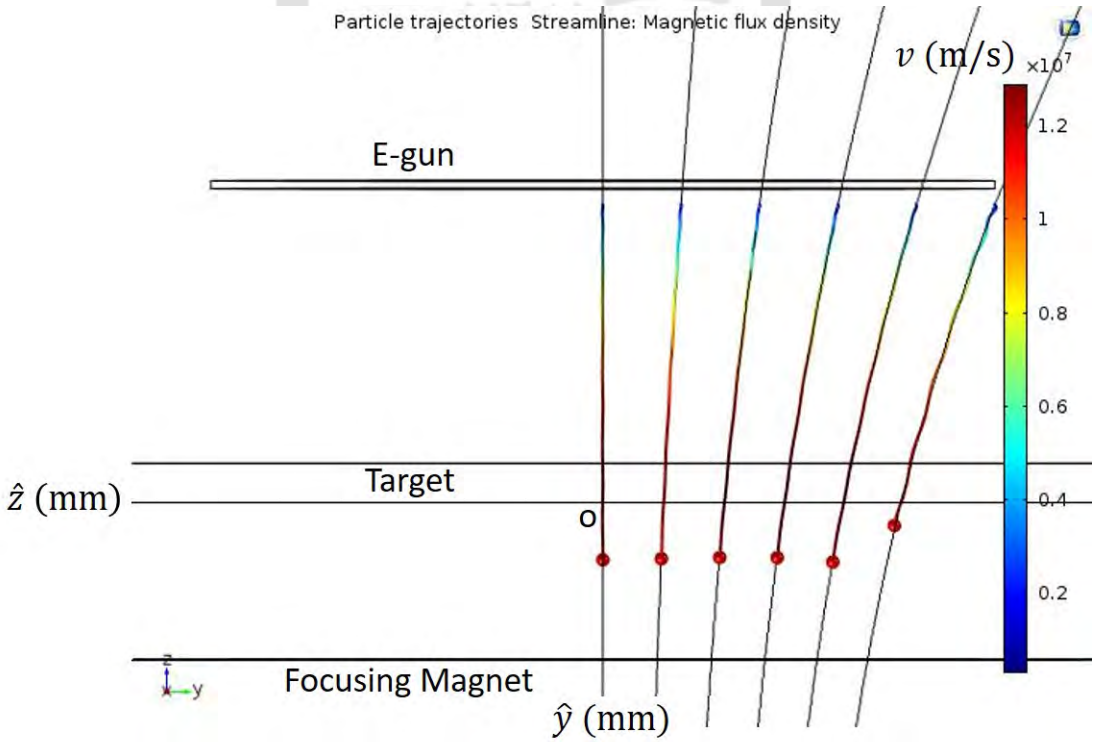

Figure 58: The electron trajectories with the initial angle equal to 60.0° in the y-z plane.

doi:10.6844/NCKU202003198

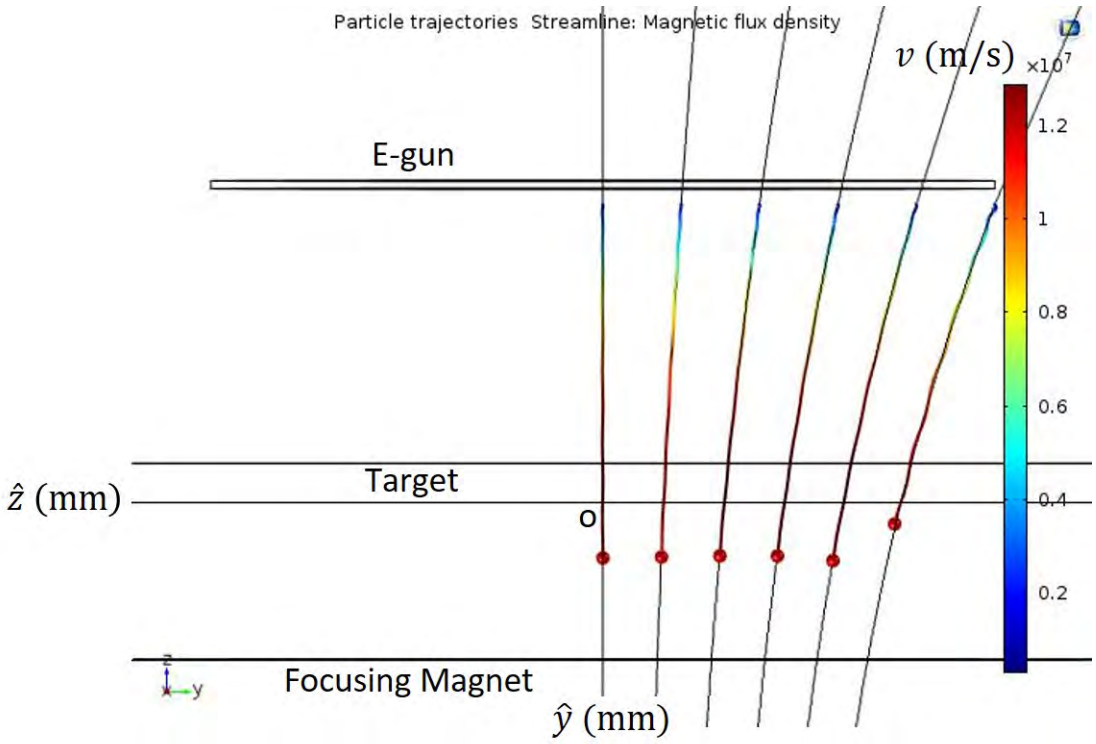

Figure 59: The electron trajectories with the initial angle equal to 70.0° in the y-z plane.

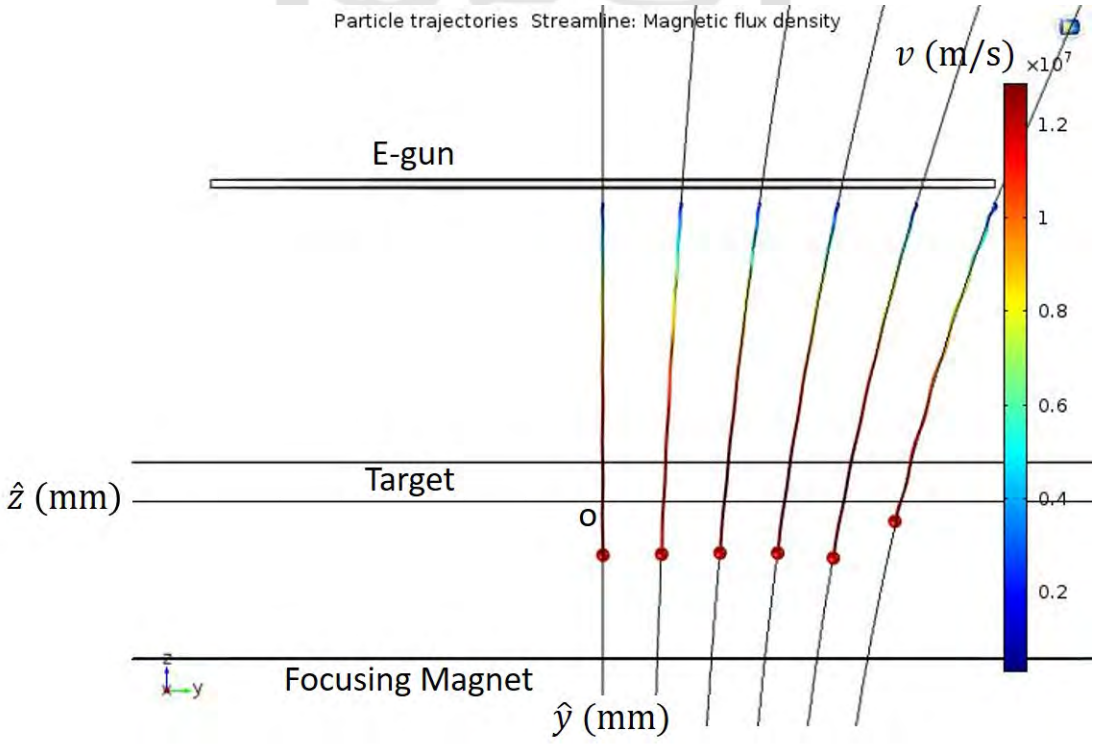

Figure 60: The electron trajectories with the initial angle equal to 80.0° in the y-z plane.

doi:10.6844/NCKU202003198

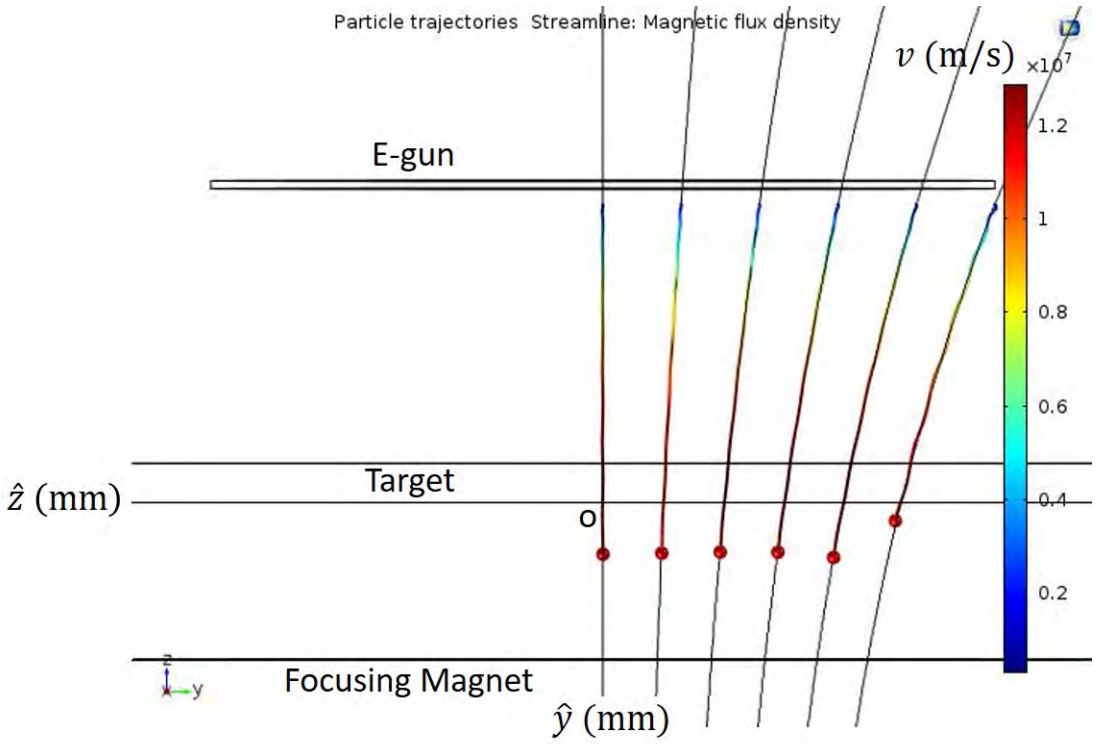

Figure 61: The electron trajectories with the initial angle equal to 90.0° in the y-z plane.

3.7 Electron trajectories in electric fields and magnetic fields with different V_{acc}

Shown in section 3.6, all electrons were accelerated by electric fields and reached the target in all cases. Therefore, we would like to lowered V_{acc} more and see if electrons could be reflected. Electrons have different accelerations with dfifferent V_{acc}. Therefore, different simulated time and steps in the simulation are needed. I chose the simulated time when the electrons passed through the target. Shown in Table 12 are different V_{acc} with different total simulated time. Initial velocities and pitch angles were 3.00×10^5 m/s and 90.0° in all cases. Simulated results are shown in Fig. 62–66 for V_{acc} = 250,100, 50, 25, and 1 V. All electrons were accelerated into the loss cone since no electrons were reflected in any cases. Nevertheless, electrons in all cases were magnetized and followed magnetic field lines.

doi:10.6844/NCKU202003198

Table 12: V_{acc} and simulated time.

V_{acc} (V)	Time (s)	Steps
250	6×10^{-10}	601
100	1.5×10^{-9}	1501
50	2×10^{-9}	2001
25	2.5×10^{-9}	2501
1	1.5×10^{-8}	15001

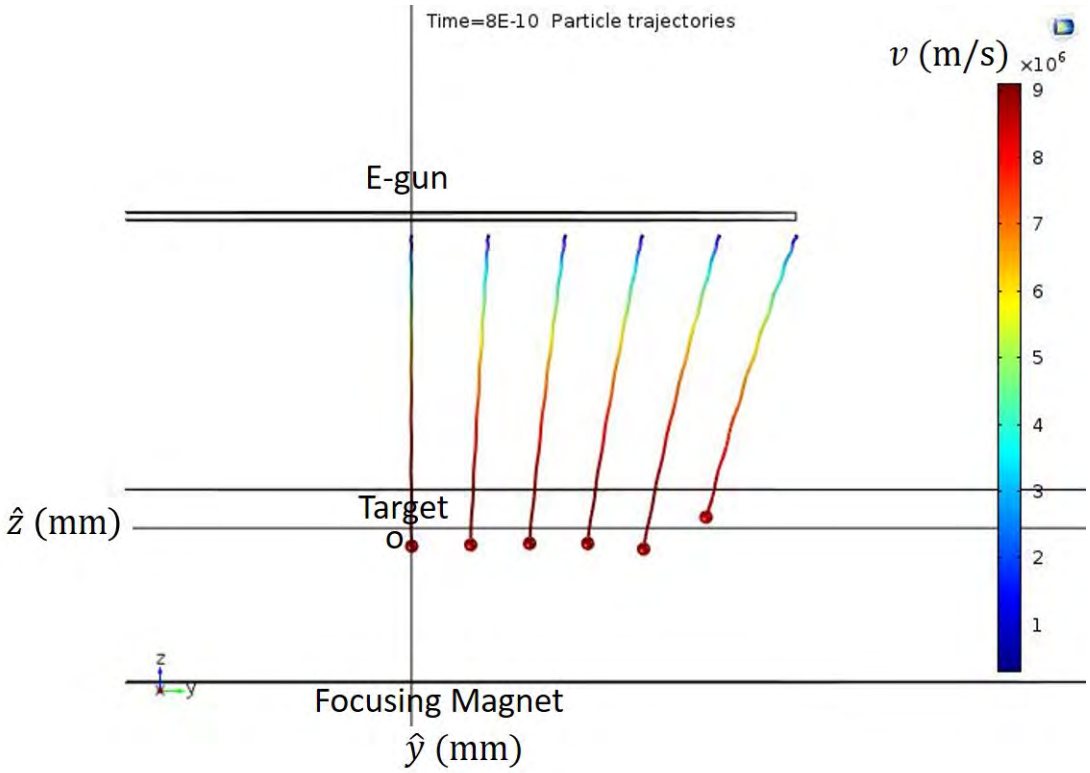

Figure 62: The electron trajectories with V_{acc}equal to 250 V in the y-z plane.

doi:10.6844/NCKU202003198

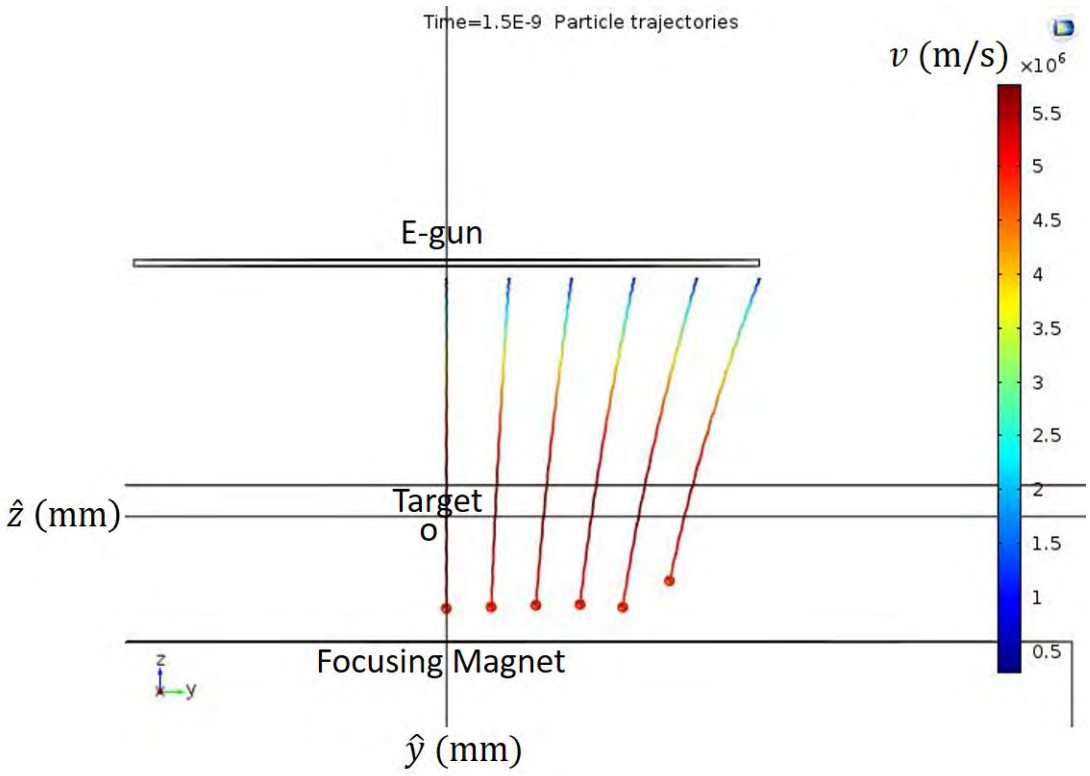

Figure 63: The electron trajectories with V_{acc}equal to 100 V in the y-z plane.

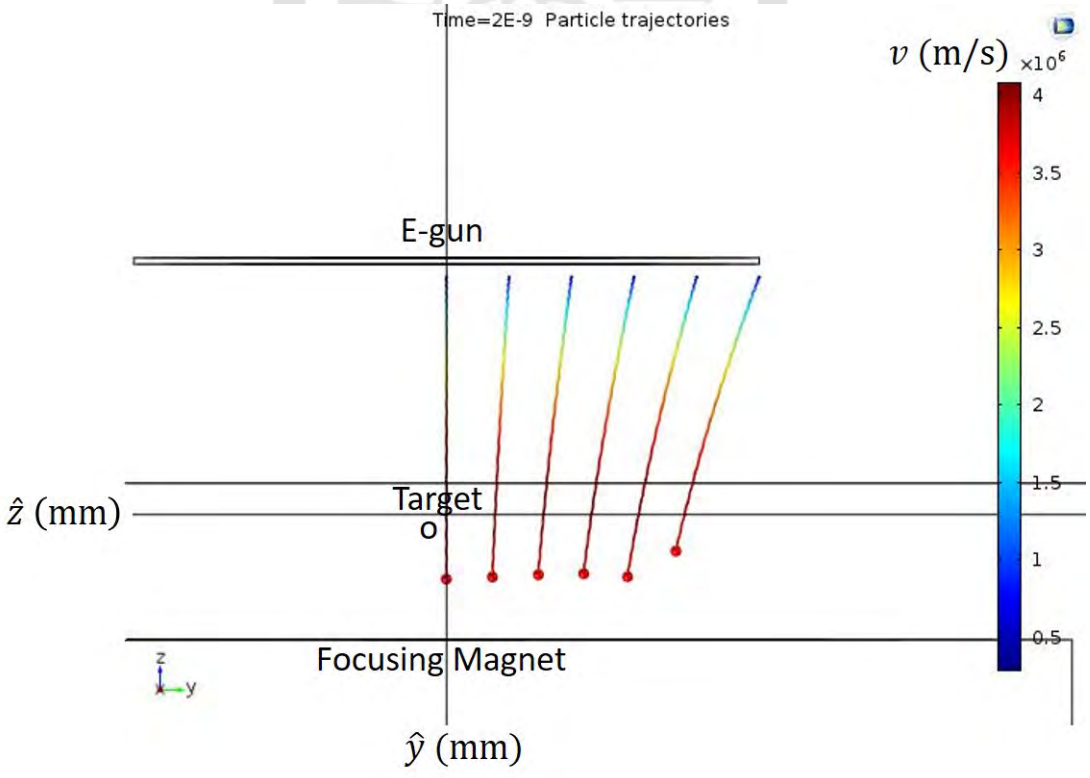

Figure 64: The electron trajectories with V_{acc}equal to 50 V in the y-z plane.

doi:10.6844/NCKU202003198

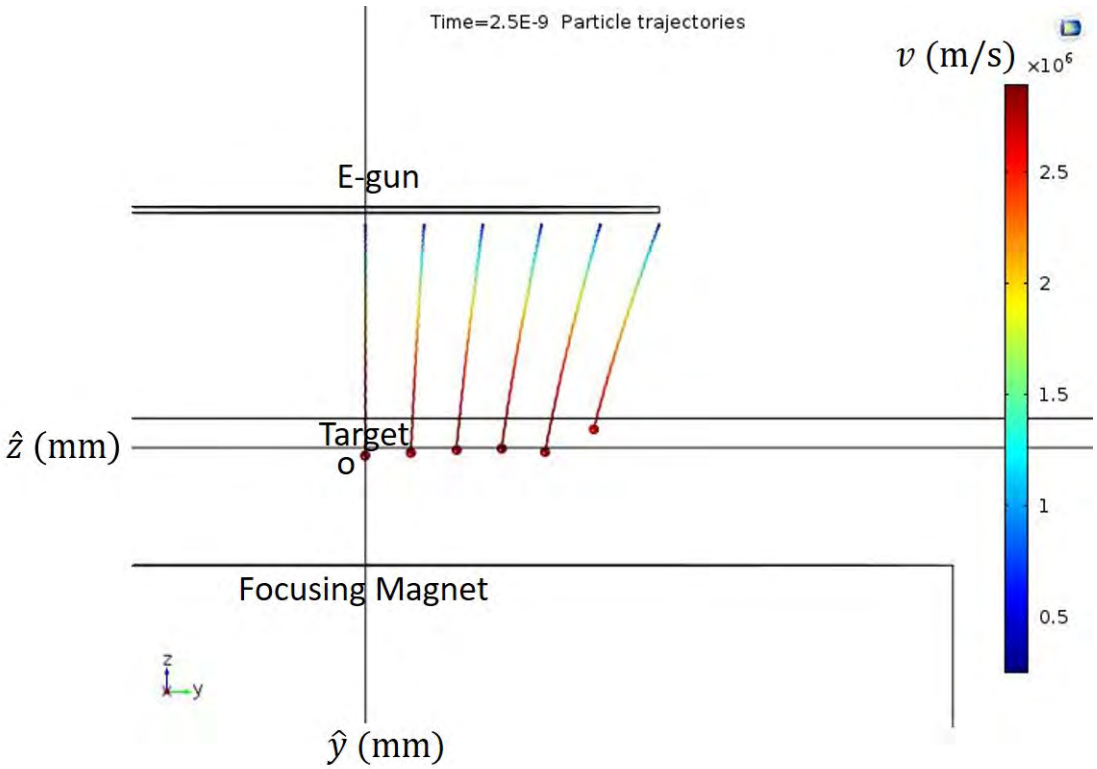

Figure 65: The electron trajectories with V_{acc}equal to 25 V in the y-z plane.

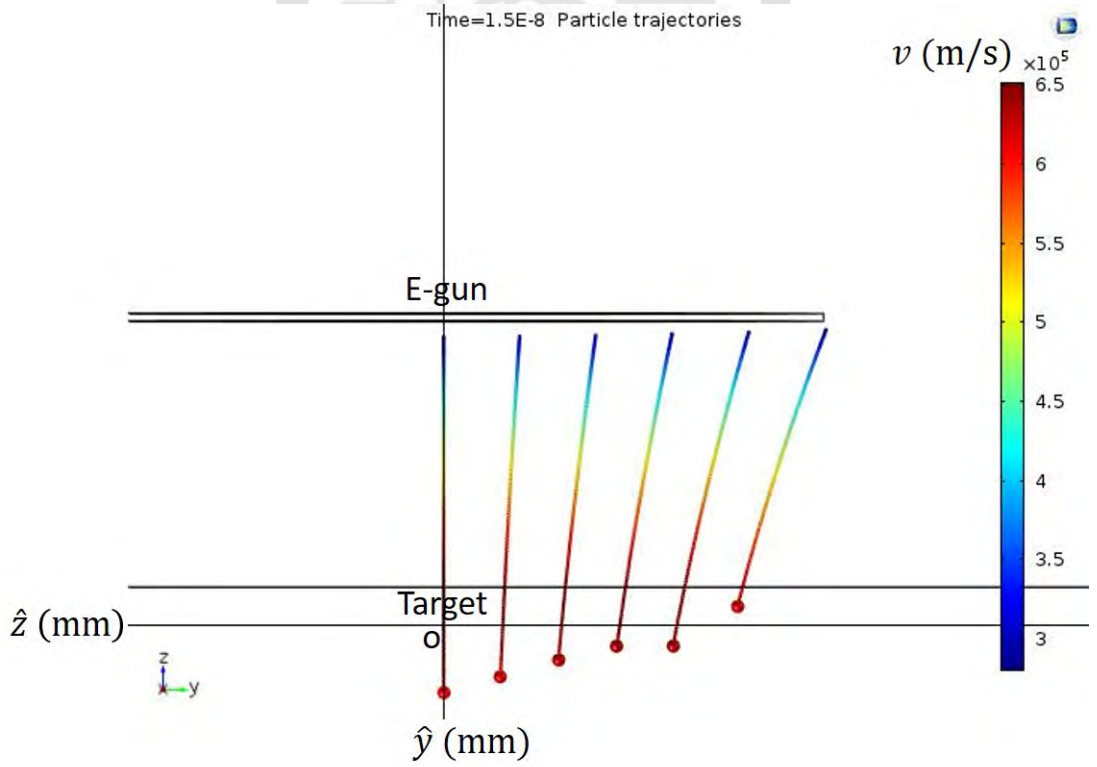

Figure 66: The electron trajectories with V_{acc}equal to 1 V in the y-z plane.

doi:10.6844/NCKU202003198

3.8 Summary

In all simulations, no electrons were reflected once there were electric fields. It means the electric force was much larger than the magnetic mirror force. Therefore, the hypothesis that electrons were confined by the magnetic mirror effect was not correct.

doi:10.6844/NCKU202003198

4 Discussions

In Chap. 2, the electric currents I_e with V_{acc} equal to 500 V, 750 V, and 1000 V were 15 mA, 10 mA, and 7.5 mA, respectively. Based on the calculated temperature of the filament as the E-gun from the power that heats the filament, the expected emission current density J using Eq. 7 with V_{acc} equal to 500 V and 1000 V were 226.07 kA/m^2 and 34.89 kA/m^2, respectively. The expected current density J with V_{acc} equal to 500 V supposed to be 6.48 times larger than J with V_{acc} equal to 1000 V. However, I_e with V_{acc} equal to 500 V was only 2 times higher than I_e with V_{acc} equal to 1000 V. I suspected that emitted electrons might not reach the target contributing to the current I_e because the magnetic mirror force might be larger than the electric force.

In Chap. 3, I simulated electron trajectories using COMSOL to verify the hypothesis. However, the simulation results showed that no electrons were reflected by the magnetic-mirror force once there was an electric force from V_{acc} greater than 1 V. Electrons originally not in the loss cone without electric forces were moved into the loss cone so that they reached the target. It means that the electric force was much larger than the magnetic-mirror force. Therefore, the result of the simulation didn't support the hypothesis.

In order to verify our simulation results, we estimated the electric force and the magnetic-mirror force. The force from the electric field F_E could be calculated by

$$|\overrightarrow{F}_E| = qE \approx q\frac{V_{acc}}{d}$$

where $d = 3.5$ mm is the distance between the filament and the target. The force from the magnetic-mirror effect F_B could be calculated by

$$|\overrightarrow{F}_B| = |-\mu\nabla_{\parallel}B| \approx \mu|\frac{\triangle B}{d}| = \frac{1}{2}\frac{m_e v_{\perp}^2}{B_0}\frac{|B' - B_0|}{d} \tag{33}$$

where m_e is the mass of the electron, $v_{\perp}$ is the velocity perpendicular to the magnetic field, $B_0 = 0.3$ T is the magnetic field at the center of the disc filament, and $B' = 0.45$ T is the magnetic field at the center of the target. For the extreme case, the initial pitch angle is set to 90^o, i.e., $v_{\perp}$ equals to the thermal velocity 3×10^5 m/s. If the electron is reflected, F_E is smaller than F_B. In other words,

doi:10.6844/NCKU202003198

$$|\overrightarrow{F}_{\mathrm{E}}| \approx q\frac{V_{\mathrm{acc}}}{d} < |F_{\mathrm{B}}| \approx \frac{1}{2}\frac{m_{\mathrm{e}}v_{\perp}^{2}}{B_0}\frac{|B^{'} - B_0|}{d} \tag{34}$$

$$\Rightarrow V_{\mathrm{acc}} < \frac{1}{2}m_{\mathrm{e}}v_{\perp}^{2}\frac{B^{'} - B_0}{B_0} = 0.13\ (\mathrm{V})\,. \tag{35}$$

The estimation shows that only when V_{acc} less than 0.13 V can electrons be reflected by the magnetic-mirror force. In other words, once V_{acc} is larger than 0.13 V, electrons will not be reflected. The estimated results support the simulation results where V_{acc} was larger than 1 V in all cases.

When I did the simulation of the electron trajectories, I assumed that initial locations of the electrons were 0.2 mm under the filament. In other words, I assumed that electrons had already been emitted from the filament since thermionic electron emission was not simulated. Therefore, even the simulation results didn't support the hypothesis we obtained from experiments, we have rolled out the magnetic mirror effect in our system. To understand more details of the electron behaviors in MIT-MEB, we need to study thermionic electron emission more carefully.

In our experiments, we set V_{acc} larger than 0.13 V which provided the electric field large enough to pull out the electrons from the thermal filament. In those case, we know that the electric force $|\overrightarrow{F}_{\mathrm{E}}|$ is much larger than the magnetic-mirror force $|\overrightarrow{F}_{\mathrm{B}}|$ when the electric force is parallel to the magnetic field as shown in Fig. 67 (a). In order to have a magnetic-mirror effect comparable to the electric field, we can redesign the system such that the electric field is not paralleled to the magnetic-mirror force. We can set the relation between the electric force and the magnetic-mirror force as shown in Fig. 67 (b). In this case, the component of the electric field $\overrightarrow{F}_{\mathrm{E}}$ paralled to $\overrightarrow{F}_{\mathrm{B}}$, writen as $\overrightarrow{F}_{\parallel}$, is much smaller $\overrightarrow{F}_{\mathrm{B}}$. Therefore, electrons can be reflected by $\overrightarrow{F}_{\mathrm{B}}$. In fact, the component of $\overrightarrow{F}_{\mathrm{E}}$ perpendicular to $\overrightarrow{F}_{\mathrm{B}}$, writen as $\overrightarrow{F}_{\perp}$, increases the component of the velocity perpendicular to $\overrightarrow{F}_{\mathrm{B}}$. The magnetic moment and thus the magnetic-mirror force increase. It also helps reflecting the electrons. Therefore, moving the filament as the E-gun sideway as shown in Fig. 67 (c) may enhance the magnetic-mirror effect. Electrons may be trapped easier.

Therefore, using other simulations which can simulate the thermionic electron emission to study the electron behavior in MIT-MEB and changing the design of the MIT-MEB are left as

doi:10.6844/NCKU202003198

the future work for our group.

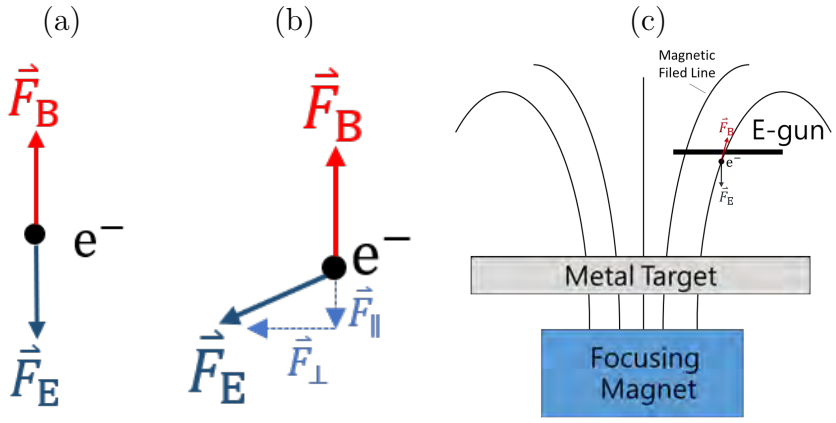

Figure 67: The Electric field (a)parallel to the magnetic field and (b)not parallel to the magnetic field, and the suggested position of the filament.

doi:10.6844/NCKU202003198

5 Summary

Electron trajectories play an important role in the MIT-MEB. Therefore, we have done a series of experiments with experments with different accelerating voltage V_{acc} and see if the performance of the MIT-MEB can be improved. In our experiments, we had V_{acc} equal to 500, 750, and 1000 V. We found that the filament as the E-gun for providing the thermionic emitted electrons I_{e} needed to be heated to much a higher temperature for $V_{\text{acc}} = 500$ V than that for $V_{\text{acc}} = 1000$ V. We could calculate the expected emitted current from the temperature using Eq. 7. We found that the expected current with $V_{\text{acc}} = 500$ V supposed to be 6.48 times higher than that with $V_{\text{acc}} = 1000$ V. However, I_{e} with V_{acc} equal to 500 V was only 2 times higher than I_{e} with V_{acc} equal to 1000 V in experiments. It means that the electric current I_{e} was much smaller than the expected current emitted from the E-gun due to the thermal emission. We suspected that electrons emitted from the E-gun were confined by the magnetic-mirror effect due to the non-uniform magnetic field. The confinement would have depended on the competition between the electric force and the magnetic-mirror force. The electric force would accelerate electrons toward the target while the magnetic-mirror force would reflect electrons back to the filament of the E-gun preventing them to reach the target. Therefore, we studied the electron trajectories in simulations. However, in simulation results, no electrons were reflected by the magnetic mirror force once there was an electric force from V_{acc} greater than 1 V. To verify the simulation results , we used a simple model to estimate the required electric potential V_{acc} such that the electric force would overcome the magnetic mirror force. We found that $V_{\text{acc}} = 0.13$ V was enough in the model. It explained all electrons reached the target in our simulations. However, it didn't explain the experimental results. Nevertheless, if we provide the electric force whose component parallel to the magnetic field, electrons may still be reflected by the magnetic-mirror effect. In fact, I assumed electrons had already been emitted from the filament since thermionic electron emission was not simulated in my simulations. In other words, we only rolled out the possibilities of electrons being reflected by the magnetic-mirror effect. However, how electrons were emitted from the filament with different V_{acc} was not considered. Therefore, using other simulations, which could simulate the thermionic electron emission, need to be conducted more carefully. It is left as the future work for our group.

doi:10.6844/NCKU202003198

References

[1] Ming-Hsueh Shen. Development of a micro ecr ion thruster for space propulsion. Master's thesis, National Cheng Kung University, 2016. Replotted from Kuriki, K. and Arakawa. Y.,Introduction to electric propulsion, U. Tokyo Press., Tokyo, 2003.

[2] K. Kuriki and Y. Arakawa. *Introduction to electric propulsion.* University of Tokyo Press, 2003.

[3] Robert G. Jahn. *Physics of electric propulsion.* Dover Publications, 2006.

[4] S. Anthony. Nasa's next ion drive breaks world record, will eventually powerinterplanetary missions., December 2012.

[5] Riccardo Albertoni Anuscheh Nawaz and Monika Auweter-Kurtz. Thrust efficiency optimization of the pulsed plasma thruster simp-lex. *Acta Astronautica, 67(3):440 – 448*, 2010.

[6] Joseph Ashkenazy, G Appelbaum, T Ram-Cohen, A Warshavsky, I Tidhar, and L Rabinovich. Venμs technological payload - the israeli hall effect thruster electric propulsion system. 2007.

[7] Mike Robin James Szabo and John Duggan. Light metal propellant hall thrusters. *IEPC-2009-138, Presented at the 31st International Electric Propulsion Conference,University of Michigan • Ann Arbor, Michigan • USA*, September 20 – 24, 2009.

[8] Kuo-Yi Chen. Development of metallic ion thruster using magnetron electron-beam bombardment. Master's thesis, National Cheng Kung University, Institute of Space and Plasma Sciences, 2019.

[9] C.R. Crowell. The richardson constant for thermionic emission in schottky barrier diodes. *Solid-State Electronics*, 1965.

[10] K.S Sree Harsha. *Principle of Vapor Deposition of Thin Films.* Elsevier Science, 2006.

[11] Thermionic emission, [online] http://spmphysics.onlinetuition.com.my/2013/06/thermionic-emission.html.

doi:10.6844/NCKU202003198

[12] Jatosado. Electron beam deposition, wikipedia.

[13] J Stefan. über die beziehung zwischen der wärmestrahlung und der temperatur. *Sitzungsberichte der Kaiserlichen Akademie der Wissenschaften in Wien, Vol. 79, Aus der k.k. Hof-und Staatsdruckerei, 391-428*, 1879.

[14] [online] https://luxel.com/wp-content/uploads/2013/04/luxel-vapor-pressure-chart.pdf.

[15] First ionization energy. wikipedia.

[16] Kuo-Yi Chen, Po-Yu Chang, and Wan-Yi Lin. Metal ion thruster using magnetron electron-beam bombardment (mit-meb). *Plasma Sources Science and Technology*, 2019.

[17] Rahla Naghma Debdeep Ghoshal Jaspreet Kaur, Dhanoj Gupta and Bobby Antony. Electron impact ionization cross sections of atoms. *Canadian Journal of Physics,93(6):617–625*, 2015.

[18] Jaro.p. Lorentz force.svg. wikipedia.

[19] Paul Urone. *College physics Vol. 1.* OpenStax, Houston, Texas, 2017.

[20] Francis Chen. *Introduction to plasma physics and controlled fusion.* Plenum Press, New York, 1984.

[21] Comsol multiphysics®, http://www.comsol.com, comsol ab, stockholm,sweden.

doi:10.6844/NCKU202003198

Appendix

A SOP of the vacuum system

A.1 抽眞空 Pumping down

1. 確認粗抽閥(角閥)與閘閥開啓。

   Open the angle valve and the gate valve.

2. 球閥(1)和球閥(2)關閉 。

   Close the ball valve(1) and the ball valve(2) .

3. 開啓粗抽泵。

   Turn on the rotary pump.

4. 確認低眞空計低於10^{-1} torr (10 Pa)。

   Check the low vacuum gauge if the pressure in the chamber is less than 10^{-1} torr (10 Pa).

5. 打開擴散泵 。

   Turn on the diffusion pump.

6. 確認低眞空計低於5.0×10^{-2} torr (6.7 Pa)或擴散泵已開啓超過一小時。

   Check the low vacuum gauge if the pressure in the chamber is less than 5.0×10^{-2} torr (6.7 Pa) or the diffusion pump has been turned on for over one hour.

7. 可開啓高眞空計(Ion gauge) 。

   Turn on the ion gauge.

   注意：氣壓大於5.0×10^{-2} torr (6.7 Pa)不可開啓高眞空計，且不使用高眞空計時記得關閉避免燒壞。

   Note: The ion gauge can't be truned on when the pressure in the chamber is higher than 5.0×10^{-2} torr (6.7 Pa) or the diffusion pump hasn't been turned on for over one hour, and should be turned off if it is not used.

8. 確認高眞空計低於4.5×10^{-5} torr (6.0×10^{-3} Pa)。

   Check the ion gauge if the pressure in the chamber is less than 4.5×10^{-5} torr (6.0×10^{-3} Pa).

doi:10.6844/NCKU202003198

9. 可開始做實驗。

10. We can start doing the experiment.

A.2 破眞空 Vacuum venting

1. 關掉高眞空計。

   Turn off the ion gauge.

   注意：高眞空計必須關閉以免燒壞 。

   Note: The ion gauge has to be turned off of it will be damaged.

2. 關掉擴散泵 。

   Turn off the diffusion pump.

3. 關閉閘閥。

   Close the gate valve.

4. 打開球閥(1)將眞空腔破眞空。

   Open the ball valve (1) to vent the chamber.

5. 等待擴散泵的溫度冷卻至 35°C以下。

   Wait until the diffusion pump cools down to less than 35°C.

   注意：擴散泵未冷卻前不可破眞空 。

   Note: Do not vent the diffusion pump before it cools down.

6. 關閉角閥。

   Close the angle valve.

7. 關閉粗抽泵。

   Turn off the rotary pump.

8. 打開球閥(2)破擴散泵的眞空 。

   Open the ball valve (2) to vent the diffusion pump .

doi:10.6844/NCKU202003198

B Experimental raw data

Table 13: Currents, voltages, and powers of filaments of E-gun and neutralizer.

Date	V_{acc}(V)	I_f(A)	std$_{I_f}$(A)	V_f(V)	std$_{V_f}$(V)	I_{nf}(A)	std$_{I_{nf}}$(A)	V_{nf}(V)	std$_{V_{nf}}$(V)
20190905	1000	2.26	0.05	2.0	0.1	2.34	0.00	2.2	0.0
20190906	1000	2.20	0.01	1.8	0.0	2.33	0.00	2.8	0.2
20190910	1000	2.16	0.39	1.8	0.3	0.00	0.00	16.3	9.3
20190911	1000	2.43	0.01	2.5	0.2	2.33	0.00	2.0	0.0
20190912	1000	2.34	0.07	2.2	0.1	2.33	0.00	2.0	0.1
20190917	1000	2.41	0.02	2.1	0.0	2.33	0.01	2.1	0.0
20190919	1000	2.37	0.01	1.9	0.0	2.34	0.00	2.2	0.2
20191007	250	2.61	0.05	3.3	0.1	2.33	0.00	2.5	0.2
20191015	1000	2.33	0.01	1.9	0.1	2.32	0.10	2.9	0.2
20191018	1000	2.23	0.02	1.9	0.0	2.35	0.03	2.4	0.1
20191025	1000	2.24	0.03	1.9	0.0	2.04	0.82	3.5	2.8
20191029	1000	2.13	0.03	2.2	0.1	2.33	0.00	2.3	0.0
20191031	1000	2.10	0.02	2.6	0.2	2.33	0.00	2.3	0.1
20191101	1000	1.94	0.04	2.8	0.1	2.34	0.00	2.3	0.0
20191104	1000	1.86	0.03	2.6	0.1	2.33	0.00	2.4	0.1
20191230	1000	2.01	0.03	3.1	0.1	2.27	0.40	3.2	0.6
20200102	1000	1.98	0.07	3.1	0.2	2.34	0.00	3.4	0.1
20200106	1000	2.00	0.06	2.9	0.2	2.36	0.17	3.4	0.1
20200109	1000	2.02	0.04	3.2	0.2	2.33	0.00	3.0	0.0
20200117	250	2.34	0.19	3.6	0.4	2.33	0.00	2.8	0.0
20200120	250	2.27	0.05	3.8	0.3	2.33	0.00	3.1	0.1
20200122	250	2.32	0.00	3.4	0.0	2.33	0.00	3.5	0.1
20200213	250	2.37	0.01	3.2	0.1	2.33	0.01	2.2	0.1
20200218	250	2.20	0.00	2.8	0.1	2.32	0.00	2.6	0.1
20200224	250	2.32	0.00	3.5	0.1	2.24	0.49	3.3	0.7
20200303	250	2.44	0.04	3.6	0.1	2.32	0.01	2.2	0.0
20200305	500	2.01	0.07	2.7	0.3	2.32	0.00	2.4	0.1
20200309	500	2.11	0.17	3.2	0.3	2.32	0.01	2.2	0.1
20200317	500	2.40	0.00	3.1	0.0	2.34	0.00	2.0	0.0
20200326	500	2.38	0.02	3.0	0.1	2.37	0.30	2.4	0.5
20200422	750	2.21	0.02	2.6	0.1	2.35	0.4	4.1	1.2
20200426	750	2.19	0.01	2.6	0.0	2.54	0.01	2.6	0.1
20200501	750	2.17	0.01	2.7	0.1	0.18	0.66	0.2	0.8
20200505	750	2.13	0.02	2.8	0.1	1.08	1.21	1.4	1.6
20200508	750	2.06	0.02	2.6	0.1	2.43	0.02	3.2	0.1
20200520	750	1.98	0.04	2.7	0.1	2.45	0.00	3	0.1
20200526	900	1.98	0.02	2.6	0.0	2.5	0.02	2.7	0.1
20200529	900	1.83	0.00	2.5	0.0	2.46	0.02	3.3	0.1
20200602	900	1.84	0.05	2.6	0.1	2.55	0.00	2.8	0.0
20200605	900	1.86	0.02	2.8	0.1	0.00	0.00	0.0	0.0
20200611	1000	1.91	0.03	2.7	0.1	2.55	0.00	3.3	0.1
20200612	1000	2.02	0.00	2.6	0.1	2.48	0.28	3.2	0.3
20200616	500	2.26	0.06	3.8	0.1	1.13	1.34	8.2	4.1
20200617	500	2.25	0.04	3.8	0.1	2.56	0.01	3.0	0.1
20200619	500	2.17	0.10	3.6	0.2	0.28	0.81	0.4	1.1
20200624	500	2.07	0.00	3.2	0.0	2.55	0.00	2.3	0
20200626	1000	1.96	0.01	2.7	0.1	2.55	0.00	3.0	0.1
20200629	1000	1.96	0.01	2.6	0.0	2.54	0.00	2.9	0.1
20200703	1000	1.95	0.01	3	0.1	2.54	0.00	2.4	0.1
20200706	1000	1.93	0.01	2.8	0.2	2.53	0.00	2.7	0
20200708	1000	1.91	0.01	3	0.1	0	0.00	0.0	0.0
20200709	1000	1.9	0.01	2.8	0.1	2.54	0.00	2.8	0
20200714	1000	1.9	0.01	2.7	0.1	1.46	1.26	1.9	1.6
20200716	750	1.89	0.01	2.9	0.2	2.55	0.00	3.5	0.1
20200722	750	1.82	0.00	3.0	0.1	2.54	0.00	3.4	0.2
20200724	750	1.97	0.01	3.0	0.1	1.23	1.30	2.1	2.6
20200729	750	2.08	0.01	3.2	0.1	2.54	0.00	2.7	0.1
20200730	750	2.06	0.02	2.9	0.0	1.49	1.27	1.8	1.6

doi:10.6844/NCKU202003198

Table 14: Currents, voltages, and powers of the E-beam.

Date	V_{acc}(V)	Actual V_{acc}(V)	std$_{V_{acc}}$(V)	I_e(mA)	std$_{I_e}$(A)	Power(W)	std$_{Power}$(W)
20190905	1000	NA	NA	14.6	1.2	14.6	1.2
20190906	1000	NA	NA	15.1	0.6	15.1	0.6
20190910	1000	NA	NA	14.1	2.1	14.1	2.1
20190911	1000	NA	NA	15.1	0.9	15.1	0.9
20190912	1000	730	276	9.6	5.4	7.1	4.8
20190917	1000	NA	NA	15.0	1.0	15.0	1.0
20190919	1000	NA	NA	14.8	0.9	14.8	0.9
20191007	250	NA	NA	6.0	0.1	1.5	0.1
20191015	1000	1008	1	14.6	2.1	14.8	2.2
20191018	1000	1007	1	14.8	1.2	14.9	1.2
20191025	1000	NA	NA	13.8	2.8	13.8	2.8
20191029	1000	877	299	12.9	4.9	12.9	5.0
20191031	1000	857	302	12.9	2.7	11.7	4.8
20191101	1000	949	165	13.7	4.5	13.2	4.7
20191104	1000	808	363	8.6	5.4	8.2	5.6
20191230	1000	916	267	13.7	4.1	13.3	4.5
20200102	1000	903	190	12.4	3.3	11.4	4.3
20200106	1000	1006	33	14.2	3.1	14.4	3.2
20200109	1000	956	182	12.8	3.7	12.4	4.3
20200117	250	251	0	8.5	0.7	2.1	0.2
20200120	250	249	1	10.1	0.2	2.5	0.1
20200122	250	249	1	5.8	0.1	1.4	0.0
20200213	250	251	0	8.0	0.1	1.9	0.4
20200218	250	252	1	9.9	0.2	2.5	0.1
20200224	250	254	2	10.1	0.1	2.6	0.0
20200303	250	251	0	6.1	0.2	1.5	0.1
20200305	500	501	1	6.3	2.3	3.1	1.2
20200309	500	500	2	9.9	6.0	5.0	3.0
20200317	500	504	1	10.0	0.2	5.0	0.1
20200326	500	503	1	9.1	0.3	4.6	0.1
20200422	750	752	1	10.0	1.6	7.5	1.2
20200426	750	751	1	10.9	0.8	8.2	0.6
20200501	750	754	2	10.6	0.4	8.0	0.3
20200505	750	752	1	10.1	0.6	7.6	0.5
20200508	750	758	56	10.2	0.6	7.7	0.6
20200520	750	752	1	10.2	0.4	7.7	0.3
20200526	900	903	0	8.7	0.8	7.8	0.8
20200529	900	903	0	8.3	0.3	7.5	0.3
20200602	900	903	1	8.0	0.5	7.2	0.5
20200605	900	898	19	7.8	0.8	7.0	0.7
20200611	1000	957	150	13.3	3.4	12.9	4.0
20200612	1000	1006	1	7.5	0.3	7.5	0.3
20200616	500	504	1	15.0	0.4	7.5	0.2
20200617	500	506	1	15.0	0.5	7.6	0.2
20200619	500	506	1	15.1	0.7	7.7	0.4
20200624	500	506	1	15.0	0.2	7.6	0.1
20200626	1000	1003	1	7.4	0.3	7.4	0.3
20200629	1000	1003	1	7.4	0.4	7.4	0.4
20200703	1000	1003	1	7.5	0.2	7.5	0.2
20200706	1000	1004	3	7.5	0.3	7.5	0.3
20200708	1000	1002	1	7.5	0.2	7.6	0.2
20200709	1000	1003	1	7.5	0.2	7.6	0.2
20200714	1000	1003	1	7.5	0.2	7.5	0.2
20200716	750	752	0	10.0	0.4	7.6	0.3
20200722	750	752	1	10.0	0.2	7.5	0.1
20200724	750	750	14	9.9	0.3	7.5	0.2
20200729	750	753	1	10.0	0.1	7.5	0.1
20200730	750	754	1	9.9	0.1	7.5	0.1

doi:10.6844/NCKU202003198

Table 15: Experimental time and evaporation rates.

Date	V_{acc}(V)	time(s)	$m_i - m_f$(g)	Evaporation rate(g/s)
20190905	1000	600	1.01E-01	1.70E-04
20190906	1000	310	6.28E-02	2.00E-04
20190910	1000	320	2.44E-02	7.60E-05
20190911	1000	390	4.01E-02	1.00E-04
20190912	1000	320	3.03E-02	9.50E-05
20190917	1000	380	6.73E-02	6.70E-02
20190919	1000	330	4.71E-02	1.40E-04
20191007	250	310	1.00E-04	3.20E-07
20191015	1000	560	4.00E-04	7.10E-07
20191018	1000	320	7.01E-02	2.20E-04
20191025	1000	360	2.10E-03	5.80E-06
20191029	1000	310	8.21E-02	2.60E-04
20191031	1000	320	7.54E-02	2.40E-04
20191101	1000	350	9.30E-02	2.70E-04
20191104	1000	310	2.34E-01	7.50E-04
20191230	1000	330	9.00E-04	2.70E-06
20200102	1000	300	3.71E-02	1.20E-04
20200106	1000	320	5.40E-03	1.70E-05
20200109	1000	380	1.33E-02	3.50E-05
20200117	250	360	1.00E-04	2.80E-07
20200120	250	600	7.00E-04	1.20E-06
20200122	250	1140	3.94E-03	3.50E-06
20200213	250	3180	1.30E-03	4.10E-07
20200218	250	2940	1.10E-03	3.70E-07
20200224	250	1320	1.87E-02	1.40E-05
20200303	250	1080	6.00E-04	5.60E-07
20200305	500	1500	1.60E-02	1.10E-05
20200309	500	120	7.70E-03	6.40E-05
20200317	500	1440	3.90E-03	2.70E-06
20200326	500	1440	4.40E-03	3.10E-06
20200422	750	180	2.50E-03	1.40E-05
20200426	750	260	-1.00E-04	-3.80E-07
20200501	750	3600	1.20E-03	3.30E-07
20200505	750	3600	6.60E-03	1.80E-06
20200508	750	1380	7.97E-02	5.80E-05
20200520	750	3600	3.28E-02	9.10E-06
20200526	900	600	2.58E-02	4.30E-05
20200529	900	360	1.74E-02	4.80E-05
20200602	900	360	4.27E-02	1.20E-04
20200605	900	360	9.82E-02	2.70E-04
20200611	1000	300	2.44E-02	8.10E-05
20200612	1000	300	1.10E-03	3.70E-06
20200616	500	600	9.00E-04	1.50E-06
20200617	500	3600	6.30E-03	1.70E-06
20200619	500	3600	5.80E-03	1.60E-06
20200624	500	3600	6.00E-03	1.70E-06
20200626	1000	720	1.70E-03	2.40E-06
20200629	1000	1800	5.10E-03	2.80E-06
20200703	1000	3600	5.40E-03	1.50E-06
20200706	1000	3600	4.70E-03	1.30E-06
20200708	1000	3600	-3.00E-04	-8.30E-08
20200709	1000	3600	2.90E-03	8.10E-07
20200714	1000	3600	4.70E-03	1.30E-06
20200716	750	780	1.58E-02	2.00E-05
20200722	750	900	-1.60E-03	-1.80E-06
20200724	750	2400	5.54E-02	2.30E-05
20200729	750	1800	1.10E-03	6.11E-07
20200730	750	2700	2.30E-03	8.52E-07

doi:10.6844/NCKU202003198

Table 16: I_{n} and β.

Date	V_{acc}	$I_{\mathrm{n}}(\mu\mathrm{A})$	$\mathrm{std}_{I_{\mathrm{n}}}(\mu\mathrm{A})$	$\beta(\%)$	$\mathrm{std}_{\beta}(\%)$	$I_{\mathrm{n(max)}}(\mu\mathrm{A})$	$\beta_{max}(\%)$
20190905	1000	54.42	53.96	2.21E-02	0.021892058	184.90	0.07501808
20190906	1000	-0.58	15.96	-1.95E-04	-0.000194851	-40.86	-0.013734336
20190910	1000	9.99	10.60	8.92E-03	0.009465937	32.32	0.02886282
20190911	1000	1.01	11.06	6.67E-04	0.0073257	-49.76	-0.032953979
20190912	1000	222.38	176.46	1.60E-01	0.126900171	613.40	0.44112165
20190917	1000	267.86	100.19	8.41E-02	0.031461261	448.90	0.140965632
20190919	1000	1.86	6.14	8.89E-04	0.002929647	-12.61	-0.006016104
20191007	250	0.56	0.61	1.18E-01	0.129578166	1.39	0.293415969
20191015	1000	9.34	18.11	9.33E-01	1.711620013	34.22	3.262235375
20191018	1000	-2.70	16.51	-8.40E-04	0.005133393	-85.84	-0.026682648
20191025	1000	156.71	76.37	1.83E+00	0.891444056	329.85	3.850409732
20191029	1000	23.46	39.67	6.03E-03	0.01019844	191.29	0.049183344
20191031	1000	200.84	195.62	5.80E-02	0.056531849	693.40	0.200387082
20191101	1000	188.01	121.61	4.82E-02	0.03116442	439.72	0.112685638
20191104	1000	110.06	90.18	9.95E-03	0.008148859	371.53	0.033572988
20191230	1000	48.71	26.37	1.22E+00	0.658275319	110.00	2.746447917
20200102	1000	372.34	373.23	2.05E-01	0.205507042	1364.30	0.751215389
20200106	1000	94.34	46.62	3.81E-01	0.188110275	192.04	0.774916963
20200109	1000	240.42	302.97	4.68E-01	0.589431506	1306.00	2.540869643
20200117	250	108.47	9.90	2.66E+01	2.427557621	131.40	32.2110675
20200120	250	11.67	2.42	6.81E-01	0.141081794	14.19	0.828214554
20200122	250	31.00	8.88	6.11E-01	0.174874815	42.02	0.827888652
20200213	250	4.38	0.53	7.29E-01	0.088863829	5.26	0.876146567
20200218	250	7.83	3.22	1.43E+00	0.586842067	19.21	3.496143597
20200224	250	2.49	5.48	1.20E-02	0.026336264	12.94	0.062197632
20200303	250	0.53	0.32	6.53E-02	0.039573327	1.00	0.12256875
20200305	500	2.18	1.88	1.39E-02	0.011988374	4.21	0.026875752
20200309	500	2.68	3.50	2.84E-03	0.00371424	6.64	0.007046377
20200317	500	-0.02	0.26	-6.03E-04	0.006549076	0.61	0.015336808
20200326	500	2.22	0.49	4.94E-02	0.011015705	3.12	0.069529909
20200422	750	18.38	20.52	2.25E+00	2.514742653	47.13	5.776665188
20200426	750	1.09	0.13	3.86E-02	0.00468612	1.39	0.049218163
20200501	750	0.36	0.48	7.35E-02	0.098518154	2.10	0.428990625
20200505	750	2.72	3.41	1.01E-01	0.126772582	12.49	0.463904148
20200508	750	9.56	21.81	1.13E-02	0.025715897	100.10	0.118021762
20200520	750	13.96	9.95	1.04E-01	0.0743811	24.33	0.181835225
20200526	900	2.52	0.98	3.98E-03	0.001548772	3.29	0.005209964
20200529	900	3.91	0.41	5.50E-03	0.000578233	4.89	0.006889209
20200602	900	17.03	18.85	9.78E-03	0.010821859	63.26	0.036317092
20200605	900	6.67	5.50	1.67E-03	0.001373996	23.90	0.005966177
20200611	1000	12.36	10.78	1.04E-02	0.009029021	53.16	0.044506522
20200612	1000	15.32	6.42	2.85E-01	0.119210694	27.98	0.519617216
20200616	500	0.30	0.27	1.37E-02	0.012157225	0.85	0.038586458
20200617	500	2.59	1.02	1.01E-01	0.03955245	3.99	0.15525375
20200619	500	69.15	46.31	2.92E+00	1.957383802	103.80	4.387115948
20200624	500	1.20	0.31	4.89E-02	0.01248932	1.51	0.061692938
20200626	1000	4.43	1.20	1.28E-01	0.034540567	6.88	0.198417177
20200629	1000	5.49	1.51	1.32E-01	0.036297904	7.69	0.184814449
20200703	1000	2.43	0.43	1.10E-01	0.01959688	3.11	0.141181042
20200706	1000	2.82	0.65	1.47E-01	0.034141479	3.85	0.200804122
20200708	1000	0.42	0.09	-3.39E-01	0.07164417	0.61	-0.49844625
20200709	1000	3.15	0.94	2.66E-01	0.079222371	4.58	0.38714819
20200714	1000	2.46	1.23	1.28E-01	0.064196946	4.39	0.228968856
20200716	750	5.38	4.92	1.66E-02	0.0166248	17.60	0.059163987
20200722	750	17.93	4.05	-6.87E-01	0.155088498	27.58	-1.056389414
20200724	750	9.12	7.99	2.69E-02	0.02356004	22.40	0.066077978
20200729	750	0.58	0.47	6.50E-02	0.052078017	3.04	0.338735455
20200730	750	0.53	0.24	4.23E-02	0.019153925	1.05	0.083932948

doi:10.6844/NCKU202003198

The raw data, which were chosen to be the experimental results shown in this thesis, are:

1. 500 V: 20200616, 20200617, 20200619, 20200624
2. 750 V: 20200422, 20200501, 20200505, 20200508, 20200520, 20200716, 20200724, 20200729, 20200730
3. 1000 V: 20200612, 20200626, 20200629, 20200703, 20200706, 20200709, 20200714

Locations of the experimental data in the lab drive are:

1. 「Shares\WYL\Data\YYYYMM\YYYYMM-MMDD.csv」, YYYY is year, MM is month, and DD is date.
2. 「 Shares\WYL\Data\OO\(YYYYMM-MMDD.csv)」, OO is the value of V_{acc}, for example: 1kV, 500 V etc..

C Raw data of electron trajectories in simulations

Locations of the simulatied data in the lab drive are:

1. $\overrightarrow{E} \times \overrightarrow{B}$ drift: 「Shares\WYL\simulation\test」
2. Electron trajectories with the electric field: 「Shares\WYL\simulation\E\OO」, OO is the value of V_{acc}, for example: 1kV, 500 V etc..
3. Electron trajectory with the magnetic field: 「Shares\WYL\simulation\B\XX」, XX is the value of the initial angle, for example: 56.4° etc..
4. Electron trajectories in electric fields and magnetic fields: 「Shares\WYL\simulation\EB\XX」, XX is the value of the initial angle, for example: 56.4° etc..

C.1 $\overrightarrow{E} \times \overrightarrow{B}$ drift

1. The initial positions: $0\hat{x} + 0\hat{y} + 0\hat{z}$ (m).
2. The initial velocities: $0\hat{x} + 0\hat{y} + 0\hat{z}$ (m/s).
3. $\overrightarrow{E} = 1\hat{x}$ (V/m).

doi:10.6844/NCKU202003198

4. $\overrightarrow{B} = 1\hat{z}$ (T).

5. The total simulated time: 4 (s).

6. Steps: 4001.

7. qx, qy, and qz are the positions in $\hat{x}$, $\hat{y}$, and $\hat{z}$, respectively.

Table 17: Raw data of electron trajectories with $\overrightarrow{E} \times \overrightarrow{B}$ drift.

q2x (m) @ t=0	0.000	q2x (m) @ t=0.46	-0.309	q2x (m) @ t=0.92	-0.355
q2y (m) @ t=0	0.000	q2y (m) @ t=0.46	-0.571	q2y (m) @ t=0.92	-1.357
q2x (m) @ t=0.02	-0.101	q2x (m) @ t=0.48	-0.36	q2x (m) @ t=0.94	-0.301
q2y (m) @ t=0.02	-0.016	q2y (m) @ t=0.48	-0.679	q2y (m) @ t=0.94	-1.463
q2x (m) @ t=0.04	-0.199	q2x (m) @ t=0.5	-0.38	q2x (m) @ t=0.96	-0.222
q2y (m) @ t=0.04	-0.065	q2y (m) @ t=0.5	-0.799	q2y (m) @ t=0.96	-1.547
q2x (m) @ t=0.06	-0.283	q2x (m) @ t=0.52	-0.368	q2x (m) @ t=0.98	-0.127
q2y (m) @ t=0.06	-0.142	q2y (m) @ t=0.52	-0.92	q2y (m) @ t=0.98	-1.604
q2x (m) @ t=0.08	-0.344	q2x (m) @ t=0.54	-0.325	q2x (m) @ t=1	-0.026
q2y (m) @ t=0.08	-0.243	q2y (m) @ t=0.54	-1.032	q2y (m) @ t=1	-1.628
q2x (m) @ t=0.1	-0.376	q2x (m) @ t=0.56	-0.255	q2x (m) @ t=1.02	0.072
q2y (m) @ t=0.1	-0.359	q2y (m) @ t=0.56	-1.125	q2y (m) @ t=1.02	-1.621
q2x (m) @ t=0.12	-0.377	q2x (m) @ t=0.58	-0.166	q2x (m) @ t=1.04	0.156
q2y (m) @ t=0.12	-0.481	q2y (m) @ t=0.58	-1.193	q2y (m) @ t=1.04	-1.584
q2x (m) @ t=0.14	-0.345	q2x (m) @ t=0.6	-0.066	q2x (m) @ t=1.06	0.218
q2y (m) @ t=0.14	-0.598	q2y (m) @ t=0.6	-1.23	q2y (m) @ t=1.06	-1.523
q2x (m) @ t=0.16	-0.285	q2x (m) @ t=0.62	0.035	q2x (m) @ t=1.08	0.251
q2y (m) @ t=0.16	-0.699	q2y (m) @ t=0.62	-1.235	q2y (m) @ t=1.08	-1.447
q2x (m) @ t=0.18	-0.202	q2x (m) @ t=0.64	0.125	q2x (m) @ t=1.1	0.252
q2y (m) @ t=0.18	-0.778	q2y (m) @ t=0.64	-1.209	q2y (m) @ t=1.1	-1.366
q2x (m) @ t=0.2	-0.105	q2x (m) @ t=0.66	0.197	q2x (m) @ t=1.12	0.222
q2y (m) @ t=0.2	-0.827	q2y (m) @ t=0.66	-1.157	q2y (m) @ t=1.12	-1.289
q2x (m) @ t=0.22	-0.004	q2x (m) @ t=0.68	0.242	q2x (m) @ t=1.14	0.162
q2y (m) @ t=0.22	-0.845	q2y (m) @ t=0.68	-1.086	q2y (m) @ t=1.14	-1.227
q2x (m) @ t=0.24	0.092	q2x (m) @ t=0.7	0.256	q2x (m) @ t=1.16	0.080
q2y (m) @ t=0.24	-0.830	q2y (m) @ t=0.7	-1.005	q2y (m) @ t=1.16	-1.187
q2x (m) @ t=0.26	0.172	q2x (m) @ t=0.72	0.237	q2x (m) @ t=1.18	-0.017
q2y (m) @ t=0.26	-0.788	q2y (m) @ t=0.72	-0.926	q2y (m) @ t=1.18	-1.177
q2x (m) @ t=0.28	0.228	q2x (m) @ t=0.74	0.189	q2x (m) @ t=1.2	-0.118
q2y (m) @ t=0.28	-0.723	q2y (m) @ t=0.74	-0.857	q2y (m) @ t=1.2	-1.199
q2x (m) @ t=0.3	0.254	q2x (m) @ t=0.76	0.114	q2x (m) @ t=1.22	-0.214
q2y (m) @ t=0.3	-0.645	q2y (m) @ t=0.76	-0.807	q2y (m) @ t=1.22	-1.252
q2x (m) @ t=0.32	0.248	q2x (m) @ t=0.78	0.022	q2x (m) @ t=1.24	-0.295
q2y (m) @ t=0.32	-0.564	q2y (m) @ t=0.78	-0.785	q2y (m) @ t=1.24	-1.334
q2x (m) @ t=0.34	0.211	q2x (m) @ t=0.8	-0.079	q2x (m) @ t=1.26	-0.351
q2y (m) @ t=0.34	-0.489	q2y (m) @ t=0.8	-0.794	q2y (m) @ t=1.26	-1.439
q2x (m) @ t=0.36	0.146	q2x (m) @ t=0.82	-0.178	q2x (m) @ t=1.28	-0.379
q2y (m) @ t=0.36	-0.431	q2y (m) @ t=0.82	-0.836	q2y (m) @ t=1.28	-1.556
q2x (m) @ t=0.38	0.059	q2x (m) @ t=0.84	-0.266	q2x (m) @ t=1.3	-0.374
q2y (m) @ t=0.38	-0.398	q2y (m) @ t=0.84	-0.907	q2y (m) @ t=1.3	-1.678
q2x (m) @ t=0.4	-0.039	q2x (m) @ t=0.86	-0.332	q2x (m) @ t=1.32	-0.337
q2y (m) @ t=0.4	-0.395	q2y (m) @ t=0.86	-1.004	q2y (m) @ t=1.32	-1.792
q2x (m) @ t=0.42	-0.141	q2x (m) @ t=0.88	-0.372	q2x (m) @ t=1.34	-0.273
q2y (m) @ t=0.42	-0.424	q2y (m) @ t=0.88	-1.117	q2y (m) @ t=1.34	-1.891
q2x (m) @ t=0.44	-0.234	q2x (m) @ t=0.9	-0.38	q2x (m) @ t=1.36	-0.187
q2y (m) @ t=0.44	-0.484	q2y (m) @ t=0.9	-1.239	q2y (m) @ t=1.36	-1.965

doi:10.6844/NCKU202003198

q2x (m) @ t=1.38	-0.088	q2x (m) @ t=1.84	0.206	q2x (m) @ t=2.3	0.214
q2y (m) @ t=1.38	-2.009	q2y (m) @ t=1.84	-2.323	q2y (m) @ t=2.3	-2.454
q2x (m) @ t=1.4	0.013	q2x (m) @ t=1.86	0.246	q2x (m) @ t=2.32	0.150
q2y (m) @ t=1.4	-2.021	q2y (m) @ t=1.86	-2.250	q2y (m) @ t=2.32	-2.395
q2x (m) @ t=1.42	0.106	q2x (m) @ t=1.88	0.255	q2x (m) @ t=2.34	0.065
q2y (m) @ t=1.42	-2.002	q2y (m) @ t=1.88	-2.169	q2y (m) @ t=2.34	-2.360
q2x (m) @ t=1.44	0.183	q2x (m) @ t=1.9	0.231	q2x (m) @ t=2.36	-0.034
q2y (m) @ t=1.44	-1.955	q2y (m) @ t=1.9	-2.090	q2y (m) @ t=2.36	-2.355
q2x (m) @ t=1.46	0.234	q2x (m) @ t=1.92	0.178	q2x (m) @ t=2.38	-0.135
q2y (m) @ t=1.46	-1.887	q2y (m) @ t=1.92	-2.023	q2y (m) @ t=2.38	-2.382
q2x (m) @ t=1.48	0.255	q2x (m) @ t=1.94	0.100	q2x (m) @ t=2.4	-0.229
q2y (m) @ t=1.48	-1.808	q2y (m) @ t=1.94	-1.978	q2y (m) @ t=2.4	-2.441
q2x (m) @ t=1.5	0.244	q2x (m) @ t=1.96	0.006	q2x (m) @ t=2.42	-0.306
q2y (m) @ t=1.5	-1.727	q2y (m) @ t=1.96	-1.961	q2y (m) @ t=2.42	-2.527
q2x (m) @ t=1.52	0.202	q2x (m) @ t=1.98	-0.096	q2x (m) @ t=2.44	-0.358
q2y (m) @ t=1.52	-1.655	q2y (m) @ t=1.98	-1.976	q2y (m) @ t=2.44	-2.634
q2x (m) @ t=1.54	0.133	q2x (m) @ t=2	-0.194	q2x (m) @ t=2.46	-0.380
q2y (m) @ t=1.54	-1.601	q2y (m) @ t=2	-2.022	q2y (m) @ t=2.46	-2.753
q2x (m) @ t=1.56	0.044	q2x (m) @ t=2.02	-0.278	q2x (m) @ t=2.48	-0.370
q2y (m) @ t=1.56	-1.572	q2y (m) @ t=2.02	-2.098	q2y (m) @ t=2.48	-2.874
q2x (m) @ t=1.58	-0.056	q2x (m) @ t=2.04	-0.341	q2x (m) @ t=2.5	-0.329
q2y (m) @ t=1.58	-1.574	q2y (m) @ t=2.04	-2.198	q2y (m) @ t=2.5	-2.987
q2x (m) @ t=1.6	-0.157	q2x (m) @ t=2.06	-0.375	q2x (m) @ t=2.52	-0.260
q2y (m) @ t=1.6	-1.608	q2y (m) @ t=2.06	-2.314	q2y (m) @ t=2.52	-3.082
q2x (m) @ t=1.62	-0.248	q2x (m) @ t=2.08	-0.378	q2x (m) @ t=2.54	-0.171
q2y (m) @ t=1.62	-1.673	q2y (m) @ t=2.08	-2.435	q2y (m) @ t=2.54	-3.151
q2x (m) @ t=1.64	-0.320	q2x (m) @ t=2.1	-0.348	q2x (m) @ t=2.56	-0.072
q2y (m) @ t=1.64	-1.765	q2y (m) @ t=2.1	-2.552	q2y (m) @ t=2.56	-3.190
q2x (m) @ t=1.66	-0.366	q2x (m) @ t=2.12	-0.289	q2x (m) @ t=2.58	0.029
q2y (m) @ t=1.66	-1.875	q2y (m) @ t=2.12	-2.655	q2y (m) @ t=2.58	-3.197
q2x (m) @ t=1.68	-0.381	q2x (m) @ t=2.14	-0.208	q2x (m) @ t=2.6	0.120
q2y (m) @ t=1.68	-1.996	q2y (m) @ t=2.14	-2.735	q2y (m) @ t=2.6	-3.173
q2x (m) @ t=1.7	-0.363	q2x (m) @ t=2.16	-0.111	q2x (m) @ t=2.62	0.193
q2y (m) @ t=1.7	-2.116	q2y (m) @ t=2.16	-2.787	q2y (m) @ t=2.62	-3.122
q2x (m) @ t=1.72	-0.315	q2x (m) @ t=2.18	-0.009	q2x (m) @ t=2.64	0.240
q2y (m) @ t=1.72	-2.225	q2y (m) @ t=2.18	-2.806	q2y (m) @ t=2.64	-3.052
q2x (m) @ t=1.74	-0.242	q2x (m) @ t=2.2	0.087	q2x (m) @ t=2.66	0.256
q2y (m) @ t=1.74	-2.315	q2y (m) @ t=2.2	-2.793	q2y (m) @ t=2.66	-2.971
q2x (m) @ t=1.76	-0.150	q2x (m) @ t=2.22	0.168	q2x (m) @ t=2.68	0.239
q2y (m) @ t=1.76	-2.378	q2y (m) @ t=2.22	-2.752	q2y (m) @ t=2.68	-2.891
q2x (m) @ t=1.78	-0.049	q2x (m) @ t=2.24	0.225	q2x (m) @ t=2.7	0.192
q2y (m) @ t=1.78	-2.410	q2y (m) @ t=2.24	-2.688	q2y (m) @ t=2.7	-2.821
q2x (m) @ t=1.8	0.051	q2x (m) @ t=2.26	0.254	q2x (m) @ t=2.72	0.119
q2y (m) @ t=1.8	-2.410	q2y (m) @ t=2.26	-2.611	q2y (m) @ t=2.72	-2.771
q2x (m) @ t=1.82	0.139	q2x (m) @ t=2.28	0.250	q2x (m) @ t=2.74	0.028
q2y (m) @ t=1.82	-2.379	q2y (m) @ t=2.28	-2.529	q2y (m) @ t=2.74	-2.747

doi:10.6844/NCKU202003198

q2x (m) @ t=2.76	-0.073	q2x (m) @ t=3.22	-0.349	q2x (m) @ t=3.68	-0.319
q2y (m) @ t=2.76	-2.754	q2y (m) @ t=3.22	-3.393	q2y (m) @ t=3.68	-4.180
q2x (m) @ t=2.78	-0.173	q2x (m) @ t=3.24	-0.378	q2x (m) @ t=3.7	-0.247
q2y (m) @ t=2.78	-2.793	q2y (m) @ t=3.24	-3.510	q2y (m) @ t=3.7	-4.272
q2x (m) @ t=2.8	-0.261	q2x (m) @ t=3.26	-0.375	q2x (m) @ t=3.72	-0.156
q2y (m) @ t=2.8	-2.863	q2y (m) @ t=3.26	-3.632	q2y (m) @ t=3.72	-4.336
q2x (m) @ t=2.82	-0.329	q2x (m) @ t=3.28	-0.340	q2x (m) @ t=3.74	-0.055
q2y (m) @ t=2.82	-2.959	q2y (m) @ t=3.28	-3.747	q2y (m) @ t=3.74	-4.370
q2x (m) @ t=2.84	-0.370	q2x (m) @ t=3.3	-0.277	q2x (m) @ t=3.76	0.045
q2y (m) @ t=2.84	-3.071	q2y (m) @ t=3.3	-3.847	q2y (m) @ t=3.76	-4.372
q2x (m) @ t=2.86	-0.380	q2x (m) @ t=3.32	-0.193	q2x (m) @ t=3.78	0.134
q2y (m) @ t=2.86	-3.193	q2y (m) @ t=3.32	-3.923	q2y (m) @ t=3.78	-4.343
q2x (m) @ t=2.88	-0.357	q2x (m) @ t=3.34	-0.094	q2x (m) @ t=3.8	0.203
q2y (m) @ t=2.88	-3.312	q2y (m) @ t=3.34	-3.969	q2y (m) @ t=3.8	-4.288
q2x (m) @ t=2.9	-0.305	q2x (m) @ t=3.36	0.007	q2x (m) @ t=3.82	0.245
q2y (m) @ t=2.9	-3.418	q2y (m) @ t=3.36	-3.983	q2y (m) @ t=3.82	-4.216
q2x (m) @ t=2.92	-0.228	q2x (m) @ t=3.38	0.101	q2x (m) @ t=3.84	0.255
q2y (m) @ t=2.92	-3.504	q2y (m) @ t=3.38	-3.965	q2y (m) @ t=3.84	-4.135
q2x (m) @ t=2.94	-0.133	q2x (m) @ t=3.4	0.179	q2x (m) @ t=3.86	0.234
q2y (m) @ t=2.94	-3.562	q2y (m) @ t=3.4	-3.920	q2y (m) @ t=3.86	-4.056
q2x (m) @ t=2.96	-0.032	q2x (m) @ t=3.42	0.232	q2x (m) @ t=3.88	0.182
q2y (m) @ t=2.96	-3.589	q2y (m) @ t=3.42	-3.853	q2y (m) @ t=3.88	-3.988
q2x (m) @ t=2.98	0.066	q2x (m) @ t=3.44	0.255	q2x (m) @ t=3.9	0.106
q2y (m) @ t=2.98	-3.583	q2y (m) @ t=3.44	-3.774	q2y (m) @ t=3.9	-3.942
q2x (m) @ t=3	0.151	q2x (m) @ t=3.46	0.246	q2x (m) @ t=3.92	0.012
q2y (m) @ t=3	-3.548	q2y (m) @ t=3.46	-3.693	q2y (m) @ t=3.92	-3.923
q2x (m) @ t=3.02	0.215	q2x (m) @ t=3.48	0.205	q2x (m) @ t=3.94	-0.089
q2y (m) @ t=3.02	-3.489	q2y (m) @ t=3.48	-3.620	q2y (m) @ t=3.94	-3.935
q2x (m) @ t=3.04	0.250	q2x (m) @ t=3.5	0.138	q2x (m) @ t=3.96	-0.188
q2y (m) @ t=3.04	-3.413	q2y (m) @ t=3.5	-3.564	q2y (m) @ t=3.96	-3.980
q2x (m) @ t=3.06	0.253	q2x (m) @ t=3.52	0.050	q2x (m) @ t=3.98	-0.274
q2y (m) @ t=3.06	-3.332	q2y (m) @ t=3.52	-3.534	q2y (m) @ t=3.98	-4.054
q2x (m) @ t=3.08	0.225	q2x (m) @ t=3.54	-0.050	q2x (m) @ t=4	-0.338
q2y (m) @ t=3.08	-3.255	q2y (m) @ t=3.54	-3.534	q2y (m) @ t=4	-4.153
q2x (m) @ t=3.1	0.167	q2x (m) @ t=3.56	-0.151		
q2y (m) @ t=3.1	-3.191	q2y (m) @ t=3.56	-3.566		
q2x (m) @ t=3.12	0.085	q2x (m) @ t=3.58	-0.243		
q2y (m) @ t=3.12	-3.150	q2y (m) @ t=3.58	-3.630		
q2x (m) @ t=3.14	-0.011	q2x (m) @ t=3.6	-0.316		
q2y (m) @ t=3.14	-3.138	q2y (m) @ t=3.6	-3.720		
q2x (m) @ t=3.16	-0.112	q2x (m) @ t=3.62	-0.364		
q2y (m) @ t=3.16	-3.158	q2y (m) @ t=3.62	-3.830		
q2x (m) @ t=3.18	-0.209	q2x (m) @ t=3.64	-0.381		
q2y (m) @ t=3.18	-3.209	q2y (m) @ t=3.64	-3.950		
q2x (m) @ t=3.2	-0.290	q2x (m) @ t=3.66	-0.365		
q2y (m) @ t=3.2	-3.290	q2y (m) @ t=3.66	-4.070		

C.2 Electron trajectory with the electric field

1. The initial positions: $0\hat{x} + 0\hat{y} + 3.8\hat{z}$ (mm).

2. The initial velocities: $0\hat{x} + 0\hat{y} + 0\hat{z}$ (m/s).

3. V_{acc}: 500 V, 750 V, and 1000 V.

doi:10.6844/NCKU202003198

4. The total simulated time: 5×10^{-10} (s).

5. Steps: 1001.

6. qz is the position in $\hat{z}$.

Table 18: Raw data of electron trajectories with $V_{\text{acc}} = 500$ V.

qz (mm) @ t=0	3.80000	qz (mm) @ t=2.3E-11	3.79319
qz (mm) @ t=5E-13	3.80000	qz (mm) @ t=2.35E-11	3.79289
qz (mm) @ t=1E-12	3.79999	qz (mm) @ t=2.4E-11	3.79258
qz (mm) @ t=1.5E-12	3.79997	qz (mm) @ t=2.45E-11	3.79227
qz (mm) @ t=2E-12	3.79995	qz (mm) @ t=2.5E-11	3.79195
qz (mm) @ t=2.5E-12	3.79992	qz (mm) @ t=2.55E-11	3.79163
qz (mm) @ t=3E-12	3.79988	qz (mm) @ t=2.6E-11	3.79129
qz (mm) @ t=3.5E-12	3.79984	qz (mm) @ t=2.65E-11	3.79096
qz (mm) @ t=4E-12	3.79979	qz (mm) @ t=2.7E-11	3.79061
qz (mm) @ t=4.5E-12	3.79974	qz (mm) @ t=2.75E-11	3.79026
qz (mm) @ t=5E-12	3.79968	qz (mm) @ t=2.8E-11	3.78990
qz (mm) @ t=5.5E-12	3.79961	qz (mm) @ t=2.85E-11	3.78954
qz (mm) @ t=6E-12	3.79954	qz (mm) @ t=2.9E-11	3.78917
qz (mm) @ t=6.5E-12	3.79946	qz (mm) @ t=2.95E-11	3.78879
qz (mm) @ t=7E-12	3.79937	qz (mm) @ t=3E-11	3.78841
qz (mm) @ t=7.5E-12	3.79928	qz (mm) @ t=3.05E-11	3.78802
qz (mm) @ t=8E-12	3.79918	qz (mm) @ t=3.1E-11	3.78762
qz (mm) @ t=8.5E-12	3.79907	qz (mm) @ t=3.15E-11	3.78722
qz (mm) @ t=9E-12	3.79896	qz (mm) @ t=3.2E-11	3.78681
qz (mm) @ t=9.5E-12	3.79884	qz (mm) @ t=3.25E-11	3.78640
qz (mm) @ t=1E-11	3.79871	qz (mm) @ t=3.3E-11	3.78598
qz (mm) @ t=1.05E-11	3.79858	qz (mm) @ t=3.35E-11	3.78555
qz (mm) @ t=1.1E-11	3.79844	qz (mm) @ t=3.4E-11	3.78511
qz (mm) @ t=1.15E-11	3.79830	qz (mm) @ t=3.45E-11	3.78467
qz (mm) @ t=1.2E-11	3.79815	qz (mm) @ t=3.5E-11	3.78422
qz (mm) @ t=1.25E-11	3.79799	qz (mm) @ t=3.55E-11	3.78377
qz (mm) @ t=1.3E-11	3.79782	qz (mm) @ t=3.6E-11	3.78331
qz (mm) @ t=1.35E-11	3.79765	qz (mm) @ t=3.65E-11	3.78284
qz (mm) @ t=1.4E-11	3.79748	qz (mm) @ t=3.7E-11	3.78237
qz (mm) @ t=1.45E-11	3.79729	qz (mm) @ t=3.75E-11	3.78189
qz (mm) @ t=1.5E-11	3.79710	qz (mm) @ t=3.8E-11	3.78140
qz (mm) @ t=1.55E-11	3.79691	qz (mm) @ t=3.85E-11	3.78091
qz (mm) @ t=1.6E-11	3.79670	qz (mm) @ t=3.9E-11	3.78041
qz (mm) @ t=1.65E-11	3.79649	qz (mm) @ t=3.95E-11	3.77991
qz (mm) @ t=1.7E-11	3.79628	qz (mm) @ t=4E-11	3.77940
qz (mm) @ t=1.75E-11	3.79606	qz (mm) @ t=4.05E-11	3.77888
qz (mm) @ t=1.8E-11	3.79583	qz (mm) @ t=4.1E-11	3.77835
qz (mm) @ t=1.85E-11	3.79559	qz (mm) @ t=4.15E-11	3.77782
qz (mm) @ t=1.9E-11	3.79535	qz (mm) @ t=4.2E-11	3.77728
qz (mm) @ t=1.95E-11	3.79510	qz (mm) @ t=4.25E-11	3.77674
qz (mm) @ t=2E-11	3.79485	qz (mm) @ t=4.3E-11	3.77619
qz (mm) @ t=2.05E-11	3.79459	qz (mm) @ t=4.35E-11	3.77563
qz (mm) @ t=2.1E-11	3.79432	qz (mm) @ t=4.4E-11	3.77507
qz (mm) @ t=2.15E-11	3.79405	qz (mm) @ t=4.45E-11	3.77450
qz (mm) @ t=2.2E-11	3.79377	qz (mm) @ t=4.5E-11	3.77392
qz (mm) @ t=2.25E-11	3.79348	qz (mm) @ t=4.55E-11	3.77334

doi:10.6844/NCKU202003198

qz (mm) @ t=4.6E-11	3.77275	qz (mm) @ t=6.9E-11	3.73869
qz (mm) @ t=4.65E-11	3.77215	qz (mm) @ t=6.95E-11	3.73780
qz (mm) @ t=4.7E-11	3.77155	qz (mm) @ t=7E-11	3.73690
qz (mm) @ t=4.75E-11	3.77094	qz (mm) @ t=7.05E-11	3.73600
qz (mm) @ t=4.8E-11	3.77033	qz (mm) @ t=7.1E-11	3.73508
qz (mm) @ t=4.85E-11	3.76971	qz (mm) @ t=7.15E-11	3.73417
qz (mm) @ t=4.9E-11	3.76908	qz (mm) @ t=7.2E-11	3.73324
qz (mm) @ t=4.95E-11	3.76845	qz (mm) @ t=7.25E-11	3.73231
qz (mm) @ t=5E-11	3.76781	qz (mm) @ t=7.3E-11	3.73138
qz (mm) @ t=5.05E-11	3.76716	qz (mm) @ t=7.35E-11	3.73043
qz (mm) @ t=5.1E-11	3.76650	qz (mm) @ t=7.4E-11	3.72948
qz (mm) @ t=5.15E-11	3.76584	qz (mm) @ t=7.45E-11	3.72853
qz (mm) @ t=5.2E-11	3.76518	qz (mm) @ t=7.5E-11	3.72756
qz (mm) @ t=5.25E-11	3.76451	qz (mm) @ t=7.55E-11	3.72660
qz (mm) @ t=5.3E-11	3.76383	qz (mm) @ t=7.6E-11	3.72562
qz (mm) @ t=5.35E-11	3.76314	qz (mm) @ t=7.65E-11	3.72464
qz (mm) @ t=5.4E-11	3.76245	qz (mm) @ t=7.7E-11	3.72365
qz (mm) @ t=5.45E-11	3.76175	qz (mm) @ t=7.75E-11	3.72266
qz (mm) @ t=5.5E-11	3.76104	qz (mm) @ t=7.8E-11	3.72165
qz (mm) @ t=5.55E-11	3.76033	qz (mm) @ t=7.85E-11	3.72065
qz (mm) @ t=5.6E-11	3.75962	qz (mm) @ t=7.9E-11	3.71963
qz (mm) @ t=5.65E-11	3.75889	qz (mm) @ t=7.95E-11	3.71861
qz (mm) @ t=5.7E-11	3.75816	qz (mm) @ t=8E-11	3.71759
qz (mm) @ t=5.75E-11	3.75742	qz (mm) @ t=8.05E-11	3.71655
qz (mm) @ t=5.8E-11	3.75668	qz (mm) @ t=8.1E-11	3.71551
qz (mm) @ t=5.85E-11	3.75593	qz (mm) @ t=8.15E-11	3.71447
qz (mm) @ t=5.9E-11	3.75517	qz (mm) @ t=8.2E-11	3.71341
qz (mm) @ t=5.95E-11	3.75441	qz (mm) @ t=8.25E-11	3.71235
qz (mm) @ t=6E-11	3.75364	qz (mm) @ t=8.3E-11	3.71129
qz (mm) @ t=6.05E-11	3.75286	qz (mm) @ t=8.35E-11	3.71022
qz (mm) @ t=6.1E-11	3.75208	qz (mm) @ t=8.4E-11	3.70914
qz (mm) @ t=6.15E-11	3.75129	qz (mm) @ t=8.45E-11	3.70805
qz (mm) @ t=6.2E-11	3.75050	qz (mm) @ t=8.5E-11	3.70696
qz (mm) @ t=6.25E-11	3.74970	qz (mm) @ t=8.55E-11	3.70586
qz (mm) @ t=6.3E-11	3.74889	qz (mm) @ t=8.6E-11	3.70476
qz (mm) @ t=6.35E-11	3.74807	qz (mm) @ t=8.65E-11	3.70365
qz (mm) @ t=6.4E-11	3.74725	qz (mm) @ t=8.7E-11	3.70253
qz (mm) @ t=6.45E-11	3.74643	qz (mm) @ t=8.75E-11	3.70141
qz (mm) @ t=6.5E-11	3.74559	qz (mm) @ t=8.8E-11	3.70028
qz (mm) @ t=6.55E-11	3.74475	qz (mm) @ t=8.85E-11	3.69914
qz (mm) @ t=6.6E-11	3.74391	qz (mm) @ t=8.9E-11	3.69800
qz (mm) @ t=6.65E-11	3.74305	qz (mm) @ t=8.95E-11	3.69685
qz (mm) @ t=6.7E-11	3.74219	qz (mm) @ t=9E-11	3.69570
qz (mm) @ t=6.75E-11	3.74133	qz (mm) @ t=9.05E-11	3.69453
qz (mm) @ t=6.8E-11	3.74045	qz (mm) @ t=9.1E-11	3.69337
qz (mm) @ t=6.85E-11	3.73958	qz (mm) @ t=9.15E-11	3.69219

doi:10.6844/NCKU202003198

qz (mm) @ t=9.2E-11	3.69101	qz (mm) @ t=1.15E-10	3.62971
qz (mm) @ t=9.25E-11	3.68982	qz (mm) @ t=1.155E-10	3.62823
qz (mm) @ t=9.3E-11	3.68863	qz (mm) @ t=1.16E-10	3.62674
qz (mm) @ t=9.35E-11	3.68743	qz (mm) @ t=1.165E-10	3.62524
qz (mm) @ t=9.4E-11	3.68622	qz (mm) @ t=1.17E-10	3.62374
qz (mm) @ t=9.45E-11	3.68501	qz (mm) @ t=1.175E-10	3.62223
qz (mm) @ t=9.5E-11	3.68379	qz (mm) @ t=1.18E-10	3.62071
qz (mm) @ t=9.55E-11	3.68256	qz (mm) @ t=1.185E-10	3.61919
qz (mm) @ t=9.6E-11	3.68133	qz (mm) @ t=1.19E-10	3.61766
qz (mm) @ t=9.65E-11	3.68009	qz (mm) @ t=1.195E-10	3.61613
qz (mm) @ t=9.7E-11	3.67884	qz (mm) @ t=1.2E-10	3.61458
qz (mm) @ t=9.75E-11	3.67759	qz (mm) @ t=1.205E-10	3.61304
qz (mm) @ t=9.8E-11	3.67633	qz (mm) @ t=1.21E-10	3.61148
qz (mm) @ t=9.85E-11	3.67507	qz (mm) @ t=1.215E-10	3.60992
qz (mm) @ t=9.9E-11	3.67379	qz (mm) @ t=1.22E-10	3.60835
qz (mm) @ t=9.95E-11	3.67252	qz (mm) @ t=1.225E-10	3.60678
qz (mm) @ t=1E-10	3.67123	qz (mm) @ t=1.23E-10	3.60520
qz (mm) @ t=1.005E-10	3.66994	qz (mm) @ t=1.235E-10	3.60361
qz (mm) @ t=1.01E-10	3.66864	qz (mm) @ t=1.24E-10	3.60202
qz (mm) @ t=1.015E-10	3.66734	qz (mm) @ t=1.245E-10	3.60042
qz (mm) @ t=1.02E-10	3.66603	qz (mm) @ t=1.25E-10	3.59881
qz (mm) @ t=1.025E-10	3.66471	qz (mm) @ t=1.255E-10	3.59720
qz (mm) @ t=1.03E-10	3.66339	qz (mm) @ t=1.26E-10	3.59558
qz (mm) @ t=1.035E-10	3.66206	qz (mm) @ t=1.265E-10	3.59396
qz (mm) @ t=1.04E-10	3.66073	qz (mm) @ t=1.27E-10	3.59233
qz (mm) @ t=1.045E-10	3.65938	qz (mm) @ t=1.275E-10	3.59069
qz (mm) @ t=1.05E-10	3.65804	qz (mm) @ t=1.28E-10	3.58904
qz (mm) @ t=1.055E-10	3.65668	qz (mm) @ t=1.285E-10	3.58739
qz (mm) @ t=1.06E-10	3.65532	qz (mm) @ t=1.29E-10	3.58573
qz (mm) @ t=1.065E-10	3.65395	qz (mm) @ t=1.295E-10	3.58407
qz (mm) @ t=1.07E-10	3.65258	qz (mm) @ t=1.3E-10	3.58240
qz (mm) @ t=1.075E-10	3.65120	qz (mm) @ t=1.305E-10	3.58072
qz (mm) @ t=1.08E-10	3.64981	qz (mm) @ t=1.31E-10	3.57904
qz (mm) @ t=1.085E-10	3.64841	qz (mm) @ t=1.315E-10	3.57735
qz (mm) @ t=1.09E-10	3.64701	qz (mm) @ t=1.32E-10	3.57565
qz (mm) @ t=1.095E-10	3.64561	qz (mm) @ t=1.325E-10	3.57395
qz (mm) @ t=1.1E-10	3.64419	qz (mm) @ t=1.33E-10	3.57224
qz (mm) @ t=1.105E-10	3.64278	qz (mm) @ t=1.335E-10	3.57053
qz (mm) @ t=1.11E-10	3.64135	qz (mm) @ t=1.34E-10	3.56881
qz (mm) @ t=1.115E-10	3.63992	qz (mm) @ t=1.345E-10	3.56708
qz (mm) @ t=1.12E-10	3.63848	qz (mm) @ t=1.35E-10	3.56534
qz (mm) @ t=1.125E-10	3.63703	qz (mm) @ t=1.355E-10	3.56360
qz (mm) @ t=1.13E-10	3.63558	qz (mm) @ t=1.36E-10	3.56186
qz (mm) @ t=1.135E-10	3.63412	qz (mm) @ t=1.365E-10	3.56010
qz (mm) @ t=1.14E-10	3.63266	qz (mm) @ t=1.37E-10	3.55834
qz (mm) @ t=1.145E-10	3.63119	qz (mm) @ t=1.375E-10	3.55657

doi:10.6844/NCKU202003198

qz (mm) @ t=1.38E-10	3.55480	qz (mm) @ t=1.61E-10	3.46629
qz (mm) @ t=1.385E-10	3.55302	qz (mm) @ t=1.615E-10	3.46421
qz (mm) @ t=1.39E-10	3.55124	qz (mm) @ t=1.62E-10	3.46213
qz (mm) @ t=1.395E-10	3.54944	qz (mm) @ t=1.625E-10	3.46004
qz (mm) @ t=1.4E-10	3.54764	qz (mm) @ t=1.63E-10	3.45795
qz (mm) @ t=1.405E-10	3.54584	qz (mm) @ t=1.635E-10	3.45585
qz (mm) @ t=1.41E-10	3.54403	qz (mm) @ t=1.64E-10	3.45374
qz (mm) @ t=1.415E-10	3.54221	qz (mm) @ t=1.645E-10	3.45163
qz (mm) @ t=1.42E-10	3.54038	qz (mm) @ t=1.65E-10	3.44951
qz (mm) @ t=1.425E-10	3.53855	qz (mm) @ t=1.655E-10	3.44738
qz (mm) @ t=1.43E-10	3.53672	qz (mm) @ t=1.66E-10	3.44525
qz (mm) @ t=1.435E-10	3.53487	qz (mm) @ t=1.665E-10	3.44311
qz (mm) @ t=1.44E-10	3.53302	qz (mm) @ t=1.67E-10	3.44096
qz (mm) @ t=1.445E-10	3.53117	qz (mm) @ t=1.675E-10	3.43881
qz (mm) @ t=1.45E-10	3.52930	qz (mm) @ t=1.68E-10	3.43665
qz (mm) @ t=1.455E-10	3.52743	qz (mm) @ t=1.685E-10	3.43449
qz (mm) @ t=1.46E-10	3.52556	qz (mm) @ t=1.69E-10	3.43232
qz (mm) @ t=1.465E-10	3.52367	qz (mm) @ t=1.695E-10	3.43014
qz (mm) @ t=1.47E-10	3.52179	qz (mm) @ t=1.7E-10	3.42795
qz (mm) @ t=1.475E-10	3.51989	qz (mm) @ t=1.705E-10	3.42576
qz (mm) @ t=1.48E-10	3.51799	qz (mm) @ t=1.71E-10	3.42357
qz (mm) @ t=1.485E-10	3.51608	qz (mm) @ t=1.715E-10	3.42136
qz (mm) @ t=1.49E-10	3.51417	qz (mm) @ t=1.72E-10	3.41915
qz (mm) @ t=1.495E-10	3.51224	qz (mm) @ t=1.725E-10	3.41694
qz (mm) @ t=1.5E-10	3.51032	qz (mm) @ t=1.73E-10	3.41471
qz (mm) @ t=1.505E-10	3.50838	qz (mm) @ t=1.735E-10	3.41248
qz (mm) @ t=1.51E-10	3.50644	qz (mm) @ t=1.74E-10	3.41025
qz (mm) @ t=1.515E-10	3.50450	qz (mm) @ t=1.745E-10	3.40801
qz (mm) @ t=1.52E-10	3.50254	qz (mm) @ t=1.75E-10	3.40576
qz (mm) @ t=1.525E-10	3.50058	qz (mm) @ t=1.755E-10	3.40350
qz (mm) @ t=1.53E-10	3.49862	qz (mm) @ t=1.76E-10	3.40124
qz (mm) @ t=1.535E-10	3.49665	qz (mm) @ t=1.765E-10	3.39897
qz (mm) @ t=1.54E-10	3.49467	qz (mm) @ t=1.77E-10	3.39670
qz (mm) @ t=1.545E-10	3.49268	qz (mm) @ t=1.775E-10	3.39442
qz (mm) @ t=1.55E-10	3.49069	qz (mm) @ t=1.78E-10	3.39213
qz (mm) @ t=1.555E-10	3.48869	qz (mm) @ t=1.785E-10	3.38984
qz (mm) @ t=1.56E-10	3.48669	qz (mm) @ t=1.79E-10	3.38754
qz (mm) @ t=1.565E-10	3.48468	qz (mm) @ t=1.795E-10	3.38523
qz (mm) @ t=1.57E-10	3.48266	qz (mm) @ t=1.8E-10	3.38292
qz (mm) @ t=1.575E-10	3.48064	qz (mm) @ t=1.805E-10	3.38060
qz (mm) @ t=1.58E-10	3.47861	qz (mm) @ t=1.81E-10	3.37827
qz (mm) @ t=1.585E-10	3.47657	qz (mm) @ t=1.815E-10	3.37594
qz (mm) @ t=1.59E-10	3.47453	qz (mm) @ t=1.82E-10	3.37360
qz (mm) @ t=1.595E-10	3.47248	qz (mm) @ t=1.825E-10	3.37126
qz (mm) @ t=1.6E-10	3.47042	qz (mm) @ t=1.83E-10	3.36891
qz (mm) @ t=1.605E-10	3.46836	qz (mm) @ t=1.835E-10	3.36655

doi:10.6844/NCKU202003198

qz (mm) @ t=1.84E-10	3.36419	qz (mm) @ t=2.07E-10	3.24851
qz (mm) @ t=1.845E-10	3.36182	qz (mm) @ t=2.075E-10	3.24584
qz (mm) @ t=1.85E-10	3.35944	qz (mm) @ t=2.08E-10	3.24317
qz (mm) @ t=1.855E-10	3.35706	qz (mm) @ t=2.085E-10	3.24049
qz (mm) @ t=1.86E-10	3.35467	qz (mm) @ t=2.09E-10	3.23781
qz (mm) @ t=1.865E-10	3.35227	qz (mm) @ t=2.095E-10	3.23512
qz (mm) @ t=1.87E-10	3.34987	qz (mm) @ t=2.1E-10	3.23242
qz (mm) @ t=1.875E-10	3.34746	qz (mm) @ t=2.105E-10	3.22972
qz (mm) @ t=1.88E-10	3.34504	qz (mm) @ t=2.11E-10	3.22701
qz (mm) @ t=1.885E-10	3.34262	qz (mm) @ t=2.115E-10	3.22429
qz (mm) @ t=1.89E-10	3.34019	qz (mm) @ t=2.12E-10	3.22157
qz (mm) @ t=1.895E-10	3.33776	qz (mm) @ t=2.125E-10	3.21884
qz (mm) @ t=1.9E-10	3.33532	qz (mm) @ t=2.13E-10	3.21610
qz (mm) @ t=1.905E-10	3.33287	qz (mm) @ t=2.135E-10	3.21336
qz (mm) @ t=1.91E-10	3.33042	qz (mm) @ t=2.14E-10	3.21061
qz (mm) @ t=1.915E-10	3.32796	qz (mm) @ t=2.145E-10	3.20785
qz (mm) @ t=1.92E-10	3.32549	qz (mm) @ t=2.15E-10	3.20509
qz (mm) @ t=1.925E-10	3.32302	qz (mm) @ t=2.155E-10	3.20233
qz (mm) @ t=1.93E-10	3.32054	qz (mm) @ t=2.16E-10	3.19955
qz (mm) @ t=1.935E-10	3.31805	qz (mm) @ t=2.165E-10	3.19677
qz (mm) @ t=1.94E-10	3.31556	qz (mm) @ t=2.17E-10	3.19398
qz (mm) @ t=1.945E-10	3.31306	qz (mm) @ t=2.175E-10	3.19119
qz (mm) @ t=1.95E-10	3.31055	qz (mm) @ t=2.18E-10	3.18839
qz (mm) @ t=1.955E-10	3.30804	qz (mm) @ t=2.185E-10	3.18558
qz (mm) @ t=1.96E-10	3.30552	qz (mm) @ t=2.19E-10	3.18277
qz (mm) @ t=1.965E-10	3.30300	qz (mm) @ t=2.195E-10	3.17995
qz (mm) @ t=1.97E-10	3.30047	qz (mm) @ t=2.2E-10	3.17713
qz (mm) @ t=1.975E-10	3.29793	qz (mm) @ t=2.205E-10	3.17430
qz (mm) @ t=1.98E-10	3.29539	qz (mm) @ t=2.21E-10	3.17146
qz (mm) @ t=1.985E-10	3.29284	qz (mm) @ t=2.215E-10	3.16861
qz (mm) @ t=1.99E-10	3.29028	qz (mm) @ t=2.22E-10	3.16576
qz (mm) @ t=1.995E-10	3.28772	qz (mm) @ t=2.225E-10	3.16290
qz (mm) @ t=2E-10	3.28515	qz (mm) @ t=2.23E-10	3.16004
qz (mm) @ t=2.005E-10	3.28257	qz (mm) @ t=2.235E-10	3.15717
qz (mm) @ t=2.01E-10	3.27999	qz (mm) @ t=2.24E-10	3.15429
qz (mm) @ t=2.015E-10	3.27740	qz (mm) @ t=2.245E-10	3.15141
qz (mm) @ t=2.02E-10	3.27481	qz (mm) @ t=2.25E-10	3.14852
qz (mm) @ t=2.025E-10	3.27221	qz (mm) @ t=2.255E-10	3.14563
qz (mm) @ t=2.03E-10	3.26960	qz (mm) @ t=2.26E-10	3.14272
qz (mm) @ t=2.035E-10	3.26699	qz (mm) @ t=2.265E-10	3.13981
qz (mm) @ t=2.04E-10	3.26437	qz (mm) @ t=2.27E-10	3.13690
qz (mm) @ t=2.045E-10	3.26174	qz (mm) @ t=2.275E-10	3.13398
qz (mm) @ t=2.05E-10	3.25910	qz (mm) @ t=2.28E-10	3.13105
qz (mm) @ t=2.055E-10	3.25647	qz (mm) @ t=2.285E-10	3.12812
qz (mm) @ t=2.06E-10	3.25382	qz (mm) @ t=2.29E-10	3.12518
qz (mm) @ t=2.065E-10	3.25117	qz (mm) @ t=2.295E-10	3.12223

doi:10.6844/NCKU202003198

qz (mm) @ t=2.3E-10	3.11928	qz (mm) @ t=2.53E-10	2.97652
qz (mm) @ t=2.305E-10	3.11632	qz (mm) @ t=2.535E-10	2.97326
qz (mm) @ t=2.31E-10	3.11335	qz (mm) @ t=2.54E-10	2.97000
qz (mm) @ t=2.315E-10	3.11038	qz (mm) @ t=2.545E-10	2.96674
qz (mm) @ t=2.32E-10	3.10740	qz (mm) @ t=2.55E-10	2.96346
qz (mm) @ t=2.325E-10	3.10441	qz (mm) @ t=2.555E-10	2.96018
qz (mm) @ t=2.33E-10	3.10142	qz (mm) @ t=2.56E-10	2.95690
qz (mm) @ t=2.335E-10	3.09842	qz (mm) @ t=2.565E-10	2.95361
qz (mm) @ t=2.34E-10	3.09542	qz (mm) @ t=2.57E-10	2.95031
qz (mm) @ t=2.345E-10	3.09241	qz (mm) @ t=2.575E-10	2.94701
qz (mm) @ t=2.35E-10	3.08939	qz (mm) @ t=2.58E-10	2.94369
qz (mm) @ t=2.355E-10	3.08637	qz (mm) @ t=2.585E-10	2.94038
qz (mm) @ t=2.36E-10	3.08334	qz (mm) @ t=2.59E-10	2.93705
qz (mm) @ t=2.365E-10	3.08030	qz (mm) @ t=2.595E-10	2.93372
qz (mm) @ t=2.37E-10	3.07726	qz (mm) @ t=2.6E-10	2.93039
qz (mm) @ t=2.375E-10	3.07421	qz (mm) @ t=2.605E-10	2.92704
qz (mm) @ t=2.38E-10	3.07115	qz (mm) @ t=2.61E-10	2.92370
qz (mm) @ t=2.385E-10	3.06809	qz (mm) @ t=2.615E-10	2.92034
qz (mm) @ t=2.39E-10	3.06502	qz (mm) @ t=2.62E-10	2.91698
qz (mm) @ t=2.395E-10	3.06195	qz (mm) @ t=2.625E-10	2.91361
qz (mm) @ t=2.4E-10	3.05887	qz (mm) @ t=2.63E-10	2.91024
qz (mm) @ t=2.405E-10	3.05578	qz (mm) @ t=2.635E-10	2.90685
qz (mm) @ t=2.41E-10	3.05268	qz (mm) @ t=2.64E-10	2.90347
qz (mm) @ t=2.415E-10	3.04958	qz (mm) @ t=2.645E-10	2.90007
qz (mm) @ t=2.42E-10	3.04648	qz (mm) @ t=2.65E-10	2.89667
qz (mm) @ t=2.425E-10	3.04336	qz (mm) @ t=2.655E-10	2.89327
qz (mm) @ t=2.43E-10	3.04025	qz (mm) @ t=2.66E-10	2.88985
qz (mm) @ t=2.435E-10	3.03712	qz (mm) @ t=2.665E-10	2.88644
qz (mm) @ t=2.44E-10	3.03399	qz (mm) @ t=2.67E-10	2.88301
qz (mm) @ t=2.445E-10	3.03085	qz (mm) @ t=2.675E-10	2.87958
qz (mm) @ t=2.45E-10	3.02770	qz (mm) @ t=2.68E-10	2.87614
qz (mm) @ t=2.455E-10	3.02455	qz (mm) @ t=2.685E-10	2.87270
qz (mm) @ t=2.46E-10	3.02139	qz (mm) @ t=2.69E-10	2.86924
qz (mm) @ t=2.465E-10	3.01823	qz (mm) @ t=2.695E-10	2.86579
qz (mm) @ t=2.47E-10	3.01506	qz (mm) @ t=2.7E-10	2.86232
qz (mm) @ t=2.475E-10	3.01188	qz (mm) @ t=2.705E-10	2.85885
qz (mm) @ t=2.48E-10	3.00870	qz (mm) @ t=2.71E-10	2.85538
qz (mm) @ t=2.485E-10	3.00551	qz (mm) @ t=2.715E-10	2.85189
qz (mm) @ t=2.49E-10	3.00231	qz (mm) @ t=2.72E-10	2.84841
qz (mm) @ t=2.495E-10	2.99911	qz (mm) @ t=2.725E-10	2.84491
qz (mm) @ t=2.5E-10	2.99590	qz (mm) @ t=2.73E-10	2.84141
qz (mm) @ t=2.505E-10	2.99269	qz (mm) @ t=2.735E-10	2.83790
qz (mm) @ t=2.51E-10	2.98947	qz (mm) @ t=2.74E-10	2.83439
qz (mm) @ t=2.515E-10	2.98624	qz (mm) @ t=2.745E-10	2.83086
qz (mm) @ t=2.52E-10	2.98300	qz (mm) @ t=2.75E-10	2.82734
qz (mm) @ t=2.525E-10	2.97976	qz (mm) @ t=2.755E-10	2.82380

doi:10.6844/NCKU202003198

qz (mm) @ t=2.76E-10	2.82026	qz (mm) @ t=2.99E-10	2.65056
qz (mm) @ t=2.765E-10	2.81672	qz (mm) @ t=2.995E-10	2.64672
qz (mm) @ t=2.77E-10	2.81316	qz (mm) @ t=3E-10	2.64287
qz (mm) @ t=2.775E-10	2.80961	qz (mm) @ t=3.005E-10	2.63902
qz (mm) @ t=2.78E-10	2.80604	qz (mm) @ t=3.01E-10	2.63517
qz (mm) @ t=2.785E-10	2.80247	qz (mm) @ t=3.015E-10	2.63130
qz (mm) @ t=2.79E-10	2.79889	qz (mm) @ t=3.02E-10	2.62743
qz (mm) @ t=2.795E-10	2.79531	qz (mm) @ t=3.025E-10	2.62356
qz (mm) @ t=2.8E-10	2.79171	qz (mm) @ t=3.03E-10	2.61967
qz (mm) @ t=2.805E-10	2.78812	qz (mm) @ t=3.035E-10	2.61578
qz (mm) @ t=2.81E-10	2.78451	qz (mm) @ t=3.04E-10	2.61189
qz (mm) @ t=2.815E-10	2.78090	qz (mm) @ t=3.045E-10	2.60799
qz (mm) @ t=2.82E-10	2.77729	qz (mm) @ t=3.05E-10	2.60408
qz (mm) @ t=2.825E-10	2.77366	qz (mm) @ t=3.055E-10	2.60017
qz (mm) @ t=2.83E-10	2.77004	qz (mm) @ t=3.06E-10	2.59624
qz (mm) @ t=2.835E-10	2.76640	qz (mm) @ t=3.065E-10	2.59232
qz (mm) @ t=2.84E-10	2.76276	qz (mm) @ t=3.07E-10	2.58838
qz (mm) @ t=2.845E-10	2.75911	qz (mm) @ t=3.075E-10	2.58444
qz (mm) @ t=2.85E-10	2.75546	qz (mm) @ t=3.08E-10	2.58050
qz (mm) @ t=2.855E-10	2.75180	qz (mm) @ t=3.085E-10	2.57655
qz (mm) @ t=2.86E-10	2.74813	qz (mm) @ t=3.09E-10	2.57259
qz (mm) @ t=2.865E-10	2.74446	qz (mm) @ t=3.095E-10	2.56862
qz (mm) @ t=2.87E-10	2.74078	qz (mm) @ t=3.1E-10	2.56465
qz (mm) @ t=2.875E-10	2.73709	qz (mm) @ t=3.105E-10	2.56067
qz (mm) @ t=2.88E-10	2.73340	qz (mm) @ t=3.11E-10	2.55669
qz (mm) @ t=2.885E-10	2.72970	qz (mm) @ t=3.115E-10	2.55270
qz (mm) @ t=2.89E-10	2.72599	qz (mm) @ t=3.12E-10	2.54870
qz (mm) @ t=2.895E-10	2.72228	qz (mm) @ t=3.125E-10	2.54470
qz (mm) @ t=2.9E-10	2.71856	qz (mm) @ t=3.13E-10	2.54069
qz (mm) @ t=2.905E-10	2.71484	qz (mm) @ t=3.135E-10	2.53668
qz (mm) @ t=2.91E-10	2.71111	qz (mm) @ t=3.14E-10	2.53265
qz (mm) @ t=2.915E-10	2.70737	qz (mm) @ t=3.145E-10	2.52863
qz (mm) @ t=2.92E-10	2.70363	qz (mm) @ t=3.15E-10	2.52459
qz (mm) @ t=2.925E-10	2.69988	qz (mm) @ t=3.155E-10	2.52055
qz (mm) @ t=2.93E-10	2.69612	qz (mm) @ t=3.16E-10	2.51650
qz (mm) @ t=2.935E-10	2.69236	qz (mm) @ t=3.165E-10	2.51245
qz (mm) @ t=2.94E-10	2.68859	qz (mm) @ t=3.17E-10	2.50839
qz (mm) @ t=2.945E-10	2.68482	qz (mm) @ t=3.175E-10	2.50432
qz (mm) @ t=2.95E-10	2.68104	qz (mm) @ t=3.18E-10	2.50025
qz (mm) @ t=2.955E-10	2.67725	qz (mm) @ t=3.185E-10	2.49617
qz (mm) @ t=2.96E-10	2.67345	qz (mm) @ t=3.19E-10	2.49209
qz (mm) @ t=2.965E-10	2.66965	qz (mm) @ t=3.195E-10	2.48800
qz (mm) @ t=2.97E-10	2.66585	qz (mm) @ t=3.2E-10	2.48390
qz (mm) @ t=2.975E-10	2.66203	qz (mm) @ t=3.205E-10	2.47979
qz (mm) @ t=2.98E-10	2.65821	qz (mm) @ t=3.21E-10	2.47568
qz (mm) @ t=2.985E-10	2.65439	qz (mm) @ t=3.215E-10	2.47157

doi:10.6844/NCKU202003198

qz (mm) @ t=3.22E-10	2.46745	qz (mm) @ t=3.45E-10	2.27098
qz (mm) @ t=3.225E-10	2.46332	qz (mm) @ t=3.455E-10	2.26656
qz (mm) @ t=3.23E-10	2.45918	qz (mm) @ t=3.46E-10	2.26214
qz (mm) @ t=3.235E-10	2.45504	qz (mm) @ t=3.465E-10	2.25770
qz (mm) @ t=3.24E-10	2.45089	qz (mm) @ t=3.47E-10	2.25327
qz (mm) @ t=3.245E-10	2.44674	qz (mm) @ t=3.475E-10	2.24882
qz (mm) @ t=3.25E-10	2.44258	qz (mm) @ t=3.48E-10	2.24437
qz (mm) @ t=3.255E-10	2.43841	qz (mm) @ t=3.485E-10	2.23992
qz (mm) @ t=3.26E-10	2.43423	qz (mm) @ t=3.49E-10	2.23545
qz (mm) @ t=3.265E-10	2.43006	qz (mm) @ t=3.495E-10	2.23098
qz (mm) @ t=3.27E-10	2.42587	qz (mm) @ t=3.5E-10	2.22651
qz (mm) @ t=3.275E-10	2.42168	qz (mm) @ t=3.505E-10	2.22203
qz (mm) @ t=3.28E-10	2.41748	qz (mm) @ t=3.51E-10	2.21754
qz (mm) @ t=3.285E-10	2.41327	qz (mm) @ t=3.515E-10	2.21305
qz (mm) @ t=3.29E-10	2.40906	qz (mm) @ t=3.52E-10	2.20854
qz (mm) @ t=3.295E-10	2.40484	qz (mm) @ t=3.525E-10	2.20404
qz (mm) @ t=3.3E-10	2.40062	qz (mm) @ t=3.53E-10	2.19952
qz (mm) @ t=3.305E-10	2.39639	qz (mm) @ t=3.535E-10	2.19501
qz (mm) @ t=3.31E-10	2.39215	qz (mm) @ t=3.54E-10	2.19048
qz (mm) @ t=3.315E-10	2.38791	qz (mm) @ t=3.545E-10	2.18595
qz (mm) @ t=3.32E-10	2.38366	qz (mm) @ t=3.55E-10	2.18141
qz (mm) @ t=3.325E-10	2.37941	qz (mm) @ t=3.555E-10	2.17687
qz (mm) @ t=3.33E-10	2.37515	qz (mm) @ t=3.56E-10	2.17232
qz (mm) @ t=3.335E-10	2.37088	qz (mm) @ t=3.565E-10	2.16776
qz (mm) @ t=3.34E-10	2.36660	qz (mm) @ t=3.57E-10	2.16319
qz (mm) @ t=3.345E-10	2.36232	qz (mm) @ t=3.575E-10	2.15863
qz (mm) @ t=3.35E-10	2.35804	qz (mm) @ t=3.58E-10	2.15405
qz (mm) @ t=3.355E-10	2.35374	qz (mm) @ t=3.585E-10	2.14947
qz (mm) @ t=3.36E-10	2.34944	qz (mm) @ t=3.59E-10	2.14488
qz (mm) @ t=3.365E-10	2.34514	qz (mm) @ t=3.595E-10	2.14029
qz (mm) @ t=3.37E-10	2.34083	qz (mm) @ t=3.6E-10	2.13568
qz (mm) @ t=3.375E-10	2.33651	qz (mm) @ t=3.605E-10	2.13108
qz (mm) @ t=3.38E-10	2.33218	qz (mm) @ t=3.61E-10	2.12646
qz (mm) @ t=3.385E-10	2.32785	qz (mm) @ t=3.615E-10	2.12184
qz (mm) @ t=3.39E-10	2.32352	qz (mm) @ t=3.62E-10	2.11722
qz (mm) @ t=3.395E-10	2.31917	qz (mm) @ t=3.625E-10	2.11259
qz (mm) @ t=3.4E-10	2.31482	qz (mm) @ t=3.63E-10	2.10795
qz (mm) @ t=3.405E-10	2.31047	qz (mm) @ t=3.635E-10	2.10330
qz (mm) @ t=3.41E-10	2.30610	qz (mm) @ t=3.64E-10	2.09865
qz (mm) @ t=3.415E-10	2.30174	qz (mm) @ t=3.645E-10	2.09400
qz (mm) @ t=3.42E-10	2.29736	qz (mm) @ t=3.65E-10	2.08933
qz (mm) @ t=3.425E-10	2.29298	qz (mm) @ t=3.655E-10	2.08466
qz (mm) @ t=3.43E-10	2.28859	qz (mm) @ t=3.66E-10	2.07999
qz (mm) @ t=3.435E-10	2.28420	qz (mm) @ t=3.665E-10	2.07530
qz (mm) @ t=3.44E-10	2.27980	qz (mm) @ t=3.67E-10	2.07062
qz (mm) @ t=3.445E-10	2.27539	qz (mm) @ t=3.675E-10	2.06592

doi:10.6844/NCKU202003198

qz (nm) @ t=3.68E-10	2.06122	qz (nm) @ t=3.91E-10	1.83823
qz (nm) @ t=3.685E-10	2.05651	qz (nm) @ t=3.915E-10	1.83324
qz (nm) @ t=3.69E-10	2.05180	qz (nm) @ t=3.92E-10	1.82824
qz (nm) @ t=3.695E-10	2.04708	qz (nm) @ t=3.925E-10	1.82323
qz (nm) @ t=3.7E-10	2.04235	qz (nm) @ t=3.93E-10	1.81822
qz (nm) @ t=3.705E-10	2.03762	qz (nm) @ t=3.935E-10	1.81320
qz (nm) @ t=3.71E-10	2.03288	qz (nm) @ t=3.94E-10	1.80817
qz (nm) @ t=3.715E-10	2.02814	qz (nm) @ t=3.945E-10	1.80314
qz (nm) @ t=3.72E-10	2.02339	qz (nm) @ t=3.95E-10	1.79810
qz (nm) @ t=3.725E-10	2.01863	qz (nm) @ t=3.955E-10	1.79306
qz (nm) @ t=3.73E-10	2.01387	qz (nm) @ t=3.96E-10	1.78801
qz (nm) @ t=3.735E-10	2.00910	qz (nm) @ t=3.965E-10	1.78295
qz (nm) @ t=3.74E-10	2.00432	qz (nm) @ t=3.97E-10	1.77789
qz (nm) @ t=3.745E-10	1.99954	qz (nm) @ t=3.975E-10	1.77282
qz (nm) @ t=3.75E-10	1.99475	qz (nm) @ t=3.98E-10	1.76775
qz (nm) @ t=3.755E-10	1.98996	qz (nm) @ t=3.985E-10	1.76267
qz (nm) @ t=3.76E-10	1.98516	qz (nm) @ t=3.99E-10	1.75758
qz (nm) @ t=3.765E-10	1.98035	qz (nm) @ t=3.995E-10	1.75248
qz (nm) @ t=3.77E-10	1.97554	qz (nm) @ t=4E-10	1.74738
qz (nm) @ t=3.775E-10	1.97072	qz (nm) @ t=4.005E-10	1.74228
qz (nm) @ t=3.78E-10	1.96589	qz (nm) @ t=4.01E-10	1.73717
qz (nm) @ t=3.785E-10	1.96106	qz (nm) @ t=4.015E-10	1.73205
qz (nm) @ t=3.79E-10	1.95622	qz (nm) @ t=4.02E-10	1.72692
qz (nm) @ t=3.795E-10	1.95138	qz (nm) @ t=4.025E-10	1.72179
qz (nm) @ t=3.8E-10	1.94652	qz (nm) @ t=4.03E-10	1.71666
qz (nm) @ t=3.805E-10	1.94167	qz (nm) @ t=4.035E-10	1.71151
qz (nm) @ t=3.81E-10	1.93680	qz (nm) @ t=4.04E-10	1.70636
qz (nm) @ t=3.815E-10	1.93193	qz (nm) @ t=4.045E-10	1.70121
qz (nm) @ t=3.82E-10	1.92706	qz (nm) @ t=4.05E-10	1.69604
qz (nm) @ t=3.825E-10	1.92218	qz (nm) @ t=4.055E-10	1.69088
qz (nm) @ t=3.83E-10	1.91729	qz (nm) @ t=4.06E-10	1.68570
qz (nm) @ t=3.835E-10	1.91239	qz (nm) @ t=4.065E-10	1.68052
qz (nm) @ t=3.84E-10	1.90749	qz (nm) @ t=4.07E-10	1.67534
qz (nm) @ t=3.845E-10	1.90259	qz (nm) @ t=4.075E-10	1.67014
qz (nm) @ t=3.85E-10	1.89767	qz (nm) @ t=4.08E-10	1.66494
qz (nm) @ t=3.855E-10	1.89275	qz (nm) @ t=4.085E-10	1.65974
qz (nm) @ t=3.86E-10	1.88783	qz (nm) @ t=4.09E-10	1.65453
qz (nm) @ t=3.865E-10	1.88290	qz (nm) @ t=4.095E-10	1.64931
qz (nm) @ t=3.87E-10	1.87796	qz (nm) @ t=4.1E-10	1.64409
qz (nm) @ t=3.875E-10	1.87301	qz (nm) @ t=4.105E-10	1.63885
qz (nm) @ t=3.88E-10	1.86806	qz (nm) @ t=4.11E-10	1.63362
qz (nm) @ t=3.885E-10	1.86311	qz (nm) @ t=4.115E-10	1.62838
qz (nm) @ t=3.89E-10	1.85814	qz (nm) @ t=4.12E-10	1.62313
qz (nm) @ t=3.895E-10	1.85317	qz (nm) @ t=4.125E-10	1.61787
qz (nm) @ t=3.9E-10	1.84820	qz (nm) @ t=4.13E-10	1.61261
qz (nm) @ t=3.905E-10	1.84322	qz (nm) @ t=4.135E-10	1.60734

doi:10.6844/NCKU202003198

qz (mm) @ t=3.68E-10	2.06122	qz (mm) @ t=3.91E-10	1.83823
qz (mm) @ t=3.685E-10	2.05651	qz (mm) @ t=3.915E-10	1.83324
qz (mm) @ t=3.69E-10	2.05180	qz (mm) @ t=3.92E-10	1.82824
qz (mm) @ t=3.695E-10	2.04708	qz (mm) @ t=3.925E-10	1.82323
qz (mm) @ t=3.7E-10	2.04235	qz (mm) @ t=3.93E-10	1.81822
qz (mm) @ t=3.705E-10	2.03762	qz (mm) @ t=3.935E-10	1.81320
qz (mm) @ t=3.71E-10	2.03288	qz (mm) @ t=3.94E-10	1.80817
qz (mm) @ t=3.715E-10	2.02814	qz (mm) @ t=3.945E-10	1.80314
qz (mm) @ t=3.72E-10	2.02339	qz (mm) @ t=3.95E-10	1.79810
qz (mm) @ t=3.725E-10	2.01863	qz (mm) @ t=3.955E-10	1.79306
qz (mm) @ t=3.73E-10	2.01387	qz (mm) @ t=3.96E-10	1.78801
qz (mm) @ t=3.735E-10	2.00910	qz (mm) @ t=3.965E-10	1.78295
qz (mm) @ t=3.74E-10	2.00432	qz (mm) @ t=3.97E-10	1.77789
qz (mm) @ t=3.745E-10	1.99954	qz (mm) @ t=3.975E-10	1.77282
qz (mm) @ t=3.75E-10	1.99475	qz (mm) @ t=3.98E-10	1.76775
qz (mm) @ t=3.755E-10	1.98996	qz (mm) @ t=3.985E-10	1.76267
qz (mm) @ t=3.76E-10	1.98516	qz (mm) @ t=3.99E-10	1.75758
qz (mm) @ t=3.765E-10	1.98035	qz (mm) @ t=3.995E-10	1.75248
qz (mm) @ t=3.77E-10	1.97554	qz (mm) @ t=4E-10	1.74738
qz (mm) @ t=3.775E-10	1.97072	qz (mm) @ t=4.005E-10	1.74228
qz (mm) @ t=3.78E-10	1.96589	qz (mm) @ t=4.01E-10	1.73717
qz (mm) @ t=3.785E-10	1.96106	qz (mm) @ t=4.015E-10	1.73205
qz (mm) @ t=3.79E-10	1.95622	qz (mm) @ t=4.02E-10	1.72692
qz (mm) @ t=3.795E-10	1.95138	qz (mm) @ t=4.025E-10	1.72179
qz (mm) @ t=3.8E-10	1.94652	qz (mm) @ t=4.03E-10	1.71666
qz (mm) @ t=3.805E-10	1.94167	qz (mm) @ t=4.035E-10	1.71151
qz (mm) @ t=3.81E-10	1.93680	qz (mm) @ t=4.04E-10	1.70636
qz (mm) @ t=3.815E-10	1.93193	qz (mm) @ t=4.045E-10	1.70121
qz (mm) @ t=3.82E-10	1.92706	qz (mm) @ t=4.05E-10	1.69604
qz (mm) @ t=3.825E-10	1.92218	qz (mm) @ t=4.055E-10	1.69088
qz (mm) @ t=3.83E-10	1.91729	qz (mm) @ t=4.06E-10	1.68570
qz (mm) @ t=3.835E-10	1.91239	qz (mm) @ t=4.065E-10	1.68052
qz (mm) @ t=3.84E-10	1.90749	qz (mm) @ t=4.07E-10	1.67534
qz (mm) @ t=3.845E-10	1.90259	qz (mm) @ t=4.075E-10	1.67014
qz (mm) @ t=3.85E-10	1.89767	qz (mm) @ t=4.08E-10	1.66494
qz (mm) @ t=3.855E-10	1.89275	qz (mm) @ t=4.085E-10	1.65974
qz (mm) @ t=3.86E-10	1.88783	qz (mm) @ t=4.09E-10	1.65453
qz (mm) @ t=3.865E-10	1.88290	qz (mm) @ t=4.095E-10	1.64931
qz (mm) @ t=3.87E-10	1.87796	qz (mm) @ t=4.1E-10	1.64409
qz (mm) @ t=3.875E-10	1.87301	qz (mm) @ t=4.105E-10	1.63885
qz (mm) @ t=3.88E-10	1.86806	qz (mm) @ t=4.11E-10	1.63362
qz (mm) @ t=3.885E-10	1.86311	qz (mm) @ t=4.115E-10	1.62838
qz (mm) @ t=3.89E-10	1.85814	qz (mm) @ t=4.12E-10	1.62313
qz (mm) @ t=3.895E-10	1.85317	qz (mm) @ t=4.125E-10	1.61787
qz (mm) @ t=3.9E-10	1.84820	qz (mm) @ t=4.13E-10	1.61261
qz (mm) @ t=3.905E-10	1.84322	qz (mm) @ t=4.135E-10	1.60734

doi:10.6844/NCKU202003198

qz (mm) @ t=4.6E-10	1.09049	qz (mm) @ t=4.83E-10	0.81517
qz (mm) @ t=4.605E-10	1.08464	qz (mm) @ t=4.835E-10	0.80904
qz (mm) @ t=4.61E-10	1.07879	qz (mm) @ t=4.84E-10	0.80290
qz (mm) @ t=4.615E-10	1.07293	qz (mm) @ t=4.845E-10	0.79676
qz (mm) @ t=4.62E-10	1.06706	qz (mm) @ t=4.85E-10	0.79061
qz (mm) @ t=4.625E-10	1.06119	qz (mm) @ t=4.855E-10	0.78446
qz (mm) @ t=4.63E-10	1.05531	qz (mm) @ t=4.86E-10	0.77830
qz (mm) @ t=4.635E-10	1.04943	qz (mm) @ t=4.865E-10	0.77213
qz (mm) @ t=4.64E-10	1.04354	qz (mm) @ t=4.87E-10	0.76596
qz (mm) @ t=4.645E-10	1.03764	qz (mm) @ t=4.875E-10	0.75978
qz (mm) @ t=4.65E-10	1.03174	qz (mm) @ t=4.88E-10	0.75360
qz (mm) @ t=4.655E-10	1.02583	qz (mm) @ t=4.885E-10	0.74741
qz (mm) @ t=4.66E-10	1.01992	qz (mm) @ t=4.89E-10	0.74121
qz (mm) @ t=4.665E-10	1.01400	qz (mm) @ t=4.895E-10	0.73501
qz (mm) @ t=4.67E-10	1.00807	qz (mm) @ t=4.9E-10	0.72880
qz (mm) @ t=4.675E-10	1.00214	qz (mm) @ t=4.905E-10	0.72258
qz (mm) @ t=4.68E-10	0.99620	qz (mm) @ t=4.91E-10	0.71636
qz (mm) @ t=4.685E-10	0.99025	qz (mm) @ t=4.915E-10	0.71013
qz (mm) @ t=4.69E-10	0.98430	qz (mm) @ t=4.92E-10	0.70390
qz (mm) @ t=4.695E-10	0.97834	qz (mm) @ t=4.925E-10	0.69766
qz (mm) @ t=4.7E-10	0.97238	qz (mm) @ t=4.93E-10	0.69141
qz (mm) @ t=4.705E-10	0.96641	qz (mm) @ t=4.935E-10	0.68516
qz (mm) @ t=4.71E-10	0.96043	qz (mm) @ t=4.94E-10	0.67890
qz (mm) @ t=4.715E-10	0.95445	qz (mm) @ t=4.945E-10	0.67264
qz (mm) @ t=4.72E-10	0.94846	qz (mm) @ t=4.95E-10	0.66637
qz (mm) @ t=4.725E-10	0.94247	qz (mm) @ t=4.955E-10	0.66009
qz (mm) @ t=4.73E-10	0.93647	qz (mm) @ t=4.96E-10	0.65381
qz (mm) @ t=4.735E-10	0.93046	qz (mm) @ t=4.965E-10	0.64752
qz (mm) @ t=4.74E-10	0.92445	qz (mm) @ t=4.97E-10	0.64123
qz (mm) @ t=4.745E-10	0.91843	qz (mm) @ t=4.975E-10	0.63493
qz (mm) @ t=4.75E-10	0.91240	qz (mm) @ t=4.98E-10	0.62862
qz (mm) @ t=4.755E-10	0.90637	qz (mm) @ t=4.985E-10	0.62231
qz (mm) @ t=4.76E-10	0.90034	qz (mm) @ t=4.99E-10	0.61599
qz (mm) @ t=4.765E-10	0.89429	qz (mm) @ t=4.995E-10	0.60966
qz (mm) @ t=4.77E-10	0.88824	qz (mm) @ t=5E-10	0.60333
qz (mm) @ t=4.775E-10	0.88219		
qz (mm) @ t=4.78E-10	0.87612		
qz (mm) @ t=4.785E-10	0.87006		
qz (mm) @ t=4.79E-10	0.86398		
qz (mm) @ t=4.795E-10	0.85790		
qz (mm) @ t=4.8E-10	0.85182		
qz (mm) @ t=4.805E-10	0.84572		
qz (mm) @ t=4.81E-10	0.83962		
qz (mm) @ t=4.815E-10	0.83352		
qz (mm) @ t=4.82E-10	0.82741		
qz (mm) @ t=4.825E-10	0.82129		

doi:10.6844/NCKU202003198

Table 19: Raw data of electron trajectories with $V_{acc} = 750$ V.

qz (mm) @ t=0	3.80000	qz (mm) @ t=2.3E-11	3.78978
qz (mm) @ t=5E-13	3.80000	qz (mm) @ t=2.35E-11	3.78933
qz (mm) @ t=1E-12	3.79998	qz (mm) @ t=2.4E-11	3.78887
qz (mm) @ t=1.5E-12	3.79996	qz (mm) @ t=2.45E-11	3.78840
qz (mm) @ t=2E-12	3.79992	qz (mm) @ t=2.5E-11	3.78793
qz (mm) @ t=2.5E-12	3.79988	qz (mm) @ t=2.55E-11	3.78744
qz (mm) @ t=3E-12	3.79983	qz (mm) @ t=2.6E-11	3.78694
qz (mm) @ t=3.5E-12	3.79976	qz (mm) @ t=2.65E-11	3.78643
qz (mm) @ t=4E-12	3.79969	qz (mm) @ t=2.7E-11	3.78592
qz (mm) @ t=4.5E-12	3.79961	qz (mm) @ t=2.75E-11	3.78539
qz (mm) @ t=5E-12	3.79952	qz (mm) @ t=2.8E-11	3.78486
qz (mm) @ t=5.5E-12	3.79942	qz (mm) @ t=2.85E-11	3.78431
qz (mm) @ t=6E-12	3.79930	qz (mm) @ t=2.9E-11	3.78375
qz (mm) @ t=6.5E-12	3.79918	qz (mm) @ t=2.95E-11	3.78319
qz (mm) @ t=7E-12	3.79905	qz (mm) @ t=3E-11	3.78261
qz (mm) @ t=7.5E-12	3.79891	qz (mm) @ t=3.05E-11	3.78203
qz (mm) @ t=8E-12	3.79876	qz (mm) @ t=3.1E-11	3.78144
qz (mm) @ t=8.5E-12	3.79860	qz (mm) @ t=3.15E-11	3.78083
qz (mm) @ t=9E-12	3.79844	qz (mm) @ t=3.2E-11	3.78022
qz (mm) @ t=9.5E-12	3.79826	qz (mm) @ t=3.25E-11	3.77960
qz (mm) @ t=1E-11	3.79807	qz (mm) @ t=3.3E-11	3.77896
qz (mm) @ t=1.05E-11	3.79787	qz (mm) @ t=3.35E-11	3.77832
qz (mm) @ t=1.1E-11	3.79766	qz (mm) @ t=3.4E-11	3.77767
qz (mm) @ t=1.15E-11	3.79745	qz (mm) @ t=3.45E-11	3.77701
qz (mm) @ t=1.2E-11	3.79722	qz (mm) @ t=3.5E-11	3.77634
qz (mm) @ t=1.25E-11	3.79698	qz (mm) @ t=3.55E-11	3.77566
qz (mm) @ t=1.3E-11	3.79674	qz (mm) @ t=3.6E-11	3.77497
qz (mm) @ t=1.35E-11	3.79648	qz (mm) @ t=3.65E-11	3.77427
qz (mm) @ t=1.4E-11	3.79621	qz (mm) @ t=3.7E-11	3.77356
qz (mm) @ t=1.45E-11	3.79594	qz (mm) @ t=3.75E-11	3.77284
qz (mm) @ t=1.5E-11	3.79565	qz (mm) @ t=3.8E-11	3.77211
qz (mm) @ t=1.55E-11	3.79536	qz (mm) @ t=3.85E-11	3.77137
qz (mm) @ t=1.6E-11	3.79505	qz (mm) @ t=3.9E-11	3.77062
qz (mm) @ t=1.65E-11	3.79474	qz (mm) @ t=3.95E-11	3.76986
qz (mm) @ t=1.7E-11	3.79442	qz (mm) @ t=4E-11	3.76909
qz (mm) @ t=1.75E-11	3.79408	qz (mm) @ t=4.05E-11	3.76832
qz (mm) @ t=1.8E-11	3.79374	qz (mm) @ t=4.1E-11	3.76753
qz (mm) @ t=1.85E-11	3.79339	qz (mm) @ t=4.15E-11	3.76673
qz (mm) @ t=1.9E-11	3.79303	qz (mm) @ t=4.2E-11	3.76593
qz (mm) @ t=1.95E-11	3.79265	qz (mm) @ t=4.25E-11	3.76511
qz (mm) @ t=2E-11	3.79227	qz (mm) @ t=4.3E-11	3.76428
qz (mm) @ t=2.05E-11	3.79188	qz (mm) @ t=4.35E-11	3.76345
qz (mm) @ t=2.1E-11	3.79148	qz (mm) @ t=4.4E-11	3.76260
qz (mm) @ t=2.15E-11	3.79107	qz (mm) @ t=4.45E-11	3.76175
qz (mm) @ t=2.2E-11	3.79065	qz (mm) @ t=4.5E-11	3.76088
qz (mm) @ t=2.25E-11	3.79022	qz (mm) @ t=4.55E-11	3.76001

doi:10.6844/NCKU202003198

qz (mm) @ t=4.6E-11	3.75913	qz (mm) @ t=6.9E-11	3.70804
qz (mm) @ t=4.65E-11	3.75823	qz (mm) @ t=6.95E-11	3.70670
qz (mm) @ t=4.7E-11	3.75733	qz (mm) @ t=7E-11	3.70535
qz (mm) @ t=4.75E-11	3.75642	qz (mm) @ t=7.05E-11	3.70400
qz (mm) @ t=4.8E-11	3.75549	qz (mm) @ t=7.1E-11	3.70263
qz (mm) @ t=4.85E-11	3.75456	qz (mm) @ t=7.15E-11	3.70125
qz (mm) @ t=4.9E-11	3.75362	qz (mm) @ t=7.2E-11	3.69987
qz (mm) @ t=4.95E-11	3.75267	qz (mm) @ t=7.25E-11	3.69847
qz (mm) @ t=5E-11	3.75171	qz (mm) @ t=7.3E-11	3.69707
qz (mm) @ t=5.05E-11	3.75074	qz (mm) @ t=7.35E-11	3.69565
qz (mm) @ t=5.1E-11	3.74976	qz (mm) @ t=7.4E-11	3.69423
qz (mm) @ t=5.15E-11	3.74877	qz (mm) @ t=7.45E-11	3.69279
qz (mm) @ t=5.2E-11	3.74777	qz (mm) @ t=7.5E-11	3.69135
qz (mm) @ t=5.25E-11	3.74676	qz (mm) @ t=7.55E-11	3.68990
qz (mm) @ t=5.3E-11	3.74574	qz (mm) @ t=7.6E-11	3.68843
qz (mm) @ t=5.35E-11	3.74471	qz (mm) @ t=7.65E-11	3.68696
qz (mm) @ t=5.4E-11	3.74367	qz (mm) @ t=7.7E-11	3.68548
qz (mm) @ t=5.45E-11	3.74263	qz (mm) @ t=7.75E-11	3.68399
qz (mm) @ t=5.5E-11	3.74157	qz (mm) @ t=7.8E-11	3.68249
qz (mm) @ t=5.55E-11	3.74050	qz (mm) @ t=7.85E-11	3.68097
qz (mm) @ t=5.6E-11	3.73942	qz (mm) @ t=7.9E-11	3.67945
qz (mm) @ t=5.65E-11	3.73834	qz (mm) @ t=7.95E-11	3.67792
qz (mm) @ t=5.7E-11	3.73724	qz (mm) @ t=8E-11	3.67638
qz (mm) @ t=5.75E-11	3.73614	qz (mm) @ t=8.05E-11	3.67483
qz (mm) @ t=5.8E-11	3.73502	qz (mm) @ t=8.1E-11	3.67327
qz (mm) @ t=5.85E-11	3.73390	qz (mm) @ t=8.15E-11	3.67170
qz (mm) @ t=5.9E-11	3.73276	qz (mm) @ t=8.2E-11	3.67013
qz (mm) @ t=5.95E-11	3.73162	qz (mm) @ t=8.25E-11	3.66854
qz (mm) @ t=6E-11	3.73046	qz (mm) @ t=8.3E-11	3.66694
qz (mm) @ t=6.05E-11	3.72930	qz (mm) @ t=8.35E-11	3.66533
qz (mm) @ t=6.1E-11	3.72812	qz (mm) @ t=8.4E-11	3.66371
qz (mm) @ t=6.15E-11	3.72694	qz (mm) @ t=8.45E-11	3.66209
qz (mm) @ t=6.2E-11	3.72575	qz (mm) @ t=8.5E-11	3.66045
qz (mm) @ t=6.25E-11	3.72455	qz (mm) @ t=8.55E-11	3.65880
qz (mm) @ t=6.3E-11	3.72333	qz (mm) @ t=8.6E-11	3.65715
qz (mm) @ t=6.35E-11	3.72211	qz (mm) @ t=8.65E-11	3.65548
qz (mm) @ t=6.4E-11	3.72088	qz (mm) @ t=8.7E-11	3.65381
qz (mm) @ t=6.45E-11	3.71964	qz (mm) @ t=8.75E-11	3.65212
qz (mm) @ t=6.5E-11	3.71839	qz (mm) @ t=8.8E-11	3.65043
qz (mm) @ t=6.55E-11	3.71713	qz (mm) @ t=8.85E-11	3.64872
qz (mm) @ t=6.6E-11	3.71586	qz (mm) @ t=8.9E-11	3.64701
qz (mm) @ t=6.65E-11	3.71458	qz (mm) @ t=8.95E-11	3.64528
qz (mm) @ t=6.7E-11	3.71329	qz (mm) @ t=9E-11	3.64355
qz (mm) @ t=6.75E-11	3.71199	qz (mm) @ t=9.05E-11	3.64181
qz (mm) @ t=6.8E-11	3.71068	qz (mm) @ t=9.1E-11	3.64006
qz (mm) @ t=6.85E-11	3.70937	qz (mm) @ t=9.15E-11	3.63829

doi:10.6844/NCKU202003198

qz (mm) @ t=9.2E-11	3.63652	qz (mm) @ t=1.15E-10	3.54459
qz (mm) @ t=9.25E-11	3.63474	qz (mm) @ t=1.155E-10	3.54236
qz (mm) @ t=9.3E-11	3.63295	qz (mm) @ t=1.16E-10	3.54013
qz (mm) @ t=9.35E-11	3.63115	qz (mm) @ t=1.165E-10	3.53788
qz (mm) @ t=9.4E-11	3.62934	qz (mm) @ t=1.17E-10	3.53563
qz (mm) @ t=9.45E-11	3.62752	qz (mm) @ t=1.175E-10	3.53337
qz (mm) @ t=9.5E-11	3.62569	qz (mm) @ t=1.18E-10	3.53109
qz (mm) @ t=9.55E-11	3.62385	qz (mm) @ t=1.185E-10	3.52881
qz (mm) @ t=9.6E-11	3.62200	qz (mm) @ t=1.19E-10	3.52652
qz (mm) @ t=9.65E-11	3.62014	qz (mm) @ t=1.195E-10	3.52421
qz (mm) @ t=9.7E-11	3.61827	qz (mm) @ t=1.2E-10	3.52190
qz (mm) @ t=9.75E-11	3.61639	qz (mm) @ t=1.205E-10	3.51958
qz (mm) @ t=9.8E-11	3.61451	qz (mm) @ t=1.21E-10	3.51725
qz (mm) @ t=9.85E-11	3.61261	qz (mm) @ t=1.215E-10	3.51491
qz (mm) @ t=9.9E-11	3.61070	qz (mm) @ t=1.22E-10	3.51256
qz (mm) @ t=9.95E-11	3.60879	qz (mm) @ t=1.225E-10	3.51020
qz (mm) @ t=1E-10	3.60686	qz (mm) @ t=1.23E-10	3.50783
qz (mm) @ t=1.005E-10	3.60492	qz (mm) @ t=1.235E-10	3.50545
qz (mm) @ t=1.01E-10	3.60298	qz (mm) @ t=1.24E-10	3.50306
qz (mm) @ t=1.015E-10	3.60102	qz (mm) @ t=1.245E-10	3.50066
qz (mm) @ t=1.02E-10	3.59906	qz (mm) @ t=1.25E-10	3.49825
qz (mm) @ t=1.025E-10	3.59708	qz (mm) @ t=1.255E-10	3.49583
qz (mm) @ t=1.03E-10	3.59510	qz (mm) @ t=1.26E-10	3.49341
qz (mm) @ t=1.035E-10	3.59311	qz (mm) @ t=1.265E-10	3.49097
qz (mm) @ t=1.04E-10	3.59110	qz (mm) @ t=1.27E-10	3.48852
qz (mm) @ t=1.045E-10	3.58909	qz (mm) @ t=1.275E-10	3.48607
qz (mm) @ t=1.05E-10	3.58707	qz (mm) @ t=1.28E-10	3.48360
qz (mm) @ t=1.055E-10	3.58503	qz (mm) @ t=1.285E-10	3.48112
qz (mm) @ t=1.06E-10	3.58299	qz (mm) @ t=1.29E-10	3.47864
qz (mm) @ t=1.065E-10	3.58094	qz (mm) @ t=1.295E-10	3.47614
qz (mm) @ t=1.07E-10	3.57888	qz (mm) @ t=1.3E-10	3.47364
qz (mm) @ t=1.075E-10	3.57681	qz (mm) @ t=1.305E-10	3.47112
qz (mm) @ t=1.08E-10	3.57473	qz (mm) @ t=1.31E-10	3.46860
qz (mm) @ t=1.085E-10	3.57264	qz (mm) @ t=1.315E-10	3.46607
qz (mm) @ t=1.09E-10	3.57054	qz (mm) @ t=1.32E-10	3.46352
qz (mm) @ t=1.095E-10	3.56843	qz (mm) @ t=1.325E-10	3.46097
qz (mm) @ t=1.1E-10	3.56631	qz (mm) @ t=1.33E-10	3.45841
qz (mm) @ t=1.105E-10	3.56418	qz (mm) @ t=1.335E-10	3.45583
qz (mm) @ t=1.11E-10	3.56204	qz (mm) @ t=1.34E-10	3.45325
qz (mm) @ t=1.115E-10	3.55989	qz (mm) @ t=1.345E-10	3.45066
qz (mm) @ t=1.12E-10	3.55774	qz (mm) @ t=1.35E-10	3.44806
qz (mm) @ t=1.125E-10	3.55557	qz (mm) @ t=1.355E-10	3.44545
qz (mm) @ t=1.13E-10	3.55339	qz (mm) @ t=1.36E-10	3.44283
qz (mm) @ t=1.135E-10	3.55121	qz (mm) @ t=1.365E-10	3.44020
qz (mm) @ t=1.14E-10	3.54901	qz (mm) @ t=1.37E-10	3.43756
qz (mm) @ t=1.145E-10	3.54680	qz (mm) @ t=1.375E-10	3.43491

doi:10.6844/NCKU202003198

qz (mm) @ t=1.38E-10	3.43225	qz (mm) @ t=1.61E-10	3.29954
qz (mm) @ t=1.385E-10	3.42958	qz (mm) @ t=1.615E-10	3.29643
qz (mm) @ t=1.39E-10	3.42691	qz (mm) @ t=1.62E-10	3.29330
qz (mm) @ t=1.395E-10	3.42422	qz (mm) @ t=1.625E-10	3.29017
qz (mm) @ t=1.4E-10	3.42152	qz (mm) @ t=1.63E-10	3.28703
qz (mm) @ t=1.405E-10	3.41881	qz (mm) @ t=1.635E-10	3.28388
qz (mm) @ t=1.41E-10	3.41610	qz (mm) @ t=1.64E-10	3.28073
qz (mm) @ t=1.415E-10	3.41337	qz (mm) @ t=1.645E-10	3.27756
qz (mm) @ t=1.42E-10	3.41063	qz (mm) @ t=1.65E-10	3.27438
qz (mm) @ t=1.425E-10	3.40789	qz (mm) @ t=1.655E-10	3.27119
qz (mm) @ t=1.43E-10	3.40513	qz (mm) @ t=1.66E-10	3.26799
qz (mm) @ t=1.435E-10	3.40237	qz (mm) @ t=1.665E-10	3.26479
qz (mm) @ t=1.44E-10	3.39959	qz (mm) @ t=1.67E-10	3.26157
qz (mm) @ t=1.445E-10	3.39681	qz (mm) @ t=1.675E-10	3.25834
qz (mm) @ t=1.45E-10	3.39402	qz (mm) @ t=1.68E-10	3.25511
qz (mm) @ t=1.455E-10	3.39121	qz (mm) @ t=1.685E-10	3.25186
qz (mm) @ t=1.46E-10	3.38840	qz (mm) @ t=1.69E-10	3.24860
qz (mm) @ t=1.465E-10	3.38558	qz (mm) @ t=1.695E-10	3.24534
qz (mm) @ t=1.47E-10	3.38275	qz (mm) @ t=1.7E-10	3.24206
qz (mm) @ t=1.475E-10	3.37990	qz (mm) @ t=1.705E-10	3.23878
qz (mm) @ t=1.48E-10	3.37705	qz (mm) @ t=1.71E-10	3.23549
qz (mm) @ t=1.485E-10	3.37419	qz (mm) @ t=1.715E-10	3.23218
qz (mm) @ t=1.49E-10	3.37132	qz (mm) @ t=1.72E-10	3.22887
qz (mm) @ t=1.495E-10	3.36844	qz (mm) @ t=1.725E-10	3.22555
qz (mm) @ t=1.5E-10	3.36555	qz (mm) @ t=1.73E-10	3.22222
qz (mm) @ t=1.505E-10	3.36265	qz (mm) @ t=1.735E-10	3.21887
qz (mm) @ t=1.51E-10	3.35974	qz (mm) @ t=1.74E-10	3.21552
qz (mm) @ t=1.515E-10	3.35682	qz (mm) @ t=1.745E-10	3.21216
qz (mm) @ t=1.52E-10	3.35389	qz (mm) @ t=1.75E-10	3.20879
qz (mm) @ t=1.525E-10	3.35096	qz (mm) @ t=1.755E-10	3.20541
qz (mm) @ t=1.53E-10	3.34801	qz (mm) @ t=1.76E-10	3.20202
qz (mm) @ t=1.535E-10	3.34505	qz (mm) @ t=1.765E-10	3.19862
qz (mm) @ t=1.54E-10	3.34208	qz (mm) @ t=1.77E-10	3.19521
qz (mm) @ t=1.545E-10	3.33911	qz (mm) @ t=1.775E-10	3.19179
qz (mm) @ t=1.55E-10	3.33612	qz (mm) @ t=1.78E-10	3.18836
qz (mm) @ t=1.555E-10	3.33313	qz (mm) @ t=1.785E-10	3.18493
qz (mm) @ t=1.56E-10	3.33012	qz (mm) @ t=1.79E-10	3.18148
qz (mm) @ t=1.565E-10	3.32710	qz (mm) @ t=1.795E-10	3.17802
qz (mm) @ t=1.57E-10	3.32408	qz (mm) @ t=1.8E-10	3.17456
qz (mm) @ t=1.575E-10	3.32105	qz (mm) @ t=1.805E-10	3.17108
qz (mm) @ t=1.58E-10	3.31800	qz (mm) @ t=1.81E-10	3.16759
qz (mm) @ t=1.585E-10	3.31495	qz (mm) @ t=1.815E-10	3.16410
qz (mm) @ t=1.59E-10	3.31189	qz (mm) @ t=1.82E-10	3.16059
qz (mm) @ t=1.595E-10	3.30881	qz (mm) @ t=1.825E-10	3.15708
qz (mm) @ t=1.6E-10	3.30573	qz (mm) @ t=1.83E-10	3.15355
qz (mm) @ t=1.605E-10	3.30264	qz (mm) @ t=1.835E-10	3.15002

doi:10.6844/NCKU202003198

qz (mm) @ t=1.84E-10	3.14648	qz (mm) @ t=2.07E-10	2.97312
qz (mm) @ t=1.845E-10	3.14292	qz (mm) @ t=2.075E-10	2.96912
qz (mm) @ t=1.85E-10	3.13936	qz (mm) @ t=2.08E-10	2.96512
qz (mm) @ t=1.855E-10	3.13579	qz (mm) @ t=2.085E-10	2.96111
qz (mm) @ t=1.86E-10	3.13221	qz (mm) @ t=2.09E-10	2.95709
qz (mm) @ t=1.865E-10	3.12862	qz (mm) @ t=2.095E-10	2.95305
qz (mm) @ t=1.87E-10	3.12502	qz (mm) @ t=2.1E-10	2.94901
qz (mm) @ t=1.875E-10	3.12140	qz (mm) @ t=2.105E-10	2.94496
qz (mm) @ t=1.88E-10	3.11778	qz (mm) @ t=2.11E-10	2.94090
qz (mm) @ t=1.885E-10	3.11415	qz (mm) @ t=2.115E-10	2.93683
qz (mm) @ t=1.89E-10	3.11052	qz (mm) @ t=2.12E-10	2.93275
qz (mm) @ t=1.895E-10	3.10687	qz (mm) @ t=2.125E-10	2.92866
qz (mm) @ t=1.9E-10	3.10321	qz (mm) @ t=2.13E-10	2.92456
qz (mm) @ t=1.905E-10	3.09954	qz (mm) @ t=2.135E-10	2.92045
qz (mm) @ t=1.91E-10	3.09586	qz (mm) @ t=2.14E-10	2.91634
qz (mm) @ t=1.915E-10	3.09218	qz (mm) @ t=2.145E-10	2.91221
qz (mm) @ t=1.92E-10	3.08848	qz (mm) @ t=2.15E-10	2.90807
qz (mm) @ t=1.925E-10	3.08477	qz (mm) @ t=2.155E-10	2.90393
qz (mm) @ t=1.93E-10	3.08106	qz (mm) @ t=2.16E-10	2.89977
qz (mm) @ t=1.935E-10	3.07733	qz (mm) @ t=2.165E-10	2.89560
qz (mm) @ t=1.94E-10	3.07359	qz (mm) @ t=2.17E-10	2.89143
qz (mm) @ t=1.945E-10	3.06985	qz (mm) @ t=2.175E-10	2.88724
qz (mm) @ t=1.95E-10	3.06610	qz (mm) @ t=2.18E-10	2.88305
qz (mm) @ t=1.955E-10	3.06233	qz (mm) @ t=2.185E-10	2.87885
qz (mm) @ t=1.96E-10	3.05856	qz (mm) @ t=2.19E-10	2.87463
qz (mm) @ t=1.965E-10	3.05478	qz (mm) @ t=2.195E-10	2.87041
qz (mm) @ t=1.97E-10	3.05098	qz (mm) @ t=2.2E-10	2.86618
qz (mm) @ t=1.975E-10	3.04718	qz (mm) @ t=2.205E-10	2.86193
qz (mm) @ t=1.98E-10	3.04337	qz (mm) @ t=2.21E-10	2.85768
qz (mm) @ t=1.985E-10	3.03955	qz (mm) @ t=2.215E-10	2.85342
qz (mm) @ t=1.99E-10	3.03572	qz (mm) @ t=2.22E-10	2.84915
qz (mm) @ t=1.995E-10	3.03188	qz (mm) @ t=2.225E-10	2.84487
qz (mm) @ t=2E-10	3.02803	qz (mm) @ t=2.23E-10	2.84058
qz (mm) @ t=2.005E-10	3.02417	qz (mm) @ t=2.235E-10	2.83628
qz (mm) @ t=2.01E-10	3.02030	qz (mm) @ t=2.24E-10	2.83197
qz (mm) @ t=2.015E-10	3.01642	qz (mm) @ t=2.245E-10	2.82765
qz (mm) @ t=2.02E-10	3.01253	qz (mm) @ t=2.25E-10	2.82333
qz (mm) @ t=2.025E-10	3.00863	qz (mm) @ t=2.255E-10	2.81899
qz (mm) @ t=2.03E-10	3.00472	qz (mm) @ t=2.26E-10	2.81464
qz (mm) @ t=2.035E-10	3.00081	qz (mm) @ t=2.265E-10	2.81028
qz (mm) @ t=2.04E-10	2.99688	qz (mm) @ t=2.27E-10	2.80592
qz (mm) @ t=2.045E-10	2.99294	qz (mm) @ t=2.275E-10	2.80154
qz (mm) @ t=2.05E-10	2.98900	qz (mm) @ t=2.28E-10	2.79716
qz (mm) @ t=2.055E-10	2.98504	qz (mm) @ t=2.285E-10	2.79276
qz (mm) @ t=2.06E-10	2.98108	qz (mm) @ t=2.29E-10	2.78836
qz (mm) @ t=2.065E-10	2.97710	qz (mm) @ t=2.295E-10	2.78394

doi:10.6844/NCKU202003198

qz (mm) @ t=2.3E-10	2.77952	qz (mm) @ t=2.53E-10	2.56576
qz (mm) @ t=2.305E-10	2.77509	qz (mm) @ t=2.535E-10	2.56089
qz (mm) @ t=2.31E-10	2.77065	qz (mm) @ t=2.54E-10	2.55601
qz (mm) @ t=2.315E-10	2.76619	qz (mm) @ t=2.545E-10	2.55112
qz (mm) @ t=2.32E-10	2.76173	qz (mm) @ t=2.55E-10	2.54622
qz (mm) @ t=2.325E-10	2.75726	qz (mm) @ t=2.555E-10	2.54131
qz (mm) @ t=2.33E-10	2.75278	qz (mm) @ t=2.56E-10	2.53640
qz (mm) @ t=2.335E-10	2.74829	qz (mm) @ t=2.565E-10	2.53147
qz (mm) @ t=2.34E-10	2.74379	qz (mm) @ t=2.57E-10	2.52653
qz (mm) @ t=2.345E-10	2.73928	qz (mm) @ t=2.575E-10	2.52159
qz (mm) @ t=2.35E-10	2.73476	qz (mm) @ t=2.58E-10	2.51663
qz (mm) @ t=2.355E-10	2.73024	qz (mm) @ t=2.585E-10	2.51167
qz (mm) @ t=2.36E-10	2.72570	qz (mm) @ t=2.59E-10	2.50669
qz (mm) @ t=2.365E-10	2.72115	qz (mm) @ t=2.595E-10	2.50171
qz (mm) @ t=2.37E-10	2.71659	qz (mm) @ t=2.6E-10	2.49671
qz (mm) @ t=2.375E-10	2.71203	qz (mm) @ t=2.605E-10	2.49171
qz (mm) @ t=2.38E-10	2.70745	qz (mm) @ t=2.61E-10	2.48670
qz (mm) @ t=2.385E-10	2.70287	qz (mm) @ t=2.615E-10	2.48168
qz (mm) @ t=2.39E-10	2.69827	qz (mm) @ t=2.62E-10	2.47665
qz (mm) @ t=2.395E-10	2.69367	qz (mm) @ t=2.625E-10	2.47161
qz (mm) @ t=2.4E-10	2.68905	qz (mm) @ t=2.63E-10	2.46655
qz (mm) @ t=2.405E-10	2.68443	qz (mm) @ t=2.635E-10	2.46150
qz (mm) @ t=2.41E-10	2.67980	qz (mm) @ t=2.64E-10	2.45643
qz (mm) @ t=2.415E-10	2.67516	qz (mm) @ t=2.645E-10	2.45135
qz (mm) @ t=2.42E-10	2.67050	qz (mm) @ t=2.65E-10	2.44626
qz (mm) @ t=2.425E-10	2.66584	qz (mm) @ t=2.655E-10	2.44116
qz (mm) @ t=2.43E-10	2.66117	qz (mm) @ t=2.66E-10	2.43605
qz (mm) @ t=2.435E-10	2.65649	qz (mm) @ t=2.665E-10	2.43094
qz (mm) @ t=2.44E-10	2.65180	qz (mm) @ t=2.67E-10	2.42581
qz (mm) @ t=2.445E-10	2.64710	qz (mm) @ t=2.675E-10	2.42068
qz (mm) @ t=2.45E-10	2.64239	qz (mm) @ t=2.68E-10	2.41553
qz (mm) @ t=2.455E-10	2.63768	qz (mm) @ t=2.685E-10	2.41038
qz (mm) @ t=2.46E-10	2.63295	qz (mm) @ t=2.69E-10	2.40521
qz (mm) @ t=2.465E-10	2.62821	qz (mm) @ t=2.695E-10	2.40004
qz (mm) @ t=2.47E-10	2.62346	qz (mm) @ t=2.7E-10	2.39486
qz (mm) @ t=2.475E-10	2.61871	qz (mm) @ t=2.705E-10	2.38967
qz (mm) @ t=2.48E-10	2.61394	qz (mm) @ t=2.71E-10	2.38446
qz (mm) @ t=2.485E-10	2.60917	qz (mm) @ t=2.715E-10	2.37925
qz (mm) @ t=2.49E-10	2.60438	qz (mm) @ t=2.72E-10	2.37403
qz (mm) @ t=2.495E-10	2.59959	qz (mm) @ t=2.725E-10	2.36880
qz (mm) @ t=2.5E-10	2.59478	qz (mm) @ t=2.73E-10	2.36356
qz (mm) @ t=2.505E-10	2.58997	qz (mm) @ t=2.735E-10	2.35831
qz (mm) @ t=2.51E-10	2.58515	qz (mm) @ t=2.74E-10	2.35306
qz (mm) @ t=2.515E-10	2.58031	qz (mm) @ t=2.745E-10	2.34779
qz (mm) @ t=2.52E-10	2.57547	qz (mm) @ t=2.75E-10	2.34251
qz (mm) @ t=2.525E-10	2.57062	qz (mm) @ t=2.755E-10	2.33722

doi:10.6844/NCKU202003198

qz (mm) @ t=2.76E-10	2.33193	qz (mm) @ t=2.99E-10	2.07813
qz (mm) @ t=2.765E-10	2.32662	qz (mm) @ t=2.995E-10	2.07239
qz (mm) @ t=2.77E-10	2.32131	qz (mm) @ t=3E-10	2.06664
qz (mm) @ t=2.775E-10	2.31598	qz (mm) @ t=3.005E-10	2.06088
qz (mm) @ t=2.78E-10	2.31065	qz (mm) @ t=3.01E-10	2.05512
qz (mm) @ t=2.785E-10	2.30531	qz (mm) @ t=3.015E-10	2.04934
qz (mm) @ t=2.79E-10	2.29995	qz (mm) @ t=3.02E-10	2.04356
qz (mm) @ t=2.795E-10	2.29459	qz (mm) @ t=3.025E-10	2.03776
qz (mm) @ t=2.8E-10	2.28922	qz (mm) @ t=3.03E-10	2.03196
qz (mm) @ t=2.805E-10	2.28384	qz (mm) @ t=3.035E-10	2.02614
qz (mm) @ t=2.81E-10	2.27845	qz (mm) @ t=3.04E-10	2.02032
qz (mm) @ t=2.815E-10	2.27305	qz (mm) @ t=3.045E-10	2.01449
qz (mm) @ t=2.82E-10	2.26764	qz (mm) @ t=3.05E-10	2.00865
qz (mm) @ t=2.825E-10	2.26222	qz (mm) @ t=3.055E-10	2.00280
qz (mm) @ t=2.83E-10	2.25679	qz (mm) @ t=3.06E-10	1.99694
qz (mm) @ t=2.835E-10	2.25136	qz (mm) @ t=3.065E-10	1.99107
qz (mm) @ t=2.84E-10	2.24591	qz (mm) @ t=3.07E-10	1.98519
qz (mm) @ t=2.845E-10	2.24045	qz (mm) @ t=3.075E-10	1.97930
qz (mm) @ t=2.85E-10	2.23499	qz (mm) @ t=3.08E-10	1.97340
qz (mm) @ t=2.855E-10	2.22951	qz (mm) @ t=3.085E-10	1.96750
qz (mm) @ t=2.86E-10	2.22403	qz (mm) @ t=3.09E-10	1.96158
qz (mm) @ t=2.865E-10	2.21853	qz (mm) @ t=3.095E-10	1.95565
qz (mm) @ t=2.87E-10	2.21303	qz (mm) @ t=3.1E-10	1.94972
qz (mm) @ t=2.875E-10	2.20752	qz (mm) @ t=3.105E-10	1.94377
qz (mm) @ t=2.88E-10	2.20199	qz (mm) @ t=3.11E-10	1.93782
qz (mm) @ t=2.885E-10	2.19646	qz (mm) @ t=3.115E-10	1.93186
qz (mm) @ t=2.89E-10	2.19092	qz (mm) @ t=3.12E-10	1.92588
qz (mm) @ t=2.895E-10	2.18537	qz (mm) @ t=3.125E-10	1.91990
qz (mm) @ t=2.9E-10	2.17981	qz (mm) @ t=3.13E-10	1.91391
qz (mm) @ t=2.905E-10	2.17424	qz (mm) @ t=3.135E-10	1.90791
qz (mm) @ t=2.91E-10	2.16866	qz (mm) @ t=3.14E-10	1.90190
qz (mm) @ t=2.915E-10	2.16308	qz (mm) @ t=3.145E-10	1.89588
qz (mm) @ t=2.92E-10	2.15748	qz (mm) @ t=3.15E-10	1.88985
qz (mm) @ t=2.925E-10	2.15187	qz (mm) @ t=3.155E-10	1.88381
qz (mm) @ t=2.93E-10	2.14625	qz (mm) @ t=3.16E-10	1.87777
qz (mm) @ t=2.935E-10	2.14063	qz (mm) @ t=3.165E-10	1.87171
qz (mm) @ t=2.94E-10	2.13499	qz (mm) @ t=3.17E-10	1.86564
qz (mm) @ t=2.945E-10	2.12935	qz (mm) @ t=3.175E-10	1.85957
qz (mm) @ t=2.95E-10	2.12370	qz (mm) @ t=3.18E-10	1.85348
qz (mm) @ t=2.955E-10	2.11803	qz (mm) @ t=3.185E-10	1.84739
qz (mm) @ t=2.96E-10	2.11236	qz (mm) @ t=3.19E-10	1.84129
qz (mm) @ t=2.965E-10	2.10668	qz (mm) @ t=3.195E-10	1.83517
qz (mm) @ t=2.97E-10	2.10099	qz (mm) @ t=3.2E-10	1.82905
qz (mm) @ t=2.975E-10	2.09529	qz (mm) @ t=3.205E-10	1.82292
qz (mm) @ t=2.98E-10	2.08958	qz (mm) @ t=3.21E-10	1.81678
qz (mm) @ t=2.985E-10	2.08386	qz (mm) @ t=3.215E-10	1.81063

doi:10.6844/NCKU202003198

qz (mm) @ t=3.22E-10	1.80447	qz (mm) @ t=3.45E-10	1.51108
qz (mm) @ t=3.225E-10	1.79830	qz (mm) @ t=3.455E-10	1.50448
qz (mm) @ t=3.23E-10	1.79212	qz (mm) @ t=3.46E-10	1.49787
qz (mm) @ t=3.235E-10	1.78594	qz (mm) @ t=3.465E-10	1.49126
qz (mm) @ t=3.24E-10	1.77974	qz (mm) @ t=3.47E-10	1.48464
qz (mm) @ t=3.245E-10	1.77353	qz (mm) @ t=3.475E-10	1.47800
qz (mm) @ t=3.25E-10	1.76732	qz (mm) @ t=3.48E-10	1.47136
qz (mm) @ t=3.255E-10	1.76109	qz (mm) @ t=3.485E-10	1.46471
qz (mm) @ t=3.26E-10	1.75486	qz (mm) @ t=3.49E-10	1.45805
qz (mm) @ t=3.265E-10	1.74862	qz (mm) @ t=3.495E-10	1.45137
qz (mm) @ t=3.27E-10	1.74236	qz (mm) @ t=3.5E-10	1.44469
qz (mm) @ t=3.275E-10	1.73610	qz (mm) @ t=3.505E-10	1.43801
qz (mm) @ t=3.28E-10	1.72983	qz (mm) @ t=3.51E-10	1.43131
qz (mm) @ t=3.285E-10	1.72355	qz (mm) @ t=3.515E-10	1.42460
qz (mm) @ t=3.29E-10	1.71726	qz (mm) @ t=3.52E-10	1.41788
qz (mm) @ t=3.295E-10	1.71096	qz (mm) @ t=3.525E-10	1.41116
qz (mm) @ t=3.3E-10	1.70465	qz (mm) @ t=3.53E-10	1.40442
qz (mm) @ t=3.305E-10	1.69834	qz (mm) @ t=3.535E-10	1.39768
qz (mm) @ t=3.31E-10	1.69201	qz (mm) @ t=3.54E-10	1.39092
qz (mm) @ t=3.315E-10	1.68567	qz (mm) @ t=3.545E-10	1.38416
qz (mm) @ t=3.32E-10	1.67933	qz (mm) @ t=3.55E-10	1.37739
qz (mm) @ t=3.325E-10	1.67297	qz (mm) @ t=3.555E-10	1.37060
qz (mm) @ t=3.33E-10	1.66661	qz (mm) @ t=3.56E-10	1.36381
qz (mm) @ t=3.335E-10	1.66023	qz (mm) @ t=3.565E-10	1.35701
qz (mm) @ t=3.34E-10	1.65385	qz (mm) @ t=3.57E-10	1.35020
qz (mm) @ t=3.345E-10	1.64746	qz (mm) @ t=3.575E-10	1.34338
qz (mm) @ t=3.35E-10	1.64106	qz (mm) @ t=3.58E-10	1.33656
qz (mm) @ t=3.355E-10	1.63465	qz (mm) @ t=3.585E-10	1.32972
qz (mm) @ t=3.36E-10	1.62823	qz (mm) @ t=3.59E-10	1.32287
qz (mm) @ t=3.365E-10	1.62180	qz (mm) @ t=3.595E-10	1.31602
qz (mm) @ t=3.37E-10	1.61536	qz (mm) @ t=3.6E-10	1.30915
qz (mm) @ t=3.375E-10	1.60891	qz (mm) @ t=3.605E-10	1.30228
qz (mm) @ t=3.38E-10	1.60245	qz (mm) @ t=3.61E-10	1.29539
qz (mm) @ t=3.385E-10	1.59599	qz (mm) @ t=3.615E-10	1.28850
qz (mm) @ t=3.39E-10	1.58951	qz (mm) @ t=3.62E-10	1.28160
qz (mm) @ t=3.395E-10	1.58303	qz (mm) @ t=3.625E-10	1.27469
qz (mm) @ t=3.4E-10	1.57653	qz (mm) @ t=3.63E-10	1.26777
qz (mm) @ t=3.405E-10	1.57003	qz (mm) @ t=3.635E-10	1.26084
qz (mm) @ t=3.41E-10	1.56352	qz (mm) @ t=3.64E-10	1.25390
qz (mm) @ t=3.415E-10	1.55699	qz (mm) @ t=3.645E-10	1.24695
qz (mm) @ t=3.42E-10	1.55046	qz (mm) @ t=3.65E-10	1.23999
qz (mm) @ t=3.425E-10	1.54392	qz (mm) @ t=3.655E-10	1.23303
qz (mm) @ t=3.43E-10	1.53737	qz (mm) @ t=3.66E-10	1.22605
qz (mm) @ t=3.435E-10	1.53081	qz (mm) @ t=3.665E-10	1.21907
qz (mm) @ t=3.44E-10	1.52424	qz (mm) @ t=3.67E-10	1.21207
qz (mm) @ t=3.445E-10	1.51766	qz (mm) @ t=3.675E-10	1.20507

doi:10.6844/NCKU202003198

qz (mm) @ t=3.68E-10	1.19805	qz (mm) @ t=3.91E-10	0.86550
qz (mm) @ t=3.685E-10	1.19103	qz (mm) @ t=3.915E-10	0.85805
qz (mm) @ t=3.69E-10	1.18400	qz (mm) @ t=3.92E-10	0.85060
qz (mm) @ t=3.695E-10	1.17696	qz (mm) @ t=3.925E-10	0.84313
qz (mm) @ t=3.7E-10	1.16991	qz (mm) @ t=3.93E-10	0.83566
qz (mm) @ t=3.705E-10	1.16285	qz (mm) @ t=3.935E-10	0.82818
qz (mm) @ t=3.71E-10	1.15578	qz (mm) @ t=3.94E-10	0.82069
qz (mm) @ t=3.715E-10	1.14871	qz (mm) @ t=3.945E-10	0.81319
qz (mm) @ t=3.72E-10	1.14162	qz (mm) @ t=3.95E-10	0.80567
qz (mm) @ t=3.725E-10	1.13452	qz (mm) @ t=3.955E-10	0.79816
qz (mm) @ t=3.73E-10	1.12742	qz (mm) @ t=3.96E-10	0.79063
qz (mm) @ t=3.735E-10	1.12030	qz (mm) @ t=3.965E-10	0.78309
qz (mm) @ t=3.74E-10	1.11318	qz (mm) @ t=3.97E-10	0.77554
qz (mm) @ t=3.745E-10	1.10605	qz (mm) @ t=3.975E-10	0.76799
qz (mm) @ t=3.75E-10	1.09891	qz (mm) @ t=3.98E-10	0.76042
qz (mm) @ t=3.755E-10	1.09176	qz (mm) @ t=3.985E-10	0.75285
qz (mm) @ t=3.76E-10	1.08459	qz (mm) @ t=3.99E-10	0.74526
qz (mm) @ t=3.765E-10	1.07743	qz (mm) @ t=3.995E-10	0.73767
qz (mm) @ t=3.77E-10	1.07025	qz (mm) @ t=4E-10	0.73007
qz (mm) @ t=3.775E-10	1.06306	qz (mm) @ t=4.005E-10	0.72246
qz (mm) @ t=3.78E-10	1.05586	qz (mm) @ t=4.01E-10	0.71483
qz (mm) @ t=3.785E-10	1.04865	qz (mm) @ t=4.015E-10	0.70720
qz (mm) @ t=3.79E-10	1.04144	qz (mm) @ t=4.02E-10	0.69957
qz (mm) @ t=3.795E-10	1.03421	qz (mm) @ t=4.025E-10	0.69192
qz (mm) @ t=3.8E-10	1.02698	qz (mm) @ t=4.03E-10	0.68426
qz (mm) @ t=3.805E-10	1.01974	qz (mm) @ t=4.035E-10	0.67659
qz (mm) @ t=3.81E-10	1.01248	qz (mm) @ t=4.04E-10	0.66892
qz (mm) @ t=3.815E-10	1.00522	qz (mm) @ t=4.045E-10	0.66123
qz (mm) @ t=3.82E-10	0.99795	qz (mm) @ t=4.05E-10	0.65354
qz (mm) @ t=3.825E-10	0.99067	qz (mm) @ t=4.055E-10	0.64584
qz (mm) @ t=3.83E-10	0.98338	qz (mm) @ t=4.06E-10	0.63812
qz (mm) @ t=3.835E-10	0.97608	qz (mm) @ t=4.065E-10	0.63040
qz (mm) @ t=3.84E-10	0.96878	qz (mm) @ t=4.07E-10	0.62267
qz (mm) @ t=3.845E-10	0.96146	qz (mm) @ t=4.075E-10	0.61493
qz (mm) @ t=3.85E-10	0.95413	qz (mm) @ t=4.08E-10	0.60718
qz (mm) @ t=3.855E-10	0.94680	qz (mm) @ t=4.085E-10	0.59942
qz (mm) @ t=3.86E-10	0.93945	qz (mm) @ t=4.09E-10	0.59166
qz (mm) @ t=3.865E-10	0.93210	qz (mm) @ t=4.095E-10	0.58388
qz (mm) @ t=3.87E-10	0.92473	qz (mm) @ t=4.1E-10	0.57609
qz (mm) @ t=3.875E-10	0.91736	qz (mm) @ t=4.105E-10	0.56830
qz (mm) @ t=3.88E-10	0.90998	qz (mm) @ t=4.11E-10	0.56049
qz (mm) @ t=3.885E-10	0.90259	qz (mm) @ t=4.115E-10	0.55268
qz (mm) @ t=3.89E-10	0.89519	qz (mm) @ t=4.12E-10	0.54486
qz (mm) @ t=3.895E-10	0.88778	qz (mm) @ t=4.125E-10	0.53702
qz (mm) @ t=3.9E-10	0.88036	qz (mm) @ t=4.13E-10	0.52918
qz (mm) @ t=3.905E-10	0.87294	qz (mm) @ t=4.135E-10	0.52133

doi:10.6844/NCKU202003198

qz (mm) @ t=3.68E-10	2.06122	qz (mm) @ t=3.91E-10	1.83823
qz (mm) @ t=3.685E-10	2.05651	qz (mm) @ t=3.915E-10	1.83324
qz (mm) @ t=3.69E-10	2.05180	qz (mm) @ t=3.92E-10	1.82824
qz (mm) @ t=3.695E-10	2.04708	qz (mm) @ t=3.925E-10	1.82323
qz (mm) @ t=3.7E-10	2.04235	qz (mm) @ t=3.93E-10	1.81822
qz (mm) @ t=3.705E-10	2.03762	qz (mm) @ t=3.935E-10	1.81320
qz (mm) @ t=3.71E-10	2.03288	qz (mm) @ t=3.94E-10	1.80817
qz (mm) @ t=3.715E-10	2.02814	qz (mm) @ t=3.945E-10	1.80314
qz (mm) @ t=3.72E-10	2.02339	qz (mm) @ t=3.95E-10	1.79810
qz (mm) @ t=3.725E-10	2.01863	qz (mm) @ t=3.955E-10	1.79306
qz (mm) @ t=3.73E-10	2.01387	qz (mm) @ t=3.96E-10	1.78801
qz (mm) @ t=3.735E-10	2.00910	qz (mm) @ t=3.965E-10	1.78295
qz (mm) @ t=3.74E-10	2.00432	qz (mm) @ t=3.97E-10	1.77789
qz (mm) @ t=3.745E-10	1.99954	qz (mm) @ t=3.975E-10	1.77282
qz (mm) @ t=3.75E-10	1.99475	qz (mm) @ t=3.98E-10	1.76775
qz (mm) @ t=3.755E-10	1.98996	qz (mm) @ t=3.985E-10	1.76267
qz (mm) @ t=3.76E-10	1.98516	qz (mm) @ t=3.99E-10	1.75758
qz (mm) @ t=3.765E-10	1.98035	qz (mm) @ t=3.995E-10	1.75248
qz (mm) @ t=3.77E-10	1.97554	qz (mm) @ t=4E-10	1.74738
qz (mm) @ t=3.775E-10	1.97072	qz (mm) @ t=4.005E-10	1.74228
qz (mm) @ t=3.78E-10	1.96589	qz (mm) @ t=4.01E-10	1.73717
qz (mm) @ t=3.785E-10	1.96106	qz (mm) @ t=4.015E-10	1.73205
qz (mm) @ t=3.79E-10	1.95622	qz (mm) @ t=4.02E-10	1.72692
qz (mm) @ t=3.795E-10	1.95138	qz (mm) @ t=4.025E-10	1.72179
qz (mm) @ t=3.8E-10	1.94652	qz (mm) @ t=4.03E-10	1.71666
qz (mm) @ t=3.805E-10	1.94167	qz (mm) @ t=4.035E-10	1.71151
qz (mm) @ t=3.81E-10	1.93680	qz (mm) @ t=4.04E-10	1.70636
qz (mm) @ t=3.815E-10	1.93193	qz (mm) @ t=4.045E-10	1.70121
qz (mm) @ t=3.82E-10	1.92706	qz (mm) @ t=4.05E-10	1.69604
qz (mm) @ t=3.825E-10	1.92218	qz (mm) @ t=4.055E-10	1.69088
qz (mm) @ t=3.83E-10	1.91729	qz (mm) @ t=4.06E-10	1.68570
qz (mm) @ t=3.835E-10	1.91239	qz (mm) @ t=4.065E-10	1.68052
qz (mm) @ t=3.84E-10	1.90749	qz (mm) @ t=4.07E-10	1.67534
qz (mm) @ t=3.845E-10	1.90259	qz (mm) @ t=4.075E-10	1.67014
qz (mm) @ t=3.85E-10	1.89767	qz (mm) @ t=4.08E-10	1.66494
qz (mm) @ t=3.855E-10	1.89275	qz (mm) @ t=4.085E-10	1.65974
qz (mm) @ t=3.86E-10	1.88783	qz (mm) @ t=4.09E-10	1.65453
qz (mm) @ t=3.865E-10	1.88290	qz (mm) @ t=4.095E-10	1.64931
qz (mm) @ t=3.87E-10	1.87796	qz (mm) @ t=4.1E-10	1.64409
qz (mm) @ t=3.875E-10	1.87301	qz (mm) @ t=4.105E-10	1.63885
qz (mm) @ t=3.88E-10	1.86806	qz (mm) @ t=4.11E-10	1.63362
qz (mm) @ t=3.885E-10	1.86311	qz (mm) @ t=4.115E-10	1.62838
qz (mm) @ t=3.89E-10	1.85814	qz (mm) @ t=4.12E-10	1.62313
qz (mm) @ t=3.895E-10	1.85317	qz (mm) @ t=4.125E-10	1.61787
qz (mm) @ t=3.9E-10	1.84820	qz (mm) @ t=4.13E-10	1.61261
qz (mm) @ t=3.905E-10	1.84322	qz (mm) @ t=4.135E-10	1.60734

doi:10.6844/NCKU202003198

qz (mm) @ t=4.6E-10	-0.20968	qz (mm) @ t=4.83E-10	-0.55919
qz (mm) @ t=4.605E-10	-0.21741	qz (mm) @ t=4.835E-10	-0.56665
qz (mm) @ t=4.61E-10	-0.22513	qz (mm) @ t=4.84E-10	-0.57411
qz (mm) @ t=4.615E-10	-0.23284	qz (mm) @ t=4.845E-10	-0.58156
qz (mm) @ t=4.62E-10	-0.24055	qz (mm) @ t=4.85E-10	-0.58901
qz (mm) @ t=4.625E-10	-0.24826	qz (mm) @ t=4.855E-10	-0.59645
qz (mm) @ t=4.63E-10	-0.25595	qz (mm) @ t=4.86E-10	-0.60388
qz (mm) @ t=4.635E-10	-0.26365	qz (mm) @ t=4.865E-10	-0.61131
qz (mm) @ t=4.64E-10	-0.27133	qz (mm) @ t=4.87E-10	-0.61874
qz (mm) @ t=4.645E-10	-0.27901	qz (mm) @ t=4.875E-10	-0.62615
qz (mm) @ t=4.65E-10	-0.28669	qz (mm) @ t=4.88E-10	-0.63357
qz (mm) @ t=4.655E-10	-0.29436	qz (mm) @ t=4.885E-10	-0.64097
qz (mm) @ t=4.66E-10	-0.30202	qz (mm) @ t=4.89E-10	-0.64837
qz (mm) @ t=4.665E-10	-0.30968	qz (mm) @ t=4.895E-10	-0.65577
qz (mm) @ t=4.67E-10	-0.31733	qz (mm) @ t=4.9E-10	-0.66316
qz (mm) @ t=4.675E-10	-0.32498	qz (mm) @ t=4.905E-10	-0.67054
qz (mm) @ t=4.68E-10	-0.33262	qz (mm) @ t=4.91E-10	-0.67792
qz (mm) @ t=4.685E-10	-0.34025	qz (mm) @ t=4.915E-10	-0.68529
qz (mm) @ t=4.69E-10	-0.34788	qz (mm) @ t=4.92E-10	-0.69266
qz (mm) @ t=4.695E-10	-0.35551	qz (mm) @ t=4.925E-10	-0.70002
qz (mm) @ t=4.7E-10	-0.36312	qz (mm) @ t=4.93E-10	-0.70738
qz (mm) @ t=4.705E-10	-0.37074	qz (mm) @ t=4.935E-10	-0.71472
qz (mm) @ t=4.71E-10	-0.37834	qz (mm) @ t=4.94E-10	-0.72207
qz (mm) @ t=4.715E-10	-0.38594	qz (mm) @ t=4.945E-10	-0.72941
qz (mm) @ t=4.72E-10	-0.39354	qz (mm) @ t=4.95E-10	-0.73674
qz (mm) @ t=4.725E-10	-0.40113	qz (mm) @ t=4.955E-10	-0.74407
qz (mm) @ t=4.73E-10	-0.40871	qz (mm) @ t=4.96E-10	-0.75139
qz (mm) @ t=4.735E-10	-0.41629	qz (mm) @ t=4.965E-10	-0.75870
qz (mm) @ t=4.74E-10	-0.42386	qz (mm) @ t=4.97E-10	-0.76601
qz (mm) @ t=4.745E-10	-0.43143	qz (mm) @ t=4.975E-10	-0.77332
qz (mm) @ t=4.75E-10	-0.43899	qz (mm) @ t=4.98E-10	-0.78061
qz (mm) @ t=4.755E-10	-0.44654	qz (mm) @ t=4.985E-10	-0.78791
qz (mm) @ t=4.76E-10	-0.45409	qz (mm) @ t=4.99E-10	-0.79519
qz (mm) @ t=4.765E-10	-0.46164	qz (mm) @ t=4.995E-10	-0.80247
qz (mm) @ t=4.77E-10	-0.46918	qz (mm) @ t=5E-10	-0.80975
qz (mm) @ t=4.775E-10	-0.47671		
qz (mm) @ t=4.78E-10	-0.48423		
qz (mm) @ t=4.785E-10	-0.49176		
qz (mm) @ t=4.79E-10	-0.49927		
qz (mm) @ t=4.795E-10	-0.50678		
qz (mm) @ t=4.8E-10	-0.51428		
qz (mm) @ t=4.805E-10	-0.52178		
qz (mm) @ t=4.81E-10	-0.52927		
qz (mm) @ t=4.815E-10	-0.53676		
qz (mm) @ t=4.82E-10	-0.54424		
qz (mm) @ t=4.825E-10	-0.55172		

doi:10.6844/NCKU202003198

Table 20: Raw data of electron trajectories with $V_{acc} = 1000$ V.

qz (mm) @ t=0	3.80000	qz (mm) @ t=2.3E-11	3.78638
qz (mm) @ t=5E-13	3.79999	qz (mm) @ t=2.35E-11	3.78578
qz (mm) @ t=1E-12	3.79997	qz (mm) @ t=2.4E-11	3.78517
qz (mm) @ t=1.5E-12	3.79994	qz (mm) @ t=2.45E-11	3.78454
qz (mm) @ t=2E-12	3.79990	qz (mm) @ t=2.5E-11	3.78391
qz (mm) @ t=2.5E-12	3.79984	qz (mm) @ t=2.55E-11	3.78326
qz (mm) @ t=3E-12	3.79977	qz (mm) @ t=2.6E-11	3.78259
qz (mm) @ t=3.5E-12	3.79968	qz (mm) @ t=2.65E-11	3.78192
qz (mm) @ t=4E-12	3.79959	qz (mm) @ t=2.7E-11	3.78123
qz (mm) @ t=4.5E-12	3.79948	qz (mm) @ t=2.75E-11	3.78053
qz (mm) @ t=5E-12	3.79936	qz (mm) @ t=2.8E-11	3.77981
qz (mm) @ t=5.5E-12	3.79922	qz (mm) @ t=2.85E-11	3.77908
qz (mm) @ t=6E-12	3.79907	qz (mm) @ t=2.9E-11	3.77834
qz (mm) @ t=6.5E-12	3.79891	qz (mm) @ t=2.95E-11	3.77759
qz (mm) @ t=7E-12	3.79874	qz (mm) @ t=3E-11	3.77682
qz (mm) @ t=7.5E-12	3.79855	qz (mm) @ t=3.05E-11	3.77605
qz (mm) @ t=8E-12	3.79835	qz (mm) @ t=3.1E-11	3.77525
qz (mm) @ t=8.5E-12	3.79814	qz (mm) @ t=3.15E-11	3.77445
qz (mm) @ t=9E-12	3.79791	qz (mm) @ t=3.2E-11	3.77363
qz (mm) @ t=9.5E-12	3.79768	qz (mm) @ t=3.25E-11	3.77280
qz (mm) @ t=1E-11	3.79742	qz (mm) @ t=3.3E-11	3.77196
qz (mm) @ t=1.05E-11	3.79716	qz (mm) @ t=3.35E-11	3.77110
qz (mm) @ t=1.1E-11	3.79688	qz (mm) @ t=3.4E-11	3.77023
qz (mm) @ t=1.15E-11	3.79659	qz (mm) @ t=3.45E-11	3.76935
qz (mm) @ t=1.2E-11	3.79629	qz (mm) @ t=3.5E-11	3.76846
qz (mm) @ t=1.25E-11	3.79598	qz (mm) @ t=3.55E-11	3.76755
qz (mm) @ t=1.3E-11	3.79565	qz (mm) @ t=3.6E-11	3.76663
qz (mm) @ t=1.35E-11	3.79531	qz (mm) @ t=3.65E-11	3.76569
qz (mm) @ t=1.4E-11	3.79495	qz (mm) @ t=3.7E-11	3.76475
qz (mm) @ t=1.45E-11	3.79459	qz (mm) @ t=3.75E-11	3.76379
qz (mm) @ t=1.5E-11	3.79421	qz (mm) @ t=3.8E-11	3.76282
qz (mm) @ t=1.55E-11	3.79381	qz (mm) @ t=3.85E-11	3.76183
qz (mm) @ t=1.6E-11	3.79341	qz (mm) @ t=3.9E-11	3.76083
qz (mm) @ t=1.65E-11	3.79299	qz (mm) @ t=3.95E-11	3.75982
qz (mm) @ t=1.7E-11	3.79256	qz (mm) @ t=4E-11	3.75880
qz (mm) @ t=1.75E-11	3.79211	qz (mm) @ t=4.05E-11	3.75776
qz (mm) @ t=1.8E-11	3.79166	qz (mm) @ t=4.1E-11	3.75671
qz (mm) @ t=1.85E-11	3.79119	qz (mm) @ t=4.15E-11	3.75565
qz (mm) @ t=1.9E-11	3.79070	qz (mm) @ t=4.2E-11	3.75458
qz (mm) @ t=1.95E-11	3.79021	qz (mm) @ t=4.25E-11	3.75349
qz (mm) @ t=2E-11	3.78970	qz (mm) @ t=4.3E-11	3.75239
qz (mm) @ t=2.05E-11	3.78918	qz (mm) @ t=4.35E-11	3.75128
qz (mm) @ t=2.1E-11	3.78864	qz (mm) @ t=4.4E-11	3.75015
qz (mm) @ t=2.15E-11	3.78810	qz (mm) @ t=4.45E-11	3.74901
qz (mm) @ t=2.2E-11	3.78754	qz (mm) @ t=4.5E-11	3.74786
qz (mm) @ t=2.25E-11	3.78696	qz (mm) @ t=4.55E-11	3.74669

doi:10.6844/NCKU202003198

qz (mm) @ t=4.6E-11	3.74551	qz (mm) @ t=6.9E-11	3.67741
qz (mm) @ t=4.65E-11	3.74432	qz (mm) @ t=6.95E-11	3.67563
qz (mm) @ t=4.7E-11	3.74312	qz (mm) @ t=7E-11	3.67383
qz (mm) @ t=4.75E-11	3.74190	qz (mm) @ t=7.05E-11	3.67202
qz (mm) @ t=4.8E-11	3.74067	qz (mm) @ t=7.1E-11	3.67020
qz (mm) @ t=4.85E-11	3.73943	qz (mm) @ t=7.15E-11	3.66837
qz (mm) @ t=4.9E-11	3.73818	qz (mm) @ t=7.2E-11	3.66652
qz (mm) @ t=4.95E-11	3.73691	qz (mm) @ t=7.25E-11	3.66466
qz (mm) @ t=5E-11	3.73563	qz (mm) @ t=7.3E-11	3.66279
qz (mm) @ t=5.05E-11	3.73433	qz (mm) @ t=7.35E-11	3.66090
qz (mm) @ t=5.1E-11	3.73303	qz (mm) @ t=7.4E-11	3.65900
qz (mm) @ t=5.15E-11	3.73171	qz (mm) @ t=7.45E-11	3.65709
qz (mm) @ t=5.2E-11	3.73037	qz (mm) @ t=7.5E-11	3.65517
qz (mm) @ t=5.25E-11	3.72903	qz (mm) @ t=7.55E-11	3.65323
qz (mm) @ t=5.3E-11	3.72767	qz (mm) @ t=7.6E-11	3.65128
qz (mm) @ t=5.35E-11	3.72630	qz (mm) @ t=7.65E-11	3.64932
qz (mm) @ t=5.4E-11	3.72491	qz (mm) @ t=7.7E-11	3.64734
qz (mm) @ t=5.45E-11	3.72352	qz (mm) @ t=7.75E-11	3.64535
qz (mm) @ t=5.5E-11	3.72211	qz (mm) @ t=7.8E-11	3.64335
qz (mm) @ t=5.55E-11	3.72069	qz (mm) @ t=7.85E-11	3.64134
qz (mm) @ t=5.6E-11	3.71925	qz (mm) @ t=7.9E-11	3.63931
qz (mm) @ t=5.65E-11	3.71780	qz (mm) @ t=7.95E-11	3.63727
qz (mm) @ t=5.7E-11	3.71634	qz (mm) @ t=8E-11	3.63521
qz (mm) @ t=5.75E-11	3.71487	qz (mm) @ t=8.05E-11	3.63315
qz (mm) @ t=5.8E-11	3.71338	qz (mm) @ t=8.1E-11	3.63107
qz (mm) @ t=5.85E-11	3.71188	qz (mm) @ t=8.15E-11	3.62898
qz (mm) @ t=5.9E-11	3.71037	qz (mm) @ t=8.2E-11	3.62687
qz (mm) @ t=5.95E-11	3.70884	qz (mm) @ t=8.25E-11	3.62476
qz (mm) @ t=6E-11	3.70730	qz (mm) @ t=8.3E-11	3.62263
qz (mm) @ t=6.05E-11	3.70575	qz (mm) @ t=8.35E-11	3.62048
qz (mm) @ t=6.1E-11	3.70419	qz (mm) @ t=8.4E-11	3.61833
qz (mm) @ t=6.15E-11	3.70261	qz (mm) @ t=8.45E-11	3.61616
qz (mm) @ t=6.2E-11	3.70102	qz (mm) @ t=8.5E-11	3.61398
qz (mm) @ t=6.25E-11	3.69942	qz (mm) @ t=8.55E-11	3.61178
qz (mm) @ t=6.3E-11	3.69780	qz (mm) @ t=8.6E-11	3.60957
qz (mm) @ t=6.35E-11	3.69617	qz (mm) @ t=8.65E-11	3.60735
qz (mm) @ t=6.4E-11	3.69453	qz (mm) @ t=8.7E-11	3.60512
qz (mm) @ t=6.45E-11	3.69288	qz (mm) @ t=8.75E-11	3.60287
qz (mm) @ t=6.5E-11	3.69121	qz (mm) @ t=8.8E-11	3.60062
qz (mm) @ t=6.55E-11	3.68953	qz (mm) @ t=8.85E-11	3.59834
qz (mm) @ t=6.6E-11	3.68784	qz (mm) @ t=8.9E-11	3.59606
qz (mm) @ t=6.65E-11	3.68613	qz (mm) @ t=8.95E-11	3.59376
qz (mm) @ t=6.7E-11	3.68441	qz (mm) @ t=9E-11	3.59145
qz (mm) @ t=6.75E-11	3.68268	qz (mm) @ t=9.05E-11	3.58913
qz (mm) @ t=6.8E-11	3.68094	qz (mm) @ t=9.1E-11	3.58679
qz (mm) @ t=6.85E-11	3.67918	qz (mm) @ t=9.15E-11	3.58444

doi:10.6844/NCKU202003198

qz (mm) @ t=9.2E-11	3.58208	qz (mm) @ t=1.15E-10	3.45954
qz (mm) @ t=9.25E-11	3.57971	qz (mm) @ t=1.155E-10	3.45658
qz (mm) @ t=9.3E-11	3.57732	qz (mm) @ t=1.16E-10	3.45360
qz (mm) @ t=9.35E-11	3.57492	qz (mm) @ t=1.165E-10	3.45061
qz (mm) @ t=9.4E-11	3.57251	qz (mm) @ t=1.17E-10	3.44760
qz (mm) @ t=9.45E-11	3.57008	qz (mm) @ t=1.175E-10	3.44459
qz (mm) @ t=9.5E-11	3.56764	qz (mm) @ t=1.18E-10	3.44156
qz (mm) @ t=9.55E-11	3.56519	qz (mm) @ t=1.185E-10	3.43851
qz (mm) @ t=9.6E-11	3.56272	qz (mm) @ t=1.19E-10	3.43546
qz (mm) @ t=9.65E-11	3.56025	qz (mm) @ t=1.195E-10	3.43239
qz (mm) @ t=9.7E-11	3.55776	qz (mm) @ t=1.2E-10	3.42931
qz (mm) @ t=9.75E-11	3.55525	qz (mm) @ t=1.205E-10	3.42621
qz (mm) @ t=9.8E-11	3.55274	qz (mm) @ t=1.21E-10	3.42311
qz (mm) @ t=9.85E-11	3.55021	qz (mm) @ t=1.215E-10	3.41999
qz (mm) @ t=9.9E-11	3.54767	qz (mm) @ t=1.22E-10	3.41686
qz (mm) @ t=9.95E-11	3.54511	qz (mm) @ t=1.225E-10	3.41371
qz (mm) @ t=1E-10	3.54254	qz (mm) @ t=1.23E-10	3.41055
qz (mm) @ t=1.005E-10	3.53996	qz (mm) @ t=1.235E-10	3.40738
qz (mm) @ t=1.01E-10	3.53737	qz (mm) @ t=1.24E-10	3.40420
qz (mm) @ t=1.015E-10	3.53476	qz (mm) @ t=1.245E-10	3.40100
qz (mm) @ t=1.02E-10	3.53215	qz (mm) @ t=1.25E-10	3.39779
qz (mm) @ t=1.025E-10	3.52951	qz (mm) @ t=1.255E-10	3.39457
qz (mm) @ t=1.03E-10	3.52687	qz (mm) @ t=1.26E-10	3.39133
qz (mm) @ t=1.035E-10	3.52421	qz (mm) @ t=1.265E-10	3.38808
qz (mm) @ t=1.04E-10	3.52154	qz (mm) @ t=1.27E-10	3.38482
qz (mm) @ t=1.045E-10	3.51886	qz (mm) @ t=1.275E-10	3.38155
qz (mm) @ t=1.05E-10	3.51616	qz (mm) @ t=1.28E-10	3.37826
qz (mm) @ t=1.055E-10	3.51345	qz (mm) @ t=1.285E-10	3.37496
qz (mm) @ t=1.06E-10	3.51073	qz (mm) @ t=1.29E-10	3.37165
qz (mm) @ t=1.065E-10	3.50800	qz (mm) @ t=1.295E-10	3.36833
qz (mm) @ t=1.07E-10	3.50525	qz (mm) @ t=1.3E-10	3.36499
qz (mm) @ t=1.075E-10	3.50249	qz (mm) @ t=1.305E-10	3.36164
qz (mm) @ t=1.08E-10	3.49972	qz (mm) @ t=1.31E-10	3.35827
qz (mm) @ t=1.085E-10	3.49693	qz (mm) @ t=1.315E-10	3.35490
qz (mm) @ t=1.09E-10	3.49413	qz (mm) @ t=1.32E-10	3.35151
qz (mm) @ t=1.095E-10	3.49132	qz (mm) @ t=1.325E-10	3.34811
qz (mm) @ t=1.1E-10	3.48849	qz (mm) @ t=1.33E-10	3.34469
qz (mm) @ t=1.105E-10	3.48566	qz (mm) @ t=1.335E-10	3.34126
qz (mm) @ t=1.11E-10	3.48281	qz (mm) @ t=1.34E-10	3.33782
qz (mm) @ t=1.115E-10	3.47994	qz (mm) @ t=1.345E-10	3.33437
qz (mm) @ t=1.12E-10	3.47707	qz (mm) @ t=1.35E-10	3.33090
qz (mm) @ t=1.125E-10	3.47418	qz (mm) @ t=1.355E-10	3.32742
qz (mm) @ t=1.13E-10	3.47128	qz (mm) @ t=1.36E-10	3.32393
qz (mm) @ t=1.135E-10	3.46836	qz (mm) @ t=1.365E-10	3.32043
qz (mm) @ t=1.14E-10	3.46544	qz (mm) @ t=1.37E-10	3.31691
qz (mm) @ t=1.145E-10	3.46250	qz (mm) @ t=1.375E-10	3.31338

doi:10.6844/NCKU202003198

qz (mm) @ t=1.38E-10	3.30984	qz (mm) @ t=1.61E-10	3.13301
qz (mm) @ t=1.385E-10	3.30628	qz (mm) @ t=1.615E-10	3.12886
qz (mm) @ t=1.39E-10	3.30271	qz (mm) @ t=1.62E-10	3.12470
qz (mm) @ t=1.395E-10	3.29913	qz (mm) @ t=1.625E-10	3.12053
qz (mm) @ t=1.4E-10	3.29554	qz (mm) @ t=1.63E-10	3.11635
qz (mm) @ t=1.405E-10	3.29193	qz (mm) @ t=1.635E-10	3.11215
qz (mm) @ t=1.41E-10	3.28831	qz (mm) @ t=1.64E-10	3.10794
qz (mm) @ t=1.415E-10	3.28468	qz (mm) @ t=1.645E-10	3.10372
qz (mm) @ t=1.42E-10	3.28103	qz (mm) @ t=1.65E-10	3.09949
qz (mm) @ t=1.425E-10	3.27737	qz (mm) @ t=1.655E-10	3.09524
qz (mm) @ t=1.43E-10	3.27370	qz (mm) @ t=1.66E-10	3.09098
qz (mm) @ t=1.435E-10	3.27002	qz (mm) @ t=1.665E-10	3.08671
qz (mm) @ t=1.44E-10	3.26632	qz (mm) @ t=1.67E-10	3.08242
qz (mm) @ t=1.445E-10	3.26261	qz (mm) @ t=1.675E-10	3.07812
qz (mm) @ t=1.45E-10	3.25889	qz (mm) @ t=1.68E-10	3.07381
qz (mm) @ t=1.455E-10	3.25515	qz (mm) @ t=1.685E-10	3.06949
qz (mm) @ t=1.46E-10	3.25140	qz (mm) @ t=1.69E-10	3.06515
qz (mm) @ t=1.465E-10	3.24764	qz (mm) @ t=1.695E-10	3.06080
qz (mm) @ t=1.47E-10	3.24387	qz (mm) @ t=1.7E-10	3.05644
qz (mm) @ t=1.475E-10	3.24008	qz (mm) @ t=1.705E-10	3.05207
qz (mm) @ t=1.48E-10	3.23628	qz (mm) @ t=1.71E-10	3.04768
qz (mm) @ t=1.485E-10	3.23247	qz (mm) @ t=1.715E-10	3.04328
qz (mm) @ t=1.49E-10	3.22865	qz (mm) @ t=1.72E-10	3.03886
qz (mm) @ t=1.495E-10	3.22481	qz (mm) @ t=1.725E-10	3.03444
qz (mm) @ t=1.5E-10	3.22096	qz (mm) @ t=1.73E-10	3.03000
qz (mm) @ t=1.505E-10	3.21709	qz (mm) @ t=1.735E-10	3.02555
qz (mm) @ t=1.51E-10	3.21322	qz (mm) @ t=1.74E-10	3.02108
qz (mm) @ t=1.515E-10	3.20933	qz (mm) @ t=1.745E-10	3.01661
qz (mm) @ t=1.52E-10	3.20543	qz (mm) @ t=1.75E-10	3.01212
qz (mm) @ t=1.525E-10	3.20151	qz (mm) @ t=1.755E-10	3.00761
qz (mm) @ t=1.53E-10	3.19759	qz (mm) @ t=1.76E-10	3.00310
qz (mm) @ t=1.535E-10	3.19365	qz (mm) @ t=1.765E-10	2.99857
qz (mm) @ t=1.54E-10	3.18969	qz (mm) @ t=1.77E-10	2.99403
qz (mm) @ t=1.545E-10	3.18573	qz (mm) @ t=1.775E-10	2.98948
qz (mm) @ t=1.55E-10	3.18175	qz (mm) @ t=1.78E-10	2.98491
qz (mm) @ t=1.555E-10	3.17776	qz (mm) @ t=1.785E-10	2.98033
qz (mm) @ t=1.56E-10	3.17375	qz (mm) @ t=1.79E-10	2.97574
qz (mm) @ t=1.565E-10	3.16973	qz (mm) @ t=1.795E-10	2.97113
qz (mm) @ t=1.57E-10	3.16570	qz (mm) @ t=1.8E-10	2.96652
qz (mm) @ t=1.575E-10	3.16166	qz (mm) @ t=1.805E-10	2.96189
qz (mm) @ t=1.58E-10	3.15761	qz (mm) @ t=1.81E-10	2.95724
qz (mm) @ t=1.585E-10	3.15354	qz (mm) @ t=1.815E-10	2.95259
qz (mm) @ t=1.59E-10	3.14946	qz (mm) @ t=1.82E-10	2.94792
qz (mm) @ t=1.595E-10	3.14536	qz (mm) @ t=1.825E-10	2.94324
qz (mm) @ t=1.6E-10	3.14126	qz (mm) @ t=1.83E-10	2.93854
qz (mm) @ t=1.605E-10	3.13714	qz (mm) @ t=1.835E-10	2.93384

doi:10.6844/NCKU202003198

qx (mm) @ t=1.2E-10	-0.0000309	qx (mm) @ t=1.35E-10	-0.0018484
qy (mm) @ t=1.2E-10	0.0005347	qy (mm) @ t=1.35E-10	0.0037443
qz (mm) @ t=1.2E-10	3.7801116	qz (mm) @ t=1.35E-10	3.7776294
qx (mm) @ t=1.21E-10	-0.0000665	qx (mm) @ t=1.36E-10	-0.0020528
qy (mm) @ t=1.21E-10	0.0007847	qy (mm) @ t=1.36E-10	0.0038927
qz (mm) @ t=1.21E-10	3.7799462	qz (mm) @ t=1.36E-10	3.7774640
qx (mm) @ t=1.22E-10	-0.0001154	qx (mm) @ t=1.37E-10	-0.0022648
qy (mm) @ t=1.22E-10	0.0010325	qy (mm) @ t=1.37E-10	0.0040300
qz (mm) @ t=1.22E-10	3.7797807	qz (mm) @ t=1.37E-10	3.7772985
qx (mm) @ t=1.23E-10	-0.0001774	qx (mm) @ t=1.38E-10	-0.0024838
qy (mm) @ t=1.23E-10	0.0012773	qy (mm) @ t=1.38E-10	0.0041558
qz (mm) @ t=1.23E-10	3.7796152	qz (mm) @ t=1.38E-10	3.7771330
qx (mm) @ t=1.24E-10	-0.0002525	qx (mm) @ t=1.39E-10	-0.0027092
qy (mm) @ t=1.24E-10	0.0015185	qy (mm) @ t=1.39E-10	0.0042698
qz (mm) @ t=1.24E-10	3.7794497	qz (mm) @ t=1.39E-10	3.7769675
qx (mm) @ t=1.25E-10	-0.0003403	qx (mm) @ t=1.4E-10	-0.0029404
qy (mm) @ t=1.25E-10	0.0017553	qy (mm) @ t=1.4E-10	0.0043715
qz (mm) @ t=1.25E-10	3.7792842	qz (mm) @ t=1.4E-10	3.7768021
qx (mm) @ t=1.26E-10	-0.0004406	qx (mm) @ t=1.41E-10	-0.0031767
qy (mm) @ t=1.26E-10	0.0019871	qy (mm) @ t=1.41E-10	0.0044607
qz (mm) @ t=1.26E-10	3.7791187	qz (mm) @ t=1.41E-10	3.7766366
qx (mm) @ t=1.27E-10	-0.0005531	qx (mm) @ t=1.42E-10	-0.0034174
qy (mm) @ t=1.27E-10	0.0022132	qy (mm) @ t=1.42E-10	0.0045372
qz (mm) @ t=1.27E-10	3.7789533	qz (mm) @ t=1.42E-10	3.7764712
qx (mm) @ t=1.28E-10	-0.0006776	qx (mm) @ t=1.43E-10	-0.0036619
qy (mm) @ t=1.28E-10	0.0024330	qy (mm) @ t=1.43E-10	0.0046008
qz (mm) @ t=1.28E-10	3.7787878	qz (mm) @ t=1.43E-10	3.7763057
qx (mm) @ t=1.29E-10	-0.0008136	qx (mm) @ t=1.44E-10	-0.0039094
qy (mm) @ t=1.29E-10	0.0026458	qy (mm) @ t=1.44E-10	0.0046511
qz (mm) @ t=1.29E-10	3.7786223	qz (mm) @ t=1.44E-10	3.7761403
qx (mm) @ t=1.3E-10	-0.0009607	qx (mm) @ t=1.45E-10	-0.0041593
qy (mm) @ t=1.3E-10	0.0028511	qy (mm) @ t=1.45E-10	0.0046882
qz (mm) @ t=1.3E-10	3.7784568	qz (mm) @ t=1.45E-10	3.7759748
qx (mm) @ t=1.31E-10	-0.0011187	qx (mm) @ t=1.46E-10	-0.0044108
qy (mm) @ t=1.31E-10	0.0030482	qy (mm) @ t=1.46E-10	0.0047119
qz (mm) @ t=1.31E-10	3.7782913	qz (mm) @ t=1.46E-10	3.7758094
qx (mm) @ t=1.32E-10	-0.0012869	qx (mm) @ t=1.47E-10	-0.0046632
qy (mm) @ t=1.32E-10	0.0032366	qy (mm) @ t=1.47E-10	0.0047221
qz (mm) @ t=1.32E-10	3.7781259	qz (mm) @ t=1.47E-10	3.7756439
qx (mm) @ t=1.33E-10	-0.0014649	qx (mm) @ t=1.48E-10	-0.0049158
qy (mm) @ t=1.33E-10	0.0034158	qy (mm) @ t=1.48E-10	0.0047189
qz (mm) @ t=1.33E-10	3.7779604	qz (mm) @ t=1.48E-10	3.7754785
qx (mm) @ t=1.34E-10	-0.0016523	qx (mm) @ t=1.49E-10	-0.0051678
qy (mm) @ t=1.34E-10	0.0035851	qy (mm) @ t=1.49E-10	0.0047021
qz (mm) @ t=1.34E-10	3.7777949	qz (mm) @ t=1.49E-10	3.7753131

doi:10.6844/NCKU202003198

qx (mm) @ t=1.2E-10	-0.0000309	qx (mm) @ t=1.35E-10	-0.0018484
qy (mm) @ t=1.2E-10	0.0005347	qy (mm) @ t=1.35E-10	0.0037443
qz (mm) @ t=1.2E-10	3.7801116	qz (mm) @ t=1.35E-10	3.7776294
qx (mm) @ t=1.21E-10	-0.0000665	qx (mm) @ t=1.36E-10	-0.0020528
qy (mm) @ t=1.21E-10	0.0007847	qy (mm) @ t=1.36E-10	0.0038927
qz (mm) @ t=1.21E-10	3.7799462	qz (mm) @ t=1.36E-10	3.7774640
qx (mm) @ t=1.22E-10	-0.0001154	qx (mm) @ t=1.37E-10	-0.0022648
qy (mm) @ t=1.22E-10	0.0010325	qy (mm) @ t=1.37E-10	0.0040300
qz (mm) @ t=1.22E-10	3.7797807	qz (mm) @ t=1.37E-10	3.7772985
qx (mm) @ t=1.23E-10	-0.0001774	qx (mm) @ t=1.38E-10	-0.0024838
qy (mm) @ t=1.23E-10	0.0012773	qy (mm) @ t=1.38E-10	0.0041558
qz (mm) @ t=1.23E-10	3.7796152	qz (mm) @ t=1.38E-10	3.7771330
qx (mm) @ t=1.24E-10	-0.0002525	qx (mm) @ t=1.39E-10	-0.0027092
qy (mm) @ t=1.24E-10	0.0015185	qy (mm) @ t=1.39E-10	0.0042698
qz (mm) @ t=1.24E-10	3.7794497	qz (mm) @ t=1.39E-10	3.7769675
qx (mm) @ t=1.25E-10	-0.0003403	qx (mm) @ t=1.4E-10	-0.0029404
qy (mm) @ t=1.25E-10	0.0017553	qy (mm) @ t=1.4E-10	0.0043715
qz (mm) @ t=1.25E-10	3.7792842	qz (mm) @ t=1.4E-10	3.7768021
qx (mm) @ t=1.26E-10	-0.0004406	qx (mm) @ t=1.41E-10	-0.0031767
qy (mm) @ t=1.26E-10	0.0019871	qy (mm) @ t=1.41E-10	0.0044607
qz (mm) @ t=1.26E-10	3.7791187	qz (mm) @ t=1.41E-10	3.7766366
qx (mm) @ t=1.27E-10	-0.0005531	qx (mm) @ t=1.42E-10	-0.0034174
qy (mm) @ t=1.27E-10	0.0022132	qy (mm) @ t=1.42E-10	0.0045372
qz (mm) @ t=1.27E-10	3.7789533	qz (mm) @ t=1.42E-10	3.7764712
qx (mm) @ t=1.28E-10	-0.0006776	qx (mm) @ t=1.43E-10	-0.0036619
qy (mm) @ t=1.28E-10	0.0024330	qy (mm) @ t=1.43E-10	0.0046008
qz (mm) @ t=1.28E-10	3.7787878	qz (mm) @ t=1.43E-10	3.7763057
qx (mm) @ t=1.29E-10	-0.0008136	qx (mm) @ t=1.44E-10	-0.0039094
qy (mm) @ t=1.29E-10	0.0026458	qy (mm) @ t=1.44E-10	0.0046511
qz (mm) @ t=1.29E-10	3.7786223	qz (mm) @ t=1.44E-10	3.7761403
qx (mm) @ t=1.3E-10	-0.0009607	qx (mm) @ t=1.45E-10	-0.0041593
qy (mm) @ t=1.3E-10	0.0028511	qy (mm) @ t=1.45E-10	0.0046882
qz (mm) @ t=1.3E-10	3.7784568	qz (mm) @ t=1.45E-10	3.7759748
qx (mm) @ t=1.31E-10	-0.0011187	qx (mm) @ t=1.46E-10	-0.0044108
qy (mm) @ t=1.31E-10	0.0030482	qy (mm) @ t=1.46E-10	0.0047119
qz (mm) @ t=1.31E-10	3.7782913	qz (mm) @ t=1.46E-10	3.7758094
qx (mm) @ t=1.32E-10	-0.0012869	qx (mm) @ t=1.47E-10	-0.0046632
qy (mm) @ t=1.32E-10	0.0032366	qy (mm) @ t=1.47E-10	0.0047221
qz (mm) @ t=1.32E-10	3.7781259	qz (mm) @ t=1.47E-10	3.7756439
qx (mm) @ t=1.33E-10	-0.0014649	qx (mm) @ t=1.48E-10	-0.0049158
qy (mm) @ t=1.33E-10	0.0034158	qy (mm) @ t=1.48E-10	0.0047189
qz (mm) @ t=1.33E-10	3.7779604	qz (mm) @ t=1.48E-10	3.7754785
qx (mm) @ t=1.34E-10	-0.0016523	qx (mm) @ t=1.49E-10	-0.0051678
qy (mm) @ t=1.34E-10	0.0035851	qy (mm) @ t=1.49E-10	0.0047021
qz (mm) @ t=1.34E-10	3.7777949	qz (mm) @ t=1.49E-10	3.7753131

doi:10.6844/NCKU202003198

qz (nm) @ t=2.76E-10	1.84533	qz (nm) @ t=2.99E-10	1.50809
qz (nm) @ t=2.765E-10	1.83827	qz (nm) @ t=2.995E-10	1.50047
qz (nm) @ t=2.77E-10	1.83121	qz (nm) @ t=3E-10	1.49283
qz (nm) @ t=2.775E-10	1.82413	qz (nm) @ t=3.005E-10	1.48519
qz (nm) @ t=2.78E-10	1.81704	qz (nm) @ t=3.01E-10	1.47753
qz (nm) @ t=2.785E-10	1.80994	qz (nm) @ t=3.015E-10	1.46986
qz (nm) @ t=2.79E-10	1.80283	qz (nm) @ t=3.02E-10	1.46217
qz (nm) @ t=2.795E-10	1.79570	qz (nm) @ t=3.025E-10	1.45448
qz (nm) @ t=2.8E-10	1.78856	qz (nm) @ t=3.03E-10	1.44677
qz (nm) @ t=2.805E-10	1.78141	qz (nm) @ t=3.035E-10	1.43904
qz (nm) @ t=2.81E-10	1.77425	qz (nm) @ t=3.04E-10	1.43131
qz (nm) @ t=2.815E-10	1.76707	qz (nm) @ t=3.045E-10	1.42357
qz (nm) @ t=2.82E-10	1.75988	qz (nm) @ t=3.05E-10	1.41581
qz (nm) @ t=2.825E-10	1.75268	qz (nm) @ t=3.055E-10	1.40804
qz (nm) @ t=2.83E-10	1.74547	qz (nm) @ t=3.06E-10	1.40025
qz (nm) @ t=2.835E-10	1.73824	qz (nm) @ t=3.065E-10	1.39246
qz (nm) @ t=2.84E-10	1.73101	qz (nm) @ t=3.07E-10	1.38465
qz (nm) @ t=2.845E-10	1.72376	qz (nm) @ t=3.075E-10	1.37683
qz (nm) @ t=2.85E-10	1.71649	qz (nm) @ t=3.08E-10	1.36900
qz (nm) @ t=2.855E-10	1.70922	qz (nm) @ t=3.085E-10	1.36115
qz (nm) @ t=2.86E-10	1.70193	qz (nm) @ t=3.09E-10	1.35330
qz (nm) @ t=2.865E-10	1.69463	qz (nm) @ t=3.095E-10	1.34543
qz (nm) @ t=2.87E-10	1.68732	qz (nm) @ t=3.1E-10	1.33754
qz (nm) @ t=2.875E-10	1.67999	qz (nm) @ t=3.105E-10	1.32965
qz (nm) @ t=2.88E-10	1.67265	qz (nm) @ t=3.11E-10	1.32174
qz (nm) @ t=2.885E-10	1.66530	qz (nm) @ t=3.115E-10	1.31382
qz (nm) @ t=2.89E-10	1.65794	qz (nm) @ t=3.12E-10	1.30589
qz (nm) @ t=2.895E-10	1.65057	qz (nm) @ t=3.125E-10	1.29795
qz (nm) @ t=2.9E-10	1.64318	qz (nm) @ t=3.13E-10	1.28999
qz (nm) @ t=2.905E-10	1.63578	qz (nm) @ t=3.135E-10	1.28203
qz (nm) @ t=2.91E-10	1.62837	qz (nm) @ t=3.14E-10	1.27405
qz (nm) @ t=2.915E-10	1.62094	qz (nm) @ t=3.145E-10	1.26605
qz (nm) @ t=2.92E-10	1.61351	qz (nm) @ t=3.15E-10	1.25805
qz (nm) @ t=2.925E-10	1.60606	qz (nm) @ t=3.155E-10	1.25003
qz (nm) @ t=2.93E-10	1.59860	qz (nm) @ t=3.16E-10	1.24200
qz (nm) @ t=2.935E-10	1.59112	qz (nm) @ t=3.165E-10	1.23396
qz (nm) @ t=2.94E-10	1.58364	qz (nm) @ t=3.17E-10	1.22591
qz (nm) @ t=2.945E-10	1.57614	qz (nm) @ t=3.175E-10	1.21784
qz (nm) @ t=2.95E-10	1.56863	qz (nm) @ t=3.18E-10	1.20976
qz (nm) @ t=2.955E-10	1.56110	qz (nm) @ t=3.185E-10	1.20167
qz (nm) @ t=2.96E-10	1.55357	qz (nm) @ t=3.19E-10	1.19356
qz (nm) @ t=2.965E-10	1.54602	qz (nm) @ t=3.195E-10	1.18545
qz (nm) @ t=2.97E-10	1.53846	qz (nm) @ t=3.2E-10	1.17732
qz (nm) @ t=2.975E-10	1.53089	qz (nm) @ t=3.205E-10	1.16918
qz (nm) @ t=2.98E-10	1.52330	qz (nm) @ t=3.21E-10	1.16103
qz (nm) @ t=2.985E-10	1.51570	qz (nm) @ t=3.215E-10	1.15286

doi:10.6844/NCKU202003198

qz (nm) @ t=3.22E-10	1.14468	qz (nm) @ t=3.45E-10	0.75524
qz (nm) @ t=3.225E-10	1.13650	qz (nm) @ t=3.455E-10	0.74649
qz (nm) @ t=3.23E-10	1.12829	qz (nm) @ t=3.46E-10	0.73772
qz (nm) @ t=3.235E-10	1.12008	qz (nm) @ t=3.465E-10	0.72894
qz (nm) @ t=3.24E-10	1.11185	qz (nm) @ t=3.47E-10	0.72015
qz (nm) @ t=3.245E-10	1.10361	qz (nm) @ t=3.475E-10	0.71135
qz (nm) @ t=3.25E-10	1.09536	qz (nm) @ t=3.48E-10	0.70253
qz (nm) @ t=3.255E-10	1.08710	qz (nm) @ t=3.485E-10	0.69370
qz (nm) @ t=3.26E-10	1.07882	qz (nm) @ t=3.49E-10	0.68486
qz (nm) @ t=3.265E-10	1.07053	qz (nm) @ t=3.495E-10	0.67601
qz (nm) @ t=3.27E-10	1.06223	qz (nm) @ t=3.5E-10	0.66715
qz (nm) @ t=3.275E-10	1.05392	qz (nm) @ t=3.505E-10	0.65827
qz (nm) @ t=3.28E-10	1.04560	qz (nm) @ t=3.51E-10	0.64938
qz (nm) @ t=3.285E-10	1.03726	qz (nm) @ t=3.515E-10	0.64048
qz (nm) @ t=3.29E-10	1.02891	qz (nm) @ t=3.52E-10	0.63157
qz (nm) @ t=3.295E-10	1.02055	qz (nm) @ t=3.525E-10	0.62264
qz (nm) @ t=3.3E-10	1.01217	qz (nm) @ t=3.53E-10	0.61370
qz (nm) @ t=3.305E-10	1.00379	qz (nm) @ t=3.535E-10	0.60475
qz (nm) @ t=3.31E-10	0.99539	qz (nm) @ t=3.54E-10	0.59579
qz (nm) @ t=3.315E-10	0.98698	qz (nm) @ t=3.545E-10	0.58681
qz (nm) @ t=3.32E-10	0.97855	qz (nm) @ t=3.55E-10	0.57783
qz (nm) @ t=3.325E-10	0.97012	qz (nm) @ t=3.555E-10	0.56883
qz (nm) @ t=3.33E-10	0.96167	qz (nm) @ t=3.56E-10	0.55981
qz (nm) @ t=3.335E-10	0.95321	qz (nm) @ t=3.565E-10	0.55079
qz (nm) @ t=3.34E-10	0.94474	qz (nm) @ t=3.57E-10	0.54175
qz (nm) @ t=3.345E-10	0.93625	qz (nm) @ t=3.575E-10	0.53270
qz (nm) @ t=3.35E-10	0.92776	qz (nm) @ t=3.58E-10	0.52364
qz (nm) @ t=3.355E-10	0.91925	qz (nm) @ t=3.585E-10	0.51457
qz (nm) @ t=3.36E-10	0.91073	qz (nm) @ t=3.59E-10	0.50549
qz (nm) @ t=3.365E-10	0.90219	qz (nm) @ t=3.595E-10	0.49639
qz (nm) @ t=3.37E-10	0.89365	qz (nm) @ t=3.6E-10	0.48728
qz (nm) @ t=3.375E-10	0.88509	qz (nm) @ t=3.605E-10	0.47818
qz (nm) @ t=3.38E-10	0.87652	qz (nm) @ t=3.61E-10	0.46908
qz (nm) @ t=3.385E-10	0.86794	qz (nm) @ t=3.615E-10	0.45997
qz (nm) @ t=3.39E-10	0.85934	qz (nm) @ t=3.62E-10	0.45087
qz (nm) @ t=3.395E-10	0.85073	qz (nm) @ t=3.625E-10	0.44177
qz (nm) @ t=3.4E-10	0.84211	qz (nm) @ t=3.63E-10	0.43266
qz (nm) @ t=3.405E-10	0.83348	qz (nm) @ t=3.635E-10	0.42356
qz (nm) @ t=3.41E-10	0.82484	qz (nm) @ t=3.64E-10	0.41445
qz (nm) @ t=3.415E-10	0.81618	qz (nm) @ t=3.645E-10	0.40535
qz (nm) @ t=3.42E-10	0.80751	qz (nm) @ t=3.65E-10	0.39625
qz (nm) @ t=3.425E-10	0.79883	qz (nm) @ t=3.655E-10	0.38714
qz (nm) @ t=3.43E-10	0.79014	qz (nm) @ t=3.66E-10	0.37804
qz (nm) @ t=3.435E-10	0.78143	qz (nm) @ t=3.665E-10	0.36894
qz (nm) @ t=3.44E-10	0.77272	qz (nm) @ t=3.67E-10	0.35983
qz (nm) @ t=3.445E-10	0.76399	qz (nm) @ t=3.675E-10	0.35073

doi:10.6844/NCKU202003198

qz (mm) @ t=3.68E-10	0.34162	qz (mm) @ t=3.91E-10	-0.07690
qz (mm) @ t=3.685E-10	0.33252	qz (mm) @ t=3.915E-10	-0.08594
qz (mm) @ t=3.69E-10	0.32342	qz (mm) @ t=3.92E-10	-0.09497
qz (mm) @ t=3.695E-10	0.31431	qz (mm) @ t=3.925E-10	-0.10400
qz (mm) @ t=3.7E-10	0.30521	qz (mm) @ t=3.93E-10	-0.11301
qz (mm) @ t=3.705E-10	0.29611	qz (mm) @ t=3.935E-10	-0.12202
qz (mm) @ t=3.71E-10	0.28700	qz (mm) @ t=3.94E-10	-0.13102
qz (mm) @ t=3.715E-10	0.27790	qz (mm) @ t=3.945E-10	-0.14002
qz (mm) @ t=3.72E-10	0.26879	qz (mm) @ t=3.95E-10	-0.14900
qz (mm) @ t=3.725E-10	0.25969	qz (mm) @ t=3.955E-10	-0.15798
qz (mm) @ t=3.73E-10	0.25059	qz (mm) @ t=3.96E-10	-0.16695
qz (mm) @ t=3.735E-10	0.24148	qz (mm) @ t=3.965E-10	-0.17591
qz (mm) @ t=3.74E-10	0.23238	qz (mm) @ t=3.97E-10	-0.18487
qz (mm) @ t=3.745E-10	0.22328	qz (mm) @ t=3.975E-10	-0.19382
qz (mm) @ t=3.75E-10	0.21417	qz (mm) @ t=3.98E-10	-0.20276
qz (mm) @ t=3.755E-10	0.20507	qz (mm) @ t=3.985E-10	-0.21169
qz (mm) @ t=3.76E-10	0.19596	qz (mm) @ t=3.99E-10	-0.22061
qz (mm) @ t=3.765E-10	0.18686	qz (mm) @ t=3.995E-10	-0.22953
qz (mm) @ t=3.77E-10	0.17776	qz (mm) @ t=4E-10	-0.23844
qz (mm) @ t=3.775E-10	0.16865	qz (mm) @ t=4.005E-10	-0.24734
qz (mm) @ t=3.78E-10	0.15955	qz (mm) @ t=4.01E-10	-0.25624
qz (mm) @ t=3.785E-10	0.15045	qz (mm) @ t=4.015E-10	-0.26512
qz (mm) @ t=3.79E-10	0.14134	qz (mm) @ t=4.02E-10	-0.27400
qz (mm) @ t=3.795E-10	0.13224	qz (mm) @ t=4.025E-10	-0.28288
qz (mm) @ t=3.8E-10	0.12313	qz (mm) @ t=4.03E-10	-0.29174
qz (mm) @ t=3.805E-10	0.11403	qz (mm) @ t=4.035E-10	-0.30060
qz (mm) @ t=3.81E-10	0.10493	qz (mm) @ t=4.04E-10	-0.30944
qz (mm) @ t=3.815E-10	0.09582	qz (mm) @ t=4.045E-10	-0.31829
qz (mm) @ t−3.82E-10	0.08672	qz (mm) @ t−4.05E-10	-0.32712
qz (mm) @ t=3.825E-10	0.07762	qz (mm) @ t=4.055E-10	-0.33594
qz (mm) @ t=3.83E-10	0.06851	qz (mm) @ t=4.06E-10	-0.34476
qz (mm) @ t=3.835E-10	0.05941	qz (mm) @ t=4.065E-10	-0.35357
qz (mm) @ t=3.84E-10	0.05030	qz (mm) @ t=4.07E-10	-0.36238
qz (mm) @ t=3.845E-10	0.04120	qz (mm) @ t=4.075E-10	-0.37117
qz (mm) @ t=3.85E-10	0.03210	qz (mm) @ t=4.08E-10	-0.37996
qz (mm) @ t=3.855E-10	0.02299	qz (mm) @ t=4.085E-10	-0.38874
qz (mm) @ t−3.86E-10	0.01389	qz (mm) @ t−4.09E-10	-0.39751
qz (mm) @ t=3.865E-10	0.00479	qz (mm) @ t=4.095E-10	-0.40628
qz (mm) @ t=3.87E-10	-0.00432	qz (mm) @ t=4.1E-10	-0.41503
qz (mm) @ t=3.875E-10	-0.01342	qz (mm) @ t=4.105E-10	-0.42378
qz (mm) @ t=3.88E-10	-0.02251	qz (mm) @ t=4.11E-10	-0.43253
qz (mm) @ t=3.885E-10	-0.03159	qz (mm) @ t=4.115E-10	-0.44126
qz (mm) @ t=3.89E-10	-0.04067	qz (mm) @ t=4.12E-10	-0.44999
qz (mm) @ t=3.895E-10	-0.04974	qz (mm) @ t=4.125E-10	-0.45871
qz (mm) @ t=3.9E-10	-0.05880	qz (mm) @ t=4.13E-10	-0.46742
qz (mm) @ t=3.905E-10	-0.06786	qz (mm) @ t=4.135E-10	-0.47612

doi:10.6844/NCKU202003198

qz (mm) @ t=4.14E-10	-0.48482	qz (mm) @ t=4.37E-10	-0.87662
qz (mm) @ t=4.145E-10	-0.49351	qz (mm) @ t=4.375E-10	-0.88496
qz (mm) @ t=4.15E-10	-0.50219	qz (mm) @ t=4.38E-10	-0.89329
qz (mm) @ t=4.155E-10	-0.51086	qz (mm) @ t=4.385E-10	-0.90162
qz (mm) @ t=4.16E-10	-0.51953	qz (mm) @ t=4.39E-10	-0.90993
qz (mm) @ t=4.165E-10	-0.52819	qz (mm) @ t=4.395E-10	-0.91824
qz (mm) @ t=4.17E-10	-0.53684	qz (mm) @ t=4.4E-10	-0.92654
qz (mm) @ t=4.175E-10	-0.54548	qz (mm) @ t=4.405E-10	-0.93483
qz (mm) @ t=4.18E-10	-0.55412	qz (mm) @ t=4.41E-10	-0.94312
qz (mm) @ t=4.185E-10	-0.56274	qz (mm) @ t=4.415E-10	-0.95140
qz (mm) @ t=4.19E-10	-0.57136	qz (mm) @ t=4.42E-10	-0.95967
qz (mm) @ t=4.195E-10	-0.57998	qz (mm) @ t=4.425E-10	-0.96793
qz (mm) @ t=4.2E-10	-0.58858	qz (mm) @ t=4.43E-10	-0.97619
qz (mm) @ t=4.205E-10	-0.59718	qz (mm) @ t=4.435E-10	-0.98443
qz (mm) @ t=4.21E-10	-0.60577	qz (mm) @ t=4.44E-10	-0.99267
qz (mm) @ t=4.215E-10	-0.61435	qz (mm) @ t=4.445E-10	-1.00090
qz (mm) @ t=4.22E-10	-0.62293	qz (mm) @ t=4.45E-10	-1.00913
qz (mm) @ t=4.225E-10	-0.63149	qz (mm) @ t=4.455E-10	-1.01735
qz (mm) @ t=4.23E-10	-0.64005	qz (mm) @ t=4.46E-10	-1.02555
qz (mm) @ t=4.235E-10	-0.64860	qz (mm) @ t=4.465E-10	-1.03376
qz (mm) @ t=4.24E-10	-0.65715	qz (mm) @ t=4.47E-10	-1.04195
qz (mm) @ t=4.245E-10	-0.66569	qz (mm) @ t=4.475E-10	-1.05014
qz (mm) @ t=4.25E-10	-0.67421	qz (mm) @ t=4.48E-10	-1.05831
qz (mm) @ t=4.255E-10	-0.68274	qz (mm) @ t=4.485E-10	-1.06649
qz (mm) @ t=4.26E-10	-0.69125	qz (mm) @ t=4.49E-10	-1.07465
qz (mm) @ t=4.265E-10	-0.69976	qz (mm) @ t=4.495E-10	-1.08281
qz (mm) @ t=4.27E-10	-0.70825	qz (mm) @ t=4.5E-10	-1.09095
qz (mm) @ t=4.275E-10	-0.71674	qz (mm) @ t=4.505E-10	-1.09909
qz (mm) @ t=4.28E-10	-0.72523	qz (mm) @ t=4.51E-10	-1.10723
qz (mm) @ t=4.285E-10	-0.73370	qz (mm) @ t=4.515E-10	-1.11535
qz (mm) @ t=4.29E-10	-0.74217	qz (mm) @ t=4.52E-10	-1.12347
qz (mm) @ t=4.295E-10	-0.75063	qz (mm) @ t=4.525E-10	-1.13158
qz (mm) @ t=4.3E-10	-0.75908	qz (mm) @ t=4.53E-10	-1.13968
qz (mm) @ t=4.305E-10	-0.76753	qz (mm) @ t=4.535E-10	-1.14778
qz (mm) @ t=4.31E-10	-0.77597	qz (mm) @ t=4.54E-10	-1.15587
qz (mm) @ t=4.315E-10	-0.78440	qz (mm) @ t=4.545E-10	-1.16395
qz (mm) @ t=4.32E-10	-0.79282	qz (mm) @ t=4.55E-10	-1.17202
qz (mm) @ t=4.325E-10	-0.80123	qz (mm) @ t=4.555E-10	-1.18008
qz (mm) @ t=4.33E-10	-0.80964	qz (mm) @ t=4.56E-10	-1.18814
qz (mm) @ t=4.335E-10	-0.81804	qz (mm) @ t=4.565E-10	-1.19619
qz (mm) @ t=4.34E-10	-0.82643	qz (mm) @ t=4.57E-10	-1.20423
qz (mm) @ t=4.345E-10	-0.83482	qz (mm) @ t=4.575E-10	-1.21226
qz (mm) @ t=4.35E-10	-0.84319	qz (mm) @ t=4.58E-10	-1.22029
qz (mm) @ t=4.355E-10	-0.85156	qz (mm) @ t=4.585E-10	-1.22831
qz (mm) @ t=4.36E-10	-0.85992	qz (mm) @ t=4.59E-10	-1.23632
qz (mm) @ t=4.365E-10	-0.86828	qz (mm) @ t=4.595E-10	-1.24432

doi:10.6844/NCKU202003198

qz (mm) @ t=4.6E-10	-1.25232	qz (mm) @ t=4.83E-10	-1.61191
qz (mm) @ t=4.605E-10	-1.26031	qz (mm) @ t=4.835E-10	-1.61954
qz (mm) @ t=4.61E-10	-1.26829	qz (mm) @ t=4.84E-10	-1.62717
qz (mm) @ t=4.615E-10	-1.27626	qz (mm) @ t=4.845E-10	-1.63480
qz (mm) @ t=4.62E-10	-1.28423	qz (mm) @ t=4.85E-10	-1.64241
qz (mm) @ t=4.625E-10	-1.29219	qz (mm) @ t=4.855E-10	-1.65002
qz (mm) @ t=4.63E-10	-1.30014	qz (mm) @ t=4.86E-10	-1.65762
qz (mm) @ t=4.635E-10	-1.30808	qz (mm) @ t=4.865E-10	-1.66521
qz (mm) @ t=4.64E-10	-1.31601	qz (mm) @ t=4.87E-10	-1.67280
qz (mm) @ t=4.645E-10	-1.32394	qz (mm) @ t=4.875E-10	-1.68038
qz (mm) @ t=4.65E-10	-1.33186	qz (mm) @ t=4.88E-10	-1.68794
qz (mm) @ t=4.655E-10	-1.33977	qz (mm) @ t=4.885E-10	-1.69551
qz (mm) @ t=4.66E-10	-1.34768	qz (mm) @ t=4.89E-10	-1.70306
qz (mm) @ t=4.665E-10	-1.35558	qz (mm) @ t=4.895E-10	-1.71061
qz (mm) @ t=4.67E-10	-1.36346	qz (mm) @ t=4.9E-10	-1.71815
qz (mm) @ t=4.675E-10	-1.37135	qz (mm) @ t=4.905E-10	-1.72568
qz (mm) @ t=4.68E-10	-1.37922	qz (mm) @ t=4.91E-10	-1.73320
qz (mm) @ t=4.685E-10	-1.38709	qz (mm) @ t=4.915E-10	-1.74072
qz (mm) @ t=4.69E-10	-1.39495	qz (mm) @ t=4.92E-10	-1.74823
qz (mm) @ t=4.695E-10	-1.40280	qz (mm) @ t=4.925E-10	-1.75573
qz (mm) @ t=4.7E-10	-1.41064	qz (mm) @ t=4.93E-10	-1.76322
qz (mm) @ t=4.705E-10	-1.41848	qz (mm) @ t=4.935E-10	-1.77071
qz (mm) @ t=4.71E-10	-1.42631	qz (mm) @ t=4.94E-10	-1.77819
qz (mm) @ t=4.715E-10	-1.43413	qz (mm) @ t=4.945E-10	-1.78566
qz (mm) @ t=4.72E-10	-1.44194	qz (mm) @ t=4.95E-10	-1.79312
qz (mm) @ t=4.725E-10	-1.44975	qz (mm) @ t=4.955E-10	-1.80058
qz (mm) @ t=4.73E-10	-1.45754	qz (mm) @ t=4.96E-10	-1.80802
qz (mm) @ t=4.735E-10	-1.46533	qz (mm) @ t=4.965E-10	-1.81546
qz (mm) @ t=4.74E-10	-1.47312	qz (mm) @ t=4.97E-10	-1.82290
qz (mm) @ t=4.745E-10	-1.48089	qz (mm) @ t=4.975E-10	-1.83032
qz (mm) @ t=4.75E-10	-1.48866	qz (mm) @ t=4.98E-10	-1.83774
qz (mm) @ t=4.755E-10	-1.49642	qz (mm) @ t=4.985E-10	-1.84515
qz (mm) @ t=4.76E-10	-1.50417	qz (mm) @ t=4.99E-10	-1.85255
qz (mm) @ t=4.765E-10	-1.51192	qz (mm) @ t=4.995E-10	-1.85995
qz (mm) @ t=4.77E-10	-1.51965	qz (mm) @ t=5E-10	-1.86733
qz (mm) @ t=4.775E-10	-1.52738		
qz (mm) @ t=4.78E-10	-1.53511		
qz (mm) @ t=4.785E-10	-1.54282		
qz (mm) @ t=4.79E-10	-1.55053		
qz (mm) @ t=4.795E-10	-1.55823		
qz (mm) @ t=4.8E-10	-1.56592		
qz (mm) @ t=4.805E-10	-1.57360		
qz (mm) @ t=4.81E-10	-1.58128		
qz (mm) @ t=4.815E-10	-1.58895		
qz (mm) @ t=4.82E-10	-1.59661		
qz (mm) @ t=4.825E-10	-1.60426		

C.3 Electron trajectory with the magnetic field

1. The initial positions: $0\hat{x} + 0\hat{y} + 3.8\hat{z}$ (mm).

2. The initial angle: 56.4^{o}.

doi:10.6844/NCKU202003198

3. The initial velocities: $0\hat{x} + 2.50 \times 10^5\hat{y} + -1.66 \times 10^5\hat{z}$ (m/s).

4. The total simulated time: 4×10^{-8} (s).

5. Steps: 40001.

6. qx, qy, and qz are the positions in $\hat{x}$, $\hat{y}$, and $\hat{z}$, respectively.

Table 21: Raw data of electron trajectories with the magnetic field.

qx (mm) @ t=0	0.0000000	qx (mm) @ t=1.5E-11	-0.0014296
qy (mm) @ t=0	0.0000000	qy (mm) @ t=1.5E-11	0.0033848
qz (mm) @ t=0	3.8000000	qz (mm) @ t=1.5E-11	3.7975100
qx (mm) @ t=1E-12	-0.0000067	qx (mm) @ t=1.6E-11	-0.0016149
qy (mm) @ t=1E-12	0.0002499	qy (mm) @ t=1.6E-11	0.0035560
qz (mm) @ t=1E-12	3.7998340	qz (mm) @ t=1.6E-11	3.7973440
qx (mm) @ t=2E-12	-0.0000266	qx (mm) @ t=1.7E-11	-0.0018090
qy (mm) @ t=2E-12	0.0004993	qy (mm) @ t=1.7E-11	0.0037171
qz (mm) @ t=2E-12	3.7996680	qz (mm) @ t=1.7E-11	3.7971781
qx (mm) @ t=3E-12	-0.0000598	qx (mm) @ t=1.8E-11	-0.0020114
qy (mm) @ t=3E-12	0.0007475	qy (mm) @ t=1.8E-11	0.0038676
qz (mm) @ t=3E-12	3.7995020	qz (mm) @ t=1.8E-11	3.7970121
qx (mm) @ t=4E-12	-0.0001063	qx (mm) @ t=1.9E-11	-0.0022215
qy (mm) @ t=4E-12	0.0009938	qy (mm) @ t=1.9E-11	0.0040072
qz (mm) @ t=4E-12	3.7993360	qz (mm) @ t=1.9E-11	3.7968461
qx (mm) @ t=5E-12	-0.0001658	qx (mm) @ t=2E-11	-0.0024388
qy (mm) @ t=5E-12	0.0012377	qy (mm) @ t=2E-11	0.0041353
qz (mm) @ t=5E-12	3.7991700	qz (mm) @ t=2E-11	3.7966801
qx (mm) @ t=6E-12	-0.0002383	qx (mm) @ t=2.1E-11	-0.0026626
qy (mm) @ t=6E-12	0.0014783	qy (mm) @ t=2.1E-11	0.0042517
qz (mm) @ t=6E-12	3.7990040	qz (mm) @ t=2.1E-11	3.7965141
qx (mm) @ t=7E-12	-0.0003236	qx (mm) @ t=2.2E-11	-0.0028923
qy (mm) @ t=7E-12	0.0017152	qy (mm) @ t=2.2E-11	0.0043560
qz (mm) @ t=7E-12	3.7988380	qz (mm) @ t=2.2E-11	3.7963481
qx (mm) @ t=8E-12	-0.0004214	qx (mm) @ t=2.3E-11	-0.0031272
qy (mm) @ t=8E-12	0.0019474	qy (mm) @ t=2.3E-11	0.0044479
qz (mm) @ t=8E-12	3.7986720	qz (mm) @ t=2.3E-11	3.7961822
qx (mm) @ t=9E-12	-0.0005316	qx (mm) @ t=2.4E-11	-0.0033667
qy (mm) @ t=9E-12	0.0021744	qy (mm) @ t=2.4E-11	0.0045272
qz (mm) @ t=9E-12	3.7985060	qz (mm) @ t=2.4E-11	3.7960162
qx (mm) @ t=1E-11	-0.0006536	qx (mm) @ t=2.5E-11	-0.0036100
qy (mm) @ t=1E-11	0.0023951	qy (mm) @ t=2.5E-11	0.0045937
qz (mm) @ t=1E-11	3.7983400	qz (mm) @ t=2.5E-11	3.7958502
qx (mm) @ t=1.1E-11	-0.0007873	qx (mm) @ t=2.6E-11	-0.0038566
qy (mm) @ t=1.1E-11	0.0026090	qy (mm) @ t=2.6E-11	0.0046470
qz (mm) @ t=1.1E-11	3.7981740	qz (mm) @ t=2.6E-11	3.7956843
qx (mm) @ t=1.2E-11	-0.0009321	qx (mm) @ t=2.7E-11	-0.0041056
qy (mm) @ t=1.2E-11	0.0028155	qy (mm) @ t=2.7E-11	0.0046872
qz (mm) @ t=1.2E-11	3.7980080	qz (mm) @ t=2.7E-11	3.7955183
qx (mm) @ t=1.3E-11	-0.0010878	qx (mm) @ t=2.8E-11	-0.0043565
qy (mm) @ t=1.3E-11	0.0030140	qy (mm) @ t=2.8E-11	0.0047140
qz (mm) @ t=1.3E-11	3.7978420	qz (mm) @ t=2.8E-11	3.7953523
qx (mm) @ t=1.4E-11	-0.0012538	qx (mm) @ t=2.9E-11	-0.0046084
qy (mm) @ t=1.4E-11	0.0032040	qy (mm) @ t=2.9E-11	0.0047275
qz (mm) @ t=1.4E-11	3.7976760	qz (mm) @ t=2.9E-11	3.7951864

doi:10.6844/NCKU202003198

qx (mm) @ t=3E-11	-0.0048606	qx (mm) @ t=4.5E-11	-0.0082156
qy (mm) @ t=3E-11	0.0047275	qy (mm) @ t=4.5E-11	0.0032033
qz (mm) @ t=3E-11	3.7950204	qz (mm) @ t=4.5E-11	3.7925319
qx (mm) @ t=3.1E-11	-0.0051126	qx (mm) @ t=4.6E-11	-0.0083816
qy (mm) @ t=3.1E-11	0.0047140	qy (mm) @ t=4.6E-11	0.0030132
qz (mm) @ t=3.1E-11	3.7948545	qz (mm) @ t=4.6E-11	3.7923660
qx (mm) @ t=3.2E-11	-0.0053634	qx (mm) @ t=4.7E-11	-0.0085372
qy (mm) @ t=3.2E-11	0.0046872	qy (mm) @ t=4.7E-11	0.0028146
qz (mm) @ t=3.2E-11	3.7946886	qz (mm) @ t=4.7E-11	3.7922002
qx (mm) @ t=3.3E-11	-0.0056125	qx (mm) @ t=4.8E-11	-0.0086820
qy (mm) @ t=3.3E-11	0.0046470	qy (mm) @ t=4.8E-11	0.0026079
qz (mm) @ t=3.3E-11	3.7945226	qz (mm) @ t=4.8E-11	3.7920343
qx (mm) @ t=3.4E-11	-0.0058590	qx (mm) @ t=4.9E-11	-0.0088157
qy (mm) @ t=3.4E-11	0.0045936	qy (mm) @ t=4.9E-11	0.0023938
qz (mm) @ t=3.4E-11	3.7943567	qz (mm) @ t=4.9E-11	3.7918685
qx (mm) @ t=3.5E-11	-0.0061024	qx (mm) @ t=5E-11	-0.0089377
qy (mm) @ t=3.5E-11	0.0045272	qy (mm) @ t=5E-11	0.0021729
qz (mm) @ t=3.5E-11	3.7941908	qz (mm) @ t=5E-11	3.7917027
qx (mm) @ t=3.6E-11	-0.0063419	qx (mm) @ t=5.1E-11	-0.0090477
qy (mm) @ t=3.6E-11	0.0044479	qy (mm) @ t=5.1E-11	0.0019459
qz (mm) @ t=3.6E-11	3.7940248	qz (mm) @ t=5.1E-11	3.7915369
qx (mm) @ t=3.7E-11	-0.0065769	qx (mm) @ t=5.2E-11	-0.0091456
qy (mm) @ t=3.7E-11	0.0043559	qy (mm) @ t=5.2E-11	0.0017132
qz (mm) @ t=3.7E-11	3.7938589	qz (mm) @ t=5.2E-11	3.7913711
qx (mm) @ t=3.8E-11	-0.0068066	qx (mm) @ t=5.3E-11	-0.0092308
qy (mm) @ t=3.8E-11	0.0042515	qy (mm) @ t=5.3E-11	0.0014757
qz (mm) @ t=3.8E-11	3.7936930	qz (mm) @ t=5.3E-11	3.7912053
qx (mm) @ t=3.9E-11	-0.0070304	qx (mm) @ t=5.4E-11	-0.0093034
qy (mm) @ t=3.9E-11	0.0041351	qy (mm) @ t=5.4E-11	0.0012340
qz (mm) @ t=3.9E-11	3.7935271	qz (mm) @ t=5.4E-11	3.7910395
qx (mm) @ t=4E-11	-0.0072477	qx (mm) @ t=5.5E-11	-0.0093629
qy (mm) @ t=4E-11	0.0040069	qy (mm) @ t=5.5E-11	0.0009887
qz (mm) @ t=4E-11	3.7933612	qz (mm) @ t=5.5E-11	3.7908737
qx (mm) @ t=4.1E-11	-0.0074579	qx (mm) @ t=5.6E-11	-0.0094092
qy (mm) @ t=4.1E-11	0.0038673	qy (mm) @ t=5.6E-11	0.0007406
qz (mm) @ t=4.1E-11	3.7931953	qz (mm) @ t=5.6E-11	3.7907080
qx (mm) @ t=4.2E-11	-0.0076603	qx (mm) @ t=5.7E-11	-0.0094423
qy (mm) @ t=4.2E-11	0.0037167	qy (mm) @ t=5.7E-11	0.0004904
qz (mm) @ t=4.2E-11	3.7930295	qz (mm) @ t=5.7E-11	3.7905422
qx (mm) @ t=4.3E-11	-0.0078544	qx (mm) @ t=5.8E-11	-0.0094620
qy (mm) @ t=4.3E-11	0.0035555	qy (mm) @ t=5.8E-11	0.0002388
qz (mm) @ t=4.3E-11	3.7928636	qz (mm) @ t=5.8E-11	3.7903765
qx (mm) @ t=4.4E-11	-0.0080397	qx (mm) @ t=5.9E-11	-0.0094683
qy (mm) @ t=4.4E-11	0.0033842	qy (mm) @ t=5.9E-11	-0.0000136
qz (mm) @ t=4.4E-11	3.7926977	qz (mm) @ t=5.9E-11	3.7902107

doi:10.6844/NCKU202003198

qx (mm) @ t=6E-11	-0.0094611	qx (mm) @ t=7.5E-11	-0.0078403
qy (mm) @ t=6E-11	-0.0002659	qy (mm) @ t=7.5E-11	-0.0035776
qz (mm) @ t=6E-11	3.7900450	qz (mm) @ t=7.5E-11	3.7875600
qx (mm) @ t=6.1E-11	-0.0094404	qx (mm) @ t=7.6E-11	-0.0076454
qy (mm) @ t=6.1E-11	-0.0005174	qy (mm) @ t=7.6E-11	-0.0037382
qz (mm) @ t=6.1E-11	3.7898792	qz (mm) @ t=7.6E-11	3.7873944
qx (mm) @ t=6.2E-11	-0.0094064	qx (mm) @ t=7.7E-11	-0.0074422
qy (mm) @ t=6.2E-11	-0.0007676	qy (mm) @ t=7.7E-11	-0.0038881
qz (mm) @ t=6.2E-11	3.7897135	qz (mm) @ t=7.7E-11	3.7872288
qx (mm) @ t=6.3E-11	-0.0093591	qx (mm) @ t=7.8E-11	-0.0072313
qy (mm) @ t=6.3E-11	-0.0010155	qy (mm) @ t=7.8E-11	-0.0040269
qz (mm) @ t=6.3E-11	3.7895478	qz (mm) @ t=7.8E-11	3.7870632
qx (mm) @ t=6.4E-11	-0.0092987	qx (mm) @ t=7.9E-11	-0.0070133
qy (mm) @ t=6.4E-11	-0.0012606	qy (mm) @ t=7.9E-11	-0.0041544
qz (mm) @ t=6.4E-11	3.7893821	qz (mm) @ t=7.9E-11	3.7868976
qx (mm) @ t=6.5E-11	-0.0092253	qx (mm) @ t=8E-11	-0.0067889
qy (mm) @ t=6.5E-11	-0.0015021	qy (mm) @ t=8E-11	-0.0042700
qz (mm) @ t=6.5E-11	3.7892164	qz (mm) @ t=8E-11	3.7867320
qx (mm) @ t=6.6E-11	-0.0091391	qx (mm) @ t=8.1E-11	-0.0065585
qy (mm) @ t=6.6E-11	-0.0017394	qy (mm) @ t=8.1E-11	-0.0043735
qz (mm) @ t=6.6E-11	3.7890508	qz (mm) @ t=8.1E-11	3.7865664
qx (mm) @ t=6.7E-11	-0.0090403	qx (mm) @ t=8.2E-11	-0.0063230
qy (mm) @ t=6.7E-11	-0.0019718	qy (mm) @ t=8.2E-11	-0.0044646
qz (mm) @ t=6.7E-11	3.7888851	qz (mm) @ t=8.2E-11	3.7864009
qx (mm) @ t=6.8E-11	-0.0089294	qx (mm) @ t=8.3E-11	-0.0060830
qy (mm) @ t=6.8E-11	-0.0021985	qy (mm) @ t=8.3E-11	-0.0045430
qz (mm) @ t=6.8E-11	3.7887194	qz (mm) @ t=8.3E-11	3.7862353
qx (mm) @ t=6.9E-11	-0.0088065	qx (mm) @ t=8.4E-11	-0.0058391
qy (mm) @ t=6.9E-11	-0.0024190	qy (mm) @ t=8.4E-11	-0.0046085
qz (mm) @ t=6.9E-11	3.7885538	qz (mm) @ t=8.4E-11	3.7860697
qx (mm) @ t=7E-11	-0.0086720	qx (mm) @ t=8.5E-11	-0.0055920
qy (mm) @ t=7E-11	-0.0026327	qy (mm) @ t=8.5E-11	-0.0046609
qz (mm) @ t=7E-11	3.7883881	qz (mm) @ t=8.5E-11	3.7859042
qx (mm) @ t=7.1E-11	-0.0085263	qx (mm) @ t=8.6E-11	-0.0053426
qy (mm) @ t=7.1E-11	-0.0028389	qy (mm) @ t=8.6E-11	-0.0047001
qz (mm) @ t=7.1E-11	3.7882225	qz (mm) @ t=8.6E-11	3.7857387
qx (mm) @ t=7.2E-11	-0.0083698	qx (mm) @ t=8.7E-11	-0.0050913
qy (mm) @ t=7.2E-11	-0.0030370	qy (mm) @ t=8.7E-11	-0.0047259
qz (mm) @ t=7.2E-11	3.7880568	qz (mm) @ t=8.7E-11	3.7855731
qx (mm) @ t=7.3E-11	-0.0082030	qx (mm) @ t=8.8E-11	-0.0048391
qy (mm) @ t=7.3E-11	-0.0032266	qy (mm) @ t=8.8E-11	-0.0047382
qz (mm) @ t=7.3E-11	3.7878912	qz (mm) @ t=8.8E-11	3.7854076
qx (mm) @ t=7.4E-11	-0.0080263	qx (mm) @ t=8.9E-11	-0.0045866
qy (mm) @ t=7.4E-11	-0.0034069	qy (mm) @ t=8.9E-11	-0.0047371
qz (mm) @ t=7.4E-11	3.7877256	qz (mm) @ t=8.9E-11	3.7852420

doi:10.6844/NCKU202003198

qx (mm) @ t=9E-11	-0.0043344	qx (mm) @ t=1.05E-10	-0.0010705
qy (mm) @ t=9E-11	-0.0047226	qy (mm) @ t=1.05E-10	-0.0030044
qz (mm) @ t=9E-11	3.7850765	qz (mm) @ t=1.05E-10	3.7825939
qx (mm) @ t=9.1E-11	-0.0040834	qx (mm) @ t=1.06E-10	-0.0009157
qy (mm) @ t=9.1E-11	-0.0046946	qy (mm) @ t=1.06E-10	-0.0028048
qz (mm) @ t=9.1E-11	3.7849110	qz (mm) @ t=1.06E-10	3.7824285
qx (mm) @ t=9.2E-11	-0.0038343	qx (mm) @ t=1.07E-10	-0.0007719
qy (mm) @ t=9.2E-11	-0.0046532	qy (mm) @ t=1.07E-10	-0.0025972
qz (mm) @ t=9.2E-11	3.7847455	qz (mm) @ t=1.07E-10	3.7822630
qx (mm) @ t=9.3E-11	-0.0035877	qx (mm) @ t=1.08E-10	-0.0006393
qy (mm) @ t=9.3E-11	-0.0045987	qy (mm) @ t=1.08E-10	-0.0023822
qz (mm) @ t=9.3E-11	3.7845800	qz (mm) @ t=1.08E-10	3.7820975
qx (mm) @ t=9.4E-11	-0.0033444	qx (mm) @ t=1.09E-10	-0.0005184
qy (mm) @ t=9.4E-11	-0.0045310	qy (mm) @ t=1.09E-10	-0.0021605
qz (mm) @ t=9.4E-11	3.7844144	qz (mm) @ t=1.09E-10	3.7819320
qx (mm) @ t=9.5E-11	-0.0031050	qx (mm) @ t=1.1E-10	-0.0004095
qy (mm) @ t=9.5E-11	-0.0044505	qy (mm) @ t=1.1E-10	-0.0019326
qz (mm) @ t=9.5E-11	3.7842489	qz (mm) @ t=1.1E-10	3.7817665
qx (mm) @ t=9.6E-11	-0.0028702	qx (mm) @ t=1.11E-10	-0.0003129
qy (mm) @ t=9.6E-11	-0.0043574	qy (mm) @ t=1.11E-10	-0.0016992
qz (mm) @ t=9.6E-11	3.7840834	qz (mm) @ t=1.11E-10	3.7816010
qx (mm) @ t=9.7E-11	-0.0026408	qx (mm) @ t=1.12E-10	-0.0002289
qy (mm) @ t=9.7E-11	-0.0042518	qy (mm) @ t=1.12E-10	-0.0014610
qz (mm) @ t=9.7E-11	3.7839179	qz (mm) @ t=1.12E-10	3.7814355
qx (mm) @ t=9.8E-11	-0.0024173	qx (mm) @ t=1.13E-10	-0.0001577
qy (mm) @ t=9.8E-11	-0.0041342	qy (mm) @ t=1.13E-10	-0.0012187
qz (mm) @ t=9.8E-11	3.7837524	qz (mm) @ t=1.13E-10	3.7812700
qx (mm) @ t=9.9E-11	-0.0022004	qx (mm) @ t=1.14E-10	-0.0000995
qy (mm) @ t=9.9E-11	-0.0040048	qy (mm) @ t=1.14E-10	-0.0009729
qz (mm) @ t=9.9E-11	3.7835869	qz (mm) @ t=1.14E-10	3.7811046
qx (mm) @ t=1E-10	-0.0019907	qx (mm) @ t=1.15E-10	-0.0000546
qy (mm) @ t=1E-10	-0.0038640	qy (mm) @ t=1.15E-10	-0.0007244
qz (mm) @ t=1E-10	3.7834214	qz (mm) @ t=1.15E-10	3.7809391
qx (mm) @ t=1.01E-10	-0.0017888	qx (mm) @ t=1.16E-10	-0.0000229
qy (mm) @ t=1.01E-10	-0.0037122	qy (mm) @ t=1.16E-10	-0.0004738
qz (mm) @ t=1.01E-10	3.7832559	qz (mm) @ t=1.16E-10	3.7807736
qx (mm) @ t=1.02E-10	-0.0015953	qx (mm) @ t=1.17E-10	-0.0000047
qy (mm) @ t=1.02E-10	-0.0035499	qy (mm) @ t=1.17E-10	-0.0002219
qz (mm) @ t=1.02E-10	3.7830904	qz (mm) @ t=1.17E-10	3.7806081
qx (mm) @ t=1.03E-10	-0.0014107	qx (mm) @ t=1.18E-10	0.0000000
qy (mm) @ t=1.03E-10	-0.0033775	qy (mm) @ t=1.18E-10	0.0000306
qz (mm) @ t=1.03E-10	3.7829249	qz (mm) @ t=1.18E-10	3.7804426
qx (mm) @ t=1.04E-10	-0.0012356	qx (mm) @ t=1.19E-10	-0.0000087
qy (mm) @ t=1.04E-10	-0.0031955	qy (mm) @ t=1.19E-10	0.0002831
qz (mm) @ t=1.04E-10	3.7827594	qz (mm) @ t=1.19E-10	3.7802771

doi:10.6844/NCKU202003198

qx (mm) @ t=1.2E-10	-0.0000309	qx (mm) @ t=1.35E-10	-0.0018484
qy (mm) @ t=1.2E-10	0.0005347	qy (mm) @ t=1.35E-10	0.0037443
qz (mm) @ t=1.2E-10	3.7801116	qz (mm) @ t=1.35E-10	3.7776294
qx (mm) @ t=1.21E-10	-0.0000665	qx (mm) @ t=1.36E-10	-0.0020528
qy (mm) @ t=1.21E-10	0.0007847	qy (mm) @ t=1.36E-10	0.0038927
qz (mm) @ t=1.21E-10	3.7799462	qz (mm) @ t=1.36E-10	3.7774640
qx (mm) @ t=1.22E-10	-0.0001154	qx (mm) @ t=1.37E-10	-0.0022648
qy (mm) @ t=1.22E-10	0.0010325	qy (mm) @ t=1.37E-10	0.0040300
qz (mm) @ t=1.22E-10	3.7797807	qz (mm) @ t=1.37E-10	3.7772985
qx (mm) @ t=1.23E-10	-0.0001774	qx (mm) @ t=1.38E-10	-0.0024838
qy (mm) @ t=1.23E-10	0.0012773	qy (mm) @ t=1.38E-10	0.0041558
qz (mm) @ t=1.23E-10	3.7796152	qz (mm) @ t=1.38E-10	3.7771330
qx (mm) @ t=1.24E-10	-0.0002525	qx (mm) @ t=1.39E-10	-0.0027092
qy (mm) @ t=1.24E-10	0.0015185	qy (mm) @ t=1.39E-10	0.0042698
qz (mm) @ t=1.24E-10	3.7794497	qz (mm) @ t=1.39E-10	3.7769675
qx (mm) @ t=1.25E-10	-0.0003403	qx (mm) @ t=1.4E-10	-0.0029404
qy (mm) @ t=1.25E-10	0.0017553	qy (mm) @ t=1.4E-10	0.0043715
qz (mm) @ t=1.25E-10	3.7792842	qz (mm) @ t=1.4E-10	3.7768021
qx (mm) @ t=1.26E-10	-0.0004406	qx (mm) @ t=1.41E-10	-0.0031767
qy (mm) @ t=1.26E-10	0.0019871	qy (mm) @ t=1.41E-10	0.0044607
qz (mm) @ t=1.26E-10	3.7791187	qz (mm) @ t=1.41E-10	3.7766366
qx (mm) @ t=1.27E-10	-0.0005531	qx (mm) @ t=1.42E-10	-0.0034174
qy (mm) @ t=1.27E-10	0.0022132	qy (mm) @ t=1.42E-10	0.0045372
qz (mm) @ t=1.27E-10	3.7789533	qz (mm) @ t=1.42E-10	3.7764712
qx (mm) @ t=1.28E-10	-0.0006776	qx (mm) @ t=1.43E-10	-0.0036619
qy (mm) @ t=1.28E-10	0.0024330	qy (mm) @ t=1.43E-10	0.0046008
qz (mm) @ t=1.28E-10	3.7787878	qz (mm) @ t=1.43E-10	3.7763057
qx (mm) @ t=1.29E-10	-0.0008136	qx (mm) @ t=1.44E-10	-0.0039094
qy (mm) @ t=1.29E-10	0.0026458	qy (mm) @ t=1.44E-10	0.0046511
qz (mm) @ t=1.29E-10	3.7786223	qz (mm) @ t=1.44E-10	3.7761403
qx (mm) @ t=1.3E-10	-0.0009607	qx (mm) @ t=1.45E-10	-0.0041593
qy (mm) @ t=1.3E-10	0.0028511	qy (mm) @ t=1.45E-10	0.0046882
qz (mm) @ t=1.3E-10	3.7784568	qz (mm) @ t=1.45E-10	3.7759748
qx (mm) @ t=1.31E-10	-0.0011187	qx (mm) @ t=1.46E-10	-0.0044108
qy (mm) @ t=1.31E-10	0.0030482	qy (mm) @ t=1.46E-10	0.0047119
qz (mm) @ t=1.31E-10	3.7782913	qz (mm) @ t=1.46E-10	3.7758094
qx (mm) @ t=1.32E-10	-0.0012869	qx (mm) @ t=1.47E-10	-0.0046632
qy (mm) @ t=1.32E-10	0.0032366	qy (mm) @ t=1.47E-10	0.0047221
qz (mm) @ t=1.32E-10	3.7781259	qz (mm) @ t=1.47E-10	3.7756439
qx (mm) @ t=1.33E-10	-0.0014649	qx (mm) @ t=1.48E-10	-0.0049158
qy (mm) @ t=1.33E-10	0.0034158	qy (mm) @ t=1.48E-10	0.0047189
qz (mm) @ t=1.33E-10	3.7779604	qz (mm) @ t=1.48E-10	3.7754785
qx (mm) @ t=1.34E-10	-0.0016523	qx (mm) @ t=1.49E-10	-0.0051678
qy (mm) @ t=1.34E-10	0.0035851	qy (mm) @ t=1.49E-10	0.0047021
qz (mm) @ t=1.34E-10	3.7777949	qz (mm) @ t=1.49E-10	3.7753131

doi:10.6844/NCKU202003198

qx (mm) @ t=1.5E-10	-0.0054186	qx (mm) @ t=1.65E-10	-0.0085689
qy (mm) @ t=1.5E-10	0.0046719	qy (mm) @ t=1.65E-10	0.0027516
qz (mm) @ t=1.5E-10	3.7751476	qz (mm) @ t=1.65E-10	3.7726670
qx (mm) @ t=1.51E-10	-0.0056674	qx (mm) @ t=1.66E-10	-0.0087107
qy (mm) @ t=1.51E-10	0.0046283	qy (mm) @ t=1.66E-10	0.0025425
qz (mm) @ t=1.51E-10	3.7749822	qz (mm) @ t=1.66E-10	3.7725017
qx (mm) @ t=1.52E-10	-0.0059136	qx (mm) @ t=1.67E-10	-0.0088411
qy (mm) @ t=1.52E-10	0.0045716	qy (mm) @ t=1.67E-10	0.0023261
qz (mm) @ t=1.52E-10	3.7748168	qz (mm) @ t=1.67E-10	3.7723364
qx (mm) @ t=1.53E-10	-0.0061564	qx (mm) @ t=1.68E-10	-0.0089597
qy (mm) @ t=1.53E-10	0.0045017	qy (mm) @ t=1.68E-10	0.0021030
qz (mm) @ t=1.53E-10	3.7746514	qz (mm) @ t=1.68E-10	3.7721711
qx (mm) @ t=1.54E-10	-0.0063951	qx (mm) @ t=1.69E-10	-0.0090663
qy (mm) @ t=1.54E-10	0.0044190	qy (mm) @ t=1.69E-10	0.0018738
qz (mm) @ t=1.54E-10	3.7744860	qz (mm) @ t=1.69E-10	3.7720058
qx (mm) @ t=1.55E-10	-0.0066290	qx (mm) @ t=1.7E-10	-0.0091605
qy (mm) @ t=1.55E-10	0.0043236	qy (mm) @ t=1.7E-10	0.0016394
qz (mm) @ t=1.55E-10	3.7743206	qz (mm) @ t=1.7E-10	3.7718405
qx (mm) @ t=1.56E-10	-0.0068575	qx (mm) @ t=1.71E-10	-0.0092420
qy (mm) @ t=1.56E-10	0.0042159	qy (mm) @ t=1.71E-10	0.0014002
qz (mm) @ t=1.56E-10	3.7741552	qz (mm) @ t=1.71E-10	3.7716752
qx (mm) @ t=1.57E-10	-0.0070800	qx (mm) @ t=1.72E-10	-0.0093107
qy (mm) @ t=1.57E-10	0.0040961	qy (mm) @ t=1.72E-10	0.0011570
qz (mm) @ t=1.57E-10	3.7739898	qz (mm) @ t=1.72E-10	3.7715099
qx (mm) @ t=1.58E-10	-0.0072957	qx (mm) @ t=1.73E-10	-0.0093662
qy (mm) @ t=1.58E-10	0.0039646	qy (mm) @ t=1.73E-10	0.0009104
qz (mm) @ t=1.58E-10	3.7738245	qz (mm) @ t=1.73E-10	3.7713447
qx (mm) @ t=1.59E-10	-0.0075041	qx (mm) @ t=1.74E-10	-0.0094085
qy (mm) @ t=1.59E-10	0.0038218	qy (mm) @ t=1.74E-10	0.0006613
qz (mm) @ t=1.59E-10	3.7736591	qz (mm) @ t=1.74E-10	3.7711794
qx (mm) @ t=1.6E-10	-0.0077045	qx (mm) @ t=1.75E-10	-0.0094374
qy (mm) @ t=1.6E-10	0.0036681	qy (mm) @ t=1.75E-10	0.0004102
qz (mm) @ t=1.6E-10	3.7734937	qz (mm) @ t=1.75E-10	3.7710142
qx (mm) @ t=1.61E-10	-0.0078965	qx (mm) @ t=1.76E-10	-0.0094529
qy (mm) @ t=1.61E-10	0.0035038	qy (mm) @ t=1.76E-10	0.0001579
qz (mm) @ t=1.61E-10	3.7733284	qz (mm) @ t=1.76E-10	3.7708490
qx (mm) @ t=1.62E-10	-0.0080794	qx (mm) @ t=1.77E-10	-0.0094548
qy (mm) @ t=1.62E-10	0.0033295	qy (mm) @ t=1.77E-10	-0.0000948
qz (mm) @ t=1.62E-10	3.7731630	qz (mm) @ t=1.77E-10	3.7706837
qx (mm) @ t=1.63E-10	-0.0082528	qx (mm) @ t=1.78E-10	-0.0094433
qy (mm) @ t=1.63E-10	0.0031457	qy (mm) @ t=1.78E-10	-0.0003473
qz (mm) @ t=1.63E-10	3.7729977	qz (mm) @ t=1.78E-10	3.7705185
qx (mm) @ t=1.64E-10	-0.0084161	qx (mm) @ t=1.79E-10	-0.0094182
qy (mm) @ t=1.64E-10	0.0029529	qy (mm) @ t=1.79E-10	-0.0005988
qz (mm) @ t=1.64E-10	3.7728323	qz (mm) @ t=1.79E-10	3.7703533

doi:10.6844/NCKU202003198

qx (mm) @ t=1.8E-10	-0.0093798	qx (mm) @ t=1.95E-10	-0.0073554
qy (mm) @ t=1.8E-10	-0.0008486	qy (mm) @ t=1.95E-10	-0.0039355
qz (mm) @ t=1.8E-10	3.7701881	qz (mm) @ t=1.95E-10	3.7677111
qx (mm) @ t=1.81E-10	-0.0093281	qx (mm) @ t=1.96E-10	-0.0071416
qy (mm) @ t=1.81E-10	-0.0010960	qy (mm) @ t=1.96E-10	-0.0040704
qz (mm) @ t=1.81E-10	3.7700229	qz (mm) @ t=1.96E-10	3.7675460
qx (mm) @ t=1.82E-10	-0.0092632	qx (mm) @ t=1.97E-10	-0.0069208
qy (mm) @ t=1.82E-10	-0.0013403	qy (mm) @ t=1.97E-10	-0.0041936
qz (mm) @ t=1.82E-10	3.7698577	qz (mm) @ t=1.97E-10	3.7673809
qx (mm) @ t=1.83E-10	-0.0091853	qx (mm) @ t=1.98E-10	-0.0066937
qy (mm) @ t=1.83E-10	-0.0015808	qy (mm) @ t=1.98E-10	-0.0043049
qz (mm) @ t=1.83E-10	3.7696925	qz (mm) @ t=1.98E-10	3.7672159
qx (mm) @ t=1.84E-10	-0.0090948	qx (mm) @ t=1.99E-10	-0.0064611
qy (mm) @ t=1.84E-10	-0.0018167	qy (mm) @ t=1.99E-10	-0.0044038
qz (mm) @ t=1.84E-10	3.7695274	qz (mm) @ t=1.99E-10	3.7670508
qx (mm) @ t=1.85E-10	-0.0089917	qx (mm) @ t=2E-10	-0.0062234
qy (mm) @ t=1.85E-10	-0.0020476	qy (mm) @ t=2E-10	-0.0044902
qz (mm) @ t=1.85E-10	3.7693622	qz (mm) @ t=2E-10	3.7668857
qx (mm) @ t=1.86E-10	-0.0088764		
qy (mm) @ t=1.86E-10	-0.0022725		
qz (mm) @ t=1.86E-10	3.7691971		
qx (mm) @ t=1.87E-10	-0.0087493		
qy (mm) @ t=1.87E-10	-0.0024910		
qz (mm) @ t=1.87E-10	3.7690319		
qx (mm) @ t=1.88E-10	-0.0086107		
qy (mm) @ t=1.88E-10	-0.0027024		
qz (mm) @ t=1.88E-10	3.7688668		
qx (mm) @ t=1.89E-10	-0.0084609		
qy (mm) @ t=1.89E-10	-0.0029061		
qz (mm) @ t=1.89E-10	3.7687017		
qx (mm) @ t=1.9E-10	-0.0083005		
qy (mm) @ t=1.9E-10	-0.0031015		
qz (mm) @ t=1.9E-10	3.7685365		
qx (mm) @ t=1.91E-10	-0.0081299		
qy (mm) @ t=1.91E-10	-0.0032881		
qz (mm) @ t=1.91E-10	3.7683714		
qx (mm) @ t=1.92E-10	-0.0079496		
qy (mm) @ t=1.92E-10	-0.0034652		
qz (mm) @ t=1.92E-10	3.7682063		
qx (mm) @ t=1.93E-10	-0.0077600		
qy (mm) @ t=1.93E-10	-0.0036325		
qz (mm) @ t=1.93E-10	3.7680412		
qx (mm) @ t=1.94E-10	-0.0075618		
qy (mm) @ t=1.94E-10	-0.0037894		
qz (mm) @ t=1.94E-10	3.7678761		

doi:10.6844/NCKU202003198

D The venders of all components

Table 22: The venders of all components.

Vender	Item	Note
振之越五金机電銷售中心	眞空電極	https://reurl.cc/2g2dQ9
東莞市圣澤金屬材料有限公司	鎢絲	https://reurl.cc/Y62Ako
陽光眞空	眞空計	https://reurl.cc/Gr93gp
眞空元器件	手高眞空插板	https://reurl.cc/Mdal9W
溫州暢宏管件	卡箍 、oring、眞空管件	https://reurl.cc/N6k7L6
溫州奇科流体設備有限公司	卡箍 、oring、眞空管件	https://reurl.cc/Xkd0oa
勁順購物	溫控器 1500W AC110/220V	https://reurl.cc/Y62Aba
科學博士	鋅片	https://reurl.cc/e8eN2K
雪鰻的家PLUS	Y-500 矽質高效能散熱膏	https://reurl.cc/OqlyWX
coolpolos的賣場	DC 5V-12V 無刷馬達 靜音水泵	https://reurl.cc/x0yrrL
台灣秋葉原電子企業社	240直寶塔水排 + 風扇	https://reurl.cc/2g2dnX
南一電子有限公司	Electronic components	
東昕實業有限公司	Vacuum product	
三美玻璃儀器行	Quartz processing	
科研市集	實驗耗材、設備儀器代購	https://www.sciket.com/
嘉展鋼鐵	不銹鋼	

doi:10.6844/NCKU202003198